Imperial College London

cep

Geochemical baselines based on stream waters: applications to environmental studies, Central Chile as a case study

A thesis submitted to Imperial College London for the degree of Doctor of Philosophy in the Faculty of Natural Sciences

By **Carmina Olivia Jorquera Zuniga**

July 2013

Centre for Environmental Policy

Imperial College London

DECLARATION OF OWN WORK

I declare that this thesis

'Geochemical baselines based on stream waters: applications to environmental studies, Central Chile as a case study' is entirely my own work and has not been submitted previously for any other degree. Any material that could be understood as the work of others, it is fully cited and referenced.

Name of student (*Please print*): Carmina Jorquera

Name of supervisor: Nikolaos Voulvoulis

Name of co-supervisor: Jane Plant

Name of external Anglo American Advisor: Christopher Oates

COPYRIGHT DECLARATION

The copyright of this thesis rests with the author and is made available under a Creative Commons Attribution-Non Commercial-No Derivatives licence. Researchers are free to copy, distribute or transmit the thesis on the condition that they attribute it, that they do not use it for commercial purposes and that they do not alter, transform or build upon it. For any reuse or redistribution, researchers must make clear to others the licence terms of this work.

This thesis is dedicated to my beloved family.

ABSTRACT

Increasing environmental regulation has resulted in mining companies monitoring levels of toxic trace elements in the environment. However, little research has been done to identify the sources of such elements as natural or manmade. Whilst the mining industry has traditionally used hydrogeochemical baselines for exploration, this study has evaluated the use of such baselines for environmental assessments of drainage systems, particularly the identification and quantification of natural and anthropogenic sources. The results are discussed in the context of water quality regulation and guideline values.

The research generated the first systematic regional geochemical baseline of Central Chile including the classic Andean copper mineral province and the Andina – Los Bronces mining district. The study area included three major catchments flowing from the Andean Cordillera into inhabited valleys, with the potential for contamination from agriculture and the urban environment. Waters were sampled at a density of 1 per 100 sq. km. over 20000 sq. km. in five seasons over three years. Multi-element chemistry and stable isotopes were determined. The geochemical baseline was prepared using high quality geochemical data.

The distribution patterns of the anomalously high geochemistry showed strong relationships with bedrock geology, including the presence of evaporites, sulphide mineralisation and hydrothermally altered rocks (differentiated using isotopes in sulphate). High concentrations of nitrate and phosphate were identified in agricultural areas reflecting pollution from fertilisers and sewage (distinguished using isotopes in nitrate). Areas affected by fertilisers and sewage were significantly greater than those affected by mining. Waters draining unmined Cu-mineralisation had much higher Cu and Ni levels and lower pH than Cu-mine area waters. Most regional geochemistry was below international guidelines and Chilean regulatory levels and where elevated it reflected natural sources and seasonal variations.

The study demonstrates that geochemical baselines have considerable potential for distinguishing between natural and anthropogenic pollutant sources in environmental assessments.

ACKNOWLEDGEMENT

My heartfelt thanks to all of the following for their support and encouragement throughout my PhD.

•Anglo American Chile for funding this amazing project and supporting my career. •Chris Oates for believing in me and being a huge support all these years. •My supervisors, Professor Jane Plant for helping when I most needed it and Nick Voulvoulis for his valuable recommendations. •My parents Cecilia Zuniga and Jaime Jorquera, my siblings Carmen Gloria, Juan Pablo and Carola, and my nephews Benjamin, Ian and Javier for giving me with all their unconditional love. •All my Chilean friends that saw me leaving and have been in contact and sending me good vibrations all the time, Carolina Munoz, Miguel Trejo, Cristina Ortega, Valentina Flores, Macarena Silva, Carlos Castro, Maria Pia Rodriguez, Angelo Castruccio, Michelle Munoz, Marion Fuentes, Carolina Alvarez, Carla Lohr, Romina Guzman, Cesar Silva, Gladys Navarro, Salvador Flores, Mauricio Carranza and so many more. •All my friends in the UK and the ones that have returned home, every one of you has been important in this journey, thanks for every laugh, shoulder, dance and love, Aisha, Alex, Khareen, James T., James B., Charlotte, Olwenn, Sally, Ho-Sik, Jilang, Rebecca, Atun, Aida, Young. A special thanks to Danelle Dhaniram, Amit and Jhasan, thanks for considering me part of your family and gave me home, I still miss you. •All the small but good Latin American community in the UK for the spontaneous friendship, excellent times and good laughs, Rocio, Elisa, Carito, Pato, Lety, Omar, Pablo, Leo, Pizzas, Vivi and specially to Pedro Galindo for his love, support, encouragement, sharing his lovely culture and remind me all the time how precious I am with a funny sense of humour.

TABLE OF CONTENTS

CHAPTER 1: INTRODUCTION 1
1.1 Introduction 1
1.2 Aim and objectives 3
1.3 Thesis Outline 4
1.4 Significance of the research 5
1.5 Publications 6
CHAPTER 2: BACKGROUND LITERATURE REVIEW 7
2.1 Geochemical baselines of drainage systems 7
2.1.1 Introduction 7
2.1.2 The concept behind the geochemical background and baselines 8
2.1.3 Historical development of geochemical baselines 11
2.2 Applications of geochemical baselines to environmental research 13
2.3 Sampling procedures to develop geochemical baselines 16
2.3.1 Sample density 16
2.3.2 Sample media 17
2.3.3 Sampling procedures 20
2.4 Quality assurance and quality control of geochemical data 21
2.4.1 Evaluating reliability of data 21
2.5 Current water guidelines and regulation values of environmental chemicals 23
2.6 Potentially toxic chemicals in the environment 25
2.6.1 Arsenic 25
2.6.2 Cadmium 28
2.6.3 Copper 30
2.6.4 Mercury 32
2.6.5 Lead 34
2.6.6 Nickel 37
2.6.7 Nitrate 39
2.6.8 Phosphorus 41
2.6.9 Sulphur 44
CHAPTER 3: METHODOLOGY 47
3.1 Data collection in Central Chile 47
3.1.1 Sampling procedures 47
3.2 Analytical methods used in the research 49
3.2.1 Multi-elemental chemistry and physico-chemical analysis 49

3.2.2 Stable isotope determinations 49
3.3 Evaluation of the reliability of the geochemical data collected 52
3.3.1 Quality assurance and quality control 52
3.3.2 Charge imbalance of water geochemical data 56
3.4 Chemical characterisation and developing the geochemical baseline 57
3.4.1 Preparation of regional hydrogeochemical baseline maps 57
3.5 Identification of the sources of anomalous geochemistry 58
3.6 Evaluating the application of the geochemical baseline to water regulation 59
CHAPTER 4: RESULTS 61
4.1 Study area 61
4.1.1 Introduction 61
4.1.2 Geology 65
4.2 Reliability of the analytical data 70
4.2.1 QA/QC 70
4.2.2 Alkalinity measured in the field and laboratory 73
4.2.3 Charge imbalance results 74
4.3 Characterisation of chemicals and developing the regional hydrogeochemical baseline 77
4.3.1 Statistical analysis of regional hydrogeochemical data 78
4.3.2 Multivariate data analysis 81
4.3.3 Stream water geochemistry 84
4.3.4 Hydrogeochemical baseline maps 88
4.4 Stable isotope results 118
4.4.1 Hydrogen (δD) and oxygen ($\delta^{18}O$) isotopes in water samples 118
4.4.2 Sulphur and oxygen isotopes in sulphate 123
4.4.3 Nitrogen and oxygen isotopes in nitrate 129
4.5 Sources of anomalous geochemistry in Central Chile 133
4.5.1 Geology 134
4.5.2 Hydrothermally altered and mineralised areas 135
4.5.3 Copper mineralisation 139
4.5.4 Agriculture and sewage 141
4.5.5 Human settlements 144
4.5.6 Mine area waters 144
4.6 Comparison of the hydrogeochemical data of the Maipo Basin with water quality regulation data 146
CHAPTER 5: DISCUSSION 149

5.1 Introduction 149
5.2 Reliability of the analytical data 149
5.3 Geochemistry of the trace elements and compounds 150
5.4 Stable isotope geochemistry 152
5.4.1 Hydrogen (δD) and oxygen ($\delta^{18}O$) isotopes in the waters 152
5.4.2 Sulphur and oxygen isotopes in sulphate 155
5.4.3 Nitrogen and oxygen isotopes in nitrate 156
5.5 Sources of anomalous chemistry 157
5.5.1 Natural sources of anomalous geochemistry 157
5.5.2 Anthropogenic sources of anomalous geochemistry 161
5.5.3 Cu-Mineralisation and mine area waters in the headwaters of Mapocho River: The Yerba Loca Stream and the San Francisco River 165
5.6 Application of the geochemical baseline to water regulation 166
5.6.1 Regional hydrogeochemical data compared with regulation and guideline values 166
5.7 Summary 170
CHAPTER 6: CONCLUSIONS 172
REFERENCES 176
APPENDIX A: Sampling protocol to collect stream waters 184
APPENDIX B: QA/QC evaluation 193
APPENDIX C: Anomalously high geochemistry 201
APPENDIX D: Hydrogeochemical baseline maps for Ag, B, Co, F, K, Mn, Sb, Se, Sn and Zn 237
APPENDIX E: Statistical summary for the regional data 248
APPENDIX F: Regional geochemical data 251

LIST OF FIGURES

Figure 3.1: Graph used to control precision 53
Figure 3.2: Graph used to control accuracy 55
Figure 3.3: Graph used to detect contamination 56
Figure 3.4: Histogram and frequency accumulation curve for regional copper data 58
Figure 4.1: Contour map showing the highest altitudes on the Chile-Argentina border 62
Figure 4.2: Profiles AA', BB' and CC' highlighting the relief of the region 63
Figure 4.3: Location of the study area 64
Figure 4.4: Geological map 69
Figure 4.5: Graph used to control precision of Zn 72
Figure 4.6: Field alkalinity versus laboratory alkalinity 74
Figure 4.7: Charge imbalance including H^+ versus pH data 76
Figure 4.8: Histogram of the CI distribution 76
Figure 4.9: Box-whisker charts of calcium for different seasons 77
Figure 4.10: Pearson correlation matrix for chemical parameters and scatter plots 80
Figure 4.11: Histogram showing the raw and logarithmic distribution for Cu 80
Figure 4.12: Factor 1 versus Factor 2 with the sources indicated 83
Figure 4.13: Sample scores calculated for Factor 1 and 2 by basin 83
Figure 4.14: EC versus pH scatter diagrams 84
Figure 4.15: Ternary diagrams 85
Figure 4.16: Calcium versus sulphate 92
Figure 4.17: Stream water baseline geochemical maps 98
Figure 4.18: Baseline geochemical map for δD and $\delta^{18}O$ 121
Figure 4.19: δD versus $\delta^{18}O$ for the three basins 123
Figure 4.20: Baseline geochemical map for $\delta^{34}S$ and $\delta^{18}O_{SO4}$ 125
Figure 4.21: $\delta^{34}S$ and $\delta^{18}O$ values of water samples 128
Figure 4.22: Baseline geochemical map for $\delta^{15}N$ and $\delta^{18}O_{NO3}$ 131
Figure 4.23: $\delta^{15}N$ and $\delta^{18}O$ values of water samples 133
Figure 4.24: Field pictures 137
Figure 5.1: Charge imbalance for regional samples versus pH and Cu 151
Figure 5.2: δD versus east UTM coordinate and altitude 154
Figure 5.3. Sources of anomalously high concentration of chemicals 164
Figure 5.4. Comparison of the regional hydrogeochemical data with the draft regulation values 169

LIST OF TABLES

Table 2.1: Water guideline and regulation values 24
Table 2.2: World average chemical content in rocks, and river sediments and waters 26
Table 3.1: Summary of sampling campaigns and data collected 47
Table 3.2: Summary of analytical methods for multi-element chemistry 50
Table 3.3: Methods for determining stable isotope values 50
Table 4.1: Geology of stratigraphic rock units in the study area 66
Table 4.2: Intrusive geological units in the study area 68
Table 4.3: Overall results of the QA/QC evaluation 73
Table 4.4: Statistics of charge imbalance results 75
Table 4.5. Charge imbalance percentage averages for the three basins 75
Table 4.6: Statistical summary and background levels 79
Table 4.7: Spearman rank correlation matrix 79
Table 4.8: List of chemicals included and excluded in the factor analysis 81
Table 4.9: Loadings for the eight factors calculated 82
Table 4.10: Concentration of elements upflow and downflow the Canal San Carlos 90
Table 4.11: Statistical summary of stable isotope results 118
Table 4.12: Summary of statistics for H, O, S and N isotopes for the three basins 119
Table 4.13: Lithology reflected in ternary diagrams and anomalous water samples 135
Table 4.14: Anomalous hydrogeochemistry associated with hydrothermal alteration and mineralisation 138
Table 4.15: Anomalous hydrogeochemistry associated with Cu-mineralised areas 140
Table 4.16: Anomalous hydrogeochemistry associated with agriculture and sewage 143
Table 4.17: Anomalous hydrogeochemistry associated with mine area waters 146
Table 4.18: Mean of the percentage difference between the data for the Maipo Basin and regulated values 148

LIST OF ABBREVIATIONS

AAplc: Anglo American plc

ATSDR: Agency for Toxic Substances and Disease Registry

BGS: British Geological Survey

CCME: Canadian Council of Ministers of the Environment

CONAMA: Corporación Nacional del Medio Ambiente

CRM: Certified Reference Material

D: Deuterium

DGA: Dirección General de Aguas

DL: Detection limit

EC: European Commission

EPA: Environmental Protection Agency

FOREGS: Forum of European Geological Surveys

G-BASE: Geochemical Baselines Survey of the Environment

GIS: Geographical Information System

GNIP: Global Network of Isotopes in Precipitation

ICP-ES: Inductively Coupled Plasma Emission Spectrometry

ICP-MS: Inductively Coupled Plasma Mass Spectrometry

IGCP: International Geological Correlation Programme

INN: Instituto Nacional de Normalización

IRMS: Isotope Ratio Mass Spectrometer

IUGS: International Union of Geological Sciences

LED: Light emitting diode

MMHg: Monomethylmercury

PCA: Principal Components Analysis

PEFR: Phosphate ester flame retardant

PTCs: Potentially Toxic Chemicals

QA/QC: Quality Assurance Quality Control

SMWL: Santiago meteorological water line

TDS: Total dissolved solids

THLD: Threshold

TOC: Total dissolved organic carbon

WGVs: Water Guideline Values

WHO: World Health Organisation

XRF: X-Ray Fractionation

CHAPTER 1: INTRODUCTION

1.1 Introduction

Geochemical baselines show the distribution of a range of chemical elements, compounds and other parameters based on chemical analysis of systematically sampled media. They have direct application in identifying areas of anomalous chemistry including of elements such as arsenic, cadmium, lead, mercury, nitrate, phosphorous and sulphate which are important for mineral exploration and environmental research.

Geochemistry as an exploration method began early in the 20th century and has been used extensively in mineral exploration since that time (Garrett et al. 2008). The availability of multi-element, high precision analytical methods and digital data processing since the 1960s (Plant & Hale 1994) facilitated geochemical data collection and increased the development of quantitative methods of geochemical mapping. This in turn increased the use of regional geochemical maps globally (Darnley 1997) and to the development of international standardised procedures for sampling and analysis (Darnley et al. 1995).

There are now diverse environmental applications of geochemical baselines including the assessment of the impact of industrial, urban and agricultural activities on the surface environment in relation to the environment and plant, animal and human health (Simpson et al. 1993; Plant et al. 1996). The development of geochemical baselines, where most of datasets were prepared for mineral exploration purposes and are owned by private companies, is particularly important in developing countries for environmental and epidemiological applications (Plant et al. 1996).

Other environmental applications of geochemical baselines include their use as a basis for environmental legislation and regulation (Van Den Oever 2000) and they can be used to identify areas where geochemical and physicochemical parameters fall outside acceptable values (Simpson et al. 1993). Such baselines can also be of value to mining companies especially in helping to understand the geochemistry of mineralised areas and define baseline levels of chemicals prior to the beginning of their mining operations and as a basis for on-going monitoring and post-closure operations.

In addition to identifying areas of deficiencies or anomalies of chemicals based on the trace element geochemistry of stream waters and stream sediments, isotopic signatures and multivariate statistical procedures can be used to discriminate between natural and anthropogenic sources of chemicals (Reimann & Garrett 2005).

In the present study, the regional geochemical baseline based on stream waters was used to develop methods of identifying and characterising areas of natural and anthropogenic sources of pollutants. The inorganic chemical composition and stable isotope data were used to identify the signature of the bedrock geology, hydrothermal alteration and metalliferous mineralisation, and differentiate them from the anthropogenic sources of potentially toxic chemicals (PTCs) including sources such as agriculture, sewage and industry.

The study focused particularly on trace elements such as As, Cd, Hg and Pb that pose a risk to human health and the environment; trace elements important to mineral exploration such as Cu, Mo, Ag and Zn; chemicals that reflect bedrock geology such as

Al, Ca, Cr, Fe, K, Mg, Mn, Na and SO_4^{-2}; and those such as Hg, NO_3^- and P which strongly reflect anthropogenic sources.

The case study centred on the three main drainage systems flowing from the Andes into inhabited valleys of Central Chile, including the La Ligua, the Aconcagua and the Maipo Basins (Figure 4.3). The methodologies described within this thesis and applied to this example area have the potential for identifying contamination from agriculture and the urban environment as well as natural mineral sources from the classic Andean copper mineral province and bedrock geology which includes volcanic and large sedimentary basins.

Finally, the surface hydrogeochemical baseline was evaluated in comparison to current water quality regulations and international guideline values for drinking water to evaluate their potential to facilitate environmental assessments, particularly to identify the hydrogeochemical signatures of various natural and anthropogenic end-member sources and to quantify their relative contributions.

1.2 Aim and objectives

The overall aim of the thesis was to evaluate the use of geochemical baselines in environmental assessment, particularly to identify the geochemical signatures of various natural and anthropogenic end-member sources and to quantify their relative contributions. This research was carried out using stream water geochemical data collected from over Central Chile and the results obtained were discussed in the context of water quality regulation and international guideline values.

Objectives were as follows:

1. To investigate and determine the sampling procedures and protocol to collect high quality water geochemical data to generate regional geochemical baselines in mountainous terrains.
2. To investigate and understand the analytical methods used in the research. Particularly, to select and analyse water samples for stable isotopes of environmental significance.
3. To evaluate the reliability of the water geochemical data collected using rigorous quality assurance and quality control (QA/QC) analysis.
4. To characterise the water chemistry of the region and develop a hydrogeochemical baseline based on multi-statistical analysis.
5. To identify natural and anthropogenic sources of potentially toxic elements and compounds based on the baselines prepared and quantify the areas affected.
6. To evaluate the use of the geochemical baseline prepared by comparing the geochemical dataset with the Chilean water quality regulation data.

1.3 Thesis Outline

The relevant background literature about the main topics of this research is reviewed first (**Chapter 2**), and the methodology to prepare the geochemical baselines based on stream water is explained in **Chapter 3**. This breaks the objectives into tasks set to obtain reliable geochemical data and to develop a high quality geochemical baseline to be applied in any regional environmental study. It is described the data collection and the sampling protocols used. This is followed by a description of the analytical methods used and the procedures used to evaluate the quality of the data collected.

Chapter 4 presents the results of the research. Firstly, the data are shown to be highly reliable and of high quality. The stream water data are statistically analysed and geochemically characterised. The geochemical baseline is determined and the regional hydrogeochemical baseline maps presented. The geochemical data and isotopic data are then used to identify the natural and anthropogenic sources of anomalous concentrations of chemicals. Finally, the results are evaluated by comparing them with international and national drinking water guideline values (WGVs) and Chilean national draft water quality regulation for surface waters of the Maipo Basin.

The results of the study are discussed in **Chapter 5.** The natural and anthropogenic sources identified are compared in terms of surface area of contribution. The applicability of the geochemical baselines to water quality regulation is discussed. The strengths and weaknesses of the development and application of hydrogeochemical baselines as a basis for regulation are then evaluated.

Finally, in the **Chapter 6** the overall conclusions are given and recommendations proposed.

1.4 Significance of the research

The contributions of the research are quantitative as it provides the first regional hydrogeochemical baselines over Central Chile and applies high quality geochemical and stable isotope data to environmental studies. It presents the first environmental isotope study at the regional scale and identifies methods of distinguishing between of the major natural and anthropogenic sources of anomalously high concentrations of chemicals.

This research provides a critical review of the new Chilean national water quality regulation, which is under development, and compares the draft regulation data prepared for the surface water of the Maipo Basin with the high quality hydrogeochemical data prepared for this study. This comparison is critical to demonstrating the validity of both datasets.

Qualitative information is given in the extensive literature reviewed about the applications of the geochemical baselines, particularly the considerable potential of mineral exploration geochemical data to environmental studies. Detailed information about some key chemicals is also given to aid in the identification of their sources.

1.5 Publications

- Jorquera, C., Oates, C.J., Plant, J.A., Kyser, K., Ihlenfeld, C., Voulvoulis, N. Regional hydrogeochemical mapping in Central Chile: natural and anthropogenic sources of chemicals. *Geochemistry: Exploration, Environment, Analysis.* ***(Accepted)***.
- Gloudon, A., Jorquera, C., Plant, J.A., Voulvoulis, N., Review of the application of geochemical baselines to environmental studies. *Applied Geochemistry.* ***(Submitted)***.
- Source assessment and implications for risk management in Central Chile. ***(In preparation)***.
- The role of environmental regulation on guideline values in regions with high background natural levels. ***(In preparation)***.
- 2012 XIII Congreso Geológico Chileno. Antofagasta, Chile: Jorquera, C.O., Ihlenfeld, C., Kyser, K., Oates, C.J., Plant, J.A., Voulvoulis, N. (2012). The application of N and O isotopes to the identification of sources of nitrate in stream waters in Central Chile. pp 774-776. ***(Conference Presentation)***

CHAPTER 2: BACKGROUND LITERATURE REVIEW

2.1 Geochemical baselines of drainage systems

2.1.1 Introduction

Geochemical baseline maps which are usually based on the systematic sampling and analysis of one sample media such as stream sediments or water show the distribution of a range of chemicals over regions. Such maps are used in mineral exploration to distinguish anomalously high concentrations of chemical elements that could indicate the presence of mineralisation above background values. They are also used for environmental and agricultural purposes including for example to identify anomalously high and low levels of chemicals which could lead to diseases in animals.

Systematic geochemical exploration began early in the 20th century and by the 1950s it was being used extensively for mineral exploration worldwide (Garrett et al. 2008). From the 1960s onward, improved drainage sampling and advances in analytical instrumentation and methods such as atomic absorption spectrophotometry, neutron activation, plasma emission and mass spectrometry enabled increasingly quantitative multi-element geochemical mapping programmes (Plant & Hale 1994). This in turn increased the use of geochemical maps worldwide (Darnley 1997), and there was increasing standardisation of sampling and analytical procedures internationally (Darnley et al. 1995).

There are now diverse environmental applications of geochemical baselines including the assessment of the impact of industrial, urban and agricultural activities on the surface environment in relation to the environment and plant, animal and human health (Plant et al. 1996; Simpson et al. 1993). They can also be used to identify areas where geochemical

and physicochemical parameters fall outside acceptable values (Simpson et al. 1993) and as a basis for environmental legislation and regulation (Van Den Oever 2000).

Although geochemical data continue to be collected for mineral exploration purposes, they can also be of value to mining companies especially in helping to understand the geochemistry of mineralised areas and define baseline levels of chemicals prior to their mining operations and as a basis for monitoring. Such geochemical datasets have been also shown to have a wide range of environmental applications. For example, in identifying acid mine drainage and the leaching of toxic metals from wastes (Simpson et al. 1993). It is important to collect such data in order to generate geochemical baselines for environmental and epidemiological applications, especially in developing countries (Plant et al. 1996) where most of these datasets are prepared for mineral exploration purposes and are owned by private companies and not available for public applications.

In this chapter we first discuss the concepts of geochemical background and geochemical baselines, the review of historical development of the terms. A range of potential applications of high quality geochemical datasets to environmental studies in mining districts are reviewed and the requirements for their implementation are discussed.

2.1.2 The concept behind the geochemical background and baselines

In developing a geochemical baseline, background concentration should be identified and defined, but how it is possible to be confident of what the background represents? First of all it is a requirement to understand the concept of geochemical backgrounds. 'Background' comes from exploration geochemistry and was defined by Hawkes and Webb in 1962 (in Reimann & Garrett 2005) as "the normal abundance of an element in

barren earth material", concluding "it is more realistic to view background as a range rather than an absolute value". This definition differentiates between elemental concentrations from an ore body which is known as an 'anomaly' if the signal exists. Hawkes and Webb (Hawkes & Webb 1962) state that a geochemical anomaly is a departure from the normal geochemical patterns for a given area or geochemical landscape. Hence, different geochemical anomalies exist for geochemically different areas and they can also operate at a different scale within a given area.

The term 'threshold' was introduced to differentiate between geochemical background and anomaly (Reimann & Garrett 2005). Traditionally an anomaly was considered a high value above the threshold, but now it is widely acknowledged that low values such as elemental deficiencies are also anomalies. A general definition from Garrett (Garrett 1991) states that "Threshold is the outer limit of background variation" which recognises upper and lower values when identifying anomalies (Reimann & Garrett 2005).

Usually the definitions of background in environmental sciences use adjectives such as 'natural' or pre-industrial. Although both of these terms suggest a pristine environment to the geochemical background values, reality is often much more complex and it can be difficult to distinguish the sources of the elements e.g. if hazardous chemicals are natural or manmade. The term 'ambient background' is used to describe the no longer pristine 'natural background' and it is recommended that it be used only when natural processes have been obscured (Reimann & Garrett 2005).

Humanity is part of the environment but things which affect adversely other types of organisms and ecosystems are generally considered as manmade pollution. Such pollution

spread widely around the world following the industrial revolution which began in Britain at the end of the 18th century but started with the Roman lead fabrication from the 1st to 3rd AD. Reimann and Garrett (2005) define background as "the elemental concentration(s) before industrialisation". The focus is now on finding appropriate methods to estimate pre-anthropogenic element levels such as isotopic and multi-element statistical procedures which could better discriminate between patterns of natural or anthropogenic origin (Reimann & Garrett 2005).

The term 'geochemical baseline' was first introduced formally in 1993 in the context of the IGCP 259 and 360 projects (Darnley et al. 1995), but it has never been well defined (Salminen & Tarvainen 1997). Although this term is used sometimes as equivalent to 'background', what it measures is 'ambient background' or elemental concentration levels at a particular date in order to be able to quantify future changes (Reimann & Garrett 2005). The main problem with the baseline concept is that it does not consider natural geochemical heterogeneity at the regional scale (Reimann & Garrett 2005). Moreover, Salminen and Tarvainen (1997) demonstrate baseline concentration depends on the sample material investigated, grain size and method used.

A more precise definition of the term 'geochemical baseline' is needed, especially when defining regulatory levels for political decision-making (Salminen & Tarvainen 1997). Natural variation should be taken into account, distinguishing for instance between regional and local baselines and separating them according to the different material sampled, the fraction analysed and the analytical method used (Reimann & Garrett 2005; Salminen & Tarvainen 1997). Salminen and Tarvainen (1997) propose a fluctuating geochemical surface as a baseline and calculate it as a median value ± one standard

deviation to take into account the variation of element in natural geological materials. Regulation levels should not be lower than natural variation, since important economic outcomes depend on these decisions (Reimann & Garrett 2005; Salminen & Tarvainen 1997).

In this study baseline values will be 'natural' background wherever it is possible to identify the pristine geochemical signatures and 'ambient' background where is not possible to differentiate natural from anthropogenic origin. The methodology to define the baseline is described in the Chapter 4.

2.1.3 Historical development of geochemical baselines

The first use of geochemical data (Johnson et al. 2005; Inacio et al. 2008) was for mineral exploration purposes. In the 1930s Russian geochemists (Fersman 1935) used stream sediments to identify secondary dispersion halos around ore deposits (Boyle & Garrett 1970); and by the 1940s stream sediment sampling was used for exploration worldwide as a result of the availability of cheap and fast spectrophotometric methods (Plant & Hale 1994). By the 1950s, authors such as Boyle and Hawkes, and Webb had begun to explore the applications of drainage geochemistry to regional geochemical mapping (Hawkes & Webb 1962; Boyle et al. 1968; Hawkes 1976).

Technical developments, especially during the Second World War (Plant & Hale 1994; Mukhopadhyay 2008), triggered the rapid development of geochemical methods, including developments in mass spectrometry, infra-red spectroscopy and nuclear magnetic resonance (Mukhopadhyay 2008). Advances in mass spectrometry allowed isotope hydrology to emerge as a key discipline (Edmunds 2009). All these advances

increased the analytical precision, sensitivity and resolution of the drainage geochemical data and decreased costs, increasing the feasibility of large-scale regional survey. For example in 1954, a two-year survey of 70,000 sq. km. of the Gaspé and New Brunswick regions of Canada based on 4,937 stream sediment samples was completed (Garrett et al. 2008).

The development of geochemical baselines at the national scale based on drainage systems started in the late 1960s, with the low-density sampling of stream sediments in Uganda undertaken by Reedman and Gould (Garrett et al. 2008), published as the Geochemical Atlas of Uganda (Uganda. Geological Survey and Mines Department & Reedman 1973). Similarly, in 1970 the British Geological Survey (BGS) began to prepare a high resolution systematic geochemical mapping of the UK (Johnson et al. 2005) known as the geochemical baselines survey of the environment (G-BASE). In 1979 a geochemical survey of China based on stream sediment samples commenced (Xie 1997) and in 1984 Shacklette and Boerngen (1984) produced a geochemical map of the USA, based on soil and drainage samples. In Scandinavia in the 1980s, the Geological Surveys of Norway, Sweden and Finland carried out and published a stream-based multi-media mapping project for the area north of 66°N which was based on diverse media such as moss, roots, groundwater, till, stream sediments, overbank sediments and stream water (Garrett et al. 2008).

Today, multi-element geochemical surveys continue to be prepared from the urban to continental scale using increasingly automated and highly sensitive multi-element analysis methods (Plant & Hale 1994), such as inductively coupled plasma emission spectrometry (ICP-ES) and mass spectrometry (ICP-MS) and X-ray fractionation (XRF).

Also computer aided data processing and geographical information system (GIS) based programs facilitate the interpretation of geochemical data and provide the most representative view of the geochemistry of a region (Darnley et al. 1995). Today's geochemical baselines are frequently multi-purpose (Thornton 2010) and are used to help in creating regulatory values, to monitor regulatory compliance and for scientific research (Garrett et al. 2008). The G-BASE programme of the BGS is an example of multi-element and multi-purpose geochemical surveying. It is based on stream sediment, stream water and soil data and is accessible via the internet.

In 1995, the International Geological Correlation Programme - IGCP (now the International Union of Geological Sciences - IUGS) stated that geochemical databases "should be considered an essential component of environmental knowledge" for the management of environmental and mineral resources (Darnley et al. 1995). In 1997 the Forum of European Geological Surveys (FOREGS) implemented these recommendations, harmonising national data to produce a European-wide geochemical baseline for assessment of contaminated land in "the context of variations in the natural geochemical background" (Plant 1997). Similarly, in China, geochemical mapping for environmental assessment has been underway since 2002 (Xie et al. 2008). In North America, a continental geochemical survey of soils was initiated between Canada, Mexico and the USA in 2005 for the assessment of contaminated land and other environmental risk assessment related to soil (Smith et al. 2006).

2.2 Applications of geochemical baselines to environmental research

Traditionally, applications of geochemical data have been focused on the identification of anomalies of ore and pathfinder elements for metal mineral deposits and their halos. For

example, anomalies of dissolved metals and pH are used as pathfinders for different mineral deposit types (Simpson et al. 1993). However, many economically viable mineralised outcrops have probably been discovered, and the focus has moved for example to identify mineral deposits covered with sedimentary deposits e.g. alluvial and lacustrine where undiscovered mineral deposits may lie (Cameron et al. 2004; de Caritat et al. 2009; Leybourne & Cameron 2010). Geochemical maps have been used in connection with geological mapping as a mineral exploration tool in developing countries, but covering mostly only mineral prospecting regions (Plant et al. 1996).

In response to the rising demand for minerals, more waste has been generated potentially damaging to the environment. Some large international mining companies have been working at high environmental standards in developing countries (Plant et al. 1996), but there is still significant pollution from small mining groups, especially in artisanal mining. In this context, geochemical baselines are necessary to determine regional pollution from industrial waste to the environment (e.g. acid mine drainage) (Simpson et al. 1993) and to assess environmental risk. At the small scale, geochemical monitoring based on waters around tailing dams and smelters are important in identifying leaks and pollution.

Exposure to potentially harmful concentration of specific chemical species e.g. of arsenic and lead in the environment may affect the health of animals and humans; consequently, they may have an effect on the food chain and human health. Research on element pathways and their effect on plant, animal and human health has been conducted using geochemical data (Simpson et al. 1993; Plant et al. 1996). On the other hand, some chemical elements are essential for agricultural production (Howarth & Thornton 1983)

e.g. boron, and for human health in trace amounts e.g. copper, iron and iodine (Plant et al. 1996; Phoon et al. 2012). This is most significant in developing countries where communities obtain their food from local agricultural activity (Plant et al. 1996). Areas at risk of trace element deficiencies or toxicity can be identified using geochemical baselines, and remediation carried out. Such applications are useful for both health and land use planning (Simpson et al. 1993).

The application of stream sediment geochemical data to fields such as health, agriculture and the environment is less direct than soil or water data. Even though, they provide regional patterns useful in identifying location and extent of areas where more detailed survey can be conducted by using other suitable media such as water, soil, air, lake or vegetation (Ottesen & Theobald 1994).

Water quality has been the focus of much research over centuries because water is vital for life. Geochemical baselines can also be used as the basis for comparison to determine areas where geochemical and physicochemical parameters lie outside acceptable values for irrigation, watering livestock and drinking water (Simpson et al. 1993).

The implementation of these applications for exploration and environmental risk assessment requires reliable and informative data for which good sampling plans and procedures are essential (Darnley et al. 1995). An orientation survey is recommended prior to sample collection to determine the strategic choices to be followed such as sampling media, analytical methods, sampling density, depending on the costs. Increasingly, standardised methods for different terrain types as advised by the IGCP are recommended (Hale 1994).

2.3 Sampling procedures to develop geochemical baselines

2.3.1 Sample density

The sample density used for geochemical mapping depends on the size of the area to be studied, its topography and geomorphology (Van Den Oever 2000) and the purpose of the study. Low-density geochemical maps (one sample per hundred to thousands of square kilometres) are suitable for identifying large-scale patterns of the distribution of chemical elements over the near surface of the Earth which might indicate large scale processes (Smith & Reimann 2008). High-density geochemical maps (one sample per one to tens of square kilometres) are more appropriate for mineral exploration or for local-scale environmental purposes such as identifying local pollution (Smith & Reimann 2008).

For national mapping programmes based on stream sediment and surface water samples, the IGCP recommends a density of 5 sample sites per 160 sq. km. using the internationally agreed sampling methods described in Darnley et al. (1995). In Plant (1997) the recommended sampling density is a minimum of 1 site per 100 sq. km. Geochemical surveys carried out by mining companies generally aim for higher resolution and this has many benefits for environmental risk assessments. Environmental risk analysis based on high resolution data (e.g. average 1 sample per 1.5 sq. km.) is useful because it includes small scale features such as mineral veins which are often overlooked in geologically focused sampling frameworks. Such density is used for example in the G-BASE programme in the UK, one sample per 1.5 to 2 sq. km. (Johnson et al. 2005).

2.3.2 Sample media

The sample media used in particular studies will depend on the purposes for which data are needed. Multi-purpose geochemical mapping must produce results which are comparable, representative and with a widespread application, while for specific purposes such as exploration media are chosen to maximise contrast between mineralised areas and background (Darnley et al. 1995). Drainage sample media include stream sediments and waters, and lake sediments. Stream sediments comprise a mixture of inorganic detrital material and clays, organic matter and chemical precipitates such as hydrous oxides of iron and manganese (Ottesen & Theobald 1994). Their chemical composition represents a close approximation to a composite sample of the products of weathering and erosion of soil and rock in the catchment area upstream (Howarth & Thornton 1983). Water consists of elements and compounds in solution as well as material in suspension, colloids, solid organic and inorganic debris; it can comprise surface water or groundwater. The chemical composition of water reflects different chemical processes between water and the environment through which it flows and depends on the solubility of mineral phases, the mobility of elements, and physicochemical properties of water and its environment such as the acidity (pH), reduction potential (Eh) and salinity (total dissolved solids or TDS) (Giblin 1994; Hale 1994).

Stream sediments and waters have distinctly different origins and properties which influence their suitability for particular surveys. Water samples are often preferred when highly soluble elements are sought (Hale 1994). Historically, stream sediment samples have been preferred for mineral exploration (Darnley et al. 1995). On the other hand, technological improvements in geochemical analysis have made water simpler and

cheaper to analyse than 30 years ago (Taufen 1997) which facilitate the use of water samples for the preparation of geochemical baselines.

The particular properties of stream sediments provide a mechanism for mapping regional geochemical characteristics of lithologies in large and different areas such as rain forest, desert, high mountainous range and arctic regions (Plant & Raiswell 1994). The distance that chemical elements can be detected away from their parental source depends mainly on the mobility of the element in water, the size fraction analysed, and the analytical method used. Hence, the logistics of collecting and analysing stream sediments depend on the aim of the research. For example, in gold exploration it has been demonstrated that finer sand fractions of the stream bed are enriched in heavy metals (Fletcher 1997), so that finer fraction are more suitable in this type of geochemical mapping.

Variations of chemical elements in stream sediments may occur naturally as a result of co-precipitation and adsorption of heavy metals on precipitated iron and manganese oxides for example Mn and In with Fe; Cd, Co, Fe and Tl with Mn; and Ag, As, Ba, Cu, Mo, Ni, Sr and Zn with both. This occurs when the Eh and pH of the groundwater are substantially lower than those of the stream waters (Howarth & Thornton 1983). In addition, precipitation of $CaCO_3$ in water can occur where calcareous rocks outcrop, diluting the concentration of other metals in the stream sediment samples (Howarth & Thornton 1983). The presence of organic matter and colloids may also affect the chemical element content (Howarth & Thornton 1983; Giblin 1994) for example mobile uranium can be absorbed in kaolinite, and hydrous ferric oxides on inert colloids (Giblin 1994).

The chemical element content in waters depends not only on the mobility of, but also the solubility of the parental mineral phase and the physicochemical properties of the water such as acidity (pH), reduction potential (Eh) and salinity (TDS) (Giblin 1994; Hale 1994). Geochemical mobility is dominated largely by three processes viz. element speciation in solution for example Cu can be present as free Cu^{2+} ion and/or as Cu-hydroxide ion complex or other species; precipitation of minerals, and surface sorption processes for example when solid surfaces are positively or negatively charged they can sorb anions or cations (Taufen 1997). Water composition can also vary over time but this can be minimised by systematic sampling, for example collecting water samples at the same time of the year to minimise the effects of seasonal variation (Simpson et al. 1993). Water samples may exhibit different geochemistry and expose different risks to human health and the environment than stream sediments which generally have less overall variation in physico-chemical properties than waters.

Groundwater can be used instead of surface water when this is not available depending on the geology such as the presence of fractured carbonates or in semi-arid or arid climate conditions (Giblin 1994), for example, in the extensive colluvial covered terrain in the Central Valley of Chile. Here there are significant copper, gold, silver and molybdenum deposits, but the average rainfall may be as low as <1 mm. Hence geochemical sampling for both exploration and environmental risk assessment requires the substitution of groundwater for surface waters to maintain systematic sampling. The TDS differences between ground and surface water must be taken into account in chemical analysis however.

2.3.3 Sampling procedures

A systematic sampling methodology must be used to obtain comparable samples. The sampling pattern must be achievable in terms of funds, site access, safety and security conditions (Darnley et al. 1995). International sampling protocol guides for a variety of sampling media have been published such as those prepared for the IGCP 259 (Darnley et al. 1995), for FOREGS (Salminen et al. 1998), and at national scale such as for G-BASE in the UK (Johnson et al. 2005).

Darnley et al (1995) recommend the collection of different sites or subsamples in each sampling location to identify multilevel analysis of variances. Site location for regional mapping is suggested at the outflow for catchments preferable not exceeding 100 sq. km. and for unreachable sampling sites the nearest basin should be used (Darnley et al. 1995; Salminen et al. 1998). Near roads and communities, sampling should be on the prevailing up-wind side to minimise anthropogenic contamination (Darnley et al. 1995). Samples are collected from second order or tributary streams, far upstream of its confluence with higher order drainage basins (Darnley et al. 1995; Salminen et al. 1998).

Surface water sampling sites depend on the drainage system and available access to it (Giblin 1994). Stream water samples are collected in midstream, below the surface, before the stream bed is disturbed and before other type of samples are collected such as stream sediments. Hardened Nalgene™ trace element free bottles (Salminen et al. 1998) and polypropylene containers (Darnley et al. 1995) are recommended and are thoroughly rinsed with the water to be sampled before the sample is collected (Darnley et al. 1995). Samples for element analysis should be filtered with 0.45 μm cellulose filter (Darnley et al. 1995; Johnson et al. 2005) with high surface areas such as capsule filters (Horowitz et

al. 1996). The latter reduces significant variations in the concentrations of some elements (Fe, Al, Cu, Zn, Pb, Co, and Ni) associated with filter systems caused mainly by the presence of colloids (Hall et al. 1996; Horowitz et al. 1996). A solution of nitric acid and potassium dichromate is recommended to preserve and stabilise the samples to be analysed for cations and mercury respectively. Samples collected for anion analysis should not be acidified. Electrical conductivity, pH and alkalinity are measured in the field; and meters should be calibrated every day before measurements are taken (Salminen et al. 1998). Samples should be kept in a cool unit (at 4°C) and sent to the laboratory as soon as possible after collection (Darnley et al. 1995; Salminen et al. 1998). Other general recommendations include systematic labelling and documentation, to follow international standards, avoiding contamination in all stages, the use of gloves (vinyl or latex), and removal of jewellery (Darnley et al. 1995).

2.4 Quality assurance and quality control of geochemical data

Errors in analytical data can lead not only to the generation of false anomalies but also to failure to identify real anomalies. Errors can be associated with sampling and/or analytical procedures and different methods have been developed to identify accuracy and precision based on the analysis of standards, replicates, blank samples and the use of randomisation (Miesch 1967; Plant et al. 1975; James & Radford 1980).

2.4.1 Evaluating reliability of data

Accuracy, from an analytical point of view, is the quality of being close to a value which is said to be true. Accuracy implies that the averages of a large number of estimates should be close to a ‘correct’ or reference value. The difference between that average and the ‘correct value’ is sometimes called bias (Miesch 1967). Certified reference materials

(CRM) are reproducible materials similar to the samples under analysis which have been thoroughly homogenised to have minimal sub-sampling variation; they are used to assess the accuracy of the analytical methods used and to calibrate equipment (Thompson 1997). The accuracy of the geochemical results of different surveys is essential for comparison (Plant et al. 1975).

Precision, from an analytical point of view, is the reproducibility of results and it is assessed by using sample duplicates and replicates collected in the field and during analysis. The variation is determined based on the analysis of standard deviations (Thompson & Howarth 1973) and on the variance (square of the standard deviation) of the logarithm of data when the distribution of the data is log-normal (Garrett 1969; Thompson & Howarth 1973; James & Radford 1980).

Blank samples comprise material similar to the samples being analysed but they have with negligible concentration of chemical elements compared with the survey samples. They are used to detect errors such as contamination during sample collection and analysis. Another quality control method is randomisation whereby randomising the numbered sequence in which samples are collected from the analytical order (Plant et al. 1975), this allows to distinguish systematic errors from the analytical and sampling procedures.

According to the internationally agreed protocol survey at a national scale, duplicate samples require to be collected from 3 per cent of sites, or at least on every 30^{th} site and CRM inserted at a similar frequency (Darnley et al. 1995). A blank sample, comprising deionised water, should be collected and filtered in the same way as an exploration water

sample every twenty samples (Salminen et al. 1998). In the BGS's G-BASE programme, 8 per cent of water samples submitted are for the control quality of analytical and sampling procedures (Johnson et al. 2005).

2.5 Current water guidelines and regulation values of environmental chemicals

Concern about chemicals in the environment that can adversely affect human health through the exposure to toxic substances has increased over the past decades. As a result guidelines for levels to which exposure poses a potential risk to human health and the environment have been set by health organisations and environment agencies worldwide. For example, international guidelines for permissible chemical concentrations in drinking-water have been developed by the World Health Organisation (WHO) and were first published in 1958 (WHO 2011b). Guidelines have been prepared also at the national scale for example in Canada for drinking water (Health Canada 2012) and for water and sediments to protect aquatic life (CCME 1999; CCME 2001).

Legislation for water quality standards has also developed not only for drinking water but also to protect the environment including surface freshwater, groundwater, estuaries and soil. Regulations have been enforced at the continental scale, for example the EU drinking-water directive (EC & European Commission 1998), and at the national scale such as those for drinking water in the US (EPA 2009). In Chile, the regulation of drinking water has applied since 1970 and was modified in 1984 and in 2005 (INN 2005) and for irrigation from 1978 (INN 1978) (Table 2.1).

Table 2.1: Total maximum concentration allowed for chemical species and compounds. Chilean regulation values for drinking (INN 2005) and irrigation water (INN 1978). Also shown are the WHO drinking-water guideline values (WHO 2011b) and the US (EPA 2009), and the European (EC & European Commission 1998) regulation values for drinking water for comparison. In parentheses are the cosmetic and aesthetic guideline values.

Chemical Specie	Drinking-Water – Health – (cosmetic/aesthetic)				Irrigation
	Chilean (mg/l)	US-EPA (mg/l)	EU (mg/l)	WHO (mg/l)	Chilean (mg/l)
Al	--	(0.05-0.2)	(0.2)	--	5
As	0.01	0.01	0.01	0.01P	0.1
Cd	0.01	0.005	0.005	0.003	0.01
Cl^-	(400)	(250)	(250)	--	200
Cu	2	(1)-1.3	2	2	0.2
EC	--	--	(2500)	--	750-7500
F^-	1.5	(2.0)-4.0	1.5	1.5	1.0
Fe	0.3	(0.3)	(0.2)	--	5.0
Pb	0.05	0.015	0.01	0.01P	5.0
Mg	125	--	--	--	--
Mn	0.1	(0.05)	(0.05)	(0.4)	0.2
Hg	0.001	0.002	0.001	0.006	0.001
Mo	--	--	--	--	0.01
Ni	--	--	0.02	0.07	0.2
NO_3^-	50	44	50	50	--
pH	(6.5-8.5)	(6.5-8.5)	(6.5-9.5)	--	5.5-9.0
TDS	(1500)	(500)	--	--	500-5000
Na	--	--	(200)	--	350
SO_4^{-2}	(500)	(250)	(250)	--	250
Zn	3	(5)	--	--	2.0

P: Provisional value.

In the area of this study in Central Chile, the government defined a programme to maintain and remediate the quality of the continental surficial waters at a national scale following the Chilean legislation for the environment, Law No. 19300 published in 1994; in the case of water quality in the Maipo Basin the draft regulation was first published for approval and public consultancy in 2004 (CONAMA 2004).

The draft regulation regarding the surface water quality of the Maipo Basin which has not been enacted yet is known as '*Anteproyecto de normas secundarias de calidad ambiental para la protección de las aguas continentales superficiales de la cuenca del Río Maipo*' (CONAMA 2004) which can be translated and understand as 'Preliminary environmental quality regulations to protect the surface continental waters of the Maipo River Basin'.

The regulated values are intended to establish allowable values for elements and substances among others which may pose a risk to the environment.

The regulated levels are derived from continuous monitoring and classification of the water catchment quality carried out by the Chilean supervisory entity DGA (Dirección General de Aguas) (DGA 2004b). Twenty three parameters are defined for 21 sub-basins of the Maipo Basin, of which 15 parameters including electrical conductivity (EC), dissolved oxygen (DO), pH, sodium absorption ratio (RAS), Al, As, Cl, Cr, Cu, Fe, Mn, Mo, Pb, SO_4, and Zn are also included in this research. The regulated values are defined by calculating the 66^{th} percentile of the data for each sub-basin.

2.6 Potentially toxic chemicals in the environment

Potentially toxic chemicals (PTCs) in the environment for the purpose of this study are those that in certain conditions, level of concentration and exposure can pose a hazard to human health and ecosystems. These chemicals can be released naturally from the weathering of rocks and sediments, but also human activities. In this context, the inorganic chemicals i.e. As, Cd, Cu, Hg, Ni, NO_3, P, Pb and S are included in this research (although organic chemicals are outside the scope of this research). In the following review of chemicals, trace elements are defined as those elements which are present at less than 0.1% (Rollinson 1993).

2.6.1 Arsenic

Arsenic is a trace element, the 53^{rd} most abundant of the 92 naturally occurring elements found in the Earth's crust with a median abundance of 1.7 mg/kg (Reimann et al. 2009). It is a metalloid found in the oxidation states of -3, 0, +3 and +5, occurring mainly as

sulphides, metal arsenides and arsenates (WHO 2011b), notably as arsenopyrite (FeAsS), realgar (AsS) and orpiment (As_2S_3), and frequently in other sulphides such as galena, pyrite and sphalerite (Plant et al. 2005). Arsenic has the highest concentrations (15 to 18 mg/kg) in shales and slates, and in some coals up to 3.5%, while it has much lower concentrations (0.83 µg/l) in natural waters (Table 2.2). All gold and copper deposits contain high concentrations of As (Pan et al. 2012). Significantly higher levels can be found locally in geothermal systems (Vaughan 2006) and hydrothermal alteration zones together with Au, Bi, Mo, Sb, Se and Te (Reimann et al. 2009). In stream waters arsenic is released under sufficiently low pH and Eh conditions in its trivalent form As^{3+}, otherwise As^{3+} is rapidly oxidised to its pentavalent form As^{+5} forming arsenate (AsO_4^{3-}) and mostly absorbed by hydrous Fe and Mn oxides, clays and organic matter (Pan et al. 2012). Dissolved As in river water has a global average of 0.83 µg/l (Vaughan 2006).

Table 2.2: World average chemical content in rocks and river sediments in mg/kg and in river waters in µg/l. References indicated as letter in brackets.

Rock/sediment/water	As [a]	Cd [b,c]	Cu [b]	Hg [c,d,e]	Pb [b,c]	Ni [b]	P [e]	S [e]
Andesite	2.7	0.09	-	0.015	35.1	-	-	-
Basalt	2.3	0.2	90	0.09	8	140	1200	900
Coal	0.3-35,000 (Range)	0.4	16	0.02-1 (Range)	15	17	150	20000
Evaporites	3.5	-	-	-	-	-	-	-
Granite	1.3	0.15	15	0.08	18	8	750	100
Limestone/dolomite	2.6	0.05	4	0.02	9	20	350	500
Sandstone	4.1	<0.03	2	0.03	10	2	30	200
Shale	15	1.4	50	0.4	23	68	800	1100
Slate/phyllite	18	-	-	-	-	-	-	-
River sediments	5	1.57	39	-	51	44	-	-
River water	0.83	0.08	1.5	0.05	0.08	2	20	400

a (Vaughan 2006); b (Callender 2003); c (Pan et al. 2012); d (Fitzgerald & Lamborg 2003); e (Reimann & de Caritat 1998)

Anthropogenic sources of arsenic released in the environment are associated with the use of pesticides, fungicides, herbicides, insecticides, animal-feed additives to stimulate growth, wood preservative which has been phased out in most countries, and also with the

glass and electronics industry (LEDs), metal treatment (alloys and bronze) and ammunition factories, in the production of dyes and colours, and in some pharmaceuticals (Reimann et al. 2009; Pan et al. 2012). Arsenic is also generated in mining, sulphide-ore roasting, as well as metal smelter and the burning of oil and coal (Reimann et al. 2009; Pan et al. 2012).

Arsenic is essential for some organisms including rats, sheep, and chickens, but it is toxic to humans (Pan et al. 2012). Humans can be exposed to As through air, food and water, more adverse effect are found after As exposure from drinking water however (Abernathy et al. 2003). Such effects in human health include gastroenteritis, nausea, vomiting, memory problems, neurological manifestations, vascular changes, diabetes, chronic As poisoning (arsenicosis), skin damage (melanosis) and cancers (skin, bladder, lung, liver, kidney and prostate) (Abernathy et al. 2003; Pan et al. 2012). Arsenic is highly toxic in the form of gas arsine (AsH_3), followed by arsenite (AsO_3^{3-}) and arsenate (AsO_4^{3-}) forms, both of which can be in solution (Vaughan 2006). Speciation plays an important role in the toxicity of As; when highly insoluble primary minerals such as metal arsenides and sulpharsenides break down in solution can form more soluble species such as oxides (Vaughan 2006). These can be converted enzymatically to the toxic As forms of methyl arsenic and dimethyl arsenic, in humans and other species (Abernathy et al. 2003). Arsenite can inhibit essential sulphydryl gropus of enzymes and proteins when it interacts with thiol groups and arsenate can replace inorganic phosphate in the production of adenosine triphosphate due to its similar structure (Pan et al. 2012). Methylation facilitate the excretion of inorganic arsenic from the body as methyl arsenic and dimethylarsenic can be identified in the urine of chronically exposed individuals (Abernathy et al. 2003;

WHO 2011b). In such cases the acute toxicity of As depends on the rate of its removal from the body (WHO 2011b).

Chronic As poisoning has been reported recently from at least 13 countries worldwide including Chile and Argentina which are known to have arsenic-rich regions where the high total concentrations of As in drinking water is a major health problem (O'Reilly et al. 2010; Campos et al. 2011; Pan et al. 2012). In a study of exposure to As in Chile, it was found that As concentrations in drinking water and urine were significantly higher in Antofagasta (north) than in Santiago (central) and Temuco (south) (Caceres et al. 2005). The main As source identified in the sediments and waters of the Rio Loa basin (north of Chile) is natural and related to the presence of volcanic rocks, hydrothermal ore deposits and geothermal waters in the Andes with anthropogenic sources such as smelters and mining waste representing additional minor sources (Romero et al. 2003). Arsenic removal from drinking water in Antofagasta started in 1970 and by 1995 the As average had been reduced from 860 to 40 µg/l (Caceres et al. 2005).

2.6.2 Cadmium

Cadmium is a rare element, the 67th most abundant in the Earth's crust with an average abundance of 0.1 mg/kg (Callender 2003). It is a chalcophile heavy metal with an oxidation state of +2 (Reimann & de Caritat 1998) and is strongly associated with sulphides rather than oxides (WHO 2011a). Typical Cd minerals include greenockite (CdS), octavite ($CdCO_3$), and monteponite (CdO) (Reimann & de Caritat 1998) but as its geochemistry is similar to zinc, is commonly associated with Zn in mineral deposits and other geological materials (Callender 2003). Cadmium occurs in lower concentrations (<0.03 to 0.2 mg/kg) in sandstones, basalts and granites and in higher concentrations (1.4

to 1.57 mg/kg) in shales and some stream sediments (Table 2.2), and in phosphorites (Pan et al. 2012). In natural aerobic fresh waters is found mostly as Cd^{2+} with pH <8 under oxidising conditions, as solid phases such as carbonate ($CdCO_3$) and hydroxide ($Cd(OH)_2$) with pH 8 to 13 and as sulphide (CdS) under reducing conditions (Callender 2003; Pan et al. 2012). It can also bound to organic matter, co-precipitate with hydrous oxides of Mn and possibly Fe, form complexes with in solution with halides (Ackerman et al. 1979), cyanides and ammonium species (Pan et al. 2012). Dissolved Cd in river water has a global average of 0.08 μg/l (Callender 2003).

Anthropogenic sources of Cd include old Pb and Zn mines and Zn smelters producing Cd as a by-product, phosphate fertilisers, sewage sludge, coal combustion, waste from cement manufacture, metallurgical work and waste incineration (Reimann & de Caritat 1998; Emsley 2011; Pan et al. 2012). Most of the historical uses of Cd such as pigment in paint, rubber, plastics, printing inks, and vitreous enamels have been phased out, and even fast-rechargeable light-weight Ni-Cd batteries are being phased out in favour of Ni metal hydride batteries (Emsley 2011; Pan et al. 2012). Cadmium is still used to protect steel in the aerospace, mining and off-shore oil industries, and in some nuclear reactors (Emsley 2011).

Cadmium is absorbed by humans by respiratory, oral and dermal exposure (Pan et al. 2012). It is absorbed by some food crops such as rice, lettuce, spinach, and turnip, and fish and shell-fish, and also grass on contaminated land grazed by animals (Emsley 2011). Smoking also increases Cd exposure because tobacco plants absorb it from contaminated land (WHO 2011a; Emsley 2011). Cadmium is toxic and cumulative and damages human health because it can replace the essential element Zn as well as Ca and Mg particularly in

those systems containing soft ligands (Pan et al. 2012). It can cause severe damage to human and animal organs including the kidney, lungs and liver. It can bind strongly to kidney tissue and tends to accumulate there and remain for up to 30 years (Emsley 2011); it is also stored in the liver (WHO 2011a) while it is slowly excreted in urine and faeces (Pan et al. 2012). Many effects on the endocrine system have been reported (Iavicoli et al. 2009) and chronic Cd poisoning can lead to Itai-Itai disease an extremely powerful form of osteoporosis (Emsley 2011; Pan et al. 2012). Other effects of acute exposure to Cd include severe abdominal pain, nausea, vomiting, diarrhoea, headache, vertigo and can lead to death (Pan et al. 2012). Other effects of chronic exposure anaemia, tooth discoloration and loss of sense of smell (Pan et al. 2012). There is some evidence of increased lung cancer risk as a result of Cd exposure (WHO 2011a), but this is controversial (Emsley 2011; WHO 2011a).

2.6.3 Copper

Copper is a trace element, the 26th most abundant element in the Earth's crust with an average abundance of 50 mg/kg (Emsley 2011). It is a chalcophile heavy metal with main oxidation states of +2, +1 and 0 (Reimann & de Caritat 1998). Typical minerals include chalcopyrite ($CuFeS_2$), bornite (Cu_5FeS_4), chalcosite (Cu_2S), covellite (CuS), malachite ($Cu_2CO_3(OH)_2$), azurite ($2CuCO_3.Cu(OH)_2$), chrysocolla ($CuSiO_3.2H_2O$) and native Cu which are found in sulphide ore deposits and the associated weathering products (Reimann & de Caritat 1998; Phoon et al. 2012). Copper concentrations are lower (2 to 4 mg/kg) in sandstones, limestones and dolomite, and higher (39 to 90 mg/kg) in stream sediments, shales and basalts (Table 2.2). In aqueous solution the most stable state is Cu^{2+} (Emsley 2011) but carbonates ($Cu(CO_3)_2^{2-}$ and $CuCO_3$) also important in river waters, being the later complex the most important near neutral pH, and at pH>8 the dihydroxo-

Cu(II) predominates (Callender 2003). The speciation of Cu is critical in geochemical and biological processes. In oxidising environments, Cu is more soluble under acid conditions while in reducing environments Cu solubility is decreased greatly and the most stable phase is Cu_2S (Callender 2003). Dissolved Cu in river water has a global average of 1.5 µg/l (Table 2.2).

Copper has been refined as a source of metal for thousands of years (Emsley 2011), with smelters being the major source of Cu pollution in the past. Currently, anthropogenic sources of Cu include fossil fuels burning and waste incineration, the application of sewage sludge, municipal compost, pig and poultry wastes to the land surface (Callender 2003). Copper is used in the electrical industry, and for water piping, alloys, coins, algaecide, bactericide, molluscicide, fungicide and insecticide (Reimann & de Caritat 1998). Copper sulphate is used to fertilise Cu-deficient soils usually overdosing the amount needed (Emsley 2011).

Copper can be obtained in some food, in drinking-water from the corrosion of Cu-pipes which increases in standing systems (WHO 2011b) and by inhalation usually occupational but also through smoking (Phoon et al. 2012). Copper is essential to all species involving many Cu-containing enzymes (Emsley 2011) but it is also considered a drinking-water contaminant (WHO 2011b; Reimann & de Caritat 1998). Copper toxicity depends on its concentration, speciation, route of exposure, bioavailability and the biological specie for example it is toxic to sheep, goats, marine invertebrates, many algae, bacteria and fungal spores but humans and pigs are less sensitive (Phoon et al. 2012). It is argued that Cu can displace Fe and Zn in the body when too much is consumed (Emsley 2011) and oppositely excessive Zn intake could cause low-Cu levels (Phoon et al. 2012).

Copper deficiency is rare in humans (Phoon et al. 2012), but low-Cu diets have been found to increase levels of cholesterol, blood pressure, the ability to digest glucose (Emsley 2011), anaemia and neurodegeneration (Phoon et al. 2012). Wilson's and Menke's diseases which are genetic are caused by the inability to use copper properly. The toxicity of Cu salts such as copper sulphate occurs when free-radicals cascades are generated by the reduction of Cu^{2+} to Cu^{+} (Phoon et al. 2012). The effects of Cu overdose include vomiting but copper sulphate in solution has been linked with some suicidal cases and survivors presented major damage in the kidneys and brain (Emsley 2011). Others effects reported of Cu toxicity include childhood cirrhosis, renal damage, fibrosis in lungs and there is some evidence of increased risk of heart disease (Phoon et al. 2012).

2.6.4 Mercury

Mercury is a trace element, the 68th most abundant element in the Earth's crust with an average abundance of 50 μg/kg (Emsley 2011). It is a chalcophile heavy metal with the principal oxidation states of +3, +2, +1 and 0 and typical minerals include cinnabar (HgS) and native Hg (Reimann & de Caritat 1998). Elemental Hg is found as inclusions in HgS in ore minerals such as sphalerite and chalcopyrite, with concentrations of up to 35% Hg in sphalerite. Mercury is mobilised tectonically, and important deposits occur in mineralised areas associated with subduction zones and deep-focus earthquakes (Fitzgerald & Lamborg 2003). Mercury has a high affinity for organic carbon and is often found in coal (Pan et al. 2012) and in sedimentary material rich in organic carbon such as black shales (0.4 mg/kg) (Table 2.2). Cinnabar under typical surface water conditions is only sparingly soluble, and its mobility usually involves sediment transport. The solubility of HgS is controlled by pH, temperature, chloride, sulphide and organic carbon content (Fitzgerald & Lamborg 2003). Mercury species in natural waters include

elemental Hg, ionic Hg (Hg^{+} and Hg^{2+}), methylated mercury including monomethylmercury (CH_3Hg^{+}) and dimethylmercury ($(CH_3)_2Hg$), and also Hg complexes with organic material via sulphide groups which affect its bioaccessibility in the aquatic environment (Ravichandran 2004). In oxidising acid conditions the ionic forms of Hg are predominant, but elemental Hg predominates under most pH-Eh conditions in media not in equilibrium with surface air and water so that it remains in stream sediments for many years (Pan et al. 2012). Dissolved Hg in river water has a world average of 0.05 μg/l (Table 2.2). Low-temperature volatilization from soils and mineralised areas also contribute Hg in the atmosphere (Fitzgerald & Lamborg 2003). Natural inputs of mercury to the surface environment are mainly from volcanoes, soil erosion, and microbial release of organo-mercury compounds (Emsley 2011).

Mercury emissions from human activities now dominate the cycle, providing most of the Hg in the atmosphere and surface ocean (Fitzgerald & Lamborg 2003). The global Hg cycle is similar to that of carbon (Pan et al. 2012). The primary source of pollutant mercury on a global scale is Hg emissions from fossil-fuel burning especially of coal and high-temperature combustion processes such as waste incineration (Fitzgerald & Lamborg 2003) where Hg is released mainly from discarded batteries and fluorescent light tubes (Emsley 2011), as well as mining and smelting (Pan et al. 2012). Mercury has been widely used as a laxative, antiseptic, antibacterial, bactericide and red pigment (Emsley 2011), and also in thermometers, barometers, diffusion pumps, Hg-vapour lamps, low-energy light bulbs and advertising signs (Pan et al. 2012). It is still used as a preservative in some vaccines such as the influenza vaccine (Pan et al. 2012) and in alloys such as Hg-Ag amalgams in teeth filling (Emsley 2011; WHO 2011b; Pan et al. 2012).

Low levels of mercury are also released from crematoria because of the incineration of teeth fillings (Emsley 2011).

The main human health concern is from exposure to the highly neurotoxic monomethylmercury (MMHg) which is almost entirely from the consumption of fish and fish products (Fitzgerald & Lamborg 2003). Food is the principal source of Hg exposure in non-occupational populations (WHO 2011b). All Hg compounds are toxic, but their toxicity depends on the Hg species, with MMHg being extremely toxic and Hg^{+} less toxic than Hg^{2+} because the former is less soluble (Emsley 2011). Mercury cations have an affinity for S which causes its interaction with biological ligands. Mercury can bind with sulph-hydryl and disulphide groups in amino acids inactivating S blocking enzymes, cofactors and hormones (Pan et al. 2012). Metallic Hg can dissolve in fatty compounds and even though is not readily taken up by organisms it exists as a vapour at room temperature and can cause intoxication through inhalation (Pan et al. 2012). It is absorbed through the lungs, skin and digestive tract (Emsley 2011) and is accumulated at higher levels in the kidneys than in the brain or liver (Pan et al. 2012). Acute exposure to Hg can cause appetite loss, headaches, fever, irritability, fatigue and vomiting, while chronic exposure to Hg can cause paralysis, memory loss, impaired physical coordination, chromosome damage, mutagenesis, cancer and death (Pan et al. 2012).

2.6.5 Lead

Lead is a trace element, the 36th most abundant element in the Earth's crust with an average abundance of 14 mg/kg (Emsley 2011). It is a chalcophile heavy metal with the principal oxidation states of +2 and +4. Typical minerals include galena (PbS), anglesite ($PbSO_4$), cerussite ($PbCO_3$) and minium (Pb_3O_4) which are ore minerals (Reimann & de

Caritat 1998; Pan et al. 2012) and pyromorphite ($Pb_5(PO_4)_3Cl$) which is very stable in the surface environment (Cotter-Howells 1996). Lead concentrations are lower (8 to 10 mg/kg) in basalts, limestones, dolomite and sandstones, than (18 to 51 mg/kg) in granites, andesites and stream sediments (Table 2.2). The major producers of Zn and Pb are sedimentary exhalative deposits which normally have distinctive isotopic signature that can be used to differentiate them from other sources of Pb in the environment (Pan et al. 2012). In aquatic environments, under acid conditions, lead is present mostly as Pb^{2+} and as complexes with carbonates, hydroxides and organic ligands (Pan et al. 2012). Lead nitrates, acetate and chlorides are significantly more soluble than Pb sulphides, sulphates, carbonates, phosphates and oxides (Pan et al. 2012). The carbonate species $Pb(CO_3)_2^{-2}$ are stable in the pH range 6 to 8, sulphates $PbSO_4$ below pH 6 and hydroxyls $Pb(OH)_2$ are stable above pH 8 (Callender 2003). The average concentration in global river water is 0.08 µg/l (Callender 2003). Natural lead sources in the atmosphere include wind-blown dust, forest fires and volcanoes (Pan et al. 2012).

In the case of anthropogenic sources of lead, vehicle emissions were an important source of Pb in the environment until 1986 when regulations were introduced to ban tetraethyl lead in petrol in most states of the USA (Pan et al. 2012) and in 2000 in the EU (European Commission 1998; European Commission 2003). It is also released as a result of Cu-Zn-Pb smelting, from battery factories, in sewage sludge, and from coal combustion and waste incineration (Callender 2003). Lead has been mined for more than 6,000 years but many of its traditional uses were banned in the last century (Emsley 2011; Pan et al. 2012) such as the use of white-lead interior paint in 1909 in France, Belgium and Austria and 1978 in the USA. It has been used as a pigment for paints and cosmetics, insecticide, as the additive tetraethyl lead in petrol, and lead acetate in hair dye (Emsley 2011). Lead

is still used for lead-acid batteries in cars, pigments, ammunition, metal alloys, solder, cable sheathing, weights for lifting, weight belts for diving, protective clothing to shield against radiation, in crystal and stained glass, tiling and plastic lining to block noise, as an anticorrosive in the chemical industry, in semiconductors, roof cladding, water pipes, cisterns, pewter and antiknock containers (Emsley 2011; Pan et al. 2012). Lead corrosion is of particular concern and is increased in waters with low pH. Concentrations of Pb also increases with the standing time of water in lead pipes (WHO 2011b).

Human uptake of lead occurs through respiratory, oral and dermal pathways, with oral exposure (ingestion of food and drink) being the most important (Pan et al. 2012). Studies in the UK showed that the major sources of Pb in housedust are paint, road dust, industry and soil which was demonstrated to be an important direct route of lead exposure for children via their hands (Thornton et al. 1994). Lead is highly toxic and can affect all human organs, accumulating in tissue independently of the route of exposure (Pan et al. 2012). Lead binds usually to proteins in red blood cells, but can also accumulate in bone (as lead phosphate) over a life time which is useful for monitoring human exposure (ATSDR 2007b; Emsley 2011). In the blood, Pb deactivates enzymes that make haemoglobin resulting in the build-up of aminolevulinic acid which causes a range of adverse health effects (Emsley 2011). Acute exposure to Pb causes anorexia, dyspepsia, weakness in fingers, wrists or ankles, and constipation, while chronic exposure causes neuropathies, memory loss, a reduced intelligence quotient, anaemia, hypertension, haematological effects, renal diseases, seizures, ataxia (failure of muscular coordination), reduced male fertility, growth problems in infants, coma and death (Pan et al. 2012). Other adverse effects of Pb on the endocrine systems of human and rats have been reported (Iavicoli et al. 2009).

2.6.6 Nickel

Nickel is a trace element, the 23rd most abundant element in the Earth's crust with an average abundance of 80 mg/kg (Emsley 2011). It is a chalcophile heavy metal with the principal oxidation states of +4, +3, +2, +1, 0 and -1, but the majority of Ni compounds are of +2 (Callender 2003). Typical minerals include nickeline (NiAs), gersorffite (NiAsS), pentlandite ($(Fe,Ni)_9S_8$), Ni-pyrrhotite ($Fe_{1-x}S$, up to 5% Ni), kullerudite ($NiSe_2$), ullmanite (NiSbS), polydymite (Ni_3S_4) and garnierite ($(Ni,Mg)_3Si_2O_5(OH)_4$) (Reimann & de Caritat 1998). The ion Ni^{+2} substitutes for Fe_{+2} and Mg^{+2} during fractionation because of its similar ionic radius and valency and it partitionates into ferromagnesian minerals such as olivine, so that it is enriched in mafic rocks rather than felsic rocks (FOREGS 2005). Nickel has lower concentrations (2 to 8 mg/kg) in sandstones and granites than (68 to 140 mg/kg) in shale and basalts, and a global Ni concentration of 44 mg/kg in stream sediments (Table 2.2). Nickel ore deposits include sulphides, principally pentlandite and pyrrhotite, and laterites formed by the weathering of ferromagnesium silicate rocks in humid regions (WHO 1991b). It is also found in significant amounts in pyrites and chalcopyrites and concentrations may correlate usually with those of Cu in sulphide-rich rocks (FOREGS 2005). In aerobic natural waters, Ni exists predominantly as Ni^{2+} in the pH range 7 to 9, but other complexes are formed (OH^- > SO_4^{2-} > Cl^- > NH_3). In anaerobic conditions its solubility is controlled by sulphide (Callender 2003). Nickel can also occur coating particles as well as associated with organic matter (WHO 1991b). The average concentration of Ni in global river water is 0.8 µg/l (Callender 2003). Nickel natural sources in the atmosphere are dominated by wind-blown dust (Callender 2003).

Anthropogenic sources of nickel include steel works, fertilisers, metal plating and coinage, fossil-fuel combustion and detergents (Reimann & de Caritat 1998), and also waste incineration (Callender 2003), pesticides and sewage sludge (WHO 1991b). Nickel is used in more than 3,000 known alloys including with Co, Fe, Mn, Mo, Ti and Zn, and also in plating and electroplating, Ni-Cd batteries, pigments and as a catalyst in hydrogenating vegetable oil such as in margarine production and in magnetic tapes (Callender 2003; Emsley 2011).

The dominant source of Ni exposure is food such as beans and tea (Emsley 2011; WHO 2011b). Water makes a minor contribution to exposure generally in the non-smoking, non-occupationally exposed population (WHO 2011b). Nickel is considered both essential and toxic depending on its concentration, speciation and bioavailability. It is essential to some species and related to growth, in humans it may be essential in concentrations as low as 5 µg per day (Emsley 2011) and it has been regarded as essential for human metabolism (FOREGS 2005). The toxicity of Ni depends on speciation, individual sensitivity, and the exposure pathway with inhalation and dermal exposure being of most concern. Nickel carbonyl ($Ni(CO)_4$) which is generated during Ni refining processes is the most acutely toxic Ni compound but exposure is occupational (Barceloux 1999; Haber et al. 2000). In the blood stream Ni can bind to the protein albumin (Emsley 2011). It can deposit in the upper and lower respiratory tract and in the lungs (ATSDR 2005). Nickel tends to accumulate in the lungs, liver, and kidneys, but excess Ni is excreted in urine (Emsley 2011) and faeces (Benson et al. 1994). Most Ni^{2+} is relatively non-toxic but some compounds can cause dermatitis, gastric irritation and cancer at high concentrations (WHO 1991a; Emsley 2011). Breathing Ni dust can cause lung and nasal cancer and the inhalation of Ni carbonyl vapour, even in small amounts, can cause death

(Emsley 2011). Nickel is thought to cause cancer by substituting for Zn and Mg atoms in DNA polymerase (Emsley 2011). Acute exposure to Ni causes nausea, vomiting, headaches, abdominal pains, weakness, tachycardia and coughs, death may occur following cerebral oedema (Webster et al. 1980; Barceloux 1999). Chronic exposure to Ni causes contact dermatitis, respiratory illness such as asthma, nasal polyposis (Barceloux 1999), and renal impairment (Vyskocil et al. 1994). The harmful effects of Ni can be exacerbated by interaction with other chemicals such as with benzo(a)pyrene present in cigarette smoke which enhances respiratory carcinogenisis (Sunderman 1973).

2.6.7 Nitrate

Nitrate (NO_3^-) is a naturally occurring inorganic nitrogen species. It is the stable form of combined nitrogen for oxygenated systems (WHO 2011c) and it takes part of the nitrogen (N) cycle along with nitrite (NO_2^-), ammonium (NH_4^+). Nitrogen is the 30th most abundant element in the Earth crust with an average abundance of 25 mg/kg, while oxygen is the most abundant element with 47% average abundance (Emsley 2011). Typical nitrate minerals include nitre (KNO_3) and soda-nitre ($NaNO_3$) (Reimann & de Caritat 1998) but nitrate-containing compounds are generally highly soluble and migrate readily into surface and groundwater (ATSDR 2007a). Speciation of N in surface water depends on pH, temperature and oxygen availability. Between 60 and 95% of the total dissolved N in fresh waters constitutes nitrate, but under anoxic conditions NH_4^+ predominates (FOREGS 2005). Chemical and biological processes can reduce nitrite to various compounds or oxidise it to nitrate (WHO 2011c).

Anthropogenic sources of nitrate include agricultural fertilisers, sewage, manure, and explosives, and also nitrogen oxides from the combustion of fossil fuels (FOREGS 2005;

WHO 2011c). Purified potassium nitrate is used for glass making and as a food preservative as well as sodium nitrite, especially in cured meats (WHO 2011c). Common inorganic fertilisers include potassium nitrate and ammonium nitrate which are produced from the fixation of atmospheric nitrogen (N_2) (Kendall 1998). Sewage sludge (biosolids) produced through the treatment of municipal waste water, is used as agricultural fertiliser as well as for reclaiming mined land (EPA 2002). Fertilisers produced by fixation of N_2 have a $\delta^{15}N$ composition of 0±3‰ Air (Macko & Ostrom 1994; Kendall 1998), while organic fertilisers produced from manure are characterised by $\delta^{15}N$ values in the range 10‰ to 25‰ Air (Kendall 1998). Ammonium nitrate fuel oil (ANFO) is used as a commercial blasting agent and in pH-regulating chemicals (Awadalla et al. 1994). Nitrates are also found in nitrous gases used in the welding industry as well as solute ammonium nitrate in cold packs (ATSDR 2007a).

Nitrate is an essential macronutrient for plant growth and is essential to all living organisms (Reimann & de Caritat 1998; FOREGS 2005). High concentrations of nitrate can have adverse effects on ecosystems and human health however. In many agricultural and industrial areas, the environment can become enriched in nitrate and regulated levels exceeded (WHO 2011c). Nitrate is not readily absorbed into sediments and after plant requirements are met, any excess is leached into surface and groundwater (FOREGS 2005). This excess together with high concentrations of phosphorous (P) can cause extensive environmental damage such as eutrophication of the aqueous environments (Edmunds 2009).

In humans, nitrates can be absorbed through inhalation, the skin and ingestion of food and drink (ATSDR 2007a; WHO 2011b), and vegetables and meat are the most important

sources (WHO 2011b). The bacteria in the saliva and stomach can reduce nitrate to nitrite, which can cause acute health disorders including methaemoglobinaemia and blue-baby syndrome (Knobeloch et al. 2000): the most affected population being bottle-fed infants (WHO 2011b). Methaemoglobinaemia resulting from acute toxicity to nitrate is one of the most commonly recognised health effects of excess nitrate and nitrite ingestion (ATSDR 2007a). Chronic nitrate exposure may be associated with carcinogenesis including non-Hodgkin's lymphoma (Ward et al. 1996; Richardson et al. 2008), stomach cancer, brain cancer (Berleur & Cordier 1995; Barrett et al. 1998), and cancers of the oesophagus, bladder and prostate (ATSDR 2007a). Studies to identify a specific causal link between cancer and nitrate exposure have been inconclusive however. The carcinogenicity of nitrate has been suggested to be related to its ability to react with amino acids to form nitrosamines cause cancer in animals (ATSDR 2007a). Other suggested impacts of chronic nitrate exposure include diabetes (Parslow et al. 1997), cardiovascular disorders (Klock 1975), reproductive problems, developmental problems, thyroid disorders and respiratory infections (ATSDR 2007a). Documented symptoms in workers include drowsiness, palpitations, headache, paresthesia, vertigo, anorexia, nausea, abdominal pain, dyspnea, vomiting and polyuria (ATSDR, 2007).

2.6.8 Phosphorus

Phosphorus is the 11th most abundant element in the Earth's crust with an average abundance of 1,000 mg/kg (Emsley 2011). It is a biophile, lithophile and siderophile light non-metal with main oxidation states of -3, +3, +4 and +5 and typical minerals are apatite ($Ca_5(PO_4,CO_3)_3(F,OH,Cl)$), monazite ($(Ce,La,Nd,Th,Sm)(PO_4,SiO_4)$) and xenotime ($YPO_4$) (Reimann & de Caritat 1998). In nature, it is never found as the element itself, always as phosphate (Emsley 2011) and it occurs mainly as orthophosphate (PO_4^{3-}). It is a

major constituent in all plants, but it is also widely found in biological material such as bone and at trace levels in minerals including olivine, pyroxene, amphibole and mica (FOREGS 2005). Phosphorus has lower concentrations (30 to 350 mg/kg) in sandstones, coal and limestone than (750 to 1200 mg/kg) in granite, shale and basalt (Table 2.2). The weathering of P-bearing minerals mostly depends on two main factors the adsorption of phosphate on clays, and the solubility of apatite and Fe-Al phosphate. Apatite is highly soluble under acid conditions and the presence of Ca^{2+} and forms HPO_4^{2-} and $H_2PO_4^-$ ions by the reaction of H+ with PO_4^{3-} (Smith et al. 1977; Ayers & Watson 1991). Aluminium and Fe phosphate are soluble in very acid environments only (pH<3). In natural water systems the main oxidation state is P^{5+} and depending on the pH it occurs as PO_4^{3-} (under alkaline conditions), HPO_4^{2-} (circum-neutral pH) or H_2PO^{4-} (between pH 4 and 6) (FOREGS 2005). Other species of P in water include inorganic polyphosphate and organic P compounds (FOREGS 2005). The average concentration of P in global river water is 20 µg/l (Reimann & de Caritat 1998).

Anthropogenic sources of phosphorus include detergents, fertilisers, chemical industry, military (explosives and warfare chemicals), pyrotechnics, semiconductors, insecticide, herbicide, fungicide and matches (Reimann & de Caritat 1998). Phosphate rocks are processed mainly by converting the phosphate to phosphoric acid (H_3PO_4) using sulphuric acid. Purified H_3PO_4 is also used to make food additives, animal feed supplements, surface cleaners and dishwasher powders, while lower grade H_3PO_4 is used as anti-corrosive and rust-remover in metals (Emsley 2011). Waste water contains complex phosphates, such as those used in detergents, which are unstable in water and are slowly hydrolysed to orthophosphate (FOREGS 2005). High concentrations of P in waters have been widely reported in agricultural areas where fertilisers are applied, but

the contribution from other sources also increase the levels of P; such was the case reported for England and Wales where sewage treatment works increased the concentration of P in large rivers (Muscutt & Withers 1996). Phosphorous is also used in the production of phosphate ester flame retardants which are added to consumer and industrial products for the purpose of reducing flammability, such as in plasticisers, hydraulic fluids, solvents, extraction agents, antifoam agents, and coating for electronics (ATSDR 2012). Other uses of P in manmade products include, sodium lamps, ceramics, leather tanning, water softener, dye manufacture and toothpaste (Emsley 2011).

Phosphorus is considered an essential element for all organisms, but it is toxic at high doses of the element or oxide (FOREGS 2005); 60 to 100 mg of P is lethal to humans (Reimann & de Caritat 1998). Phosphate is an important plant nutrient but its excessive use in agriculture, together with nitrate, and detergents lead to eutrophication and algal blooms in stream waters and lakes where the surface run off from fields end (FOREGS 2005). These algal blooms can lead to the excessive growth of cyanobacterial biomass, their toxins can reach concentrations in water that are potentially hazardous to human health (WHO 2011b). The phosphate ester flame retardants (PEFR) are considered an emerging pollutant, they are poorly soluble in water but adsorb strongly to soil and biodegrade in aquatic and terrestrial environments. The most common route of exposure to PEFRs is by eating contaminated food, but they can also leak from plastic into drinking water, they can contaminate air from plastics, adhesives, foams, electronics and hydraulic fluid. Limited data are available to determine health effects in humans, but studies in animals have shown damage in developing organs, the liver, kidneys and urinary systems (ATSDR 2012). Phosphine (PH_3) and elemental P_4 are very toxic to fish (FOREGS 2005).

2.6.9 Sulphur

Sulphur is the 17th most abundant element in the Earth's crust with an average abundance of 260 mg/kg (Emsley 2011). It is a biophile and chalcophile light non-metal with main oxidation states of -2, 0, +2, +4 and +6. It has four naturally occurring stable isotopes (^{32}S, ^{33}S, ^{34}S, and ^{36}S) of which ^{32}S is the most abundant (Reimann & de Caritat 1998). Typical minerals are native sulphur (S), pyrite (FeS_2), galena (PbS), sphalenite (ZnS), and other sulphides, gypsum ($CaSO_4 \bullet 2H_2O$), anhydrite ($CaSO_4$) and other sulphates (Reimann & de Caritat 1998). Sulphur has lower concentrations (100 to 500 mg/kg) in granite, sandstones, and limestone than (900 to 1100 mg/kg) in basalt and shale, and the very high concentration of 20000 mg/kg in coal (Table 2.2). Evaporite deposits, including gypsum and anhydrite, generally have approximately 20% of sulphur. In igneous rocks, the most important occurrence of S is in metal sulphide mineralisation (FOREGS 2005). Iron pyrite and other insoluble compounds precipitate into sediments and are eventually cycled into sedimentary rocks (Charlson et al. 2000).

Sulphur in soils occurs mainly as a component of organic matter, but many S compounds may be present, especially in sub-humid or arid environments. Sulphate minerals are found in aerobic environments while sulphides are usually restricted to anaerobic soils (Fanning & Burch 2001). Metal sulphates of Fe, Al, and Ca, can occur under oxidising soil conditions. They are readily soluble and are therefore greatly involved in soil equilibrium processes, and available to plants (Kabata-Pendias 2011). Dissolved sulphate ions (SO_4^{2-}) are the most important S species in the stream waters and the behaviour depends significantly on the redox state. Under acid conditions (pH<4), sulphuric acid is not completely dissociated and some HSO_4^- may be present. In very reducing conditions, hydrogen sulphide (H_2S) can be significant (FOREGS 2005). The H_2S gas has the

characteristic odour of rotten eggs and is released from crude petroleum, natural gas, volcanic gases, hot springs and as a result of bacterial breakdown of organic matter (ATSDR 2006). Micro-organisms can affect the oxidation state of sulphur, capable of either oxidation or reduction depending on microbial species and environment (Kabata-Pendias & Pendias 2001). Systems controlled by gypsum usually contain no more than 1500 mg/l SO_4^{2-} and 650 mg/l Ca, but can result in oversaturation with respect to gypsum due to the tendency of SO_4^{2-} to form neutrally charged ion-pair associations (FOREGS 2005). The average concentration in global river water is 400 µg/l (Reimann & de Caritat 1998).

Anthropogenic sources of sulphur include chemical and rubber industries, matches, fungicide, pharmacy and gunpowder (Reimann & de Caritat 1998). Sulphates are discharged into waters in wastes from industries that use sulphates and sulphuric acid, such as mining and smelting operations, kraft pulp, and paper mills, textile mills and tanneries may contain H_2S. Other sources include the use and production of fertilisers and pesticides, coal combustion, petrol refining, and vulcanisation of rubber (FOREGS 2005). The gas sulphur dioxide (SO_2) in the air can come from fossil fuel combustion or from copper smelting, but in nature it can be released from volcanic eruptions (ATSDR 1998a).

Sulphur is essential to life because the sulphur-containing amino acids are essential components of living cells (Emsley 2011). It is a major element in all plants, and a minor constituent of all parts of the human body, including fats, body fluids and skeletal minerals (FOREGS 2005). Sulphate is one of the least toxic anions, although relatively high levels (>1000 - 1200 mg/l) may have a laxative effect in humans and can also result in a noticeble taste in drinking water (WHO 2011b). Sulphate in concentrations above

1500 mg/l may affect aquatic life in fresh soft waters (~20 mg/l CaCO3) with low chloride (~5 mg/l) (Soucek & Kennedy 2005; Davies 2007). The gases SO_2 and H_2S are toxic through inhalation; the latter being dangerous even at small doses (Emsley 2011). Sulphur dioxide affects the lungs in the long-term exposure and at high levels may cause nose and throat burning, breathing difficulties and severe airway obstructions in humans and animals (ATSDR 1998a). A few breaths of high levels of H_2S can cause death and lower level long-term exposure can cause eye irritation, headache, and fatigue (ATSDR 2006). Sulphur trioxide (SO_3) is formed from SO_2 and SO_3 in contact with water forms sulphuric acid (H_2SO_4). The H_2SO_4 can cause burns to the skin, eyes, lungs, and digestive tract, and severe exposure can result in death. The SO_3 forming H_2SO_4 in water in the air is the major cause of acidity in both natural and polluted rainwater (ATSDR 1998b). Here the sulphur plays a significant role in geochemical, atmospheric, and biological processes such as the weathering of rocks, acid rain, and rates of denitrification (Mészáros 1988).

CHAPTER 3: METHODOLOGY

3.1 Data collection in Central Chile

Data collection followed the international procedures which are discussed in the Chapter 2. A sampling protocol was prepared for the study and for future studies for Anglo American plc. (AA), the company supporting the project (Appendix A). Regional scale sampling was carried out over 4 seasons together with 2 detailed sampling campaigns (Table 3.1). The sampling seasons were: high flow 2006-07 (late Oct '06 to early Feb '07, 8 weeks), low flow 2007 (late Feb to late Apr '07, 8 weeks), high flow 2007-08 (late Nov '07 to early Feb '08, 13 weeks), and low flow 2008 (mid Feb to mid-May '08, 13 weeks).

Table 3.1: Summary of sampling campaigns and data collected.

Campaign	Period	No. of Weeks	No. of Samples	Chemicals	Data Points
High Flow	late Oct'06 - early Feb'07	8	193	79	15,247
Low Flow	late Feb - late Apr'07	8	190	80	15,200
High Flow	late Nov'07 - early Feb'08	13	292	158	46,136
Low Flow	mid Feb - mid May'08	13	266	158	42,028
Low Flow	mid Jan - early Apr'09	1.1	17	158	2,686

3.1.1 Sampling procedures

The sample density used was approximately 1 sample per 50 sq. km. and the regional baseline was produced using 1 sample per 100 sq. km. Much of the area is remote and somewhat inaccessible. Hence, the locations of the sampling sites were chosen first to follow existing roads to facilitate sample collection using a 4 wheel drive vehicle and in the case of more remote sites horses and a helicopter were used. The sampling sites used are predominantly in second order drainage basins, upstream of the confluence point with the main stream. Selected control samples were also collected in the main rivers. The same sampling sites were used for low flow and high flow, however during low flow some streams were dry and no samples could be collected.

All samples (Table 3.1) of stream water were collected systematically to international standards (Darnley 1997; Salminen et al. 1998). Samples were collected in HDPE Nalgene^{TM} bottles using a manually-operated peristaltic pump with trace metal free Tygon® 2001 tubing connected to Aquaprep^{TM} 0.45 µm filter capsules. Samples were collected from the side of streams, fixing the hose under the water, without touching the stream bed, and extending to the middle of the stream as far as possible. Ultra-clean procedures were used in order to avoid cross-contamination between samples.

At each site, prior to sample collection, the pump and tubing were rinsed in the water to be collected and then rinsed with the filter attached. Separate sub-samples were collected for the determination of cations, anions, stable isotopes (δD, $\delta^{18}O$, $\delta^{34}S$ and $\delta^{15}N$) and dissolved organic carbon (DOC). Samples used to determine major cations and trace elements were acidified to 2% with ultra-pure nitric acid. Samples collected for $\delta^{15}N$ isotopic signature were stabilised with 20 drops of mercury chloride ($HgCl_2$) as a biocide. This was obtained by preparing a solution 0.129 M of $HgCl_2$ (15.75 g of $HgCl_2$ in 450 ml of deionised water) (Kattner 1999). All samples were refrigerated at 4°C after collection until dispatched for analysis. Photographs were taken at each sampling location.

Electrical conductivity (EC), pH, dissolved oxygen (DO), temperature and alkalinity were measured in the field. Alkalinity was measured as HCO_3^- using the digital titrator HACH® model 16900 by both the phenolphthalein and total method (HACH 2006). The $CaCO_3$ phenolphthalein alkalinity of all of the samples was zero, while the total alkalinity measured after adding Bromocresol Green-Methyl Red Indicator indicated bicarbonate alkalinity (HCO_3^-).

For quality control, one field duplicate was collected for every 10 samples. One international water standard was submitted with every twenty samples and two field blanks were prepared using ultra-pure deionised water for every 20 samples collected. One of these was added directly to an unwashed bottle and the other was added after filtering by pumping.

3.2 Analytical methods used in the research

3.2.1 Multi-elemental chemistry and physico-chemical analysis

The water samples were submitted to Acme Analytical Laboratories Ltd.©, Vancouver for chemical analysis and the method used are summarised in Table 3.2. These analyses included 73 chemical elements, F, nitrate, pH, EC, total dissolved solids (TDS), alkalinity and total dissolved organic carbon (TOC).

3.2.2 Stable isotope determinations

Stable isotopes (δD, $\delta^{18}O$ in water; $\delta^{34}S$ and $\delta^{18}O$ in sulphate; and $\delta^{15}N$ and $\delta^{18}O$ in nitrate) were prepared and determined at the Queen's Facility for Isotope Research (QFIR) at Queen's University, Kingston, Ontario, Canada. The analytical methods including the standards used to calibrate the equipment are summarised in Table 3.3. Oxygen-18 signatures ($\delta^{18}O$) were determined by analysing 1.5 ml of sample in a GasBench II coupled to a Thermo Finnigan Delta^{plus} XP stable isotope ratio mass spectrometer using continuous flow technology. Deuterium isotopes (δD) were determined by a Thermo Finnigan hydrogen device coupled to a Finnigan MAT 252 isotope ratio mass spectrometer (IRMS) using the dual inlet system. An aliquot of 0.3 ml of sample is injected into a chrome metal at 850°C. The oxygen stays in chrome as chrome oxide, while the hydrogen gas is released and analysed in the mass spectrometer.

Table 3.2: Summary of analytical methods for multi-element chemistry

Analytical method	Full name of method	Technique used
2C-MS	Group 2C ICP-MS Analysis of Water	Major and trace elements were analysed using a 10 ml aliquot directly into an Elan 6000 inductively coupled plasma-mass spectrometry (ICP-MS) if total dissolved solids (TDS) were <0.1% or diluted by a factor of 10, 100 or 1000 prior to ICP-MS if the TDS value was above 0.1%
2BIC-NO3	Group 2B Anion Analysis by ion chromatography	Milligrams per litre concentrations determined by a Dionex ICS 2000 Ion Chromatograph. Equipped with IonPac AS 17 separator column and NaOH eluent
2B-F	Group 2B Water Analysis	Micrograms per litre concentrations determined by specific ion electrode
2B-ALK	Group 2B Water Analysis	Alkalinity in milligrams per litre determined by titration
2B-pH	Group 2B Water Analysis	pH units determined using an electrode
2B-uS	Group 2B Water Analysis	EC in µS/cm determined using an electrode
2B-TDS	Group 2B Water Analysis	TDS in milligrams per litre determined by meter based on the measurement of EC
Water-TOC	Water TOC	Total Dissolved Organic Carbon (TOC) in milligrams per litre determined using a Shimadzu TOC analyser

Table 3.3: Methods for determining stable isotope values of δD, $\delta^{18}O$ in water; $\delta^{34}S$ and $\delta^{18}O$ in sulphate; and $\delta^{15}N$ and $\delta^{18}O$ in nitrate.

Isotope	Method	Aliquot	Preparation	Standards
δD	Thermo Finnigan H-device coupled to a Finnigan MAT 252-IRMS using dual inlet	0.3 ml	N/A	UofS and Q1 (in-house)
$\delta^{18}O$	GasBench II coupled to a Thermo Finnigan Delta^{plus} XP-MS using continuous flow	1.5 ml	N/A	UofS and Q1 (in-house)
$\delta^{34}S$	Carlo Erba Elemental Analyser NCS 2500 coupled to a Finnigan MAT 252-IRMS using continuous flow	40 ml	Precipitated as $BaSO_4$	NBS127, NBS123 (intl.) and MRC-pyrite, PRN022-alunite, $BaSO_4$-chem1 (in-house)
$\delta^{18}O$ in SO_4^{-2}	TC/EA continuous flow technology interfaced to a Thermo Finnigan Delta^{plus} XP-MS	40 ml	Precipitated as $BaSO_4$	NIST8446, NIST8493, NBS127 (intl.) and PRN022-alunite, $BaSO_4$-chem1 (in-house)
$\delta^{15}N$	Costech EA interfaced to a Thermo Finnigan Delta^{plus} XP-MS	250 ml	Precipitated as $AgNO_3$	NIST8550, NIST8551 (intl.) and αKNO_3, QFIR1 $AgNO_3$, QFIR2 $AgNO_3$, QFIR3 $AgNO_3$, eil62 (in-house)
$\delta^{18}O$ in NO_3^-	TC/EA continuous flow technology interfaced to a Thermo Finnigan Delta^{plus} XP-MS	250 ml	Precipitated as $AgNO_3$	NIST8446, NIST8493 (intl.) and QFIR1 $AgNO_3$, QFIR2 $AgNO_3$, QFIR3 $AgNO_3$, eil62 (in-house)

Intl. = international

To determine the signatures of the S-34/S-32 ratio in sulphate ($\delta^{34}S_{SO4}$) in water samples a method modified from Wasserman et al. (1992) was used. Sulphate in the samples was precipitated as barium sulphate ($BaSO_4$) by adding a saturated solution of barium chloride ($BaCl_2$) (40 ml of sample plus 10 ml of $BaCl_2$). Carbonates were removed from the precipitate by adding hydrochloric acid (HCl) at 20%, then washing the sample three times with 18 meg ohm water to remove residual Cl and dried at 60°C. An aliquot of ~0.5 mg of the precipitated sample was then loaded into tin capsules with 0.5 mg of vanadium pentoxide (V_2O_5) and analysed using a Carlo Erba Elemental Analyser NCS 2500 coupled to a Finnigan MAT 252 IRMS using continuous flow technology. To determine the signatures of the O-18/O-16 ratio in precipitated $BaSO_4$ ($\delta^{18}O_{SO4}$), ~0.1 mg of $BaSO_4$ were loaded into silver capsules and analysed by a TC/EA continuous flow technology interfaced to a Thermo Finnigan Delta^{plus} XP-MS with H_2/He auxiliary gas to aid combustion.

To determine the signatures of the N-15/N-14 ratio ($\delta^{15}N$) and the O-18/O-16 ratio ($\delta^{18}O$) of dissolved nitrate in water samples, the anion NO_3^- was precipitated as silver nitrate ($AgNO_3$) from samples following the procedure defined by Silva et al. (2000). Solute nitrate in the sample was concentrated by passing the water-sample through 5 ml of pre-cleaned anion exchanging resin columns. Nitrate was eluted from the anion columns with 15 ml of 3 M HCl in 3 ml increments. The nitrate-bearing acid eluant was then neutralised with silver oxide (Ag_2O), filtered and split into two aliquots; one was evaporated at 60°C to obtain solid $AgNO_3$ which is then analysed for $\delta^{15}N$ by a Costech EA interfaced to a Thermo Finnigan Delta^{plus} XP stable isotope ratio mass spectrometer. The second was separated for subsequent preparation and measurements of $\delta^{18}O$ in the nitrate ($\delta^{18}O_{NO3}$).

All oxygen-bearing compounds must be removed from the aliquot split to determine $\delta^{18}O_{NO3}$ accurately. Two ml of 1 M $BaCl_2$ solution was added to the 13 ml split to precipitate and remove sulphate and phosphate from the sample. The solution was then passed through 5 ml of pre-cleaned cation exchange resin columns in which Ba^{+2} and Ag^{+} are replaced by H^{+}. The sample was then neutralised with Ag_2O and the excess of Ag_2O removed from solution by filtering at 0.2 μm. The solution was evaporated at 60°C to obtain solid $AgNO_3$. The precipitated nitrate was outgassed for one hour at 100°C in the oven to remove H_2O and then analysed for $\delta^{18}O_{NO3}$ using a TC/EA continuous flow technology interfaced to a Thermo Finnigan Delta^{plus} XP stable isotope ratio mass spectrometer.

3.3 Evaluation of the reliability of the geochemical data collected

Four different techniques were used for quality control of the data viz. duplicate samples to determine precision, international water certified reference materials (CRMs) to determine accuracy, blank samples to identify any contamination and calculation of charge imbalance to control neutrality.

3.3.1 Quality assurance and quality control

One hundred (10%) field-sample duplicates were collected to determine sampling site reproducibility and the precision of the analytical methods. Fifty eight (6%) samples of international CRMs were used to evaluate the accuracy of the analytical methods. Fifty four (5%) blank samples were used to determine levels of contamination, during analysis (simple blank, B1) and during sample collection (process blank, B2).

Field duplicates

The duplicate results for each chemical were evaluated using graphs of the percentage relative difference plotted against the original-duplicate mean (Figure 3.1). These were calculated using the formulae (1) and (2) below:

$$\text{y axis:} \qquad 100 * \frac{\text{Original} - \text{Duplicate}}{\frac{1}{2}(\text{Original} + \text{Duplicate})} \tag{1}$$

$$\text{x axis:} \qquad \frac{1}{2}(\text{Original} + \text{Duplicate}) \tag{2}$$

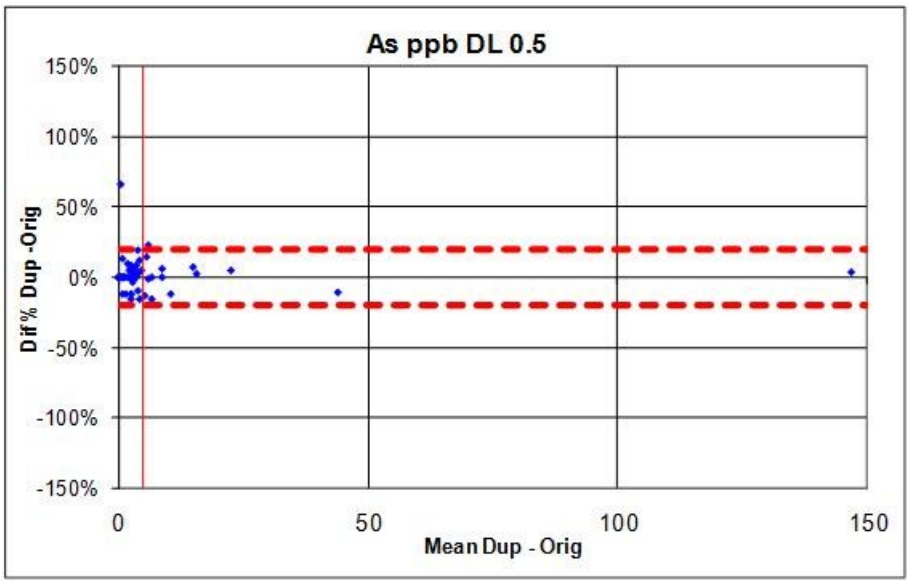


Figure 3.1: Graph used to control precision of As. Segmented red lines represent ±20% error margins. Continuous vertical red line represents 10 times the lower detection limit (DL). This case showed high precision for As data.

The data were considered precise or reproducible if 95% of values were within ±20% of the percentage relative difference for each chemical; and the entire dataset was considered precise if the average of the percentage relative difference of the all chemicals was within <±20%. This criterion considers the high variability of concentrations close to the detection limit (DL) and reflects the overall behaviour of the dataset. Sample

concentrations below 10 times the DL were excluded from the evaluation. Chemicals that had more than 50% of their concentration values below 10 times the DL were also excluded.

Control reference materials

In order to evaluate the analytical accuracy of the 2C-MS method (Table 3.2), samples of TM-27.2 (for the first 3 sampling campaigns in Table 3.1) and TM-23.3 (late in the third and the last sampling campaigns) certified reference materials were used. For 2B-IC, 2B-F and physicochemical analyses (Table 3.2) samples of TROIS-94 CRM were used. The results were compared against the known certified mean and standard deviation values for 25 chemicals using graphs (Figure 3.2).

Ideally, 95% of all samples should fall between ±2 standard deviations (warning lines), with 99% between ±3 standard deviations (failure lines). A batch of analyses is not considered accurate if one or more samples fall outside the failure lines (Figure 3.2). The analytical method was considered adequately accurate if ≤3 analysed standard samples for each chemical were outside ±25% of the mean for that standard. Elements below or close to the detection limit (DL) were excluded from the evaluation.

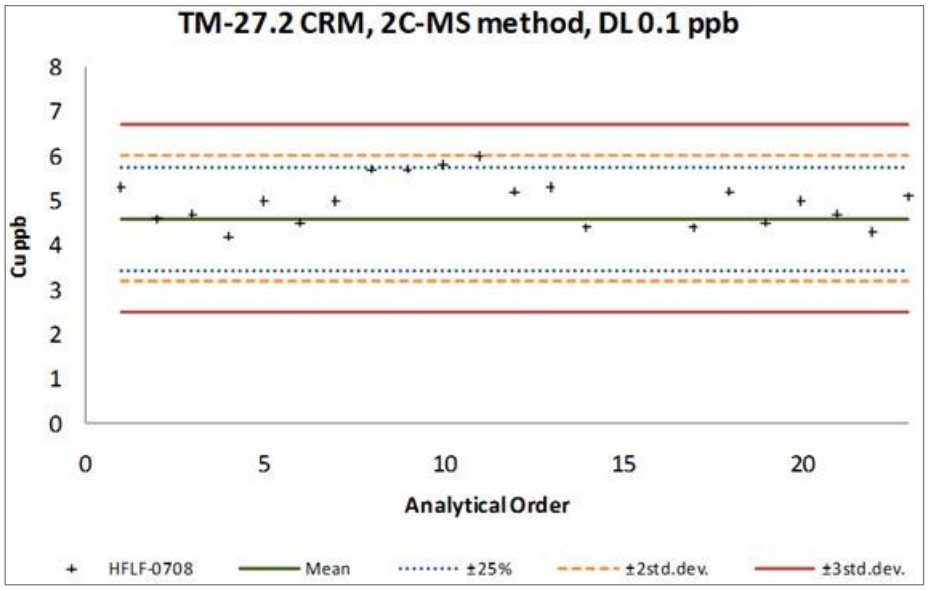


Figure 3.2: Graph used to control accuracy of Cu. The analytical concentrations for the CRM were plotted against the analytical order. The lines were calculated from the certified mean and standard deviation values. DL: detection limit. This case showed accurate Cu data.

Field Blanks

In order to detect any contamination during analysis and sampling procedures, distilled water (for the first sampling campaign) and ultra-pure deionised water (for later campaigns) were used as blank materials. Two types of blanks were prepared in the field: samples of blank 1 (B1) were prepared by filling Nalgene® sample bottles directly, and samples of blank 2 (B2) were collected as normal water samples by pumping and filtering the distilled and deionised water through all the sampling equipment.

Contamination of samples during analysis and sampling procedures considered to have occurred if concentrations in blank samples were higher than 3 times the DL supplied by the analytical laboratory (Figure 3.3). Contamination was also considered significant if concentrations in blank samples were higher than 10 times the DL.

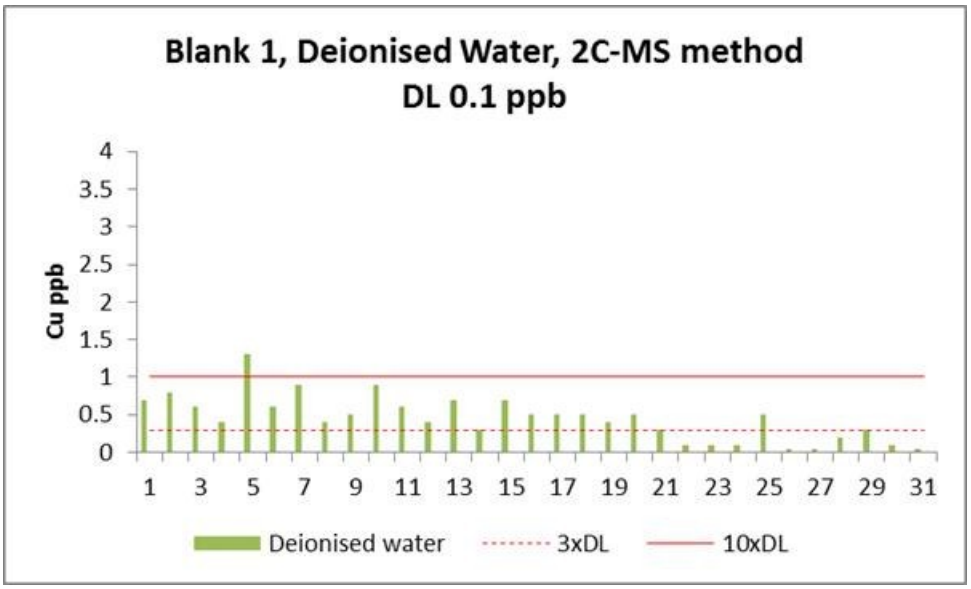


Figure 3.3: Graph used to detect any contamination of Cu in distilled water for blank 1. Red dashed line represents 3 times the DL. Red solid line represents 10 times the DL. Concentrations are in analytical batch order.

3.3.2 Charge imbalance of water geochemical data

Dissolved ions in solution should be electrically neutral, with cations balancing anions and vice versa. The charge imbalance (CI) is calculated as the quotient between the subtraction of the sum of cations less anions and the average of the sum of cations and anions multiplied by 100 (Nordstrom et al. 2009) as the formula (3) below:

$$CI\ (\%) = \frac{(\sum_i^n c_i^+ - \sum_i^m c_i^-)}{(\sum_i^n c_i^+ + \sum_i^m c_i^-)/2} \times 100 \qquad (3)$$

The CI was calculated for 812 water samples from a total of 1005 samples collected during the four regional sampling campaigns (Table 3.1) (the other 193 samples lacked alkalinity data). Field alkalinity measurements (HCO_3^-) were used for the calculations as 40 samples were lacking the laboratory alkalinity results and the low difference between these measurements as it is shown later. A charge imbalance of ±20% was used as the limit where the CI can be explained (Nordstrom et al. 2009).

3.4 Chemical characterisation and developing the geochemical baseline

In order to obtain a representative regional scale dataset, the sampling periods are compared based on number of samples sites and area covered, and on the resolution of the data between different seasons (Table 3.1).

The water samples were characterised geochemically by preparing:

- Descriptive statistics of the hydrogeochemical data
- Scatter plots of chemicals
- Pearson correlation, and Spearman correlation based on ranks
- Multivariate data analysis, factor analysis
- Scatter plots of pH versus EC by TDS concentration
- Ternary diagrams or piper plots of the major cations and anions by basins
- Population analysis using PROBPLOT (Stanley 1988)

3.4.1 Preparation of regional hydrogeochemical baseline maps

The geographic information system (GIS) Geosoft Inc. OasisMontaj software was used to prepare regional hydrogeochemical baseline maps assuming that each sample site represents the chemistry of the catchment area upstream. The frequency distribution of each determinant identifies breaks in the cumulative probability curve which were used to select class intervals (Stanley 1988) using the ProbPlot tool and revising manually the intervals for each parameter (Figure 3.4). Each population of a particular parameter was plotted in a different colour. The major population breaks defined the thresholds from which the mean background and anomalous concentrations (values above the threshold) were determined (Table 4.6).

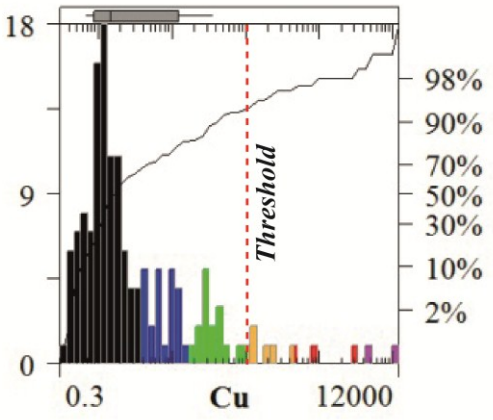


Figure 3.4: Histogram and frequency accumulation curve for regional copper data. The populations are coloured by the class intervals, being the three below the threshold (red dashed line) the background range (black, blue and green) and those above are the anomalous concentrations (orange, red and pink).

Regional hydrogeochemical baseline maps were prepared for Ca, Mg, K, Al, Fe, Cl, SO_4^{-2} and NO_3-, and the trace elements As, Cd, Cu, F^-, Hg, Mo, Ni, P, Pb and Zn, and other key chemical parameters including bicarbonate alkalinity (HCO_3^-), pH and TDS.

3.5 Identification of the sources of anomalous geochemistry

The resulting baseline maps were used to identify and group anomalously high concentrations of chemicals for each sampling site and area of occurrence. The chemicals associations identified were classified according to their sources which included natural sources such as bedrock geology, and areas of hydrothermal alteration and metal mineralisation. Anthropogenic sources of anomalous chemicals included agriculture, human settlements and mining activities. A table was prepared by chemical and sampling site, highlighting the background range, threshold, water guideline values (WGVs), values above the WGV, and anomalously high chemicals associated by their source wherever it was possible to be identified (Appendix C).

The sources of dissolved sulphate and nitrate were identified using their stable isotope values. The $\delta^{34}S$ and $\delta^{18}O_{SO4}$ values were plotted as a scatter plot with all documented sources of dissolved sulphate indicated. Similarly, the $\delta^{15}N$ and $\delta^{18}O_{NO3}$ values were plotted as scatter plot with all documented sources of dissolved nitrate identified.

3.6 Evaluating the application of the geochemical baseline to water regulation

Many of the chemical parameters analysed in this study are or may be subjected to water quality regulation in the future. The regional hydrogeochemical dataset was compared with international and Chilean guideline values for drinking water in the Table 2.1. The regional hydrogeochemical data for the Maipo Basin collected over four seasons in this study were compared with the Chilean government draft regulation values of the water quality for the Maipo Basin (CONAMA 2004). This was prepared for the 15 equivalent parameters included in both datasets: EC, DO, pH, sodium absorption ratio (SAR), Al, As, Cl, Cr, Cu, Fe, Mn, Mo, Pb, SO_4, and Zn (see section 2.5). The SAR or RAS for its translation in Spanish (razón de adsorción de sodio) is a measure of the suitability of water for the use in agricultural irrigation. It gives the relative activity of the sodium ions in the exchange reactions with calcium and magnesium in the soil by the formula (4) (Lenntech B.V. 2013). Generally, the higher the SAR is, the less suitable the water is for irrigation as the use of that water in the long term can cause Na displacing Ca and Mg in the soil.

$$RAS\ or\ SAR\ = \frac{Na^{+}}{\sqrt{\frac{1}{2}\left(Ca^{2+} + Mg^{2+}\right)}} \times 100 \qquad (4)$$

Where Na, Ca and Mg are concentrations in milliequivalents per litre.

The methodology used was as follow:

- The 22 sites equivalent to those used in the regulation data were selected close to the closure of each sub-basin
- For each site the 66th percentile, as defined in the draft regulation, and the mean of the data were calculated for data collected over 2 seasons (high flow and low flow) and for two different years (2006-07 and 2007-08)
- The percentage difference between both the mean and the 66th percentile, and the regulation levels were calculated according to equation (5) below

$$\% \, Difference = \left[\frac{X - Regulation}{Regulation}\right] \times 100 \qquad (5)$$

Where X is either the mean or the 66th percentile of the regional hydrogeochemical data. The values that were lower than the detection limits were not considered further. The regulation values are above the detection limits for the majority of the sub-basins by a factor of 10 for EC, DO, Cl, SO4, Cu, Fe, Mn, Mo, Zn, Al, As and Pb, and at or below DL for Cr in one site.

CHAPTER 4: RESULTS

4.1 Study area

4.1.1 Introduction

The research area comprises approximately 20,000 sq. km. and extends from the Andean Cordillera (AC) across the Coastal Cordillera (CC) including the Central Valley (CV) (32°5'S, 69°47'W; 34°19'S, 71°26'W) (Figures 4.1, 4.2 and 4.3), it covers 3 principal catchment basins viz. those of La Ligua, Aconcagua and Maipo. Chile's capital city Santiago is situated in the CV at 520 m, it has a population estimated to be approximately 7 million (INE 2012b). Most other communities and agricultural activities are also mainly in the CV. Livestock rearing takes place in both the CV and the valleys of the AC and CC. Mining activities, mainly copper extraction, takes place in the AC (~3,500 m a.s.l.) and CC (~800 m a.s.l.). The altitude in the region increases markedly from sea level in the west to approximately 6,000 m in the AC over a distance of ~170 km with the highest points being the Tupungato and Maipo volcanoes at 6,570 m and 5,264 m respectively, and Aconcagua at 6,962 m (Figure 4.2).

The climate in the CV is of temperate Mediterranean type and is characterised by a long dry season in the summer (December-April) and a cold winter with temperatures down to zero. Annual average temperatures are 14.5°C in Santiago and 15.2°C in Los Andes with maximum temperatures from 27-35°C in summer. Precipitation in the CV averages 300 mm/y annually and 536 mm/y at higher altitudes (~2,000 m) in the AC where the annual average temperature is of 14.2°C (DGA 2004b; DGA 2004a).

Energy in Chile was in the past predominantly from hydroelectric power plants and it represented 80% of the installed capacity in 1990. In the mid-90s gas and coal powered

thermoelectric plants began to dominate the power investment. Particularly in Central Chile, in the study area, the current (2012) installed capacity is ~3800 MW with 60% from natural gas (~2300 MW), 17% from coal (~650 MW), 15% from hydroelectric plants (~580MW) and 8% from diesel (~320 MW) (Central Energía 2012).

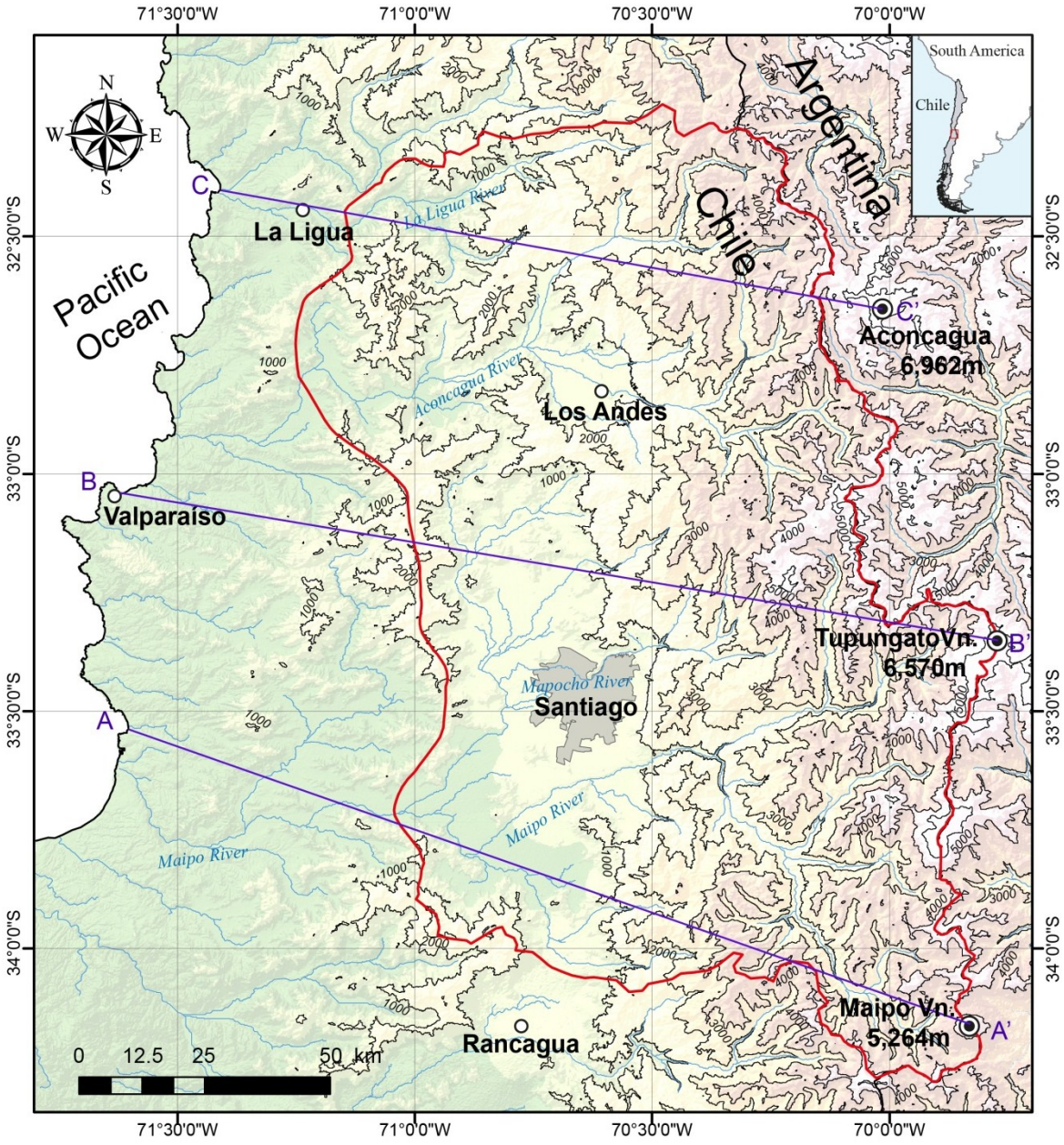


Figure 4.1: Contour map showing the highest altitudes on the Chile-Argentina border, Maipo Volcano at 5,264 m a.s.l. and Tupungato Volcano at 6,570 m a.s.l. and in Argentina, Aconcagua at 6,962 m. a.s.l. The study area is outlined in red. The three profiles, AA', BB' and CC' are shown in Figure 4.2.

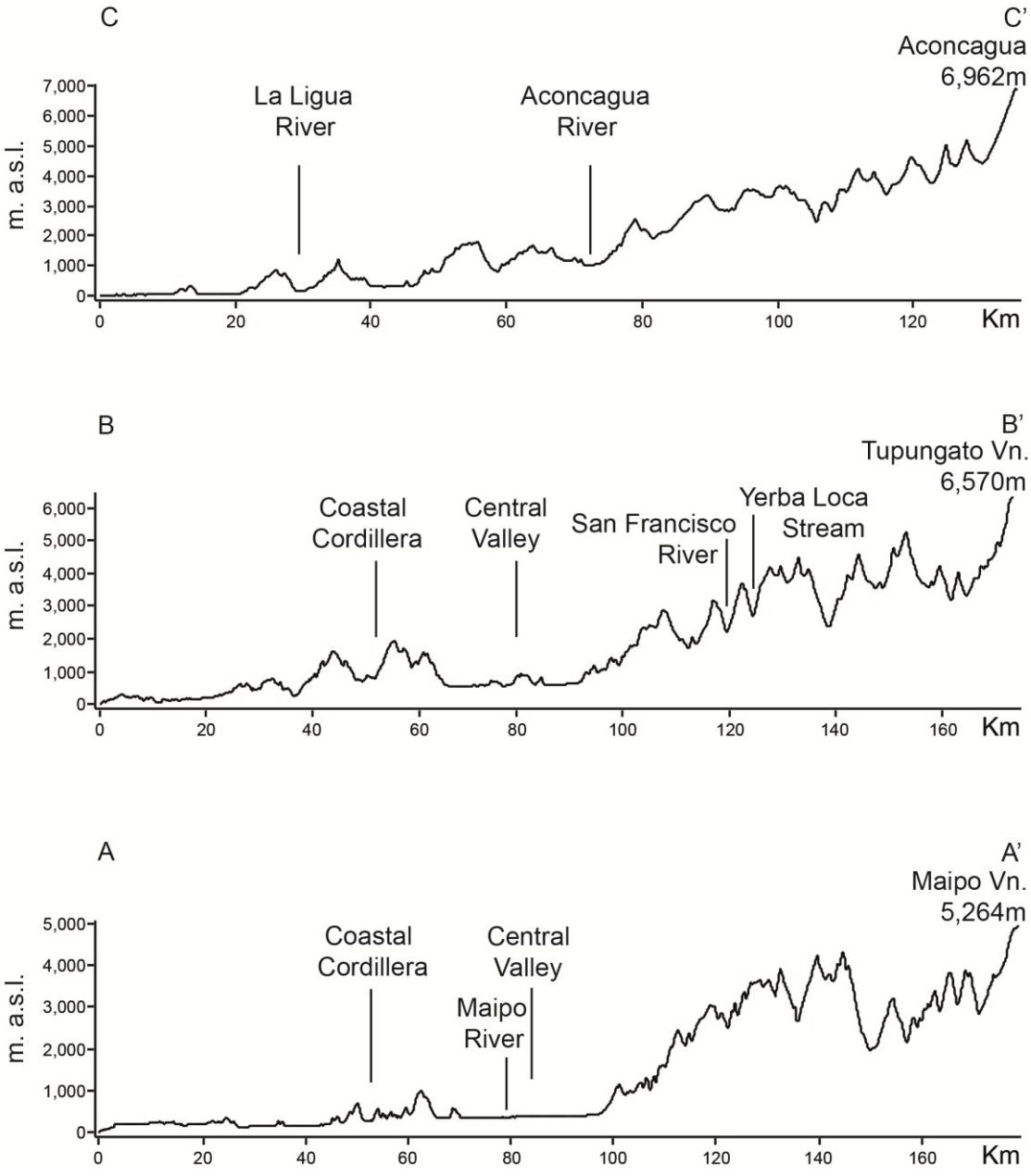


Figure 4.2: Profiles AA', BB' and CC' highlighting the relief of the region. The principal peaks, rivers and valleys are indicated.

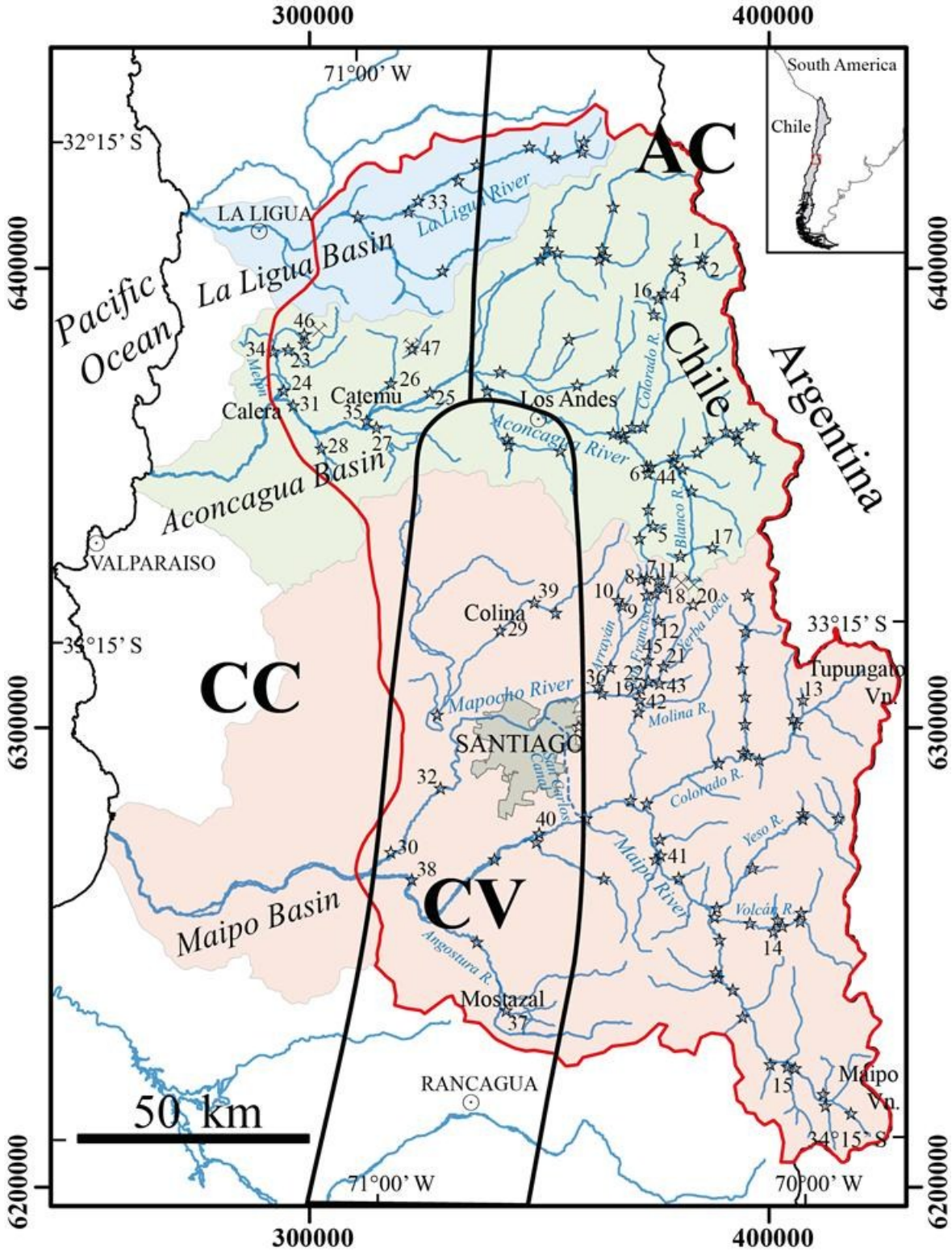


Figure 4.3: Study area outlined in red in Central Chile (upper right corner) and the catchment basins south to north: the Maipo, the Aconcagua and the La Ligua basins. CC: Coastal Cordillera, AC: Andean Cordillera and CV: Central Valley. Sample site numbers according to text.

4.1.2 Geology

A general description of the geology of the stratigraphic units (Table 4.1) and of the intrusive rocks units (Table 4.2) is summarised. The rocks in the area range from Triassic to Tertiary in age. Mesozoic stratigraphic units outcrop in N-S bands, along both the CC and the AC (Figure 4.4). The units in the CC are mainly discordant Cretaceous sedimentary and volcanic rocks of continental origin, and of marine origin in intercalations towards the west. In the AC, the units are mainly concordant Jurassic and Cretaceous marine and continental sediments, associated with extensive evaporites composed mainly of gypsum. It is important to note that these sequences are predominantly vertical, complexly folded and exposed over a horizontal E-W distance of 25 to 30 km and a N-S distance of 100 km in the headwaters of the Maipo Basin (Figures 4.3 and 4.4). The youngest stratified sediments which are of Cenozoic age occur in inactive Pliocene and Holocene volcanic structures, as well in the region are volcanoes which have been active historically. There are also fluvio-alluvial-glacial deposits of Quaternary age in the CV.

The oldest Cenozoic stratified units, which outcrop in the AC in a north-south belt, are volcanic and volcano-sedimentary sequences of Lower-Middle Miocene and Oligocene-Miocene, respectively.

Batholiths and stocks ranging in composition from diorites to granodiorites and granites were emplaced in the CC in Jurassic-Cretaceous times (Table 4.2). In the AC, plutons and porphyries ranging in composition from diorites, granodiorites, granites and monzonites range in age from Upper Cretaceous-Miocene. Generally, these intrusions occur as N-S oriented bodies which young progressively to the east. The Mesozoic intrusive bodies

intrude Mesozoic formations in the CC while the Cenozoic intrusive bodies intrude Cenozoic and Mesozoic formations in the AC.

Table 4.1: Geology of stratigraphic rock units in the study area.

Era	Age	Geological Unit	Description	Location	Reference
Cenozoic	Quaternary	Alluvial deposits	Blocks, gravel, sand, silt and clays	Fill in the CV and valleys. In the Maipo River layout as terraces	3
		Lacustrine deposits	Finely laminated silts and clays, deposited in lakes behind some moraines	In the valleys of Colina, Colorado, Maipo and Yeso rivers	3
		Gravitational deposits	Debris and talus accumulation as a result of landslide and breaking off of weathered rock	At the base of streams and cliffs in the whole area	3
		Glacial deposits	Marginal moraines and debris of rock glaciers	Head of streams in glacial cirques from 2500 m a.s.l.	3
	Holocene	Unidad Volcánica Nueva	Volcanoes with historic activity. Andesitic lavas, interbedded with breccias and minor pyroclastics	In valleys of the AC and in the CV. Tupungatito and San José volcanoes	3
	Pleistocene	Unidad Volcánica Antigua	Skeletons of extinct volcanoes, andesite and trachyandesite lavas	In the AC at the Chile-Argentina border. Tupungato Vn., Cerro Marmolejo Hill and Cerro Castillo Hill	3
		Pudahuel Ignimbrite	Pyroclastic deposits mainly rhyiolitic, related to calderas	In the CV	11
	Lower-Middle Miocene	Farellones Fm.	Andesites and pyroclastic rocks interbedded with continental sediments	In the AC as a NS orientated band	3; 5, 14
	Upper Eocene-Lower Miocene	Abanico Fm.	Andesites, basalts, rhyolite, pyroclastic and volcanoclastic rocks interbedded with continental sedimentary rocks	In the AC it exposures as two NS swaths separated by Farellones Fm. Spread outcrops in the CV	13; 14
Mesozoic	Maastrichtian	Lo Valle Fm.	Continental. Welded tuffs and dacitic tuffs. Interbedded with andesitic tuffs of the Las Chilcas Fm. at the base	Eastern part of the CC	4; 8
	Aptian-Campanian	Las Chilcas Fm.	Continental. Acid pyroclastic rocks interbedded with basalts. Through the top conglomerates and sandstones with plant remains, interbedded with basaltic and basaltic-andesitic lavas, and minor marine sandstones	Eastern part of the CC	1; 4; 9
	Barremian-Albian	Cristo Redentor Fm.	Continental. Conglomerates, fine and argillaceous sandstones and mudstones, and gypsum	In the AC at the Chile-Argentina border around the homonym border crossing	4, 6
	Barremian-Albian	Veta Negra Fm.	Continental. Porphyritic andesites interbedded with tuffaceous	In the CC as a NS orientated band	2

		sandstones and sedimentary breccias		
Hauterivian-Albian	Colimapu Fm.	Continental. Sandstones, shales, conglomerates, interbedded with pyroclastic rocks, andesites and basalts	In the AC as a NS orientated band. South of the Volcán River to the north of the Colorado River	3
Berriasian-Valanginian (Neocomian)	Lo Prado Fm.	Marine. Fossiliferous limestones, fetid calcareous mudstone, breccias, andesitic tuffs and lavas, interbedded with conglomerates, sandstones, andesites and keratophyres	In the CC as a NS orientated band	2; 12
Tithonian-Lower Hauterivian	San José Fm.	Littoral marine. Calcareous sandstones, calcilutites, calcareous breccias and gypsum	In the AC at the Chile-Argentina border as NS oriented band	6
Tithonian-Hauterivian	Lo Valdés Fm.	Marine. Limestones, shales, calcareous sandstones, conglomerates, breccias, interbedded with gypsum, basalts and andesites	In the AC as a NS orientated band. From the Yeso River to the Colorado River	3
Kimmeridgian	Río Damas Fm.	Continental. Conglomerates and conglomeratic breccias interbedded with sandstones, siltstones and andesites. Minor gypsum layers	Eastern of the AC as a NS orientated band	3
Callovian?-Oxfordian	Río Colina Fm.	Marine. Fossiliferous clastic sandstones, conglomerates, limestones and shales, interbedded with volcanic rocks and gypsum intrusions	Discontinuous outcrops in the eastern of the AC	3
Bathonian-Kimeridgean	Lagunillas Fm.	Continental. Conglomerates with matrix rich in quartz, plagioclase and K-feldespar, andesites and basaltic andesites, gypsum intrusions	In the AC at the Chile-Argentina border	4, 15
Bathonian-Lower Callovian	Nieves Negras Fm.	Marine. Black shales interbedded with fine and medium sandstones, and thin and nodular mudstones	In the AC at the Chile-Argentina border	7, 10
Toarciano-Bajociano	Horqueta Fm.	Continental. Epiclastic and pyroclastic rocks, and andesitic to rhyolitic lavas. Interbedded with tuffaceous sandstones, breccias and conglomerates	In the CC as a NS orientated band	2
Upper Triassic	La Ligua Fm.	Continental. Keratophyres lavas, breccias and tuffs interbedded with phyllite schist, slates, sandstones, quartzites and conglomerates	In the CC at the north side of the La Ligua Valley and near La Ligua Township	1; 2

[1](Thomas 1958); [2](Piracés & Maksaev 1977); [3](Thiele 1980); [4](Moscoso et al. 1982); [5](Warnaars 1985); [6](Rivano et al. 1993); [7](Alvarez et al. 1997); [8](Gana & Wall 1997); [9](Wall et al. 1999); [10](Alvarez et al. 2000); [11](Sellés & Gana 2001); [12](Boric 2002); [13](Charrier 2002); [14](Muñoz et al. 2006); [15](Charrier et al. 2007)

Table 4.2: Intrusive geological units in the study area (SERNAGEOMIN 2003).

Age Ma	Geological Unit	Description	Location
(8-5)	Upper Miocene intrusive units (Msh)	Hornblende andesite, dacite and granodiorite porphyries, bearing mineralisation 'Giant porphyry copper' type and breccia chimneys	In the AC in a scattered NS oriented belt intruding Farellones Fm.
(13-7)	Upper Miocene intrusive units (Msg)	Hornblende-biotite granodiorites. Minor monzogranites, quartz monzonites, and monzodiorites.	In the AC in a scattered NS oriented belt intruding cenozoic and Mesozoic stratified units.
(20-12)	Miocene intrusive units (Mh)	Hornblend-piroxene-biotite dacite, andesite, monzodiorite and diorite porphyry	In the AC in scattered a NS oriented belt intruding Abanico and Farellones Fm.
(22-16)	Lower-Middle Miocene intrusive units (Mimg)	Biotite-hornblend granodiorite, monzogranite, monzodiorite, monzonite and diorite	In the AC in a scattered NS oriented belt intruding Abanico and Farellones Fm.
-	Upper Cretaceous-Lower Tertiary intrusive units (KTg)	Granodiorite, diorite and granitie porphyry	In the transition between the AC and the CC, north of San Felipe town. Scattered in a NS oriented belt intruding Lo Valle and Las Chilcas Fm.
(90-65)	Upper Cretaceous intrusive units (Ksg)	Pyroxene, biotite and hornblende monzodiorite, granodiorite, gabbro and diorite; andesite and diorite porphyry	In the CC in a scattered NS oriented belt intruding Las Chilcas and Veta Negra Fm.
(84-66)	Upper Cretaceous intrusive units (Ksh)	Stoks mainly composed by andesite-diorite, dacite and rhyolite porphyry	In the CC in a scattered NS oriented belt intruding Lo Prado and Las Chilcas Fm., and Kiag intrusive unit
(123-85)	Lower-Upper Cretaceous intrusive units (Kiag)	Batholiths composed mainly by pyroxene-hornblende diorite and monzodiorite, hornblende-biotite granodiorite and monzogranite	In the CC as a NS oriented belt intruding Cretaceous and Jurassic stratified units
(180-142)	Middle-Upper Jurassic intrusive units (Jsg)	Batholiths and stocks composed mainly by biotite, pyroxene and hornblende quartz monzodiorites, diorites and granodiorites	In the CC intruding Jurassic and Paleozoic rock units

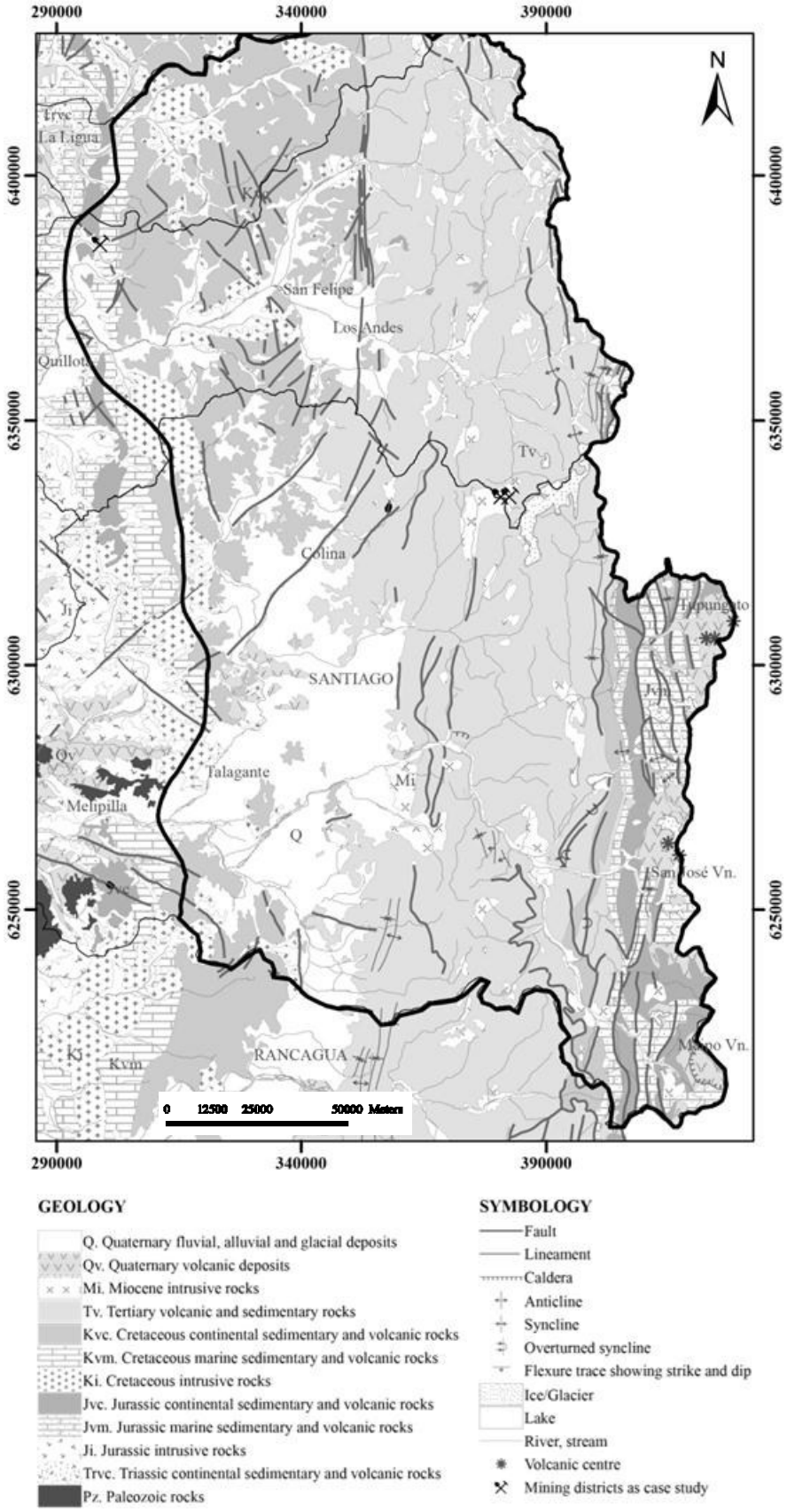


Figure 4.4: Geological map including outlined the study area and the basins. Modified from (SERNAGEOMIN 2003)

4.2 Reliability of the analytical data

4.2.1 QA/QC

The overall results are summarised in the Table 4.3. The QA/QC of all data was prepared as a report for the company sponsoring the project (Appendix B).

Precision

The evaluation of field duplicate samples showed that only 7 (9%) of the 79 parameters analysed had less than 95% of their relative difference within the ±20% variation defined as acceptable, these were Al, B. Ba, Cu, Mn, S and Zn. Of these, Zn was found to be less precise with 63% of the relative differences inside the limits while others very between 89-94% (Table B-4 Appendix B). This is thought to reflect signal noise near the detection limits (Figure 4.5). The overall average percentage relative difference is 8%, which reflects the high precision of the dataset overall, with variation well within the acceptable level of ±20%.

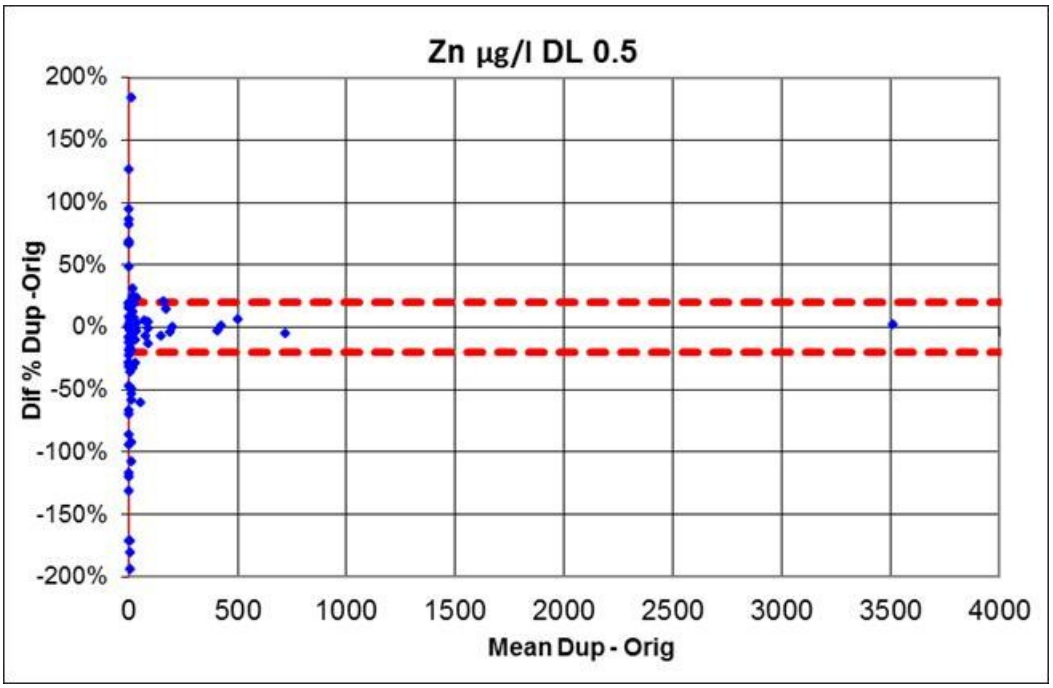
Accuracy

The evaluation of the international CRMs showed that TM-27.2 which was used to control the accuracy of cation analysis had 94% of the samples within the acceptable variation (Table 4.3). TM-23.3 which was also used to control the accuracy of cation analysis had 65% of elements within the acceptable variation. These values reflect the better accuracy of TM-27.2 over TM-23.3 overall for this analysis. Only aluminium was significantly outside the acceptable limits but its reproducibility was high with a positive bias of 23% for TM-27.2 and of 36% for TM-23.3 (Tables B-1 and B-2, Appendix B). The former had values not far from ten times the DL and the difference may reflect signal noise near the DL, but the latter values were significantly higher than DL and showed

exactly the same behaviour. This is thought to be a problem with the Al concentration in the CRMs and the analysis but as the overall data have an average ~100 and ~10 times higher than the TM-27.2 and TM-23.3 means respectively, it is not considered a major problem. TRIOS-94 which was used to control the accuracy of anions and physicochemical analyses had a 100% of chemicals within the acceptable variability.

The evaluation of both type of blanks prepared in the field, blank 1 (B1) and blank 2 (B2) showed that between 82% and 88% of chemicals had concentrations below the maximum acceptable level for both blanks which used distilled and deionised water (Table 4.3). For distilled water, nine chemicals had one or more values above 10 times DL for B1 (B, Ba, Cu, Li, Mn, Pb, Si, Sr and Zn) and ten chemicals for B2 (Al, B, Ba, Cu, Li, Mn, Sb, Si, Sr and Zn). For deionised water, fourteen chemicals had one or more values above 10 times DL for B1 (Al, Ba, Ca, Ce, Cu, Hg, Na, Rb, Si, Sn, Sr, Zn and Zr) and fourteen chemicals for B2 (Al, Ba, Ca, Ce, Cu, Hg, Mn, Na, Rb, Si, Sn, Sr, Zn and Zr) (Appendix B). However, no carryover from sample analysed previously and/or from the previously field sample analysed was detected for any of these elements. Overall the B1 and the B2 results are closely similar for both distilled and deionised water allowing for the normal analytical variation close to the DL. Therefore, the tubing, bottles and filters have not contributed any contaminating elements to the results.

a)



b)

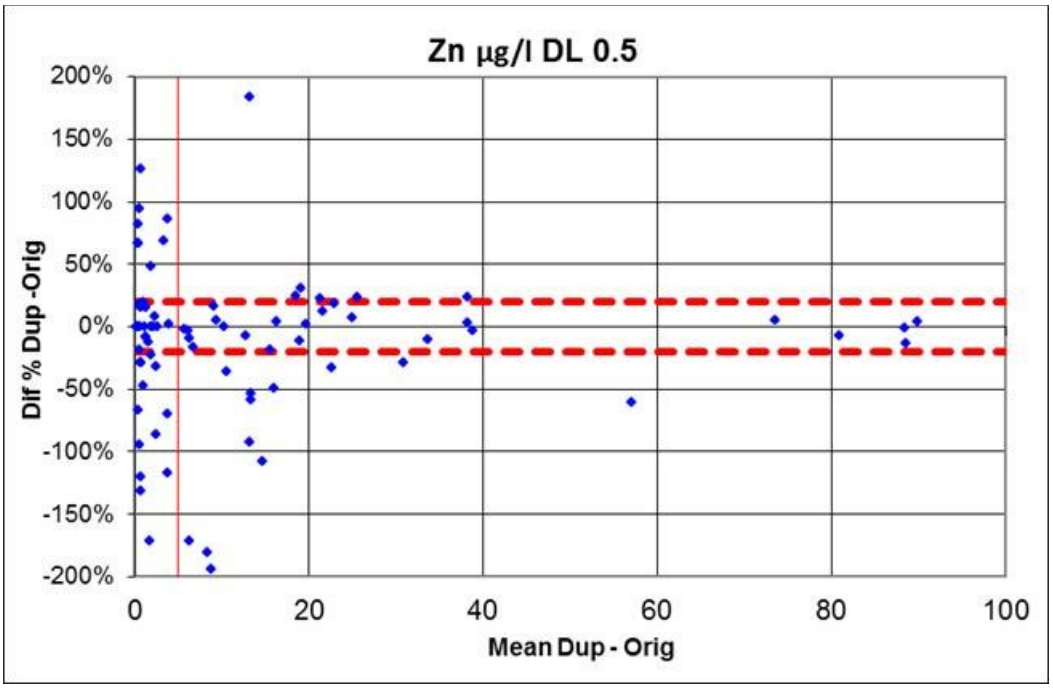


Figure 4.5: (a) Graph used to control precision of Zn. Segmented red lines represent ±20% error margins. Continuous vertical red line represents 10 times the lower detection limit (10xDL). (b) Zoom to 100 µg/l showing the variability increasing near 10xDL.

The results for the blanks, together with the high accuracy and precision demonstrated previously, indicated that the dataset is of high quality and fit for purpose.

Table 4.3: Overall results of the QA/QC evaluation. TM-27.2 and -23.3 are CRMs used to evaluate multi-element analysis and TROIS-94 to evaluate nitrate and physicochemical analysis.

Parameter	QA/QC evaluation	Result
Precision:		
Filed duplicates	Average of % relative difference of all chemicals	8%
Accuracy:		
TM-27.2	% elements within ±3 std. dev. and/or ±25%	94%
TM-23.3	% elements within ±3 std. dev. and/or ±25%	65%
TROIS-94	% chemicals within ±3 std. dev. and/or ±25%	100%
Contamination:		
SB-distilled water	% chemicals ratio max. blanks/3x detection limit ≤ 3	88%
PB-distilled water	% chemicals ratio max. blanks/3x detection limit ≤ 3	87%
SB-deionised water	% chemicals ratio max. blanks/3x detection limit ≤ 3	82%
PB-deionised water	% chemicals ratio max. blanks/3x detection limit ≤ 3	82%

4.2.2 Alkalinity measured in the field and laboratory

Alkalinity data obtained from field measurements were compared with analytical results obtained in the laboratory. The results showed a positive highly significant correlation coefficient of 0.97 and a slight positive bias of 11 mg/l on average between field and laboratory data (Figure 4.6). TDS and pH do not affect the results.

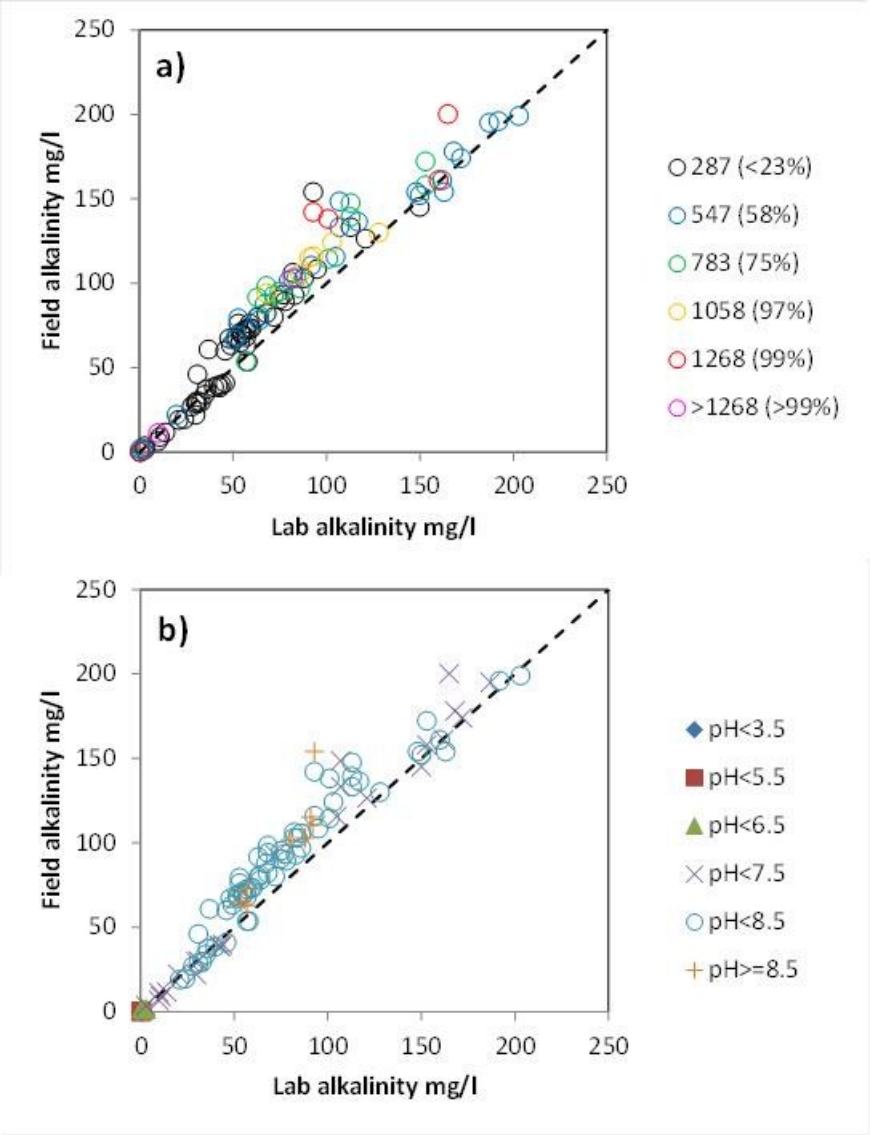


Figure 4.6: Field alkalinity versus laboratory alkalinity by (a) TDS and (b) pH. Black dashed line indicating directly proportional 1:1.

4.2.3 Charge imbalance results

A charge imbalance of ±20% was used as the limit where the charge imbalance (CI) can be explained and interpreted (Nordstrom et al. 2009). The mean, median and standard deviation of CI results are -8.4%, -4.2% and 24.7% respectively (Table 4.4). While the mean and the median are close to 0% which is the ideal balance theoretically, the standard deviation indicates a slight dispersion of the CI results, although the maximum and minimum values are far away from the mean. The latter values are very high which could

be an error in the analytical procedure and/or another chemical process may be involved such as speciation.

The charge imbalance (CI) averages were also calculated for the three main drainage basins in the study region, for the different sampling periods (Table 4.5). A total of 167 samples are outside ±20%, however the CI averages for the three main drainage basins are < ±20%.

Table 4.4: Statistics of charge imbalance results for all 812 water samples and for 645 water samples within < ±20% CI range.

Charge Imbalance	**All**	**<±20%**
Mean	-8.4	-0.6
Standard Error	0.9	0.4
Median	-4.2	-0.5
Standard Deviation	24.7	10.1
Sample Variance	608.7	101.7
Range	254.8	39.6
Minimum	-198.8	-19.9
Maximum	56.0	19.7
Sum	-6799.4	-368.5
Count	812	645
Confidence Level (95%)	1.7	0.8

Table 4.5: CI % averages for the Maipo, the Aconcagua and the La Ligua basins by different season sampling campaigns.

	Low Flow-2007	High Flow-2007/2008	Low Flow-2008	**Total**
Maipo Basin	-3.5	-3.7	-3.8	**-11.9**
Aconcagua Basin	-10.3	-2.3	-7.4	**-6.3**
La Ligua Basin	11.7	14.2	9.8	**11.9**

Nordstrom et al. (2009) established two errors in calculating charge imbalance for water of low pH. These include the omission of H^+ concentration as a cation, and the omission of speciation data. Fifteen of the water samples analysed were below pH 4, most of them collected in areas of hydrothermal alteration. The hydrogen concentration correction was calculated for the samples, but the corrected CI values did not change substantially

(Figure 4.7). Some high CI % values also occurred around neutral to basic pH values, suggesting that another chemical process such as speciation could be affecting these samples.

A histogram of the charge imbalance results was plotted for the 645 water samples in which the CI values were lower than ±20% (Figure 4.8). The distribution was similar to a Normal distribution where the mean and the standard deviation are -0.6% and 10.1% respectively (Table 4.4).

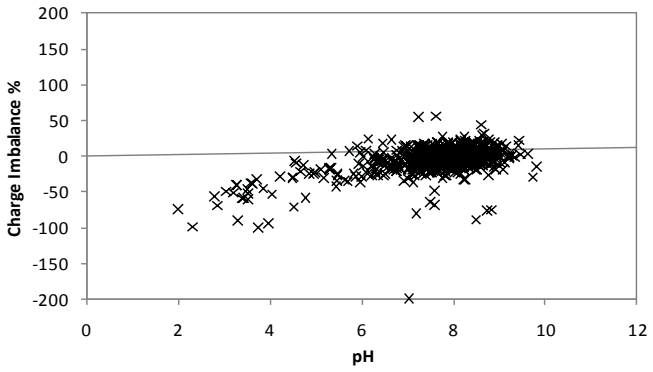


Figure 4.7: Charge imbalance including H^+ versus pH data for water samples.

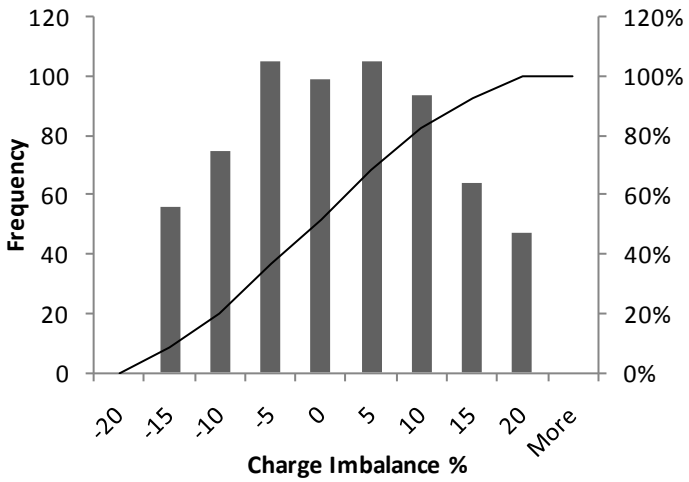


Figure 4.8: Histogram of the CI distribution and accumulated frequency for all the water samples having CI <±20%.

Overall, the CI values calculated for the all samples and the separate drainage basins are acceptable and follow a normal distribution. However, the results showed that some chemical reactions occurring in the waters affect the CI. As was demonstrated by Nordstrom et al. (2009) the speciation must be calculated for waters of low pH when calculating CI; in this study speciation of ions and compounds may be affecting waters of neutral to high pH.

4.3 Characterisation of chemicals and developing the regional hydrogeochemical baseline

One hundred and forty five samples collected during the low flow period from February to June 2008 were selected to prepare the regional hydrogeochemical dataset (Table 3.1). The selection of the sample set used was based on a comparison with previous season datasets and the annual data. This sampling period included more sampling sites than the previous year. An example of this comparison is shown for calcium (Figure 4.9).

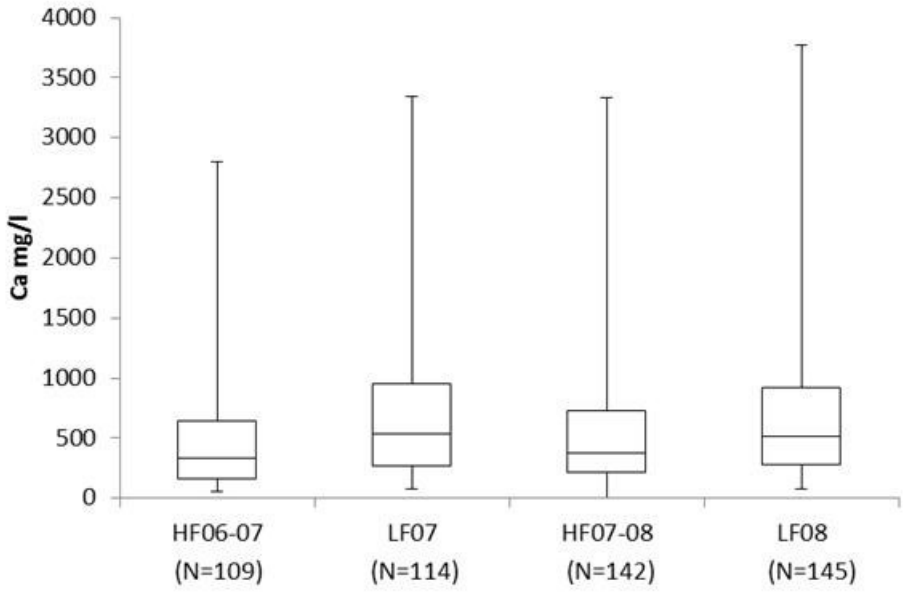


Figure 4.9: Box-whisker charts of calcium for season high flow (HF) and low flow (LF) between 2006 and 2008. The number of samples (N) is in brackets. The last season covered more sampling sites and is less diluted than previous seasons.

4.3.1 Statistical analysis of regional hydrogeochemical data

Summary statistics for the regional surface water sample data for major ions, selected trace elements and other chemical parameters are listed in Table 4.6; the full statistical summary of all measured parameters is in Appendix E and the list of analytical results is given in Appendix F.

Pearson product-moment correlation coefficients were calculated to a significant level p of 0.001 for major ions, selected trace elements and other chemical parameters using Geosoft Oasis Montaj© v 8.0 (Figure 4.10). The logarithmic transformation tool was applied to the selected chemicals because their distribution was found to be log-normal (Figure 4.11).

Spearman rank correlation coefficient rho (r_s) and significance p-values (p) were calculated for major ions, selected trace elements and other chemical parameters using MATLAB (Table 4.7). Pairs of data with medium-low ($r_s \geq 0.4$) to very strong ($r_s \geq 0.9$) correlation coefficient values with very high significance levels ($p \leq 0.001$) were considered to be correlated significantly. P-values are interpreted as the probability of the correlation r_s calculated to be the result of random chance, and the smaller the p-value is the less likely it is that the correlation r_s is false.

Table 4.6: Statistical summary and background levels for major ions, selected trace elements and other chemical parameters. The WGVs correspond to Chilean drinking water regulated values and to (*) WHO guideline values where no Chilean regulated values were available and to (**) EU regulated values where no Chilean or WHO were available. The percentage of samples above the WGV is shown in bold.

Chemical	Unit	DL	Min	Max	Median	Mean	SD	Background		WGV	%Samples >WGV
								Mean	THLD		
Ag	µg/l	0.05	<0.05	0.16	<0.05	<0.05	0.01	<0.05	<0.05	N/A	N/A
Al	µg/l	1	1	12287	15	325	1482	25	170	200**	**6.9**
As	µg/l	0.5	<0.5	65.9	3.1	4.7	7.4	3.2	10	10	**6.9**
Ca	mg/l	0.05	8	377	51	76	71	43	120	N/A	N/A
Cd	µg/l	0.05	<0.05	3.31	<0.05	0.15	0.39	0.07	0.63	10	0
Cl^-	mg/l	1	<1	426	8	34	67	12	81	400	**0.7**
Co	µg/l	0.02	<0.02	88	0.1	3.4	10.7	0.4	6	N/A	N/A
Cu	µg/l	0.1	0.3	11693	1.6	150	1056	6.2	102	2000	**2.0**
EC	µS/cm	0.1	66	1577	324	440	356	340	940	2500**	0
F^-	µg/l	20	22	1010	120	164	136	136	335	1500	0
Fe	µg/l	10	<10	44860	13	528	3822	19	170	300	**6.9**
HCO_3^-	mg/l	0	0	220	78	80	52	67	145	N/A	N/A
Hg	µg/l	0.1	<0.1	8.6	0.2	0.4	0.8	0.3	1	1	**4.8**
K	mg/l	0.05	0.1	25	1	2	3	1.2	3.9	N/A	N/A
Mg	mg/l	0.05	0.8	38	8	10	7	8	20	125	0
Mo	µg/l	0.1	<0.1	38.5	2.1	3	3.8	2.4	8.1	70*	0
Na	mg/l	0.05	0.2	240	12	26	39	12	42	N/A	N/A
Ni	µg/l	0.2	<0.2	59.1	<0.2	2.8	7.9	0.5	5	70*	0
NO_3^-	mg/l	0.05	<0.05	34	0.31	2	5.5	0.5	3	50	0
P^-	µg/l	20	<20	9021	34	134	60	34	67	N/A	N/A
Pb	µg/l	0.1	<0.1	4	<0.1	0.2	0.5	0.1	0.8	50	0
pH	pH	N/A	2	9	7.8	7.6	1.1	7.8	6.5-9	6.5-8.5	**13.8**
SO_4^{-2}	mg/l	3	12	1360	114	204	229	99	314	500	**8.3**
TDS	mg/l	2	34	1524	287	391	320	290	783	1500	**0.7**
Zn	µg/l	0.5	<0.5	345	1.5	21	54	3.9	28	3000	0

THLD: threshold; EC: electrical conductivity; TDS: total dissolved solids; N/A: not applicable.

Table 4.7: Spearman rank correlation matrix for chemical parameters. Rho values ≥0.4 are in bold.

	Al	HCO3	As	Ca	Cd	Cl	Cu	EC	F	Fe	Hg	K	Mg	Mn	Mo	Na	Ni	NO3	P	Pb	pH	SO4	TDS	Zn
Al	1.00																							
HCO3	-0.33*	1.00																						
As	-0.13	0.22	1.00																					
Ca	0.26	**0.44***	-0.06	1.00																				
Cd	**0.49***	**-0.50***	-0.35*	0.19	1.00																			
Cl	0.12	**0.48***	0.19	**0.67***	-0.01	1.00																		
Cu	**0.53***	-0.12	-0.30*	0.33*	**0.62***	0.17	1.00																	
EC	0.24	**0.51***	0.01	**0.95***	0.15	**0.75***	0.36*	1.00																
F	**0.53***	-0.10	-0.22	**0.59***	0.39*	0.32*	**0.48***	**0.57***	1.00															
Fe	0.28*	-0.11	-0.14	0.19	0.21	0.09	0.28*	0.19	0.26	1.00														
Hg	0.11	-0.04	0.18	0.06	0.06	0.14	-0.03	0.09	0.05	0.15	1.00													
K	0.33	0.33*	-0.02	**0.81***	0.19	**0.74***	0.37*	**0.83***	**0.59***	0.21	0.08	1.00												
Mg	0.18	**0.57***	-0.11	**0.85***	0.15	**0.62***	0.34*	**0.88***	**0.52***	0.19	0.06	**0.74***	1.00											
Mn	**0.66***	-0.10	-0.26	**0.52***	**0.59***	**0.43***	**0.61***	**0.52***	**0.60***	**0.46***	0.09	**0.59***	**0.50***	1.00										
Mo	-0.07	0.24	0.26	0.39*	-0.11	**0.48***	0.02	0.38*	0.23	-0.23	0.00	**0.50***	0.21	0.00	1.00									
Na	0.09	**0.61***	0.28*	**0.63***	-0.04	**0.88***	0.18	**0.77***	0.31*	0.06	0.09	**0.67***	**0.68***	**0.41***	0.36*	1.00								
Ni	**0.48***	-0.26	-0.35*	**0.50***	**0.67***	0.20	**0.54***	**0.47***	**0.66***	**0.43***	0.08	**0.46***	**0.43***	**0.67***	-0.02	0.16	1.00							
NO3	0.09	**0.43***	-0.06	**0.41***	0.11	**0.42***	**0.46***	**0.44***	0.20	0.14	-0.06	**0.40***	**0.53***	0.36*	0.10	**0.45***	0.24	1.00						
P	-0.30*	0.22	0.11	-0.13	-0.14	0.00	0.08	-0.08	-0.24	0.04	0.05	-0.04	-0.02	-0.11	-0.02	0.01	-0.19	0.25	1.00					
Pb	0.05	0.20	-0.19	0.24	0.04	0.06	0.24	0.26	0.16	0.11	-0.18	0.20	0.31*	0.17	-0.02	0.14	0.19	0.33*	0.27*	1.00				
pH	-0.31*	**0.41***	0.33*	0.01	**-0.49***	0.14	-0.38*	0.04	-0.18	-0.34*	0.04	-0.03	-0.01	**-0.41***	0.20	0.19	-0.38*	-0.08	-0.10	-0.20	1.00			
SO4	**0.44***	0.14	-0.15	**0.92***	0.34*	**0.55***	**0.42***	**0.86***	**0.75***	0.29*	0.11	**0.79***	**0.75***	**0.64***	0.36*	**0.49***	**0.64***	0.31*	-0.21	0.26	-0.15	1.00		
TDS	0.27*	**0.45***	-0.02	**0.97***	0.20	**0.71***	0.36*	**0.98***	**0.61***	0.23	0.07	**0.83***	**0.88***	**0.55***	0.36*	**0.71***	**0.52***	**0.43***	-0.09	0.28*	-0.01	**0.90***	1.00	
Zn	**0.50***	-0.25	-0.25	0.37*	**0.66***	0.14	**0.72***	0.35*	**0.53***	0.35*	0.07	0.36*	0.29*	**0.60***	0.03	0.13	**0.65***	0.31*	-0.05	0.27	**-0.47***	**0.53***	0.39*	1.00

*p<0.001

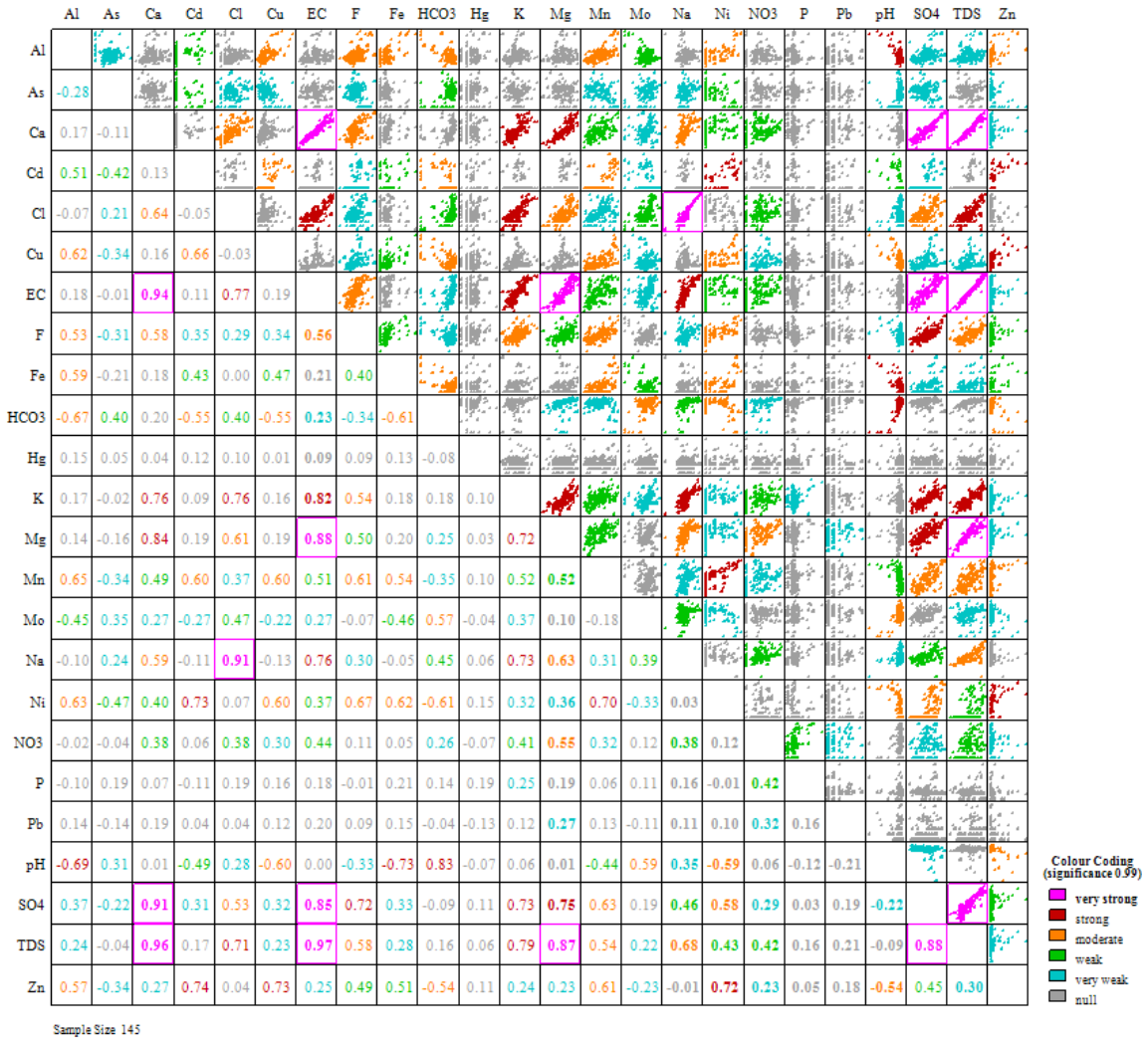


Figure 4.10: Pearson correlation matrix for chemical parameters in the lower-left and scatter plots in the upper-right. Correlation coefficients and scatter plots coloured by the degree of correlation given by default.

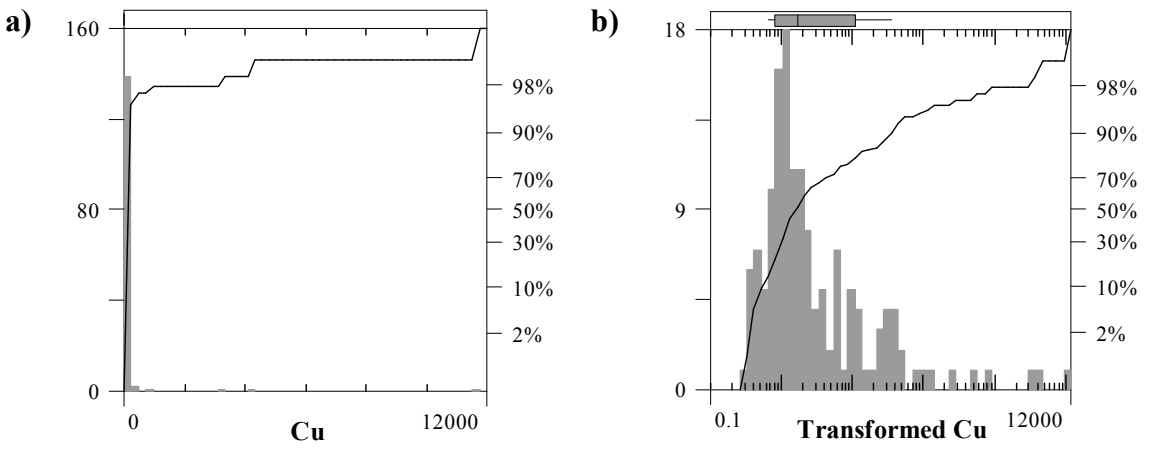


Figure 4.11: Histogram for Cu showing the (a) raw distribution and the (b) logarithmic transformation of the data

4.3.2 Multivariate data analysis

Factor analysis was performed after excluding those parameters with more than 50% of the sample concentrations below the detection limits (Table 4.8). The data were log-transformed (Figure 4.11). The factor loadings were extracted using principal components analysis (PCA) and the results were rotated as varimax normalised.

Table 4.8: List of chemicals included and excluded in the factor analysis

	Included	Excluded
Elements/Chemicals	Al, As, B, Ba, Br, Ca, Cd, Cl, Co, Cs, Cu, F, Fe, HCO3, Hg, K, Li, Mg, Mn, Mo, Na, Nd, Ni, No3, P, Pb, pH, Pr, Rb, S, Sb Sc, Se, Si, Sr, TDS Tl, U, V, W, Zn, Zr	Ag, Au, Be, Bi, Ce, Cr, Dy, Er, Eu, Ga, Gd, Ge, Hf, Ho, In, Ir, La, Lu, Nb, Os, Pd, Pt, Re, Rh, Ru, Sm, Sn, Ta, Tb, Te, Th, Ti, Tm, W, Y, Yb, DOC

The first two factors (Table 4.9) account for the 52.6% of the total variation. The first (Factor 1) correlates positively with alkaline earth metals (Sr, Ca, Mg, Ba), alkali metals (K, Rb, Li, Na, Cs), non-metals (S, Se), halogens (Cl, F) and TDS (Table 4.9) which dominate the dissolved salts from the evaporites (Figure 4.12). The second (Factor 2) correlates very positively with the rare earth metals (Nd, Pr), transition metals (Co, Cu, Zn, Ni, Cd, Mn, Fe), the metal Al, and correlates highly negatively with HCO_3 and pH (Table 4.9) which reflect dissolved metals from areas of metalliferous mineralisation and hydrothermal alteration (Figure 4.12).

The scores were calculated for each sample by the factor loadings for both Factor 1 and 2 (Figure 4.13). Samples from the Maipo Basin have groups of samples with high scores for Factor 1, reflecting the presence of evaporites, as well as Factor 2, which reflects the presence of metalliferous mineralisation and hydrothermal alteration.

Table 4.9: Loadings for the eight factors calculated. Coloured by the highest (pink) to the lowest (black) loading.

ASSAY	F1	ASSAY	F2	ASSAY	F3	ASSAY	F4	ASSAY	F5	ASSAY	F6	ASSAY	F7	ASSAY	F8
Sr	0.939	Nd	0.916	Sc	0.921	Sb	0.781	Cs	0.445	Zr	0.627	Se	0.312	Hg	0.878
Ca	0.924	Pr	0.888	Si	0.891	W	0.775	Tl	0.427	As	0.519	Pb	0.217	P	0.335
TDS	0.914	Co	0.838	Br	0.497	Mo	0.625	Li	0.236	P	0.386	F	0.210	Cs	0.166
S	0.885	Cu	0.829	V	0.431	As	0.383	F	0.214	V	0.365	P	0.149	Fe	0.165
K	0.862	Zn	0.813	Na	0.368	Se	0.305	Al	0.118	Fe	0.319	S	0.143	As	0.125
Rb	0.831	Ni	0.805	Pb	0.291	Cs	0.251	Rb	0.096	U	0.275	Pr	0.138	Cl	0.107
Mg	0.806	Cd	0.804	P	0.279	Br	0.233	W	0.095	Al	0.251	Fe	0.098	Rb	0.101
Li	0.786	Al	0.804	Mg	0.233	pH	0.208	Ni	0.078	Li	0.162	Nd	0.095	Li	0.088
Cl	0.749	Mn	0.709	NO3	0.195	B	0.204	Co	0.069	Pb	0.152	Ni	0.084	Br	0.086
Na	0.707	Fe	0.690	Se	0.168	Rb	0.199	As	0.060	Cs	0.137	Sc	0.061	Ni	0.073
Se	0.703	F	0.476	Cl	0.166	P	0.190	Pr	0.039	B	0.136	Ca	0.054	Co	0.072
F	0.639	Rb	0.324	Tl	0.160	Cl	0.152	Fe	0.011	Rb	0.133	U	0.046	K	0.053
Ba	0.635	Cs	0.322	F	0.156	Cu	0.145	Nd	0.006	W	0.126	Hg	0.035	Se	0.044
Cs	0.606	S	0.311	Fe	0.137	K	0.140	Se	0.001	Pr	0.117	W	0.015	W	0.039
Tl	0.588	Tl	0.307	TDS	0.123	Li	0.127	B	-0.002	Nd	0.099	Zn	0.008	Sb	0.039
U	0.588	Zr	0.297	W	0.123	Zn	0.116	Na	-0.011	K	0.081	Sr	0.004	Na	0.035
B	0.525	Sc	0.160	Nd	0.101	Na	0.115	Hg	-0.019	Br	0.073	Al	0.001	Cd	0.032
Br	0.521	Li	0.139	B	0.085	HCO3	0.084	pH	-0.026	Na	0.062	Cu	-0.002	Tl	0.025
Mn	0.464	TDS	0.130	Zn	0.079	U	0.065	S	-0.032	TDS	0.059	Zr	-0.041	Mn	0.012
Mo	0.381	Si	0.123	K	0.078	NO3	0.050	Cd	-0.034	Cl	0.059	TDS	-0.057	F	0.001
Ni	0.350	K	0.097	Pr	0.067	Cd	0.008	Sr	-0.041	Tl	0.056	Mo	-0.069	Sc	-0.009
Co	0.348	Hg	0.096	Mn	0.050	F	0.008	Cl	-0.078	Sc	0.051	Tl	-0.079	V	-0.011
NO3	0.324	Pb	0.089	Ni	0.045	Hg	0.003	Sc	-0.078	Hg	-0.006	Rb	-0.085	S	-0.017
HCO3	0.216	Mg	0.081	Ca	0.037	S	-0.017	Zr	-0.086	Sr	-0.007	Si	-0.099	Al	-0.018
Zn	0.196	NO3	0.067	Zr	0.035	Sc	-0.017	Zn	-0.091	F	-0.016	Cd	-0.113	Zn	-0.022
Pb	0.160	Ca	0.066	HCO3	0.027	Zr	-0.026	Si	-0.098	Si	-0.022	Mg	-0.114	TDS	-0.023
Zr	0.158	Ba	0.064	As	0.016	V	-0.031	Mn	-0.109	Se	-0.031	Sb	-0.119	Pr	-0.030
Al	0.145	Sr	0.050	Cu	0.009	Co	-0.063	Mo	-0.114	Ca	-0.038	K	-0.143	HCO3	-0.038
Fe	0.133	Se	0.040	Hg	0.005	Mn	-0.079	Br	-0.126	Mn	-0.040	Cs	-0.150	B	-0.040
Sb	0.125	P	-0.007	Co	-0.007	Nd	-0.096	Ca	-0.132	NO3	-0.042	NO3	-0.180	pH	-0.041
Hg	0.093	Sb	-0.101	S	-0.022	Ca	-0.099	K	-0.158	Mo	-0.043	Co	-0.193	Mg	-0.049
pH	0.081	U	-0.134	U	-0.023	Ba	-0.108	TDS	-0.163	Co	-0.047	HCO3	-0.249	Nd	-0.056
Cd	0.076	W	-0.136	Rb	-0.047	TDS	-0.109	Sb	-0.185	Cu	-0.058	Mn	-0.250	Mo	-0.056
P	0.054	Cl	-0.149	Cd	-0.056	Si	-0.111	V	-0.248	HCO3	-0.068	pH	-0.260	Sr	-0.058
Si	0.045	Na	-0.214	pH	-0.068	Sr	-0.119	Pb	-0.285	S	-0.070	Ba	-0.274	U	-0.061
Sc	0.035	Br	-0.223	Al	-0.074	Ni	-0.126	HCO3	-0.294	Sb	-0.091	Li	-0.318	Ca	-0.062
Cu	0.032	B	-0.326	Cs	-0.135	Tl	-0.137	Mg	-0.333	Ni	-0.102	As	-0.341	Si	-0.064
Nd	0.007	As	-0.424	Sr	-0.160	Pb	-0.153	Ba	-0.346	Mg	-0.118	V	-0.361	Cu	-0.085
V	0.003	Mo	-0.472	Sb	-0.165	Al	-0.153	Cu	-0.354	Ba	-0.119	Br	-0.402	Ba	-0.089
Pr	-0.028	V	-0.549	Li	-0.200	Pr	-0.162	U	-0.442	Zn	-0.142	Cl	-0.462	Zr	-0.108
As	-0.054	pH	-0.778	Mo	-0.251	Fe	-0.213	P	-0.637	pH	-0.251	Na	-0.474	NO3	-0.142
W	-0.148	HCO3	-0.813	Ba	-0.290	Mg	-0.233	NO3	-0.725	Cd	-0.356	B	-0.606	Pb	-0.432

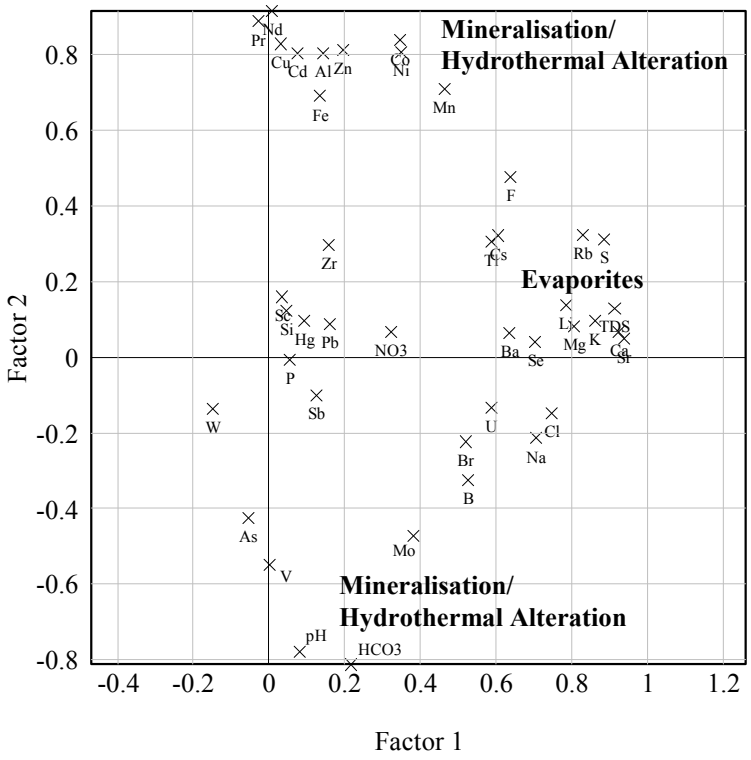


Figure 4.12: Factor 1 versus Factor 2 with the sources indicated.

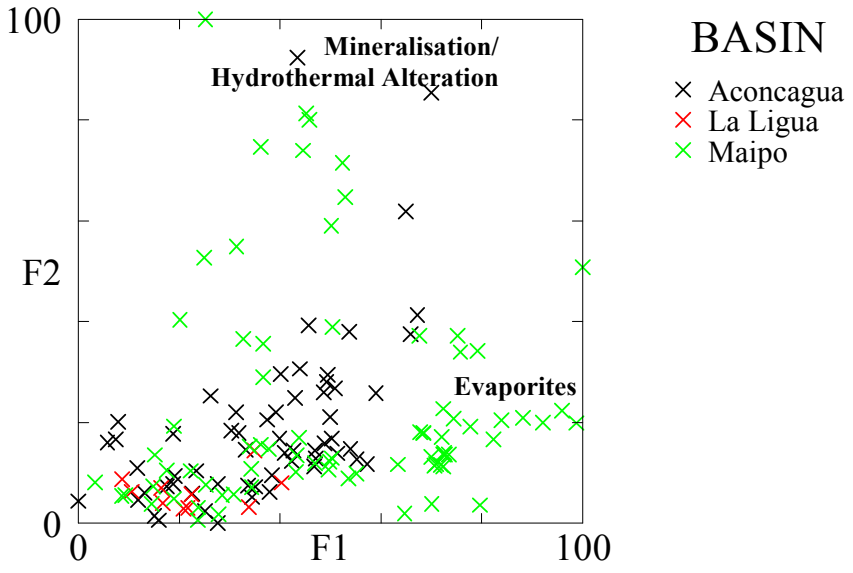


Figure 4.13: Sample scores calculated for Factor 1 (F1) and 2 (F2) for the Aconcagua, La Ligua and Maipo basins. The presence of mineralisation, hydrothermal alteration and evaporites reflected in the correlation of the elements in the factors are shown.

4.3.3 Stream water geochemistry

Field determinations of EC, pH, and TDS results show that most of the samples are neutral to alkaline and have low TDS and EC (Figure 4.14). Samples which have neutral to alkaline pH values with high TDS and EC levels reflect the presence of evaporites in the headwaters of the Maipo and Aconcagua rivers in the AC. Samples which have low pH values with low to high TDS and EC levels reflect the presence of mineralisation and hydrothermally altered areas in the Maipo and Aconcagua basins.

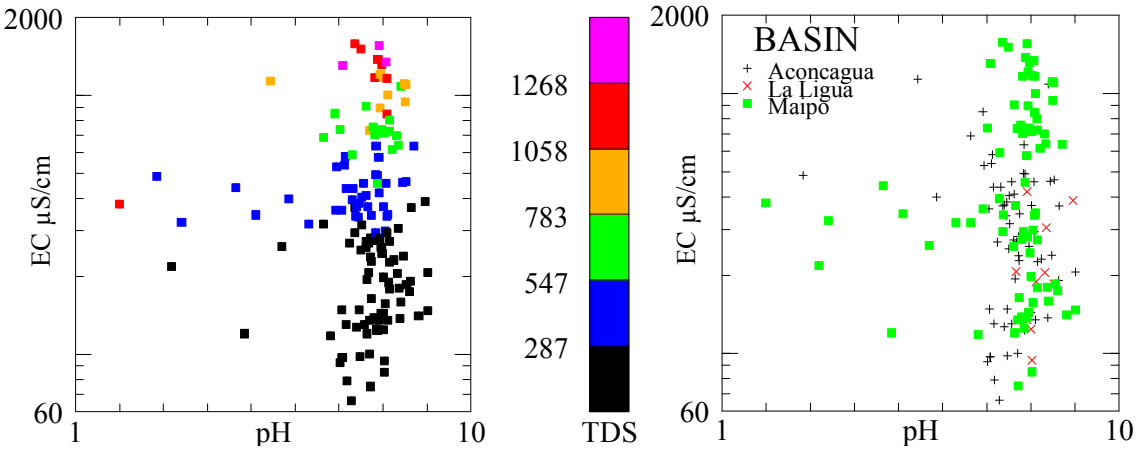


Figure 4.14: EC versus pH scatter diagrams for TDS in mg/l (left) and the Aconcagua, La Ligua and Maipo basins (right).

Piper ternary diagrams of the major cations in the water samples (Figures 4.15 a and b) showed the low TDS samples trend to Ca type for all three basins, although seven samples from the Maipo Basin predominantly with high TDS concentration trend towards the Na+K type reflecting the presence of evaporites. Ternary diagram of major anions showed the samples are dominantly of SO_4 type trending to HCO_3 type with low TDS concentrations for all three basins. Some samples with higher TDS concentration are of SO_4 type trending to Cl in the Maipo Basin reflecting also the presence of evaporites. There is no influence of NO_3^- in the water type except for one sample in the Maipo Basin

that shows a slight trend to NO_3^- (Figures 4.15 e and f). This probably reflects the presence of fertilisers and sewage drainage from a local agricultural community.

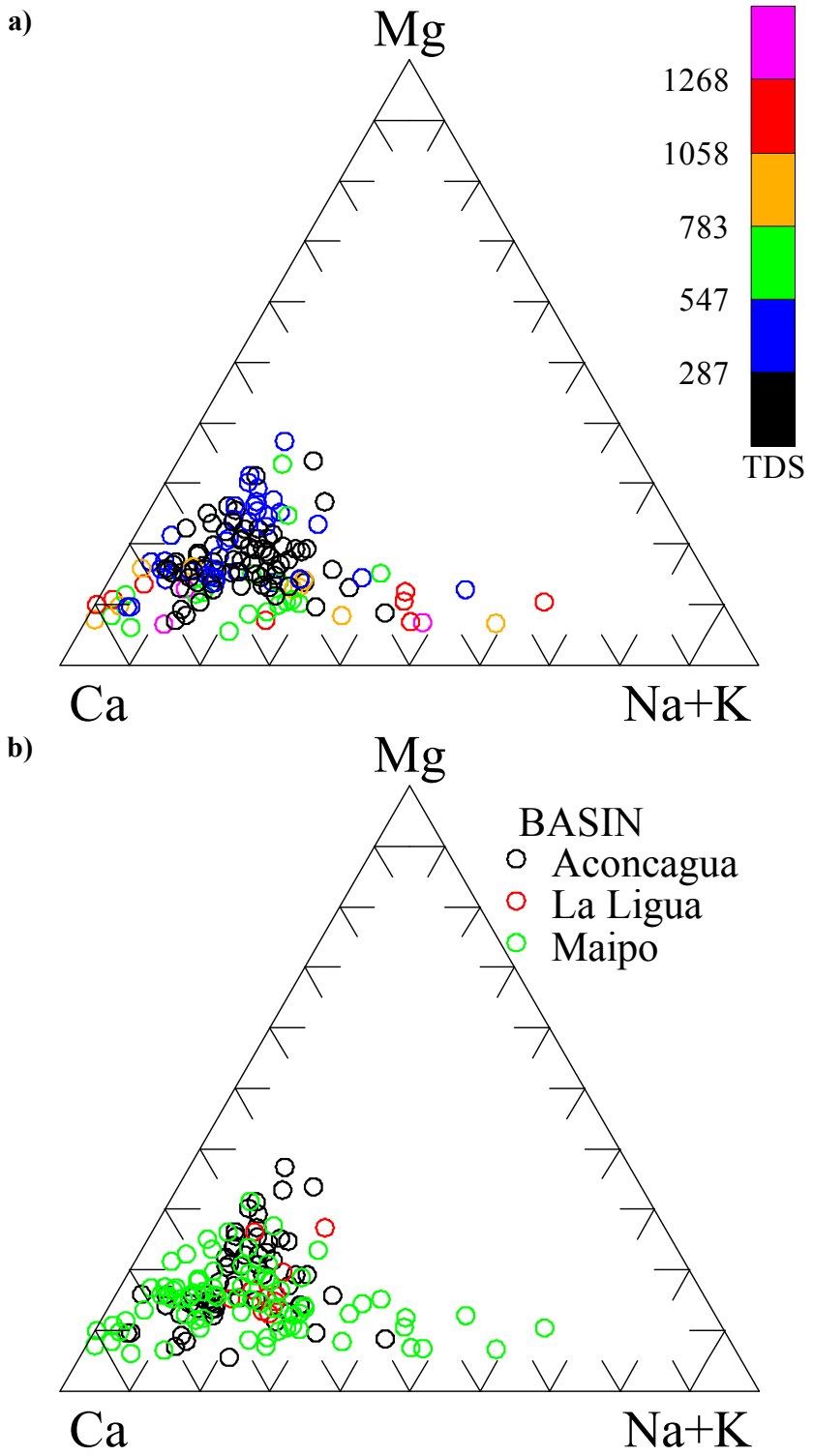
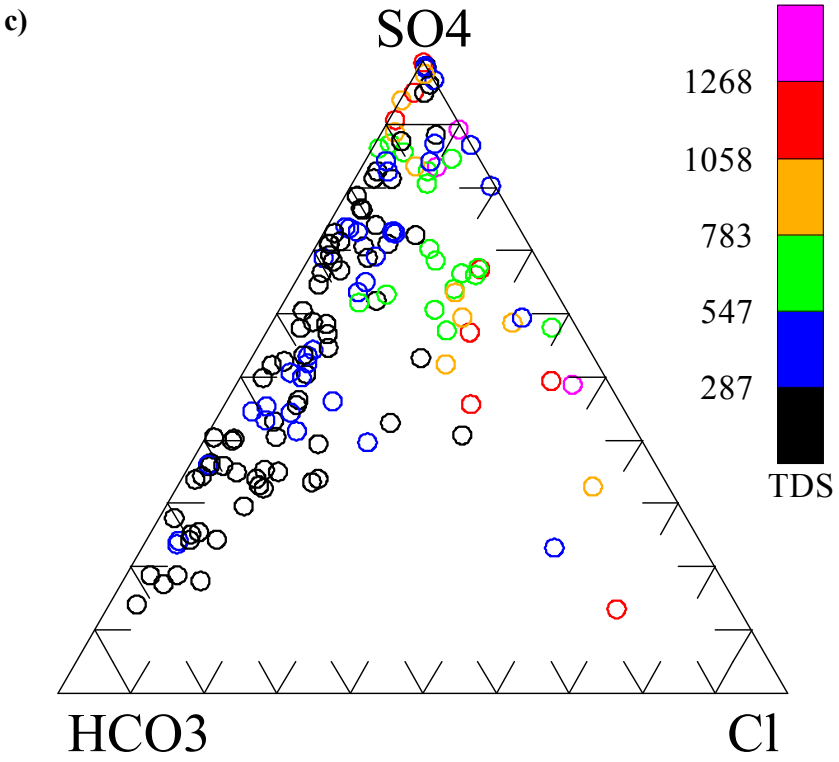
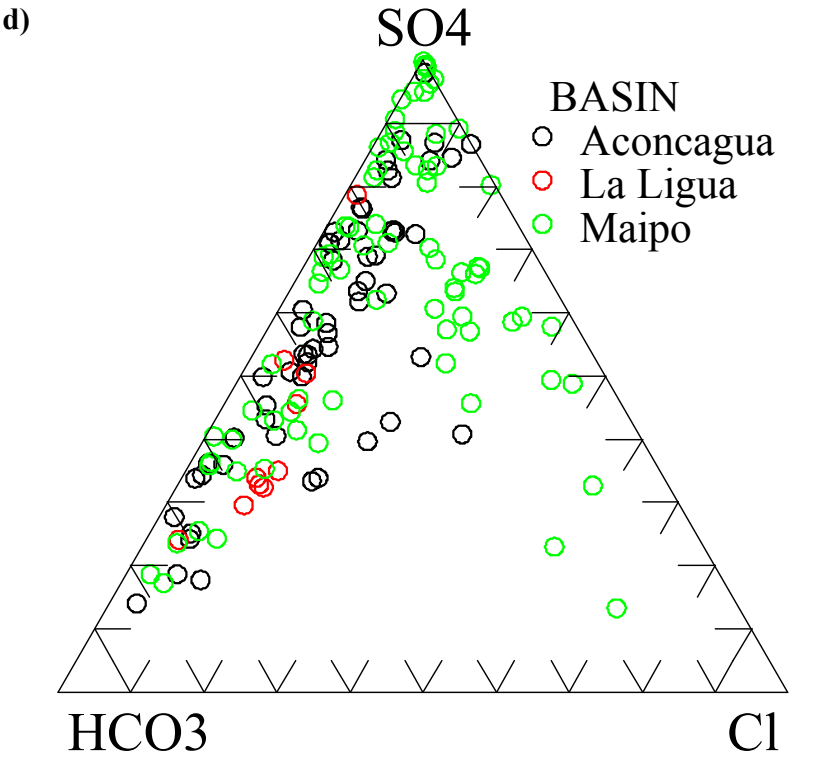
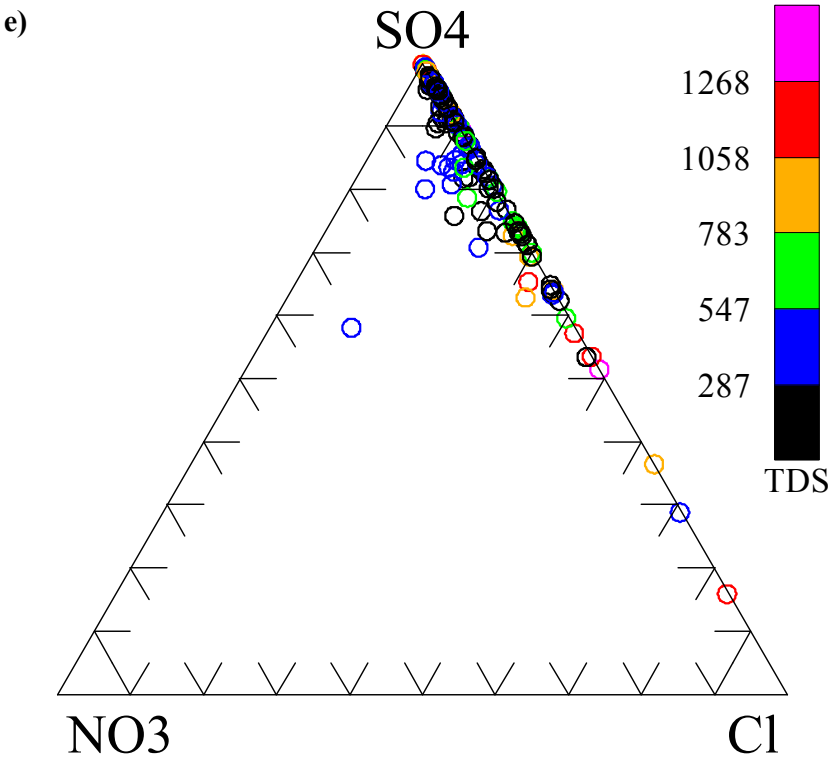


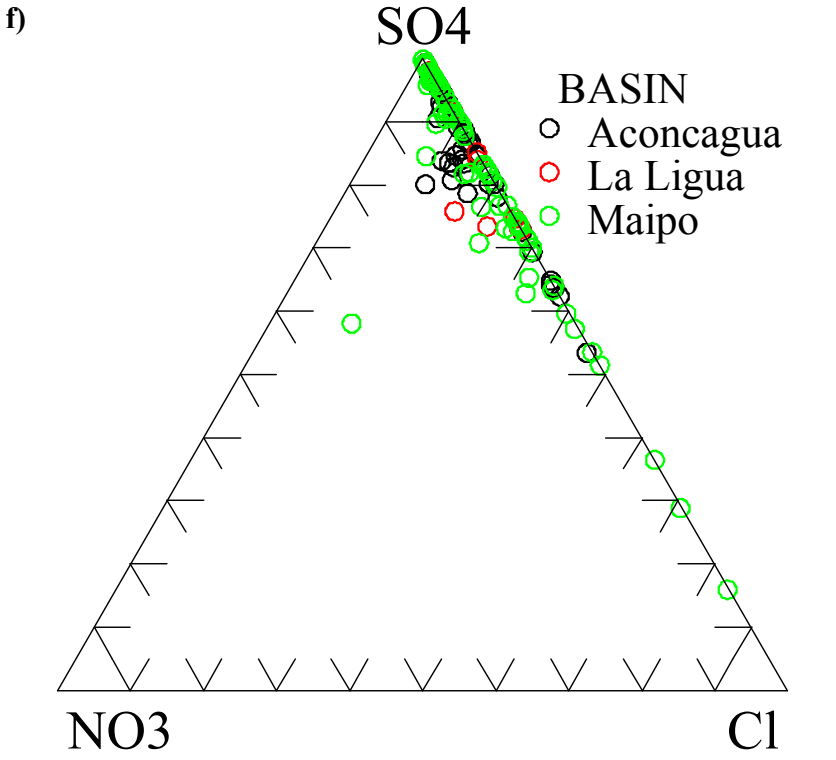
Figure 4.15: Ternary diagrams of major cations (a,b), anions (c,d) and anions compared to nitrate (e,f) coloured by TDS content in mg/l and by basin: Aconcagua (black), La Ligua (red) and Maipo (green).





Continuation **Figure 4.15**





Continuation **Figure 4.15**

4.3.4 Hydrogeochemical baseline maps

The hydrogeochemical baseline maps presented here are for the parameters pH and TDS; the major anions HCO_3^-, Cl, NO_3, P and SO_4; the major cations Ca, Na, Mg Fe and Al; and for the trace elements Cu, As, Ni, Cd, Hg and Pb (Figure 4.17). Other maps including for Ag, B, Co, F, K, Mn, Sb, Se, Sn and Zn are in Appendix D. Histograms showing the frequency distributions of the different populations are included with the maps for each chemical and orange, red and pink colours are used for concentration values above the threshold. Descriptive statistics, samples above the WGVs if any and the location of anomalously high concentrations are indicated for each chemical.

Hydrogen ion activity (pH)

The pH values range from a 2 to 9, with a median of 7.8 and mean of 7.6 with a SD of 1.1 (Table 4.6). The pH data are negatively correlated with Cd, Zn and Mn data and positively correlated with HCO_3^- data (Figure 4.10 and Table 4.7). This negative correlation is also reflected in the factor analysis, Factor 2 (Table 4.9) where the acid values and low HCO_3^- data are highly correlated with the metals reflecting the presence of mineralisation and hydrothermal alteration. Twenty samples (13.6%) fall outside the WGV range of 6.5-8.5 (Table 4.6). The low pH values (2 to <5.5) are related to known Cu-mineralisation which outcrops in the Yerba Loca Stream, Barriga River and Colorado River and to hydrothermal alteration in the Arrayán River (Figures 4.3 and 4.17), none of which has been mined. The highly alkaline values (>8.5) are part of the normal range of background levels and in the AC are related to the bedrock geology including the presence of sedimentary and intermediate to basic volcanic rocks (Figures 4.4 and 4.17).

Total Dissolved Solids (mg/l)

TDS values range from 34 to 1524, with a median of 287 and mean of 391 with a SD of 320 (Table 4.6). TDS data are positively correlated with EC, Ca, SO_4^{-2}, Mg, K, Cl, Na, F, Mn, Ni, HCO_3^- and NO_3^- data (Figure 4.10 and Table 4.7). These correlations are also reflected in the factor analysis, Factor 1 (Table 4.9) where TDS and Ca, Mg, K, Na, S, Cl, F reflect the presence of evaporites. One sample (0.7%) is above the WGV of 1500 mg/l (Table 4.6). Samples with anomalously high concentrations are widely distributed in the Maipo Basin in the Andes and downstream in the CV. They reflect the presence of dissolved major ions, principally high concentrations of Ca and SO_4^{-2} from carbonates and sulphates from limestone and evaporites. There are also anomalously high concentrations of TDS locally in the headwaters of the Yerba Loca Stream and the Barriga River and these are associated with mineralisation (Figures 4.3 and 4.17).

Bicarbonate Alkalinity (HCO_3^-, mg/l)

Bicarbonate alkalinity values range from 0 to 220, with a median of 78 and mean of 80 with a SD of 52 (Table 4.6). HCO_3^- data are positively correlated with Na, Mg, EC, Cl, TDS, Ca, NO_3^- and pH data and negatively correlated with Cd data (Figure 4.10 and Table 4.7). The relation of HCO_3^- data in the factor analysis is explained in the section on pH above. Samples with anomalously high concentrations in the CV reflect the dissolution of carbonates from agricultural liming (Figures 4.3 and 4.17) and in the CC the presence of calcareous rocks (Figures 4.4 and 4.17).

Chlorine (mg/l)

Chlorine values range from <1 to 426, with a median of 8 and mean of 34 with a SD of 67 (Table 4.6). Chlorine data are positively correlated with Na, EC, K, TDS, Ca, Mg, SO_4^{-2},

HCO_3^-, Mo, Mn and NO_3^- data (Figure 4.10 and Table 4.7). The relationship of Cl^- data in the factor analysis is the same as TDS and is associated with the presence of evaporites as shown in Factor 1. One sample (0.7%) is above the WGV of 400 mg/l (Table 4.6). Samples with the highest concentrations reflect the dissolution of the evaporites in the AC with dilution downstream in the Maipo valley (Figures 4.4 and 4.17). They also reflect the presence of salt (NaCl) from the salting of mine and industrial roads in the AC, and the presence of sewage treatment plants and landfill sites in the Mapocho River. This is also mixed with water diverted from the Maipo River through the Canal San Carlos (Figures 4.3 and 4.17). This mixing can be traced using Cl. This conservative element stays dissolved in the water after mixing with the water from the Mapocho River which has a lower Cl concentration than that from the Maipo River (Table 4.10).

Table 4.10: Concentration of elements upflow and downflow the Canal San Carlos

Sample site location	Al µg/l	As µg/l	Ca mg/l	Cl mg/l	Cu µg/l	HCO_3^- mg/l	K mg/l	Na mg/l	SO_4^{-2} mg/l
Mapocho River, up flow the canal	71	1.2	39	7	28.3	37.3	0.8	9	108
Maipo River, water diverted through the canal	8	4.2	141	209	13.7	220	17	146	383
Mapocho River, down flow the canal	60	3.9	173	194	1.3	105.6	4	127	467

Nitrate (mg/l)

Nitrate values range from <0.05 to 34, with a median of 0.31 and mean of 2 with a SD of 5.5 (Table 4.6). Nitrate data are positively correlated with Mg, Cu, Na, EC, HCO_3^-, TDS, Cl, Ca and K data (Figure 4.10 and Table 4.7). There are no samples above the WGV of 50 mg/l (Table 4.6). Samples with anomalously high concentrations are thought to be contaminated with predominantly with fertiliser, and with a minor component of manure and/or sewage in the CV and CC (Figures 4.3 and 4.17).

Phosphorus (µg/l)

Phosphorous values range from <20 to 9021, with a median of 34 and mean of 134 with a SD of 60 (Table 4.6). No significant correlation with other chemicals was found (Table 4.7). Samples with anomalously high concentrations in the CV reflect the use of fertilisers and households sewage, while in the AC they reflect the presence of apatite in porphyry copper mineralisation (Williams & Cesbron 1977; Bouzari et al. 2011) in the Yerba Loca and Riecillos rivers and in the vicinity of the Tupungato Volcano (Figures 4.3 and 4.17).

Sulphate (mg/l)

Sulphate values range from 12 to 1360, with a median of 114 and mean of 204 with a SD of 229 (Table 4.6). Sulphate data are positively correlated with Ca, TDS, EC, K, F, Mg, Mn, Ni, Cl, Zn, Na, Al and Cu data (Figure 4.10 and Table 4.7). This correlation is also reflected in the factor analysis (Table 4.9) where S and TDS, Ca, Mg, K, Na, Cl, F are related in Factor 1 reflecting the presence of evaporites. The relationship between SO_4 and Ca is positive and linear with a R^2 of ~0.9 and the sulphate dissolved from sulphides can be interpreted as a linear relationship but with a slope slightly lower than 0.2989 (Figure 4.16). Thirteen samples (8.3%) are above the WGV of 500 mg/l (Table 4.6). These are mainly in the Maipo Valley and in the headwaters of the Mapocho and Blanco Rivers (Figure 4.3). Samples with anomalously high concentrations reflect the presence of evaporites containing gypsum in the AC with dilution downstream in the CV (Figures 4.4 and 4.17). Also, in the low pH waters of the Yerba Loca, Barriga, and Arrayán rivers the anomalously high concentrations of SO_4^{-2} reflect the presence of sulphides in hydrothermally altered and mineralised rocks.

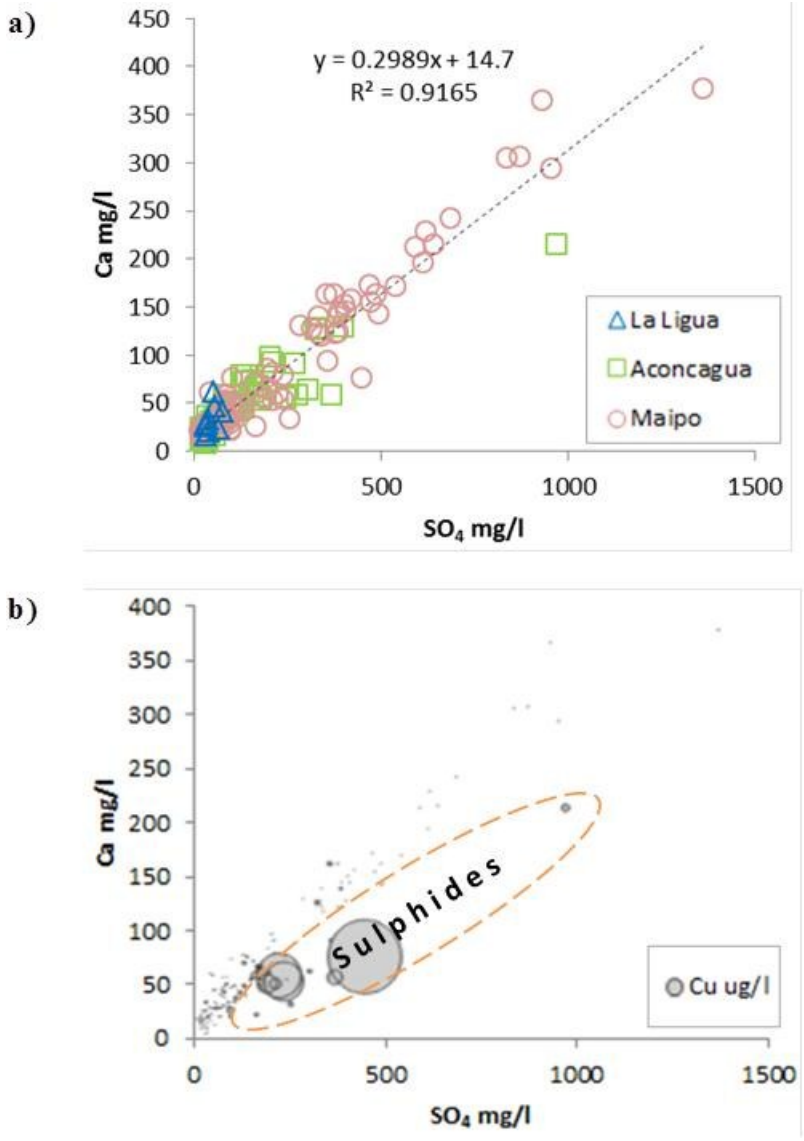


Figure 4.16: Calcium versus sulphate. (a) The relationship between Ca and SO4 is linear with a R^2 of ~0.9. (b) The higher concentrations of Cu reflect the presence of sulphide mineralisation in the system.

Calcium (mg/l)

Calcium values range from 8 to 377, with a median of 51 and mean of 76 with a SD of 71 (Table 4.6). Calcium data are positively correlated with TDS, EC, SO_4^{-2}, Mg, K, Cl, Na, F, Mn, Ni, HCO_3^- and NO_3^- data (Table 4.7). Calcium has an important loading in Factor 1 (evaporites) (Table 4.9) and it has a positive linear relationship with SO_4 (Figure 4.16). Samples with anomalously high concentrations reflect the presence of sulphates and

calcium carbonates in evaporites and limestone in the AC with dilution downstream in the CV, mainly in the Maipo Basin (Figures 4.4 and 4.17).

Sodium (mg/l)

Sodium values range from 0.2 to 240, with a median of 12 and mean of 26 with a SD of 39 (Table 4.6). Sodium data are positively correlated with Cl, EC, TDS, Mg, K, Ca, HCO_3^-, SO_4^{-2}, NO_3^- and Mn data (Table 4.7). Sodium has an important loading in Factor 1 reflecting the presence of evaporites (Table 4.9). Samples with anomalously high concentrations reflect the dissolution of the evaporites in the AC with dilution downstream in the Maipo valley (Figures 4.4 and 4.17). They also reflect the presence of salt as a result of salting of mine and industrial roads in the AC, as well as sewage treatment plants and landfill sites in the Mapocho River. Here it is also mixed with water diverted from the Maipo River through the Canal San Carlos (Figures 4.3 and 4.17 and Table 4.10).

Magnesium (mg/l)

Magnesium values range from 0.8 to 38, with a median of 8 and mean of 10 with a SD of 7 (Table 4.6). Magnesium data are positively correlated with EC, TDS, Ca, SO_4^{-2}, K, Na, Cl, HCO_3^-, NO_3^-, F, Mn and Ni data (Table 4.7). Magnesium has an important loading in Factor 1 reflecting the presence of evaporites (Table 4.9). There are no samples above the WGV of 125 mg/l (Table 4.6). Samples with anomalously high concentrations occur in areas of mineralisation and hydrothermal alteration of the dominant host rock andesitic lithology in the Barriga River catchment and near the Maipo Volcano in the AC (Figures 4.3 and 4.17). They also occur near Catemu and Calera townships in CC and near Santiago in the CV and are thought to reflect the presence of fertiliser and sewage.

Aluminium (µg/l)

Aluminium values range from 1 to 12287, with a median of 15 and mean of 325 with a SD of 1482 (Table 4.6). Aluminium data are positively correlated with Mn, Cu, F, Zn, Cd, Ni and SO_4^{-2} data (Table 4.7). Aluminium has an important loading in Factor 2 reflecting the presence of mineralisation and hydrothermal alteration (Table 4.9). Ten samples (6.8%) are above the WGV of 200 µg/l (Table 4.6). Samples with anomalously high concentrations occur in areas of mineralisation in the Yerba Loca, Barriga and Colorado Rivers and areas of hydrothermal alteration in the Arrayán River in the AC (Figures 4.3 and 4.17). These areas of mineralisation and hydrothermal alteration have not been mined.

Iron (µg/l)

Iron values range from <10 to 44860, with a median of 13 and mean of 528 with a SD of 3822 (Table 4.6). Iron data are positively correlated with Mn and Ni data (Table 4.7). Iron has an important loading in Factor 2 reflecting the presence of mineralisation and hydrothermal alteration (Table 4.9). Ten samples (6.8%) are above the WGV of 300 µg/l (Table 4.6). Samples with anomalously high concentrations occur in areas of mineralisation in the Yerba Loca, San Francisco, Barriga and Colorado Rivers and areas of hydrothermal alteration in the Arrayán River, and near the Maipo Volcano in the AC (Figures 4.3 and 4.17). They also occur in mine area waters near Catemu in the CC.

Copper (µg/l)

Copper values range from 0.3 to 11693, with a median of 1.6 and mean of 150 with a SD of 1056 (Table 4.6). Copper data are positively correlated with Zn, Cd, Mn, Ni, Al, F, NO_3^- and SO_4^{-2} data (Table 4.7). Copper has an important loading in Factor 2 reflecting

the presence of mineralisation and hydrothermal alteration (Table 4.9) and correlates with low pH values. Three samples (2%) are above the WGV of 2000 µg/l (Table 4.6). Samples with anomalously high concentrations occur in areas of mineralisation in the Yerba Loca, San Francisco, Barriga and Colorado Rivers in the AC (Figures 4.3 and 4.17), none of which have been mined.

Arsenic (µg/l)

Arsenic values range from <0.5 to 65.9, with a median of 3.1, mean of 4.7 with a SD of 7.4 (Table 4.6). No significant correlation was found with other chemicals (Figure 4.10 and Table 4.7). Ten samples (6.8%) are above the WGV of 10 µg/l (Table 4.6). Samples with anomalously high concentrations are principally in the Yerba Loca River associated with mineralisation, and in the Riecillos and Arrayán River, and near the Maipo Volcano in the AC reflecting the presence of hydrothermal alteration (Figures 4.3 and 4.17). There is also an anomalous sample near Colina which might be associated with an active geothermal spring which is upstream and it is used as spa.

Nickel (µg/l)

Nickel values range from <0.2 to 59.1, with a median of <0.2 and mean of 2.8 with a SD of 7.9 (Table 4.6). More than 50% of the Ni data (64%) are below the DL of 0.2. Nickel data are positively correlated with Cd, Mn, F, Zn, SO_4^{-2}, Cu, TDS, Ca, Al, EC, K, Fe and Mg data (Table 4.7). Nickel has an important loading in Factor 2 reflecting the presence of mineralisation and hydrothermal alteration (Table 4.9). There are no samples above the WGV of 70 µg/l (Table 4.6). Samples with anomalously high concentrations occur in areas of mineralisation in the Yerba Loca, San Francisco, Barriga and Colorado Rivers

and areas of hydrothermal alteration in the Arrayán and Colorado Rivers, and near the Maipo Volcano in the AC (Figures 4.3 and 4.17).

Cadmium (µg/l)

Cadmium values range from <0.05 to 3.31, with a median of <0.05 and mean of 0.15 with a SD of 0.39 (Table 4.6). More than 50% of the Cd data (79%) are below the DL of 0.05. Cadmium data are positively correlated with Ni, Zn, Cu, Mn and Al and negatively correlated with HCO_3^- and pH (Table 4.7). Cadmium has an important loading in Factor 2 reflecting the presence of mineralisation and hydrothermal alteration (Table 4.9). There are no samples above the WGV of 10 µg/l (Table 4.6). Samples with anomalously high concentrations occur in areas of mineralisation in the San Francisco, Barriga and Colorado Rivers and areas of hydrothermal alteration in the Colorado River in the AC (Figures 4.3 and 4.17). There is also one anomalous sample in the mine area waters of Los Bronces in the San Francisco River.

Mercury (µg/l)

Mercury values range from <0.1 to 8.6, with median of 0.2 and mean of 0.4 with a SD of 0.8 (Table 4.6). No significant correlation was found with other chemicals (Figure 4.10 and Table 4.7). Seven samples (4.8%) are above the WGV of 1 µg/l (Table 4.6). Samples with anomalously high concentrations occur in areas of unmined mineralisation in the Barriga River and areas of hydrothermal alteration in the Arrayán and Colorado Rivers in the AC (Figures 4.3 and 4.17). There are also anomalously high concentrations of Hg in the Molina and Maipo Rivers in the AC and downstream of Santiago possibly related to the disposal of batteries, thermometers and/or the use of pesticides there. There is no authorised waste incineration in the study area that might contribute to these anomalous

values. The two coal power plants in the region are near Valparaiso city on the coast 50-80 km to the W of the study area (Figure 4.1) and the prevailing wind direction in Central Chile is from the S and SW during spring and summer and from N and NW in autumn and winter (INE 2012a). These settings do not indicate that coal burning is the source of the anomalous Hg values

Lead (µg/l)

Lead values range from <0.1 to 4, with median of <0.1 and mean of 0.2 with a SD of 0.5 (Table 4.6). More than 50% of the Pb data (61%) are below the DL of 0.05 (Pb map, Figure 4.17). No significant correlation was found with other chemicals (Figure 4.10 and Table 4.7). There are no samples above the WGV of 50 µg/l. (Table 4.6). Samples with anomalously high concentrations occur in the mineralised area in the Colorado River and in the vicinity of the abandoned La Poza and Restauradora Pb-mines near Catemu in the CC (Figures 4.3 and 4.17). There are also anomalously high concentrations of Pb in the vicinity of Catemu, Mostazal and Pirque townships probably related to fly-tipping of batteries, paint and lead pipes.

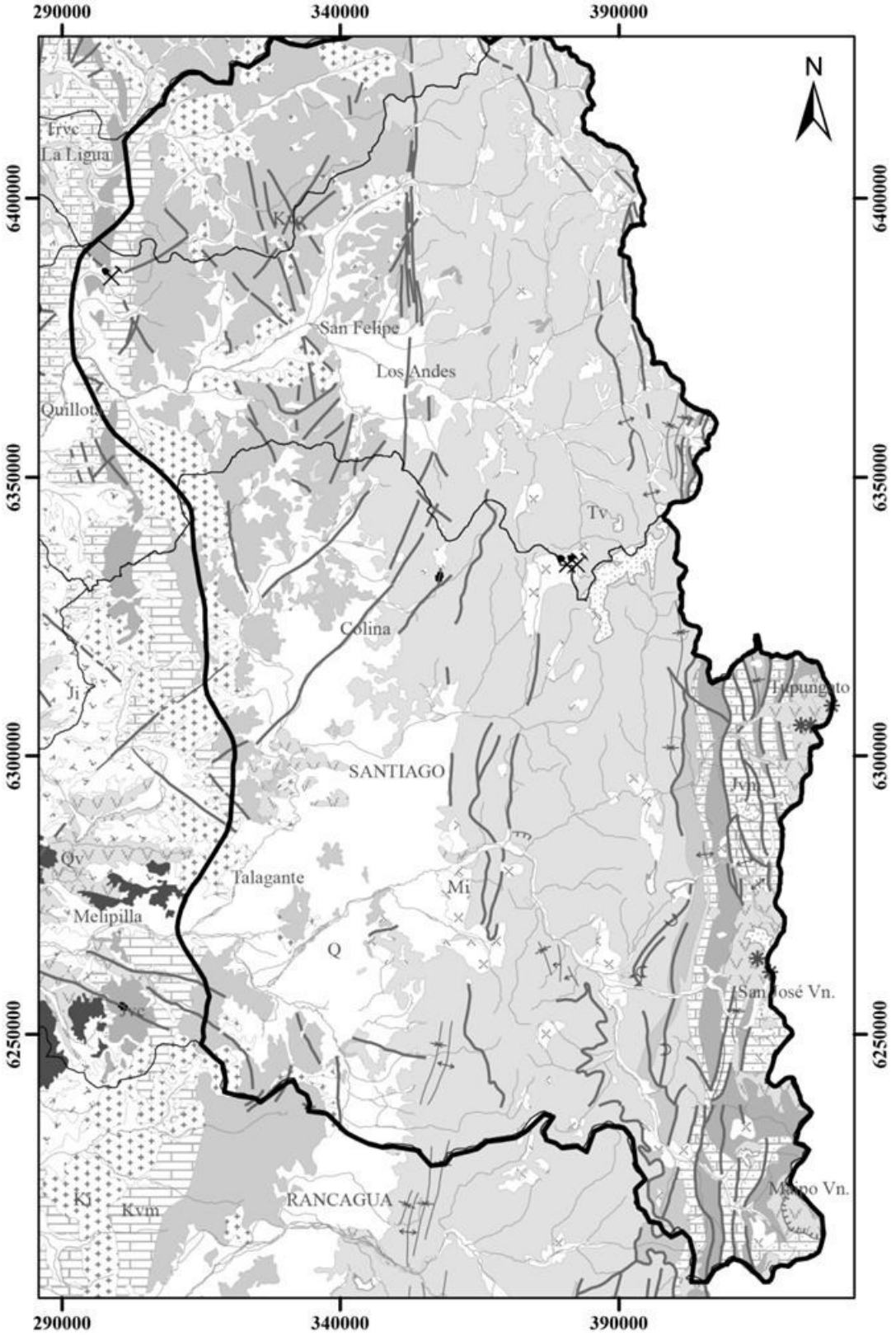
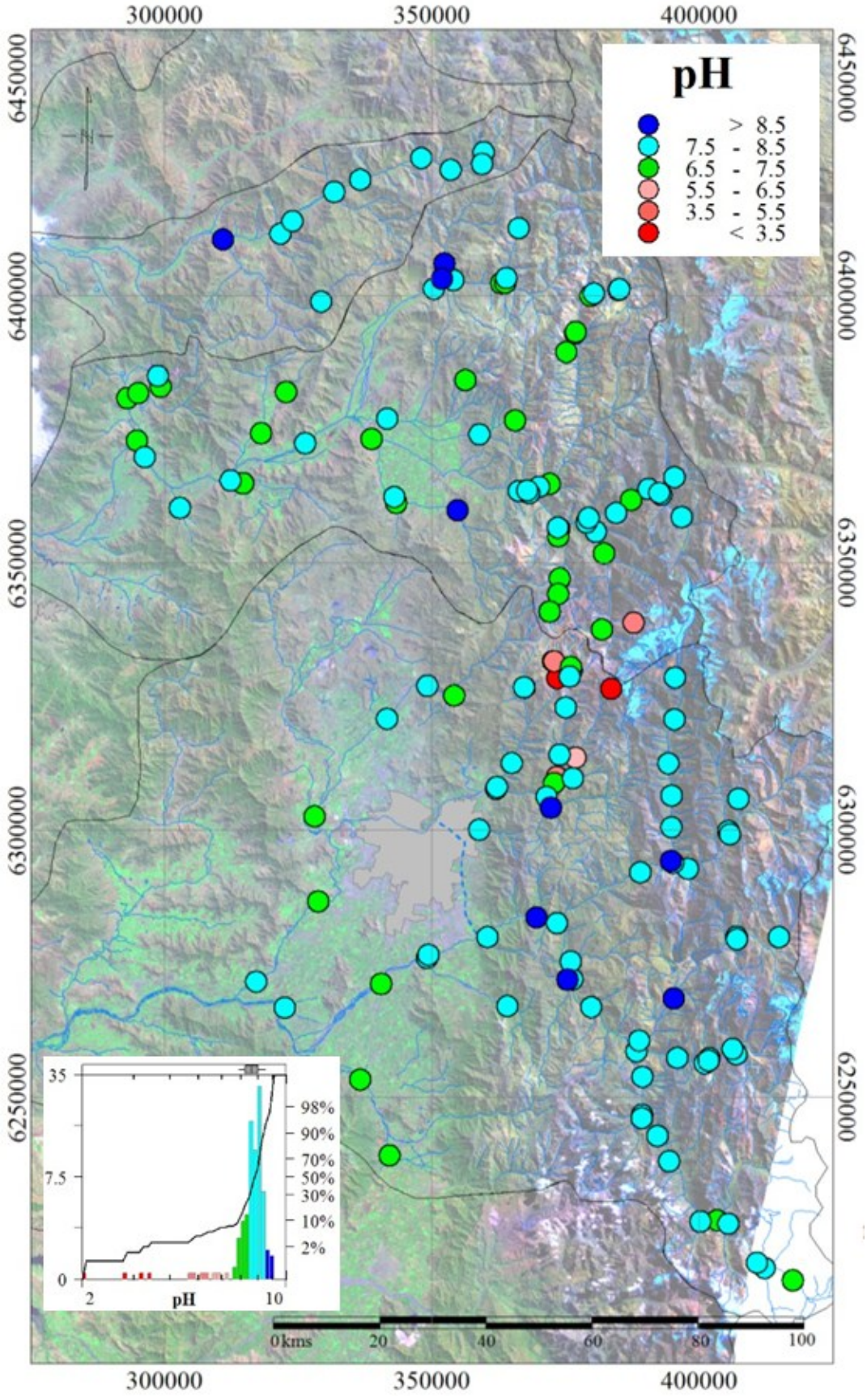
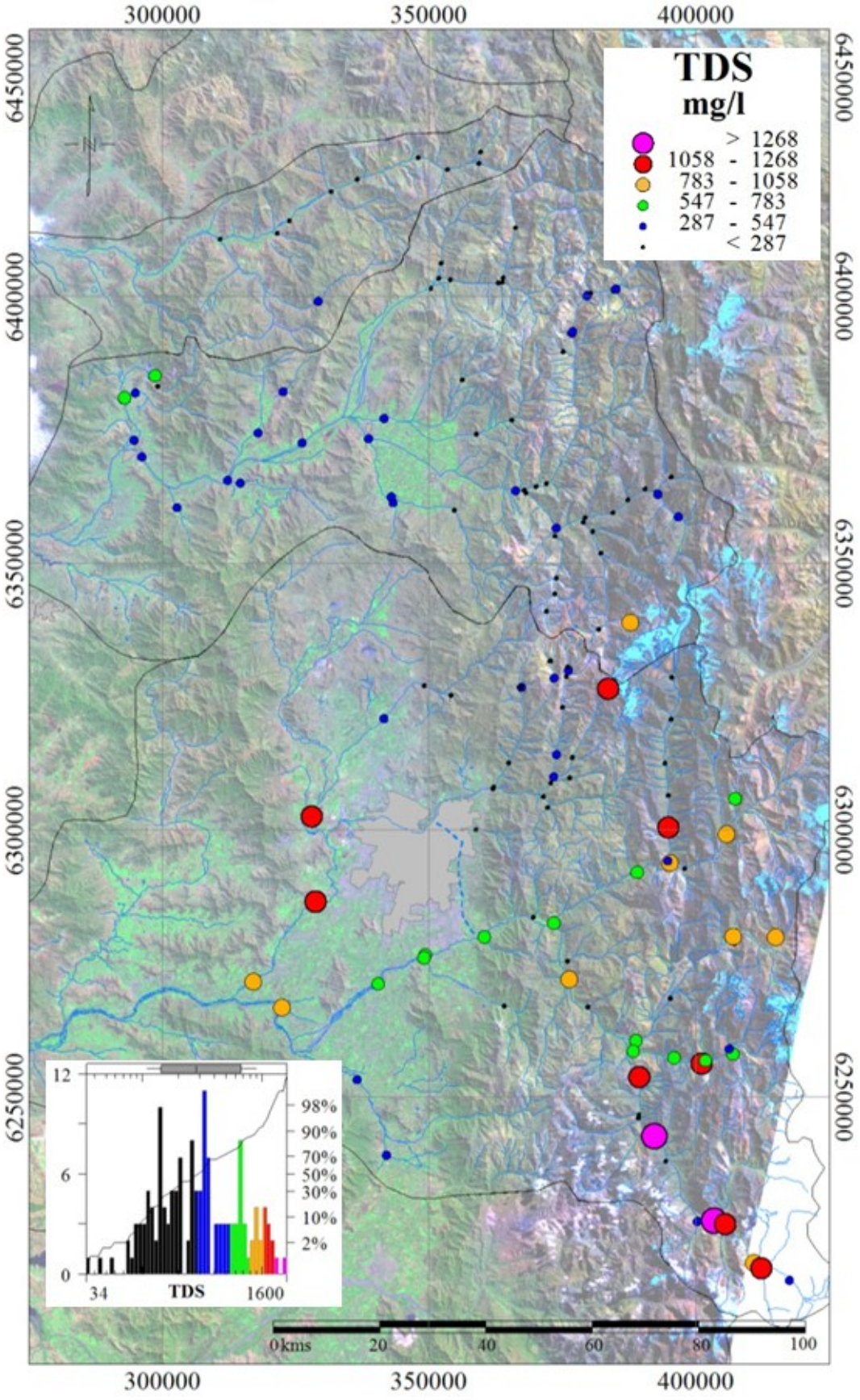
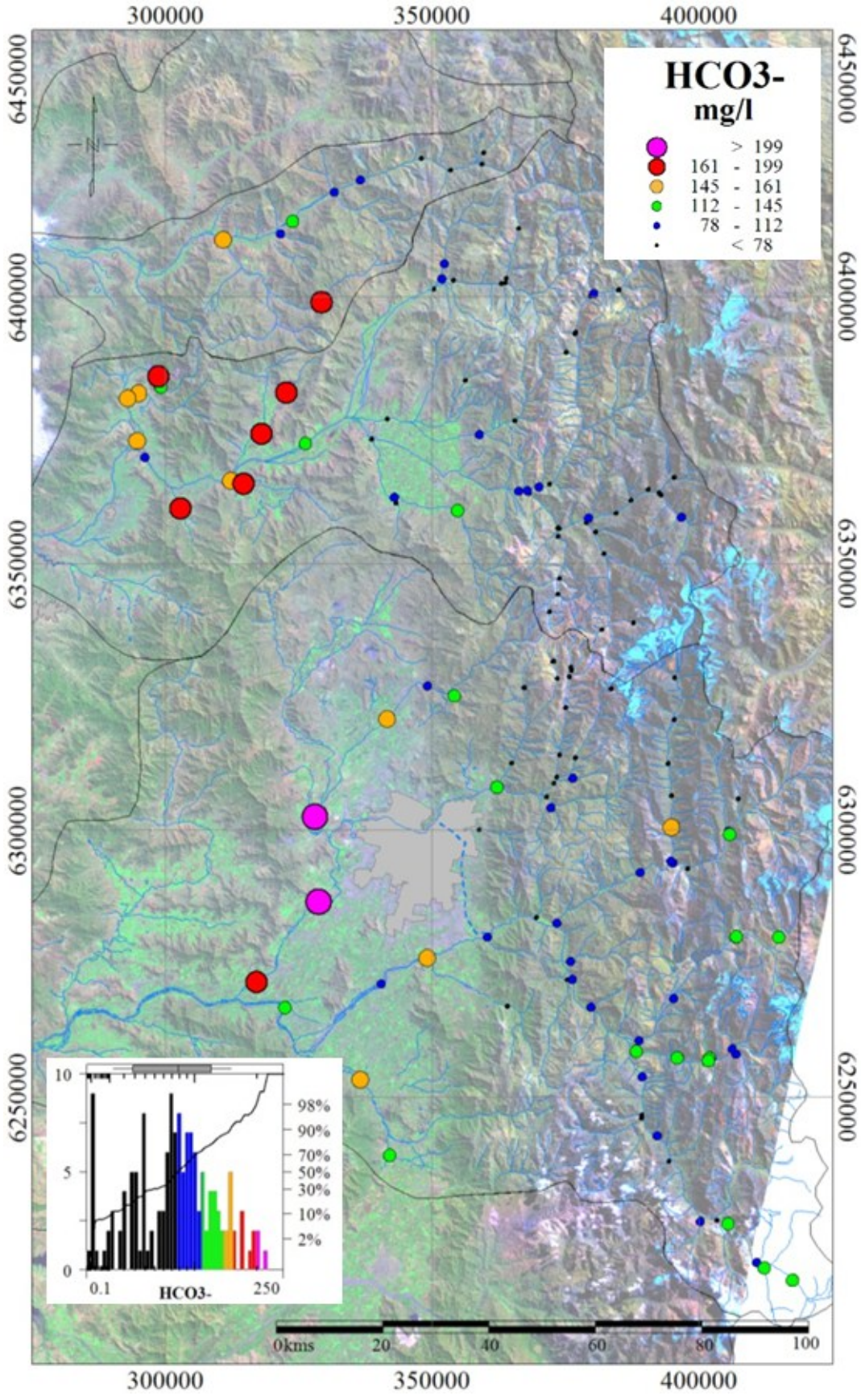
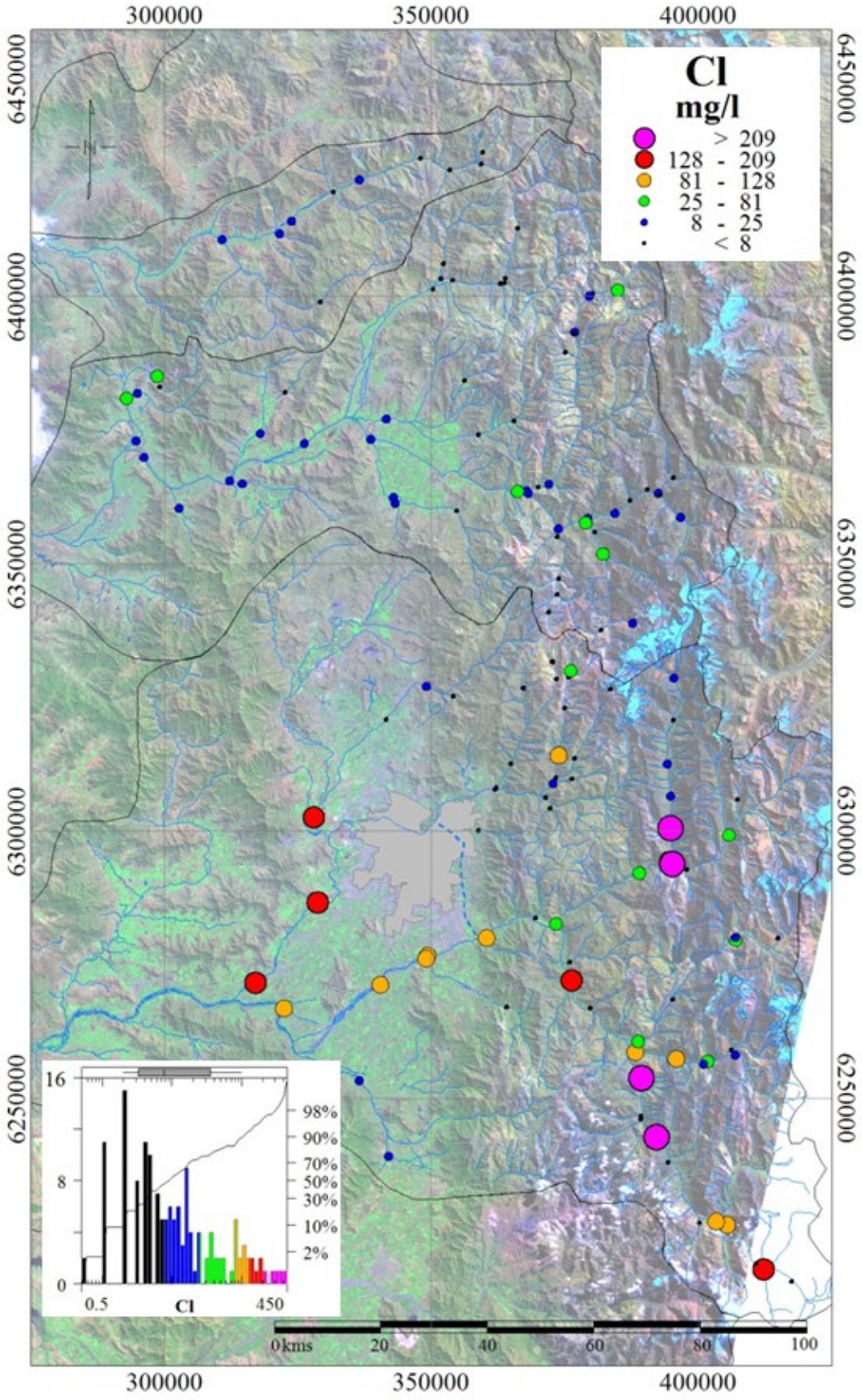


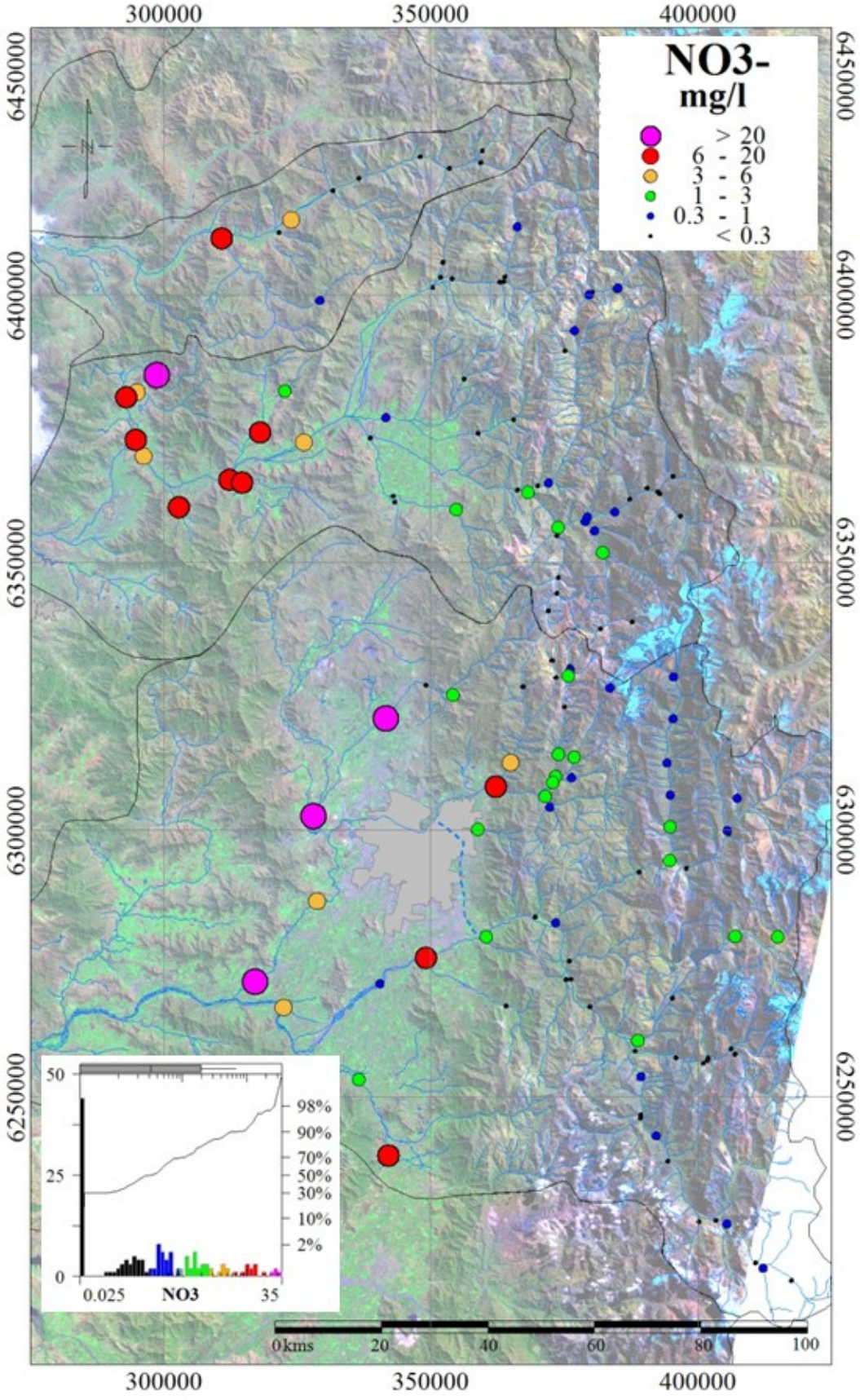
Figure 4.17: The first map is the geology of the area from Figure 4.4. Stream water baseline geochemical map coloured in relation to different populations of concentrations for pH, TDS, HCO_3^-, Cl, NO_3^-, P, SO_4^{-2}, Ca, Na, Mg, Al, Fe, Ni, Cd, Cu, As, Mo, Hg and Pb. Cold colours (black, blue and green) show the background range and the warm colours (orange, red and pink) the anomalous concentrations above threshold.

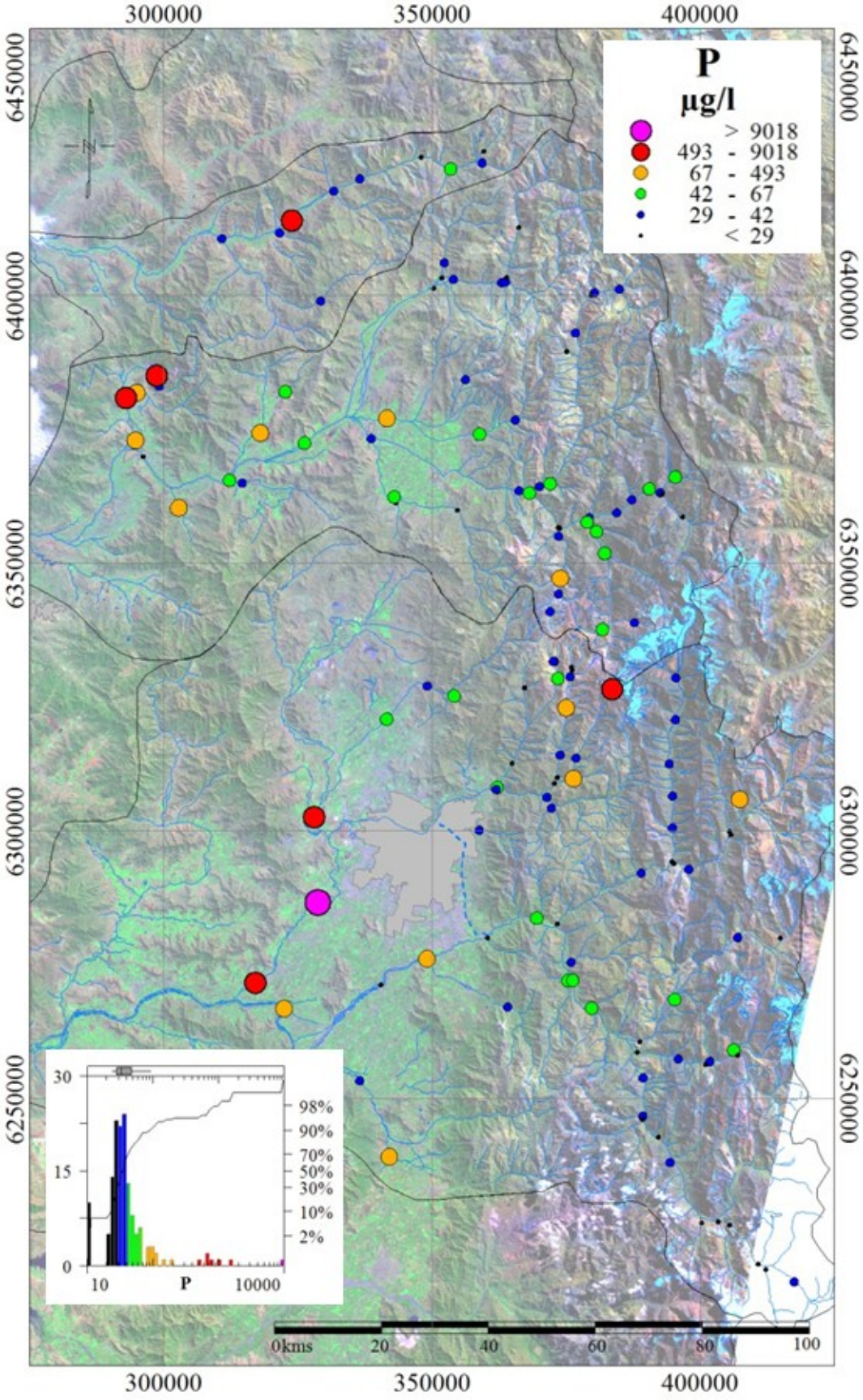

300000
350000
400000
6450000
6400000
6350000
6300000
6250000
pH
> 8.5
7.5 - 8.5
6.5 - 7.5
5.5 - 6.5
3.5 - 5.5
< 3.5
35
7.5
0
2
pH
10
98%
90%
70%
50%
30%
10%
2%
0kms
20
40
60
80
100

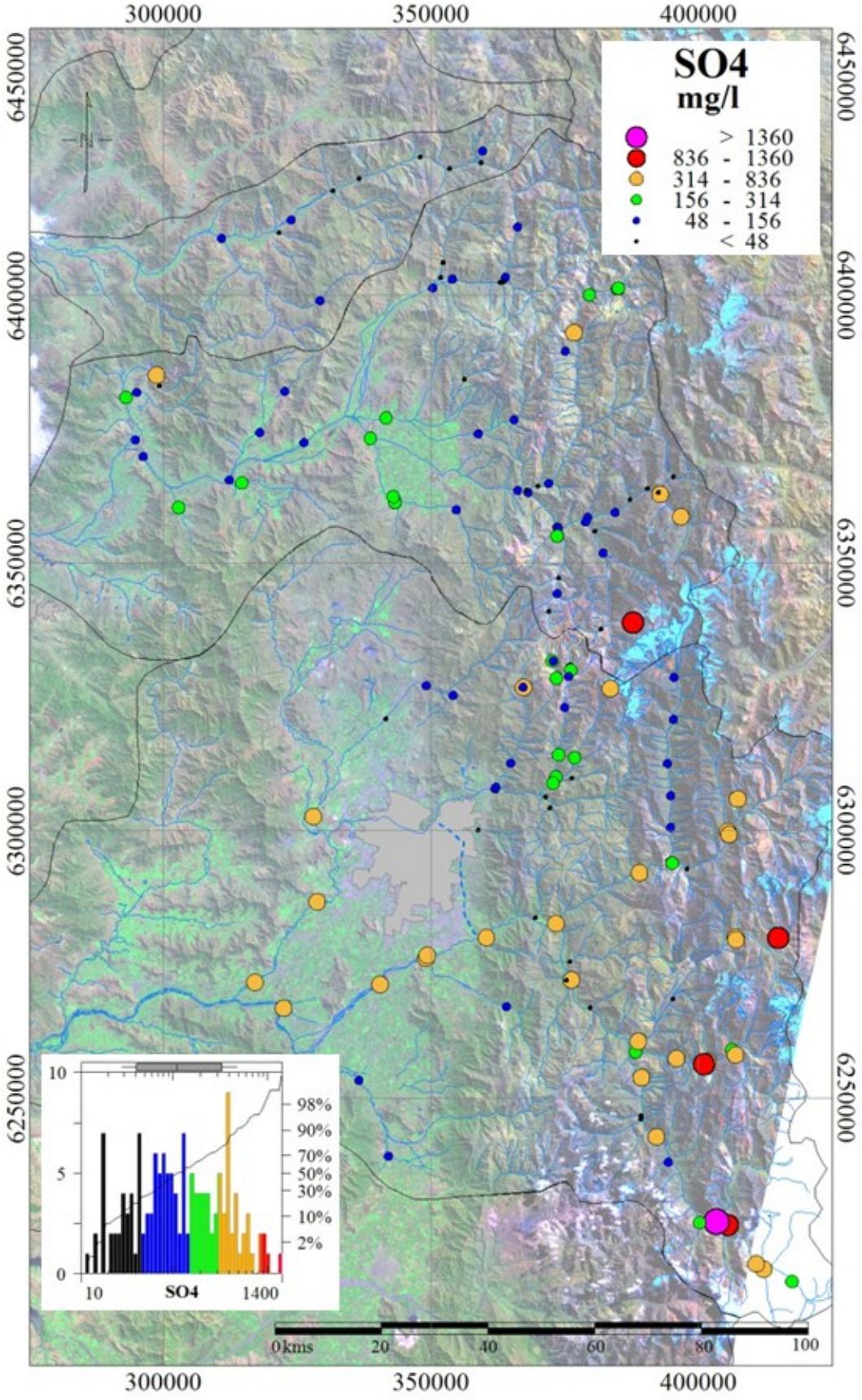

TDS
mg/l
> 1268
1058 - 1268
783 - 1058
547 - 783
287 - 547
< 287
300000
350000
400000
6450000
6400000
6350000
6300000
6250000
12
6
0
34
TDS
1600
98%
90%
70%
50%
30%
10%
2%
0kms
20
40
60
80
100

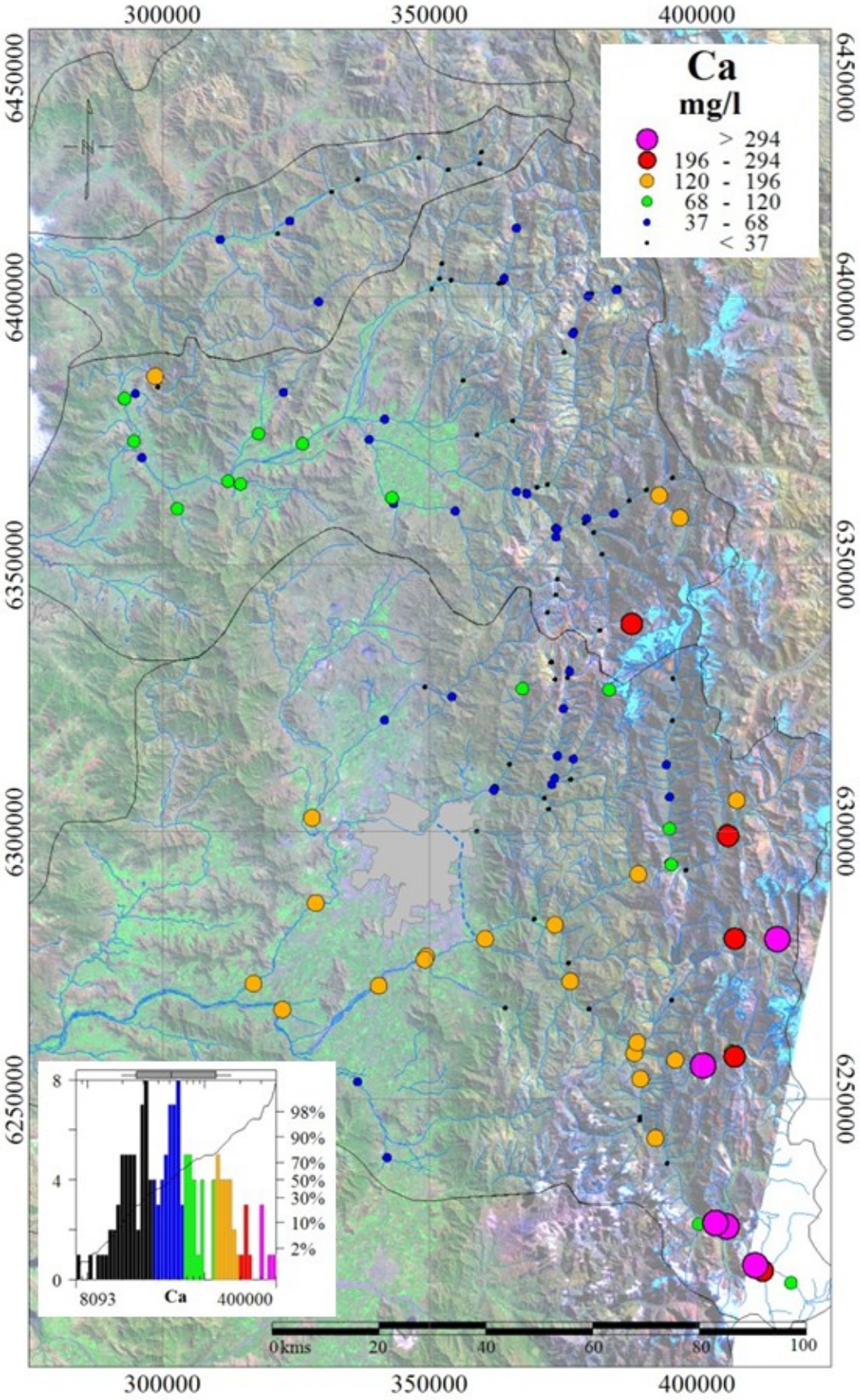

HCO3-
mg/l
> 199
161 - 199
145 - 161
112 - 145
78 - 112
< 78
300000
350000
400000
6450000
6400000
6350000
6300000
6250000
N
10
5
0
0.1
HCO3-
250
98%
90%
70%
50%
30%
10%
2%
0kms
20
40
60
80
100

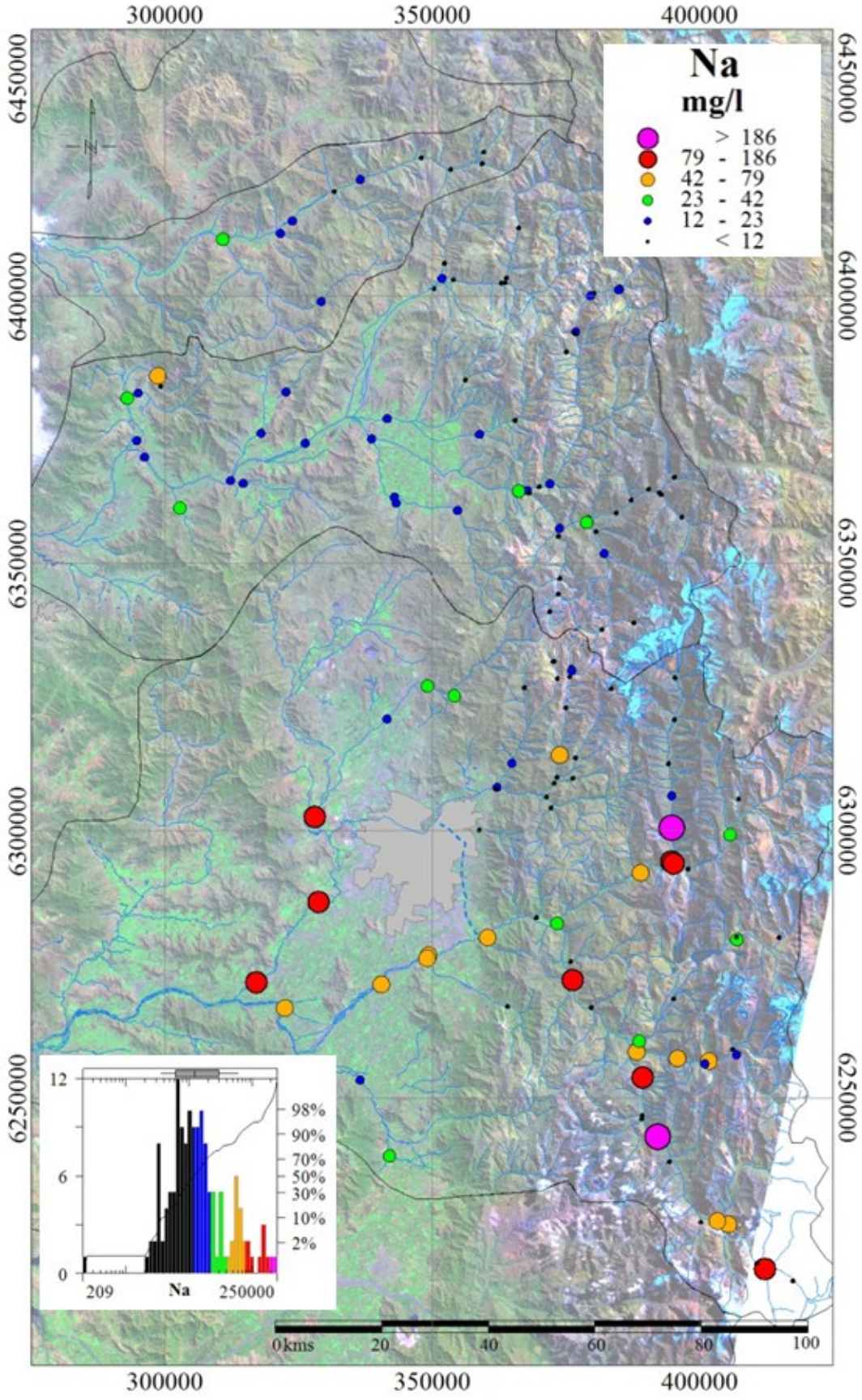

Cl
mg/l
> 209
128 - 209
81 - 128
25 - 81
8 - 25
< 8
300000
350000
400000
6450000
6400000
6350000
6300000
6250000
16
8
0
0.5
Cl
450
98%
90%
70%
50%
30%
10%
2%
0kms
20
40
60
80
100

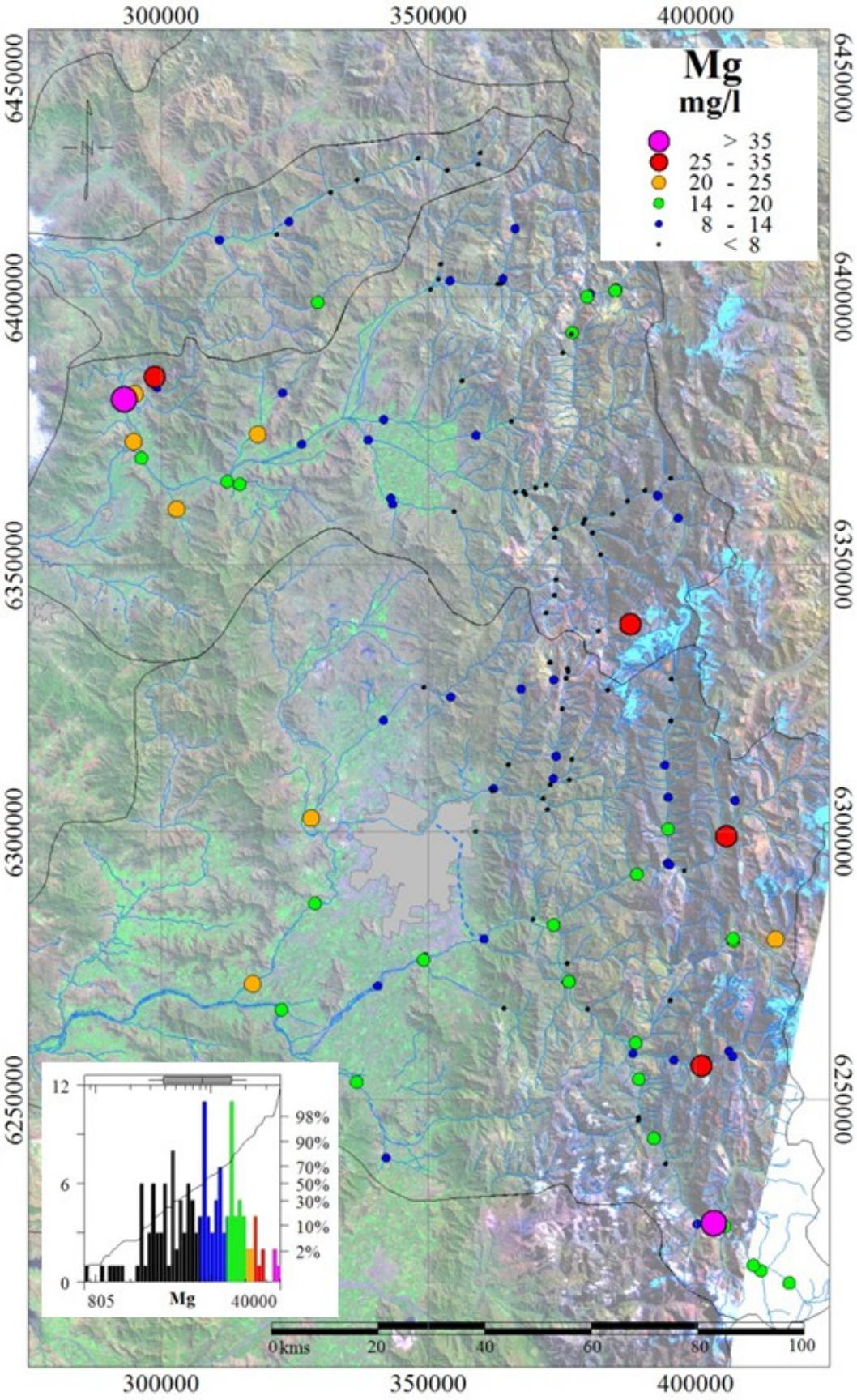

NO3-
mg/l
> 20
6 - 20
3 - 6
1 - 3
0.3 - 1
< 0.3
300000
350000
400000
6450000
6400000
6350000
6300000
6250000
50
25
0
0.025
NO3
35
98%
90%
70%
50%
30%
10%
2%
0kms
20
40
60
80
100

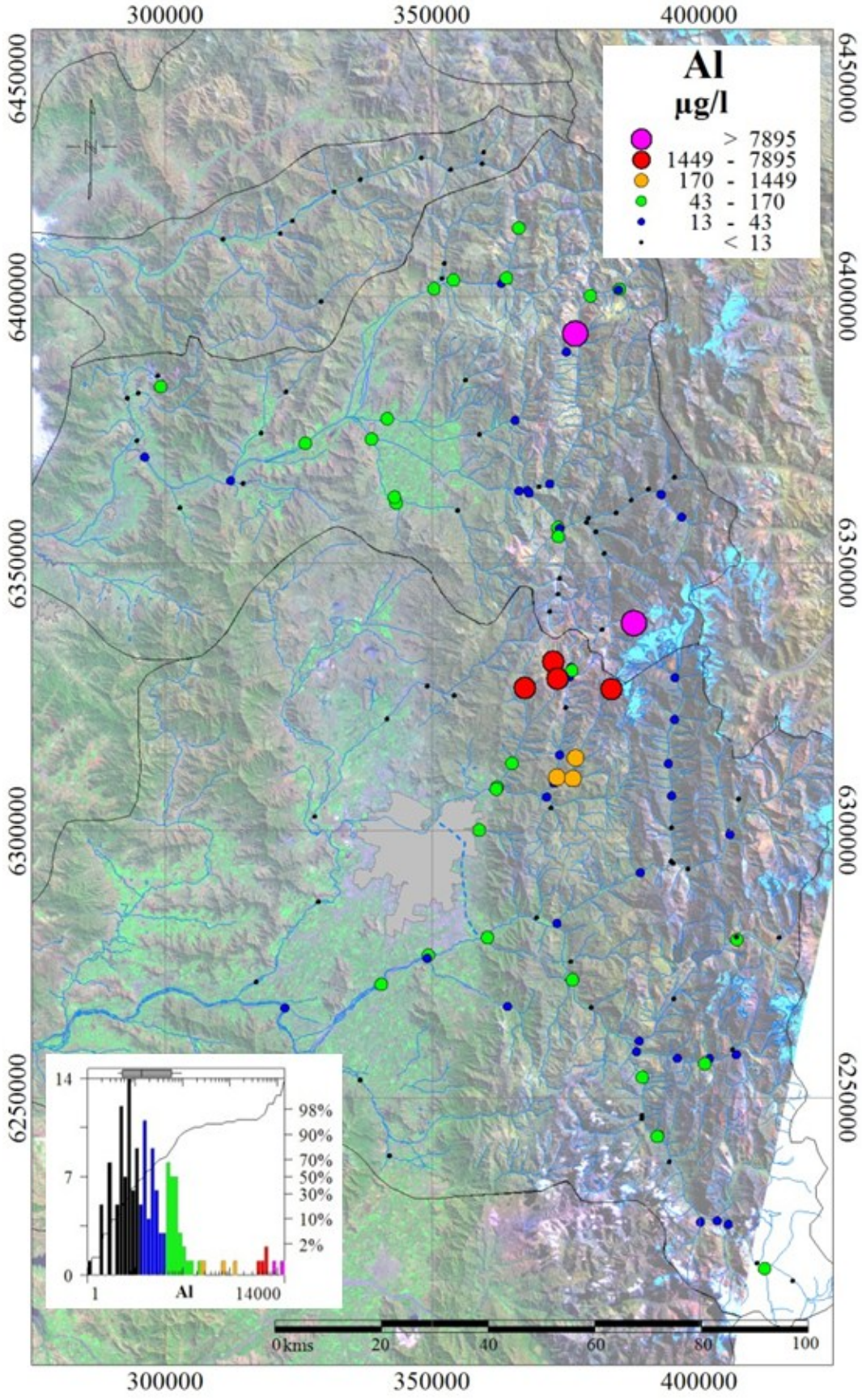

300000
350000
400000
6450000
6400000
6350000
6300000
6250000
P
µg/l
> 9018
493 - 9018
67 - 493
42 - 67
29 - 42
< 29
N
30
15
0
10
P
10000
98%
90%
70%
50%
30%
10%
2%
0kms
20
40
60
80
100

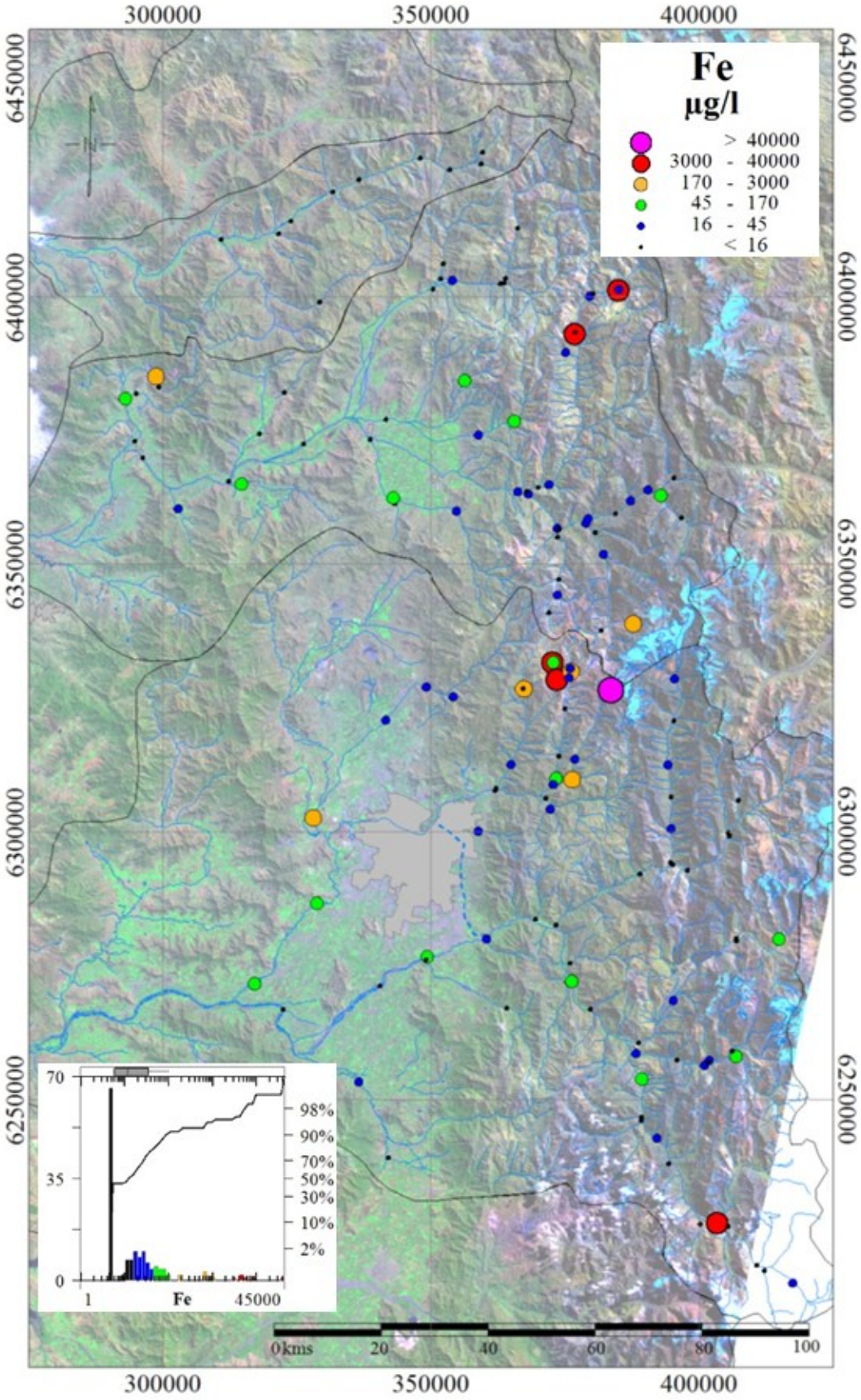

SO4
mg/l
> 1360
836 - 1360
314 - 836
156 - 314
48 - 156
< 48
300000
350000
400000
6450000
6400000
6350000
6300000
6250000
98%
90%
70%
50%
30%
10%
2%
SO4
10
1400
0kms
20
40
60
80
100

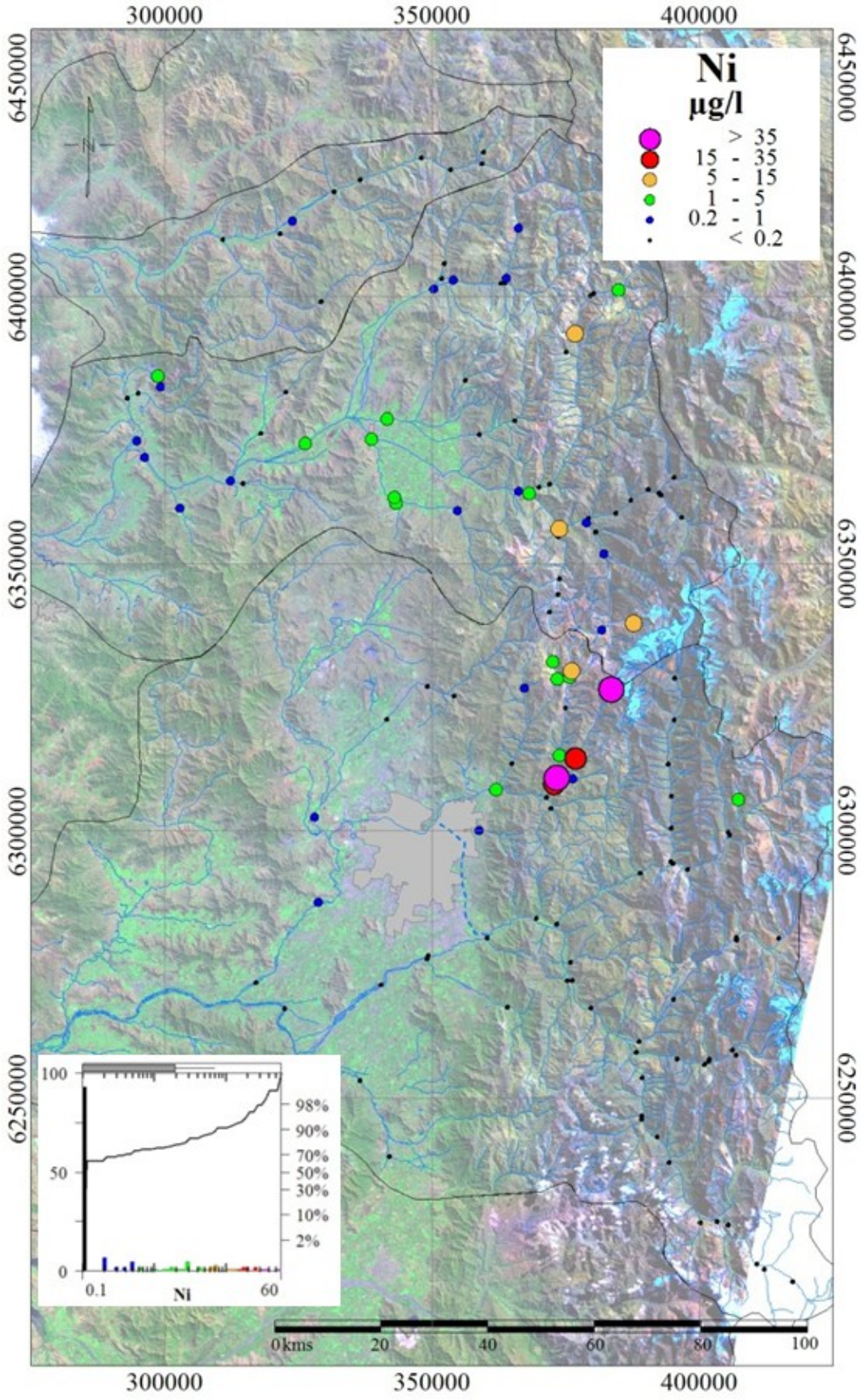

Ca
mg/l
> 294
196 - 294
120 - 196
68 - 120
37 - 68
< 37
300000
350000
400000
6450000
6400000
6350000
6300000
6250000
N
8
4
0
8093
Ca
400000
98%
90%
70%
50%
30%
10%
2%
0kms
20
40
60
80
100

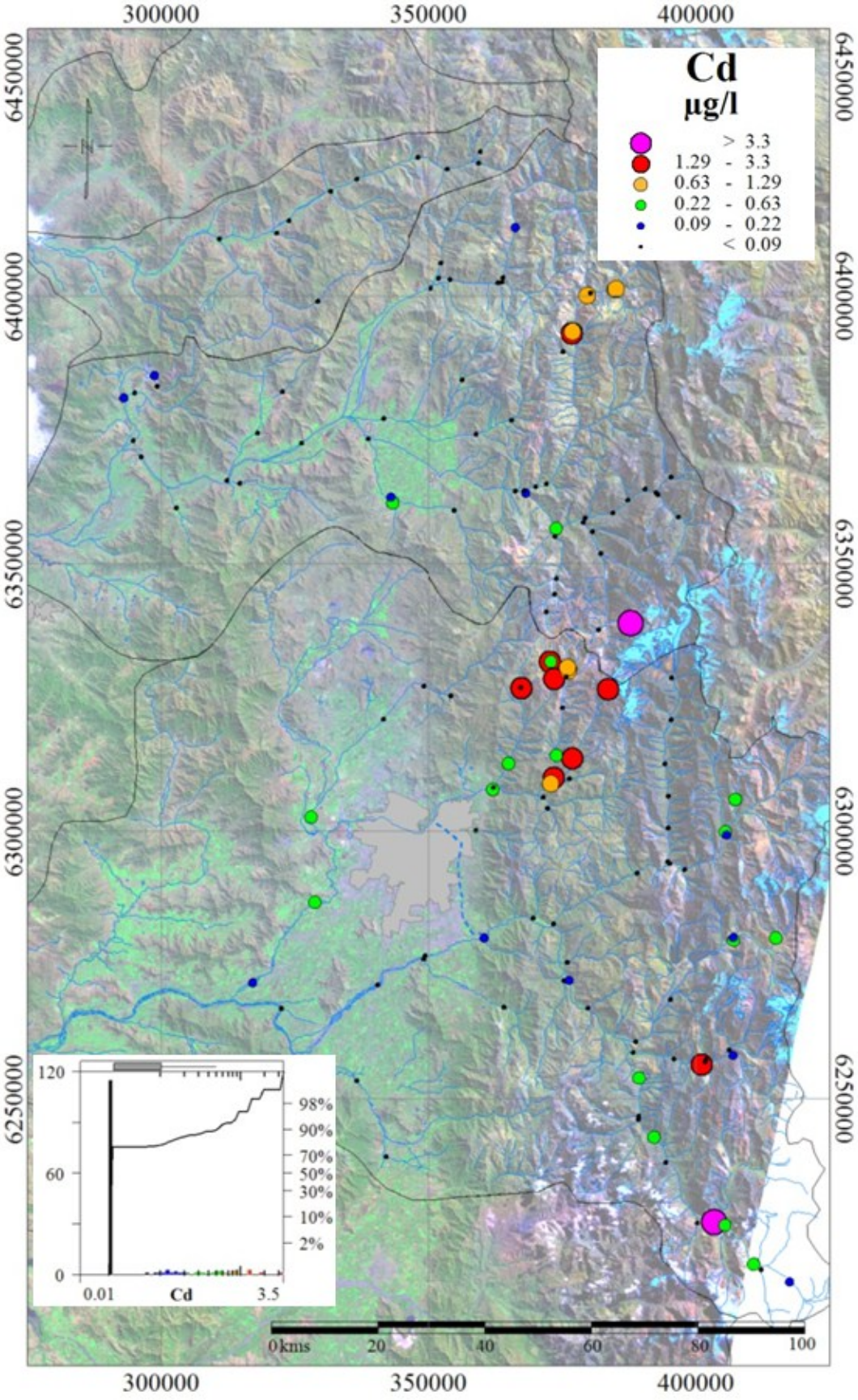

Na
mg/l
> 186
79 - 186
42 - 79
23 - 42
12 - 23
< 12
300000
350000
400000
6450000
6400000
6350000
6300000
6250000
12
6
0
209
Na
250000
98%
90%
70%
50%
30%
10%
2%
0kms
20
40
60
80
100

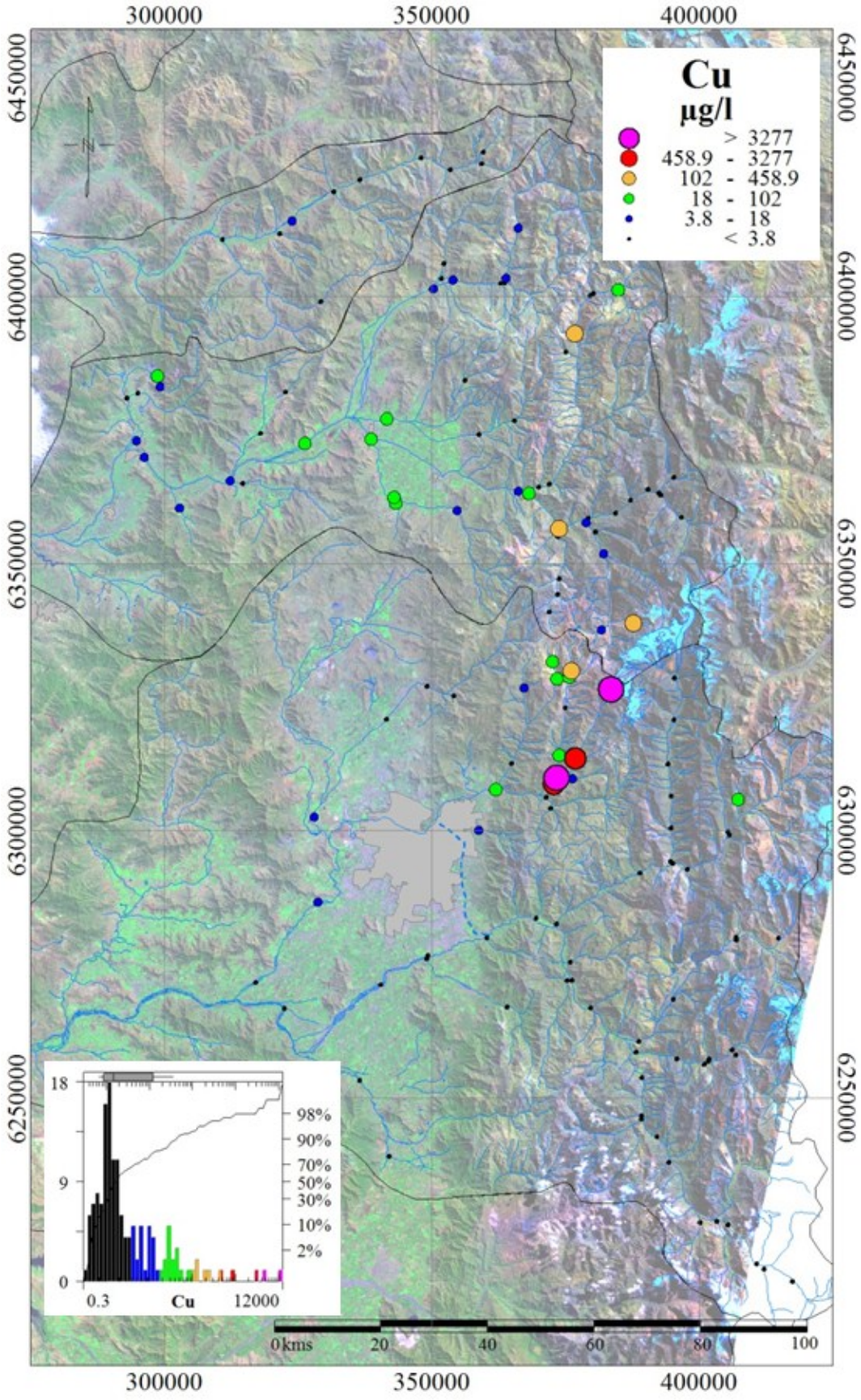

Mg
mg/l
> 35
25 - 35
20 - 25
14 - 20
8 - 14
< 8
N
300000
350000
400000
6450000
6400000
6350000
6300000
6250000
12
6
0
805
Mg
40000
98%
90%
70%
50%
30%
10%
2%
0kms
20
40
60
80
100

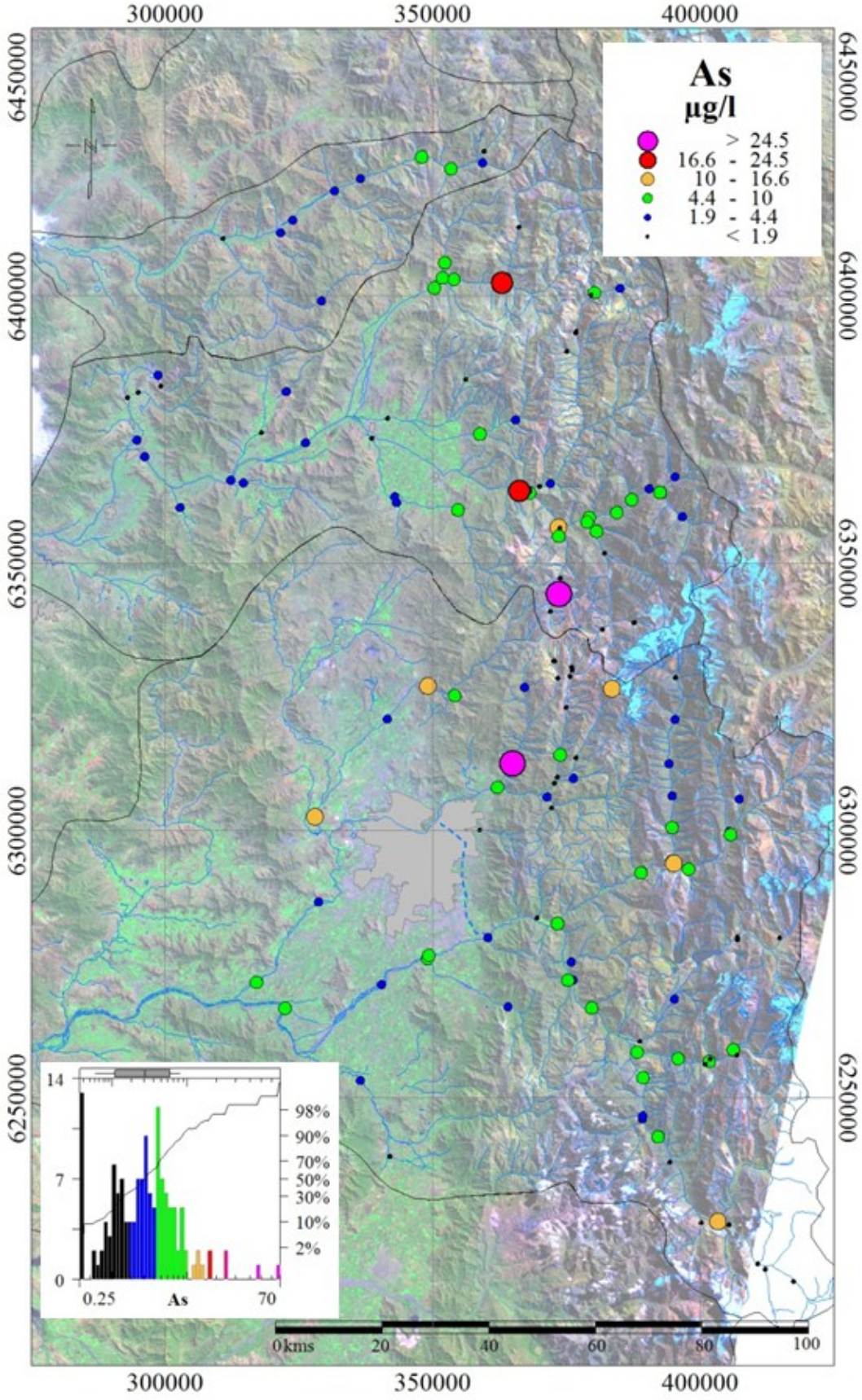

Al
µg/l
> 7895
1449 - 7895
170 - 1449
43 - 170
13 - 43
< 13
N
300000
350000
400000
6450000
6400000
6350000
6300000
6250000
14
7
0
1
Al
14000
98%
90%
70%
50%
30%
10%
2%
0kms
20
40
60
80
100

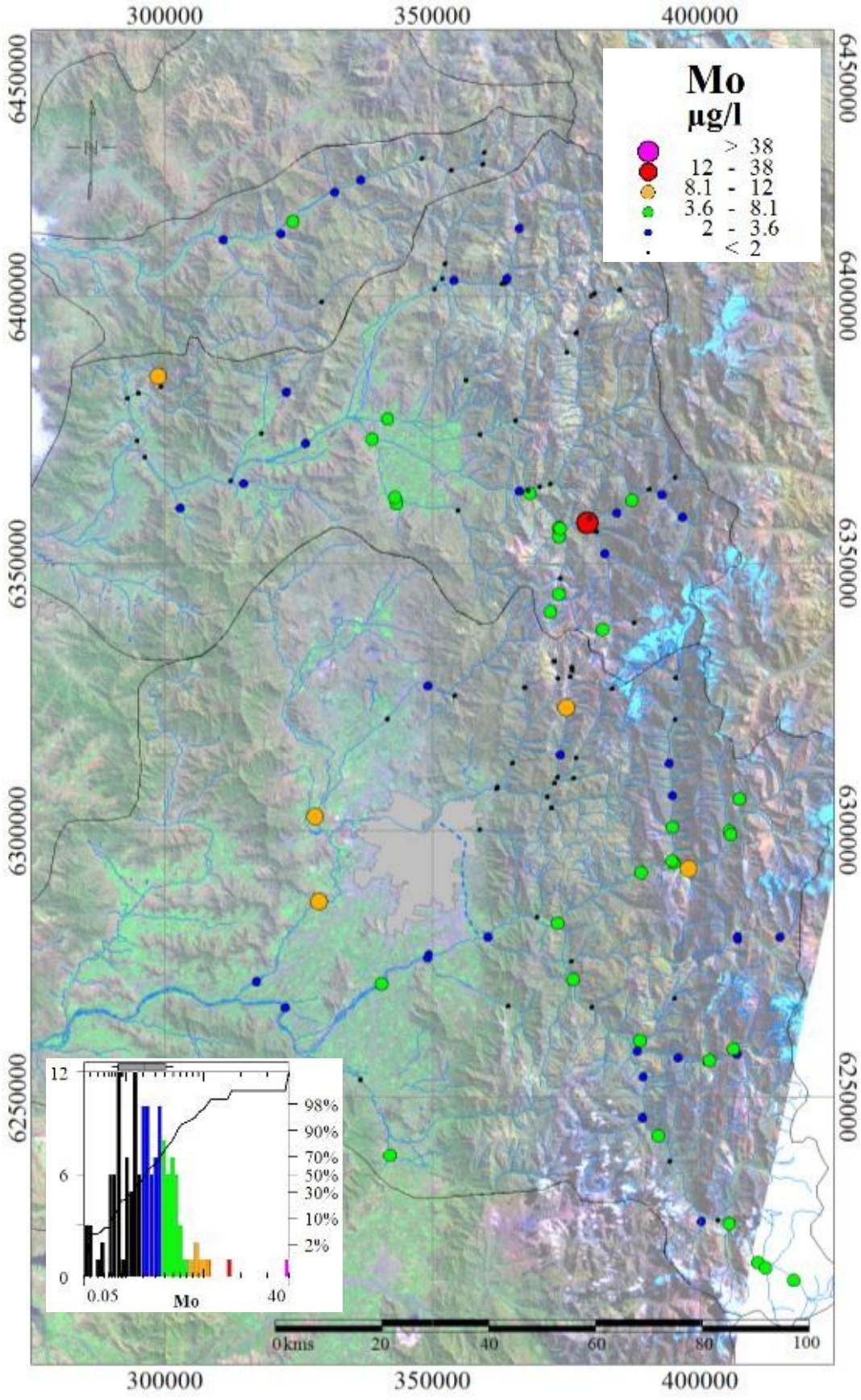

Fe
µg/l
> 40000
3000 - 40000
170 - 3000
45 - 170
16 - 45
< 16
300000
350000
400000
6450000
6400000
6350000
6300000
6250000
70
35
0
1
Fe
45000
98%
90%
70%
50%
30%
10%
2%
0kms
20
40
60
80
100

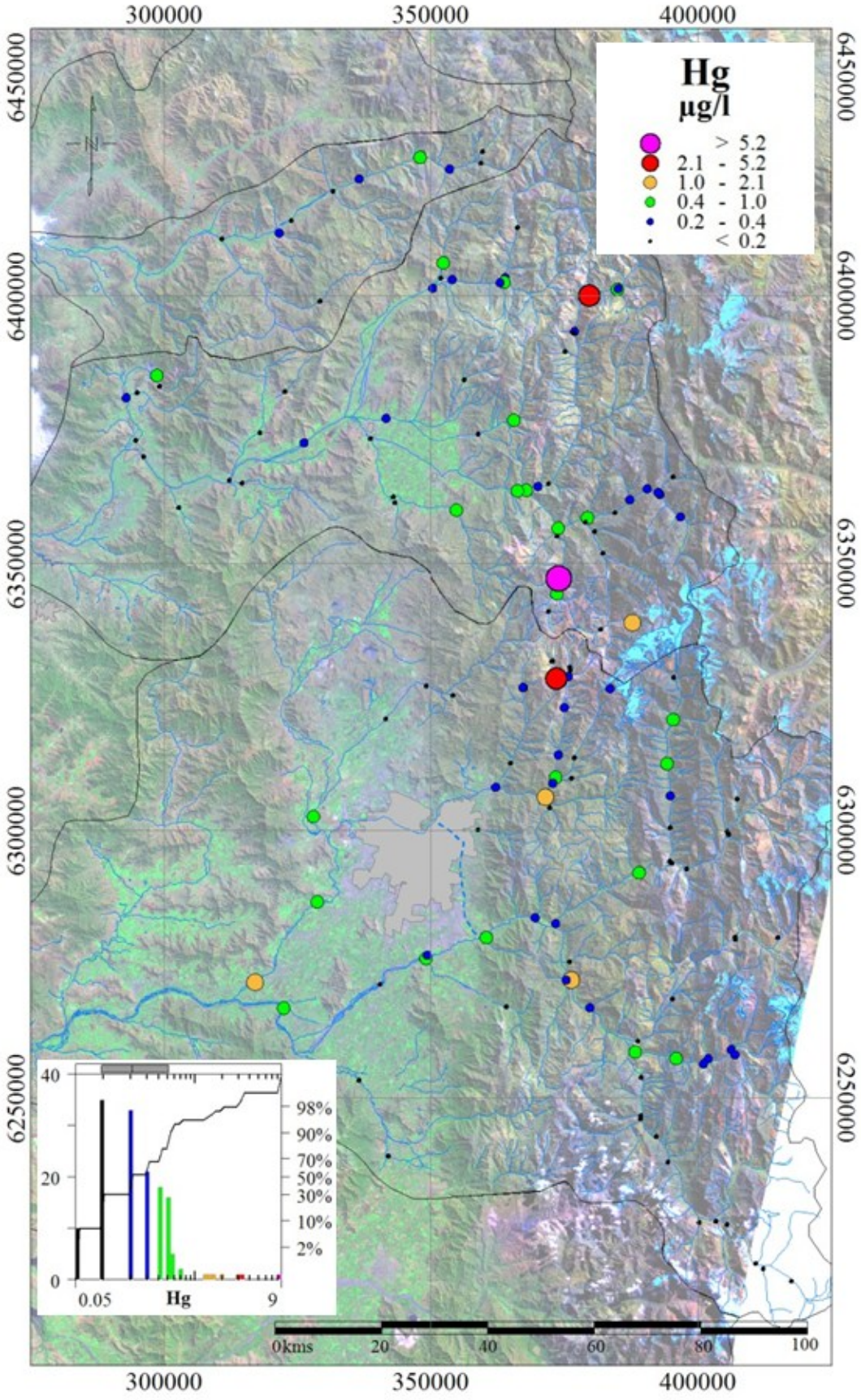

Ni
µg/l
> 35
15 - 35
5 - 15
1 - 5
0.2 - 1
< 0.2
N
300000
350000
400000
6450000
6400000
6350000
6300000
6250000
100
50
0
0.1
Ni
60
98%
90%
70%
50%
30%
10%
2%
0 kms
20
40
60
80
100

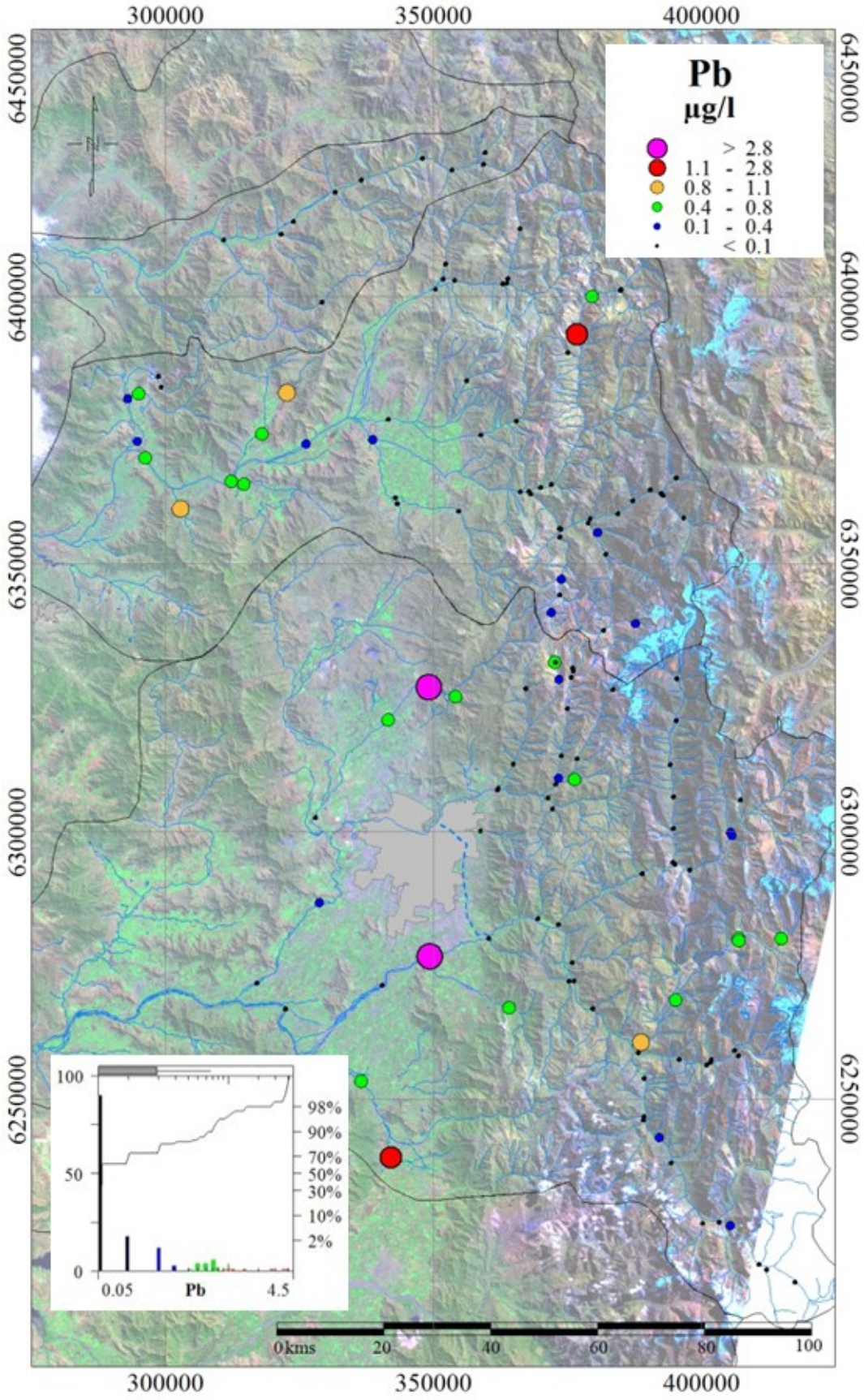

300000
350000
400000
6450000
6400000
6350000
6300000
6250000
Cd
µg/l
> 3.3
1.29 - 3.3
0.63 - 1.29
0.22 - 0.63
0.09 - 0.22
< 0.09
120
60
0
0.01
Cd
3.5
98%
90%
70%
50%
30%
10%
2%
0kms
20
40
60
80
100


Cu
µg/l
> 3277
458.9 - 3277
102 - 458.9
18 - 102
3.8 - 18
< 3.8
300000
350000
400000
6450000
6400000
6350000
6300000
6250000
18
9
0
0.3
Cu
12000
98%
90%
70%
50%
30%
10%
2%
0 kms
20
40
60
80
100


As
µg/l
> 24.5
16.6 - 24.5
10 - 16.6
4.4 - 10
1.9 - 4.4
< 1.9
300000
350000
400000
6450000
6400000
6350000
6300000
6250000
14
7
0
0.25
As
70
98%
90%
70%
50%
30%
10%
2%
0kms
20
40
60
80
100


Mo
µg/l
> 38
12 - 38
8.1 - 12
3.6 - 8.1
2 - 3.6
< 2
300000
350000
400000
6450000
6400000
6350000
6300000
6250000
12
6
0
0.05
Mo
40
98%
90%
70%
50%
30%
10%
2%
0kms
20
40
60
80
100


300000
350000
400000
6450000
6400000
6350000
6300000
6250000
Hg
µg/l
> 5.2
2.1 - 5.2
1.0 - 2.1
0.4 - 1.0
0.2 - 0.4
< 0.2
N
40
20
0
0.05
Hg
9
98%
90%
70%
50%
30%
10%
2%
0kms
20
40
60
80
100


Pb
µg/l
> 2.8
1.1 - 2.8
0.8 - 1.1
0.4 - 0.8
0.1 - 0.4
< 0.1
300000
350000
400000
6450000
6400000
6350000
6300000
6250000
100
50
0
0.05
Pb
4.5
98%
90%
70%
50%
30%
10%
2%
0kms
20
40
60
80
100

4.4 Stable isotope results

Summary statistics for δD, $\delta^{18}O$ in water, $\delta^{34}S$, $\delta^{18}O$ in sulphate and $\delta^{15}N$, $\delta^{18}O$ in nitrate are given in Table 4.11.

Table 4.11: Summary statistics of stable isotope determinations.

Isotope	Unit	DL	Samples	Min	Max	Median	Mean	SD
δD	‰ V-SMOW	N/A	145	-137	-54	-108	-107	16
$\delta^{18}O$	‰ V-SMOW	N/A	145	-18.7	-7.5	-14.8	-14.5	2.3
$\delta^{34}S$	‰ CDT	30 mg/l SO_4^{-2}	109	-4.2	14.3	4.9	5.5	4.3
$\delta^{18}O$ in SO_4^{-2}	‰ V-SMOW	30 mg/l SO_4^{-2}	104	-8	27.2	6.4	5.6	6.4
$\delta^{15}N$	‰ Air	2 mg/l NO_3^-	28	-1.5	11.9	4.3	4.5	3.5
$\delta^{18}O$ in NO_3^-	‰ V-SMOW	2 mg/l NO_3^-	28	7.8	40.4	27.2	26.2	9.8

V-SMOW: Vienna Standard Mean Ocean Water; CDT: Canyon Diablo Troilite; N/A: not applicable.

4.4.1 Hydrogen (δD) and oxygen ($\delta^{18}O$) isotopes in water samples

The overall δD values range from -137‰ to -54‰ and the $\delta^{18}O$ values from -18.7‰ to -7.5‰ (Table 4.11). In the La Ligua Basin, the δD values range from -102 to -64 with a median of -89‰ (Table 4.12); and the $\delta^{18}O$ values from -15 to -8 with a median of -11‰. The highest values (δD > -95‰ and $\delta^{18}O$ > -11.9‰) are towards the CC (Figure 4.18) and the lowest values (δD < -95‰ and $\delta^{18}O$ < -11.9‰) are in the headwaters of the La Ligua River.

The meteorological water line is a linear relationship with a worldwide average defined as $\delta D = 8 * \delta^{18}O + 10‰$ relative to SMOW (Craig 1961) but it varies globally (latitude and continental) and locally (altitude and amount of precipitation). The Santiago meteorological water line (SMWL) was obtained from the Global Network of Isotopes in Precipitation (GNIP) database for the Santiago station (Figure 4.19) of the International Atomic Energy Authority ($\delta D = 8.279 \times \delta^{18}O - 13.36$). Variation from the meteorological water line indicates evaporation and water-mineral interaction for waters with isotope values below the curve (Figure 4.19a).

The δD and $\delta^{18}O$ relationship in the waters of the La Ligua Basin is linear (Figure 4.19a), and the slope of the regression line (5.922) is lower than the SMWL slope (8.279) which reflects evaporation in the CC.

Table 4.12: Summary of statistics for H, O, S and N isotopes values for the La Ligua, Aconcagua and Maipo Basins.

Basin/Area	δD ‰	$\delta^{18}O$ ‰	$\delta^{34}S$ ‰	$\delta^{18}O_{SO4}$ ‰	$\delta^{15}N$ ‰	$\delta^{18}O_{NO3}$ ‰
La Ligua						
Min	-102	-15	3.4	7.6	4.8	31.3
Max	-64	-8	10.1	18.9	4.8	31.3
Median	-89	-11	5.4	10.2	4.8	31.3
Aconcagua						
Min	-129	-18	-4.2	-8.0	0.0	9.5
Max	-54	-8	11.7	19.8	11.9	34.8
Median	-106	-14	3.5	2.8	4.6	18.1
Maipo						
Min	-137	-19	-3.8	-13.2	-1.5	7.8
Max	-79	-11	14.3	27.2	10.1	40.4
Median	-115	-15	7.1	7.4	3.0	35.6

In the Aconcagua Basin, the δD values range from -129‰ to -54‰ with a median of -106‰ and the $\delta^{18}O$ values from -18‰ to -8‰ with a median of -14‰ (Table 4.12). The highest values (δD > -71‰ and $\delta^{18}O$ > -10.5‰) are near Catemu in the CC (Figure 4.18) and have an isotopic composition closer to evaporated ocean water (0‰) derived from meteoric water (Figure 4.19b). The high δD (-95‰ to -71‰) and $\delta^{18}O$ (-11.9‰ to -10.5‰) values are in the CC and along the west side of the AC. They reflect the composition of meteoric water away from the Pacific Ocean and at high altitude. The lower δD (-126‰ to -95‰) and $\delta^{18}O$ (-16.4‰ to -11.9‰) values along the AC and downstream in the CV reflect meteoric water distal to the seawater source as a result of the rainout effect that favours the preferential loss of deuterium (D) and ^{18}O. The lowest values (δD < -126‰ and $\delta^{18}O$ < -16.4‰) are in the headwaters of the AC as would be expected for precipitation far from the coast at high altitude. The relationship of δD and $\delta^{18}O$ in the waters of the Aconcagua Basin is linear (Figure 4.19b), and the slope of the

regression line (7.349) is lower than the SMWL slope (8.279) reflecting evaporation in the CC.

In the Maipo Basin, the δD values range from -137‰ to -29‰ with a median of -115‰ and the $\delta^{18}O$ values from -19‰ to -11‰ with a median of -15‰ (Table 4.12). The highest values (δD > -95‰ and $\delta^{18}O$ > -11.9‰) are along the west side of the AC and in the south in the CV (Figure 4.18) and again reflect the composition of meteoric water away from the Pacific Ocean at high altitude (Figure 4.19c). Like the Aconcagua Basin, the lower δD (-126‰ to -95‰) and $\delta^{18}O$ (-16.4‰ to -11.9‰) values are along the AC and downstream in the CV and reflect meteoric water distal to the seawater source as a result of the rainout effect that favours the preferential loss of D and ^{18}O. The lowest values (δD < -126‰ and $\delta^{18}O$ < -16.4‰) are in the headwaters of the AC as would be expected for precipitation at high altitudes far from the coast. The relationship of δD and $\delta^{18}O$ in the waters of the Maipo Basin is linear (Figure 4.19c), and the slope of the regression line (7.251) as well as for the Aconcagua Basin is lower than the SMWL slope (8.279) reflecting evaporation in the CC.

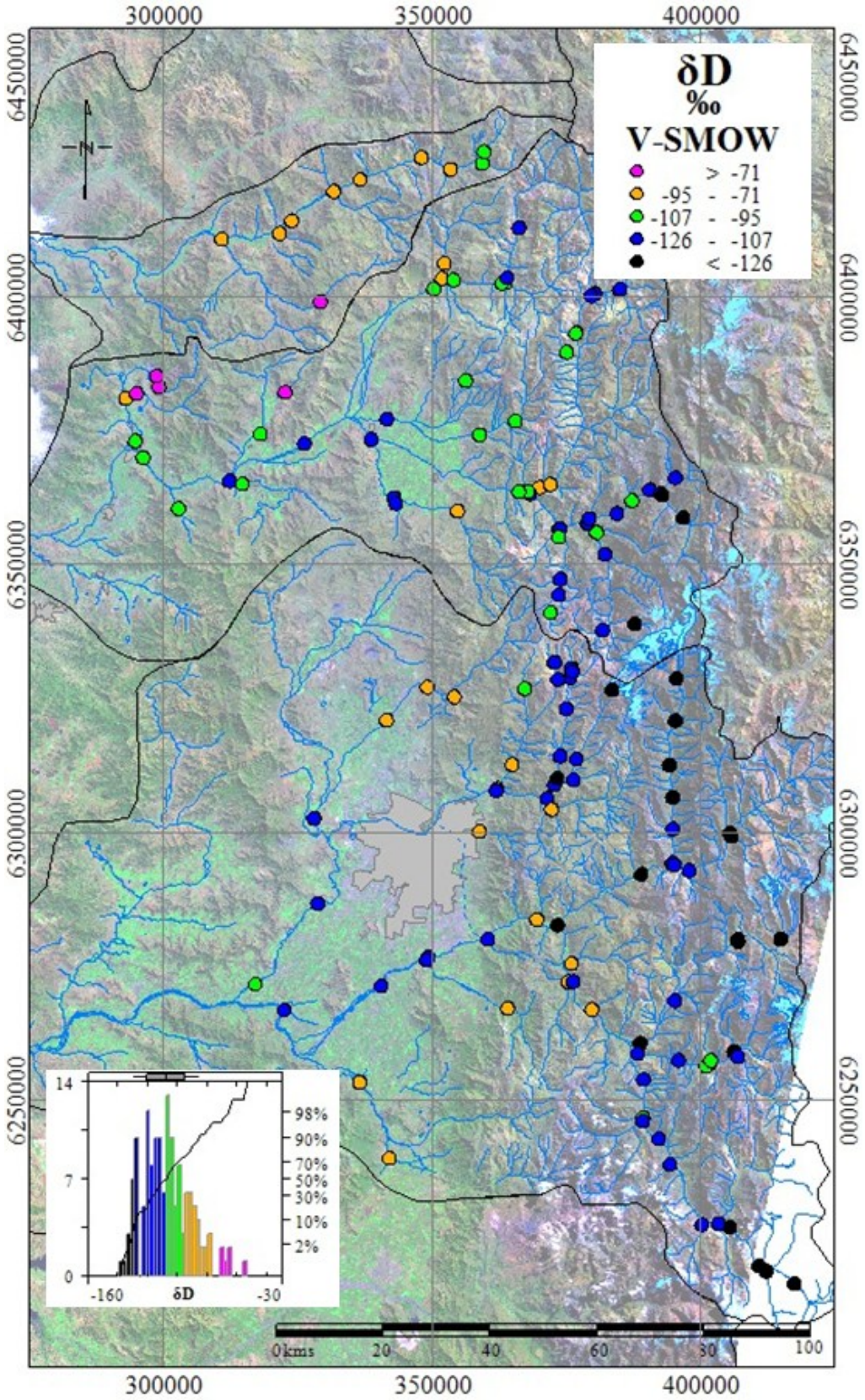
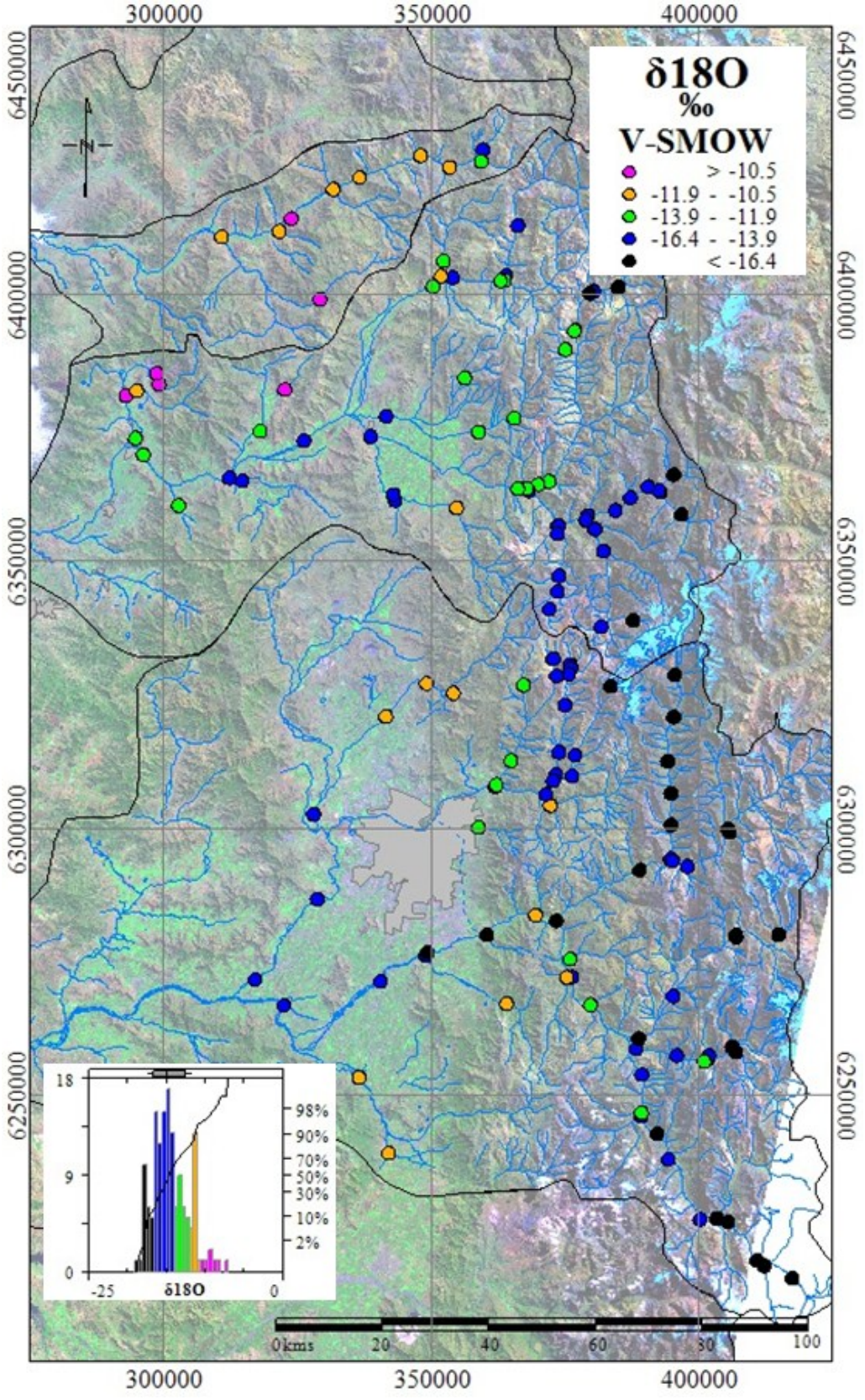


Figure 4.18: Baseline geochemical map coloured in relation to different populations for δD and $\delta^{18}O$ values in water samples.



Continuation Figure 4.18

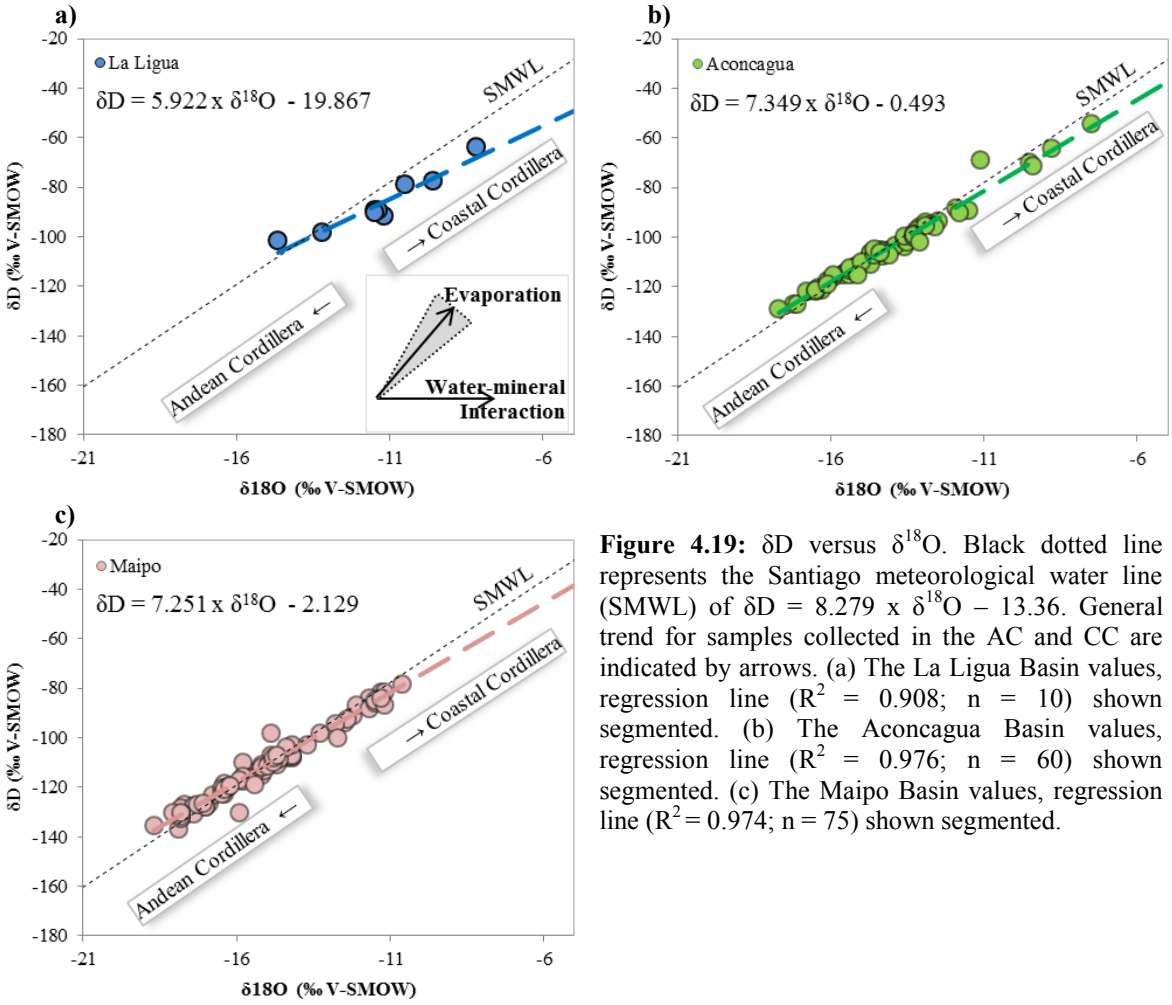


Figure 4.19: δD versus $\delta^{18}O$. Black dotted line represents the Santiago meteorological water line (SMWL) of δD = 8.279 x $\delta^{18}O$ – 13.36. General trend for samples collected in the AC and CC are indicated by arrows. (a) The La Ligua Basin values, regression line (R^2 = 0.908; n = 10) shown segmented. (b) The Aconcagua Basin values, regression line (R^2 = 0.976; n = 60) shown segmented. (c) The Maipo Basin values, regression line (R^2 = 0.974; n = 75) shown segmented.

4.4.2 Sulphur and oxygen isotopes in sulphate

The $\delta^{34}S$ values of dissolved sulphate in the waters range from -4.2‰ to 14.3‰ and the $\delta^{18}O_{SO4}$ values from -8‰ to 27.2‰ (Table 4.11). In the La Ligua Basin, the $\delta^{34}S$ values range from 3.4 to 10.1 with a median of 5.4‰ (Table 4.12). The highest $\delta^{34}S$ value of ~10‰ with a $\delta^{18}O_{SO4}$ value of 7.6‰ is in the headwaters of the La Ligua River in the AC and it has ~70 mg/l of SO_4^{-2} (Figure 4.20). These values indicate an evaporite source (Figure 4.21) but this cannot be confirmed using available geological maps (Figure 4.4). Downstream $\delta^{34}S$ values decrease from ~7‰ to ~3‰ with $\delta^{18}O_{SO4}$ values of ~8‰ to ~19‰ which indicate mixing with fertilisers (Figure 4.21) however; the exact amount of fertiliser cannot be calculated.

In the Aconcagua Basin the $\delta^{34}S$ values range from -4.2 to 11.7 with a median of 3.5‰ (Table 4.12). The highest $\delta^{34}S$ values (> 10‰) with $\delta^{18}O_{SO4}$ values of ~8 to ~15‰ are in the headwaters of the Juncal River and have a mean SO_4^{-2} concentration of ~200 mg/l (Figure 4.20). These values indicate an evaporite source (Figure 4.21) which is the Upper Jurassic marine evaporites in the Lagunilla Formation (Table 4.1) which outcrops upstream. Downstream in the CV, $\delta^{34}S$ values range from ~4‰ to 7‰ with $\delta^{18}O_{SO4}$ values of ~0‰ to ~20‰ and a mean SO_4^{-2} concentration of ~150 mg/l. These values indicate dilution and/or mixing with sources such as sulphides and fertilisers. The lowest $\delta^{34}S$ values ~-4‰ to ~4‰ with $\delta^{18}O_{SO4}$ values of ~-8‰ to ~14‰ have a mean SO_4^{-2} concentration of ~180 mg/l. These values reflect waters that have reacted with sulphide sources. These include mineralisation in the Yerba Loca, Colorado and Barroso rivers; and hydrothermal alteration in the Colorado and Riecillos rivers in the AC; and mine area waters near El Soldado and the La Poza and La Restauradora abandoned Pb-Zn mines in the CC, and near Los Bronces and Andina in the AC.

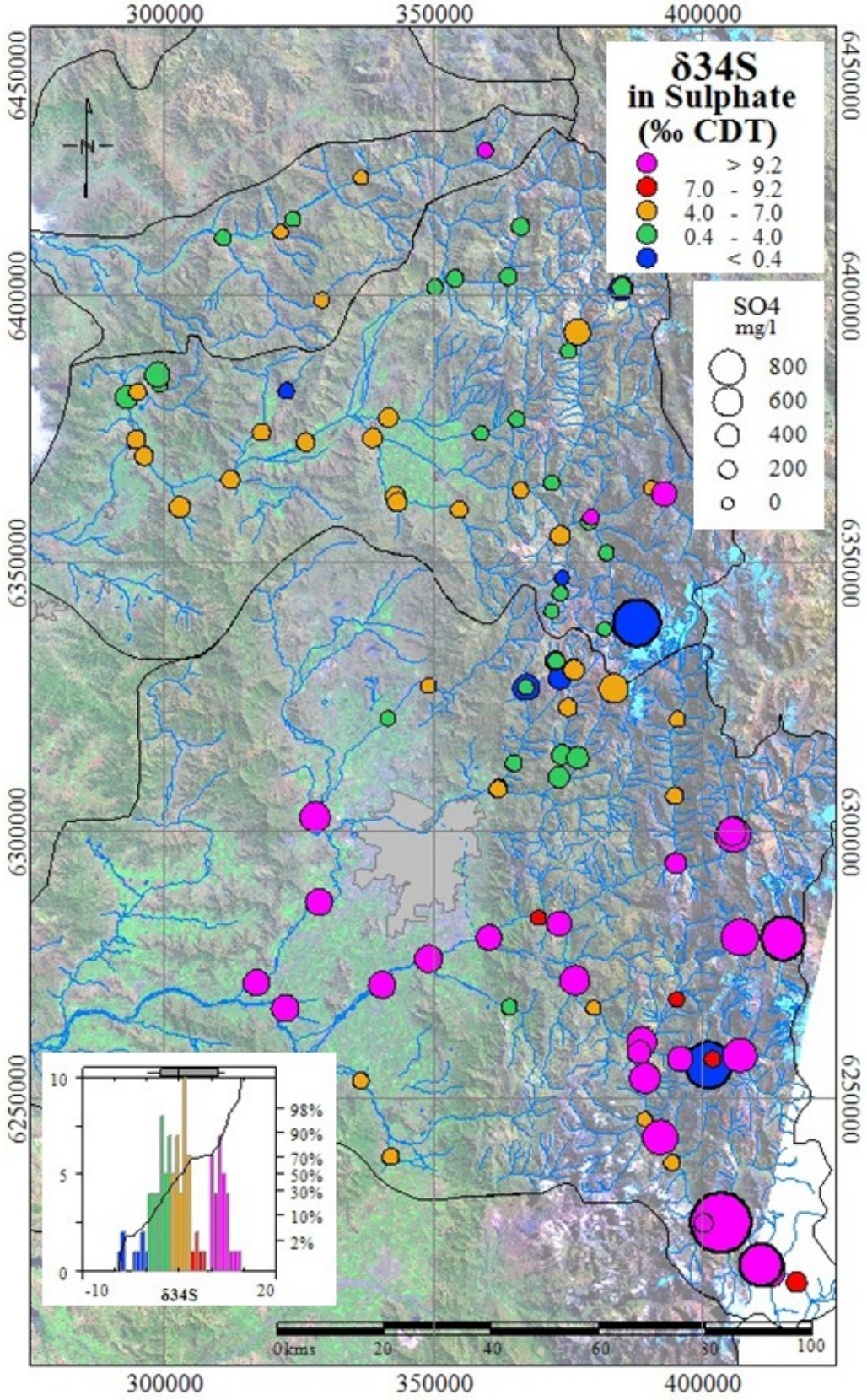
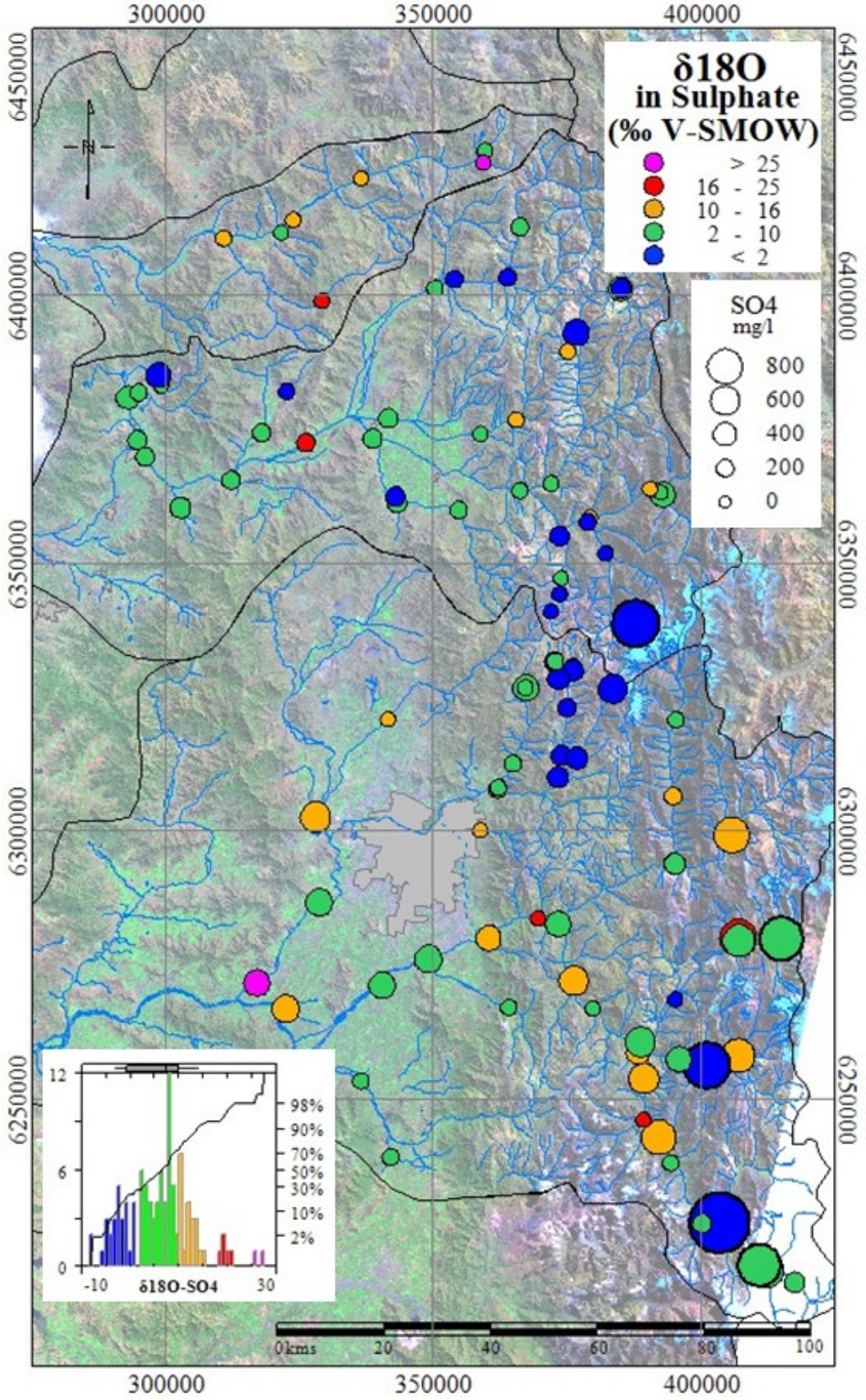


Figure 4.20: Baseline geochemical map coloured in relation to different populations for $\delta^{34}S$ and $\delta^{18}O_{SO4}$ values in precipitated sulphate of the water samples.



Continuation Figure 4.20

In the Maipo Basin, the $\delta^{34}S$ values range from -3.8‰ to 14.3‰ with a median of 7.1‰ (Table 4.12). The highest $\delta^{34}S$ values (> 9‰) with $\delta^{18}O_{SO4}$ values of ~5‰ to ~27‰ are along the Andes and downstream in the CV and have a mean SO_4^{-2} concentration of ~500 mg/l (Figure 4.20). These values indicate an evaporite source (Figure 4.21) consistent with the presence of Upper Jurassic marine evaporites in the Rio Colina, Rio Damas and Lo Valdes formations (Table 4.1) in the headwaters of the Maipo River. The $\delta^{34}S$ values between 7‰ and 9‰ with $\delta^{18}O_{SO4}$ values of ~4‰ to ~19‰ are also from the headwaters of the Maipo River and have a mean SO_4^{-2} concentration of ~90 mg/l. These values probably reflect a volcanic sulphate source ($\delta^{34}S$ ~3‰ to ~15‰ (Clark & Fritz 1997)) from the Early Cenozoic Abanico and Farellones volcanic formations and recent volcanic deposits in the vicinity of Maipo Volcano (Table 4.1). Lower $\delta^{34}S$ values of 4‰ to 7‰ with $\delta^{18}O_{SO4}$ values of ~-3‰ to ~21‰ have a mean SO_4^{-2} concentration of ~120 mg/l and indicate dilution and/or mixing with fertilisers, detergents and sulphur from volcanic rocks in the CV (Figure 4.21). The exception is in the AC in the Yerba Loca Stream where waters reacted with sulphide mineralisation and isotopes values of $\delta^{34}S$ -4.1‰ and $\delta^{18}O_{SO4}$ -13 with SO_4^{-2} concentration of ~450 mg/l indicate sulphide oxidation. The lowest $\delta^{34}S$ values of ~-4‰ to ~4‰ with $\delta^{18}O_{SO4}$ values of ~-8‰ to ~8‰ have a mean SO_4^{-2} value of ~200 mg/l. These values reflect waters that have reacted with sulphide sources in the headwaters of the Mapocho, Clarillo and Volcán rivers in the AC. One sample in the Colina Stream in the CV has isotopes values of $\delta^{34}S$ 3‰ and $\delta^{18}O_{SO4}$ of ~12.5‰ however which indicate a fertiliser source.

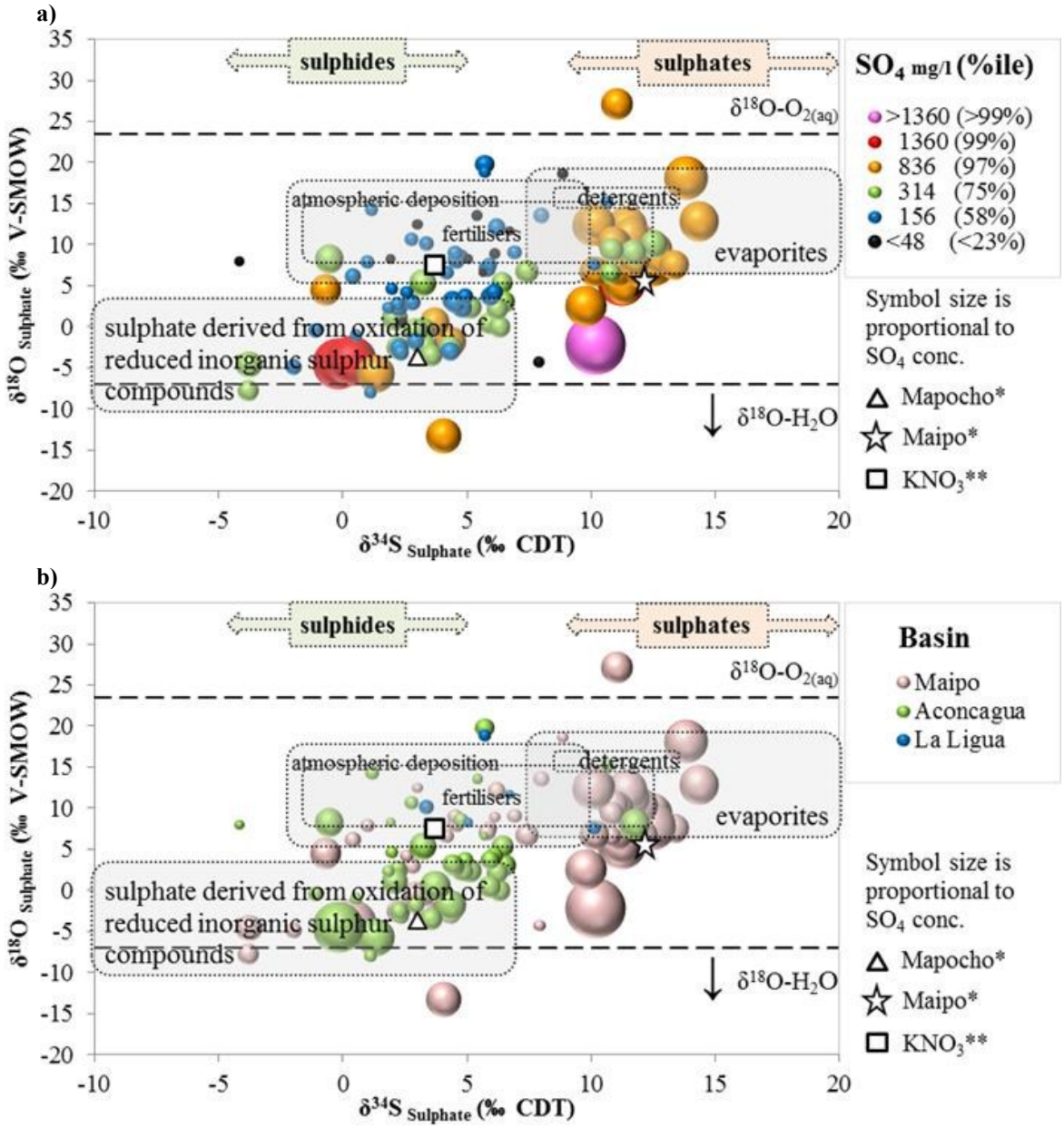


Figure 4.21: $\delta^{34}S$ and $\delta^{18}O$ values of water samples and typical sulphate sources. The size of the symbol corresponds to the concentration of dissolved sulphate in mg/l. Typical $\delta^{34}S$ and $\delta^{18}O$ values are shown by shaded areas (Krouse & Mayer 2000; Vitòria et al. 2004) and dashed lines show oxygen isotopic values expected from atmospheric (23.5‰ (Kroopnick & Craig 1972)) and regional meteoric waters (-18 to -7‰, data this project). Previous isotopic data are shown for the Mapocho* and Maipo* rivers (Iriarte et al. 2009) and KNO_3 Chilean fertiliser** (Vitòria et al. 2004). The $\delta^{34}S$ range of values for sulphides and sulphates are also indicated. (a) The symbol colour represents the sulphate frequency population, and in (b) the symbol colour represents the three basins, La Ligua, Aconcagua and Maipo.

4.4.3 Nitrogen and oxygen isotopes in nitrate

The $\delta^{15}N$ values of dissolved nitrate in the waters range from -1.5‰ to 11.9‰ and the $\delta^{18}O_{NO3}$ values from 7.8‰ to 40.4‰ (Table 4.11 and Figure 4.22). The isotope values obtained for the fertilisers in this study are 2.1‰ $\delta^{15}N_{NO3}$ with 15.6‰ $\delta^{18}O_{NO3}$ for $NH_4H_2PO_4$ and -3.4‰ $\delta^{15}N_{NO3}$ for KCl with insufficient nitrate to analyse $\delta^{18}O_{NO3}$. These values are consistent with published values (Kendall 1998), but differ from the Chilean KNO_3 fertiliser isotopic values in another study (Vitòria et al. 2004) (Figure 4.23). In the La Ligua Basin, nitrate isotopes were determined in only one sample; it has a $\delta^{15}N$ value of 4.8‰ with $\delta^{18}O_{NO3}$ of 31.3‰ (Table 4.12 and Figure 4.22). These values indicate mixing between two sources; sewage and nitrate derived predominantly from the atmosphere (Figure 4.23).

In the Aconcagua Basin, the $\delta^{15}N$ values range from 0 to ~12 with a median of 4.6‰ (Table 4.12). The highest $\delta^{15}N$ value of ~12‰ with a $\delta^{18}O_{NO3}$ value of ~30‰ is near the township of Calera in the CC (Figure 4.3) and has a NO_3^- concentration of ~4 mg/l (Figure 4.22). These values indicate a nitrate source from septic waste and/or manure consistent with the presence of sewage in the area (Figure 4.23). The $\delta^{15}N$ values between ~6‰ and 9‰ with $\delta^{18}O_{NO3}$ values of 12‰ and ~31‰ are near the townships of Calera and Catemu in the CC and have a mean NO_3^- concentration of ~10 mg/l. These values indicate a mixture of nitrate fertilisers and septic waste reflecting the presence of agricultural communities in these areas. The $\delta^{15}N$ values between ~3.5‰ and 6‰ with $\delta^{18}O_{NO3}$ values of ~15‰ and ~19‰ are near the townships of Calera in the CC and have a mean NO_3^- concentration of ~12 mg/l. These values indicate a source from fertilisers used in agriculture in the area. The lowest $\delta^{15}N$ values between 0‰ and 3.3‰ with $\delta^{18}O_{NO3}$ values between ~27‰ and 35‰ are in the headwaters of the Barriga and Blanco rivers in

the Andina mine district and have a mean NO_3^- concentration of ~1 mg/l. These values indicate that this nitrate is derived from the atmosphere. One sample in the Catemu Stream in the CC is an exception; it has a NO_3^- concentration of ~20 mg/l with $\delta^{15}N$ of 2.8‰ but lower $\delta^{18}O_{NO3}$ value of ~9‰ consistent with an ammonium fertiliser source.

In the Maipo Basin, the $\delta^{15}N$ values range from 0‰ to ~10‰ with a median of 3‰ (Table 4.12). The highest $\delta^{15}N$ value of ~10‰ with a $\delta^{18}O_{NO3}$ value of 21‰ is in the Mapocho River downstream of Santiago in the CV (Figure 4.3) and it has a NO_3^- concentration of ~5 mg/l (Figure 4.22). These values indicate a septic waste source consistent with this river being the main outflow of treated sewage waters from the city. The $\delta^{15}N$ values between ~6‰ and 9‰ with $\delta^{18}O_{NO3}$ values of ~21‰ and ~30‰ are in the southern and northern CV and have a mean NO_3^- concentration of ~9 mg/l. These values indicate mixed fertilisers and septic waste sources consistent with the presence of agricultural communities in the area. The $\delta^{15}N$ values between ~3.5‰ and 6‰ with $\delta^{18}O_{NO3}$ values of ~8‰ and ~14‰ are in the southern CV and near the Colina Township and have a mean NO_3^- concentration of ~30 mg/l. These values indicate the presence of nitrate from fertilisers which is used by the agricultural communities in the area. One sample in the Andes, in the headwaters of the Yeso River in an exception; it has a NO_3^- concentration of ~2 mg/l with $\delta^{15}N$ of 4.2‰ and a much higher $\delta^{18}O_{NO3}$ value of ~40‰ consistent with nitrate derived from the atmosphere. The lowest $\delta^{15}N$ values between -1.5‰ and 2.3‰ with $\delta^{18}O_{NO3}$ values between ~34‰ and 40‰ are in the Mapocho, San Francisco, Yerba Loca, and Arrayán rivers in the AC and have a mean NO_3^- concentration of ~3 mg/l. These values also indicate nitrate derived from the atmosphere.

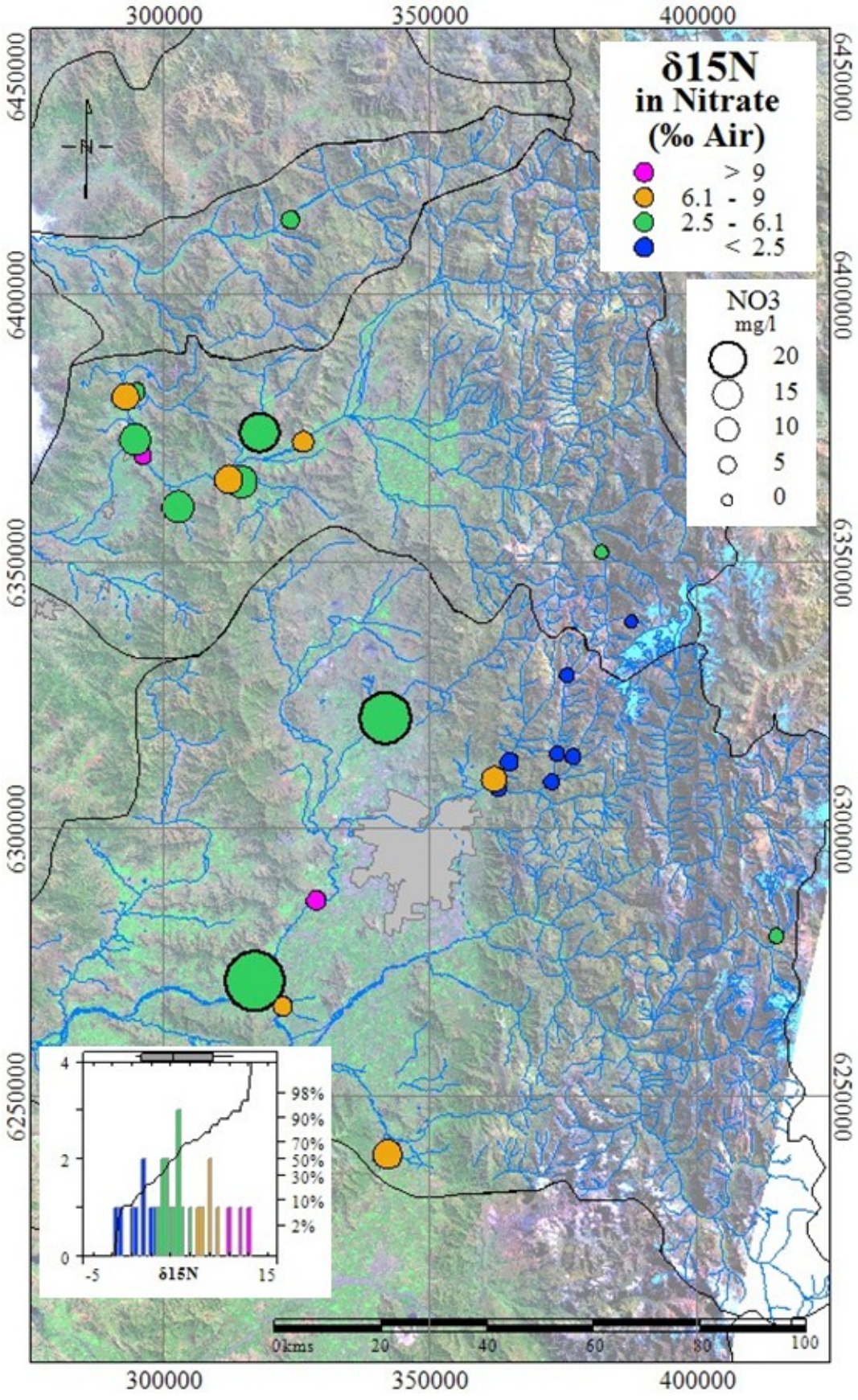
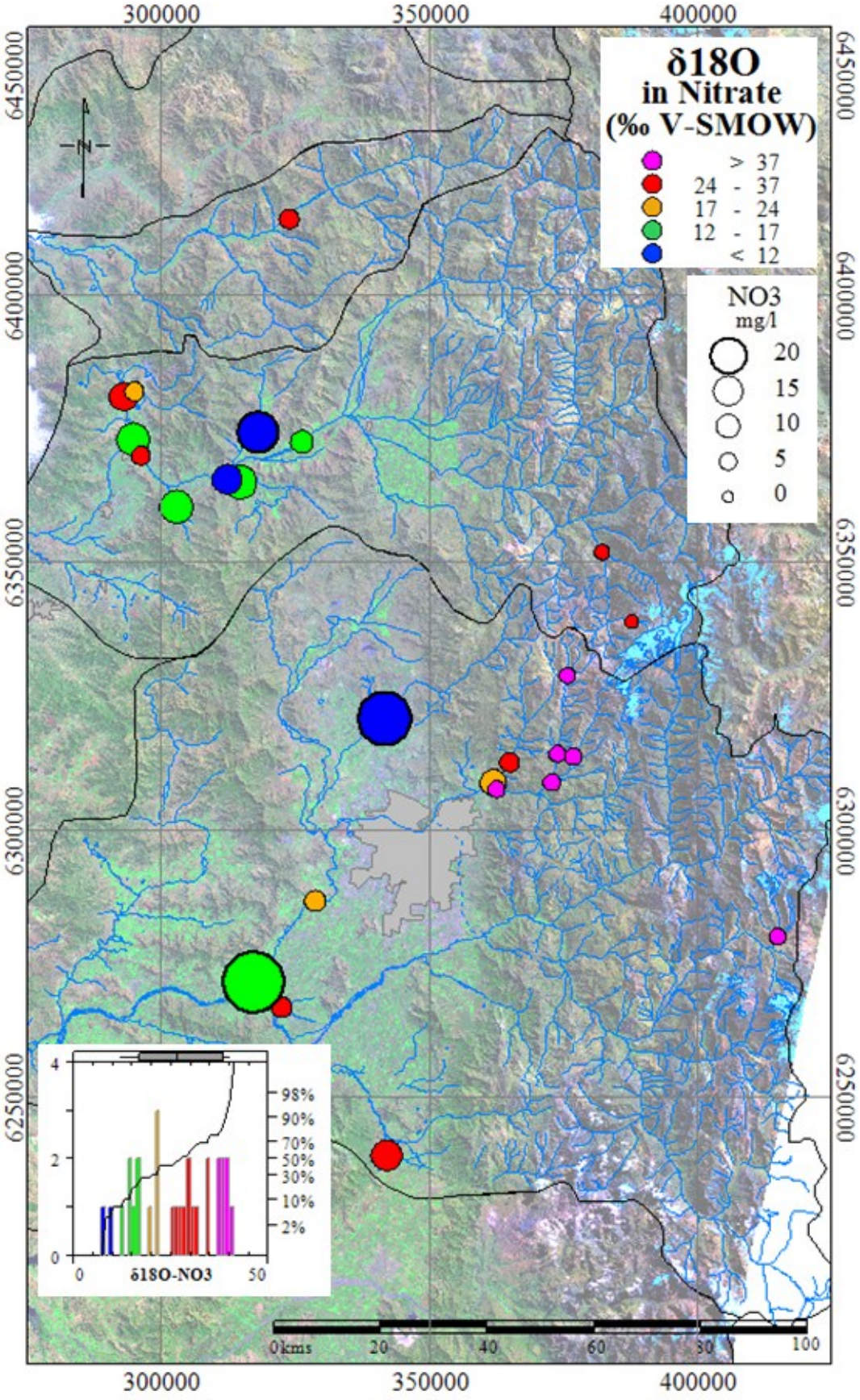


Figure 4.22: Baseline geochemical map coloured in relation to different populations for $\delta^{15}N$ and $\delta^{18}O_{NO3}$ values in precipitated nitrate of the water samples.



Continuation Figure 4.22

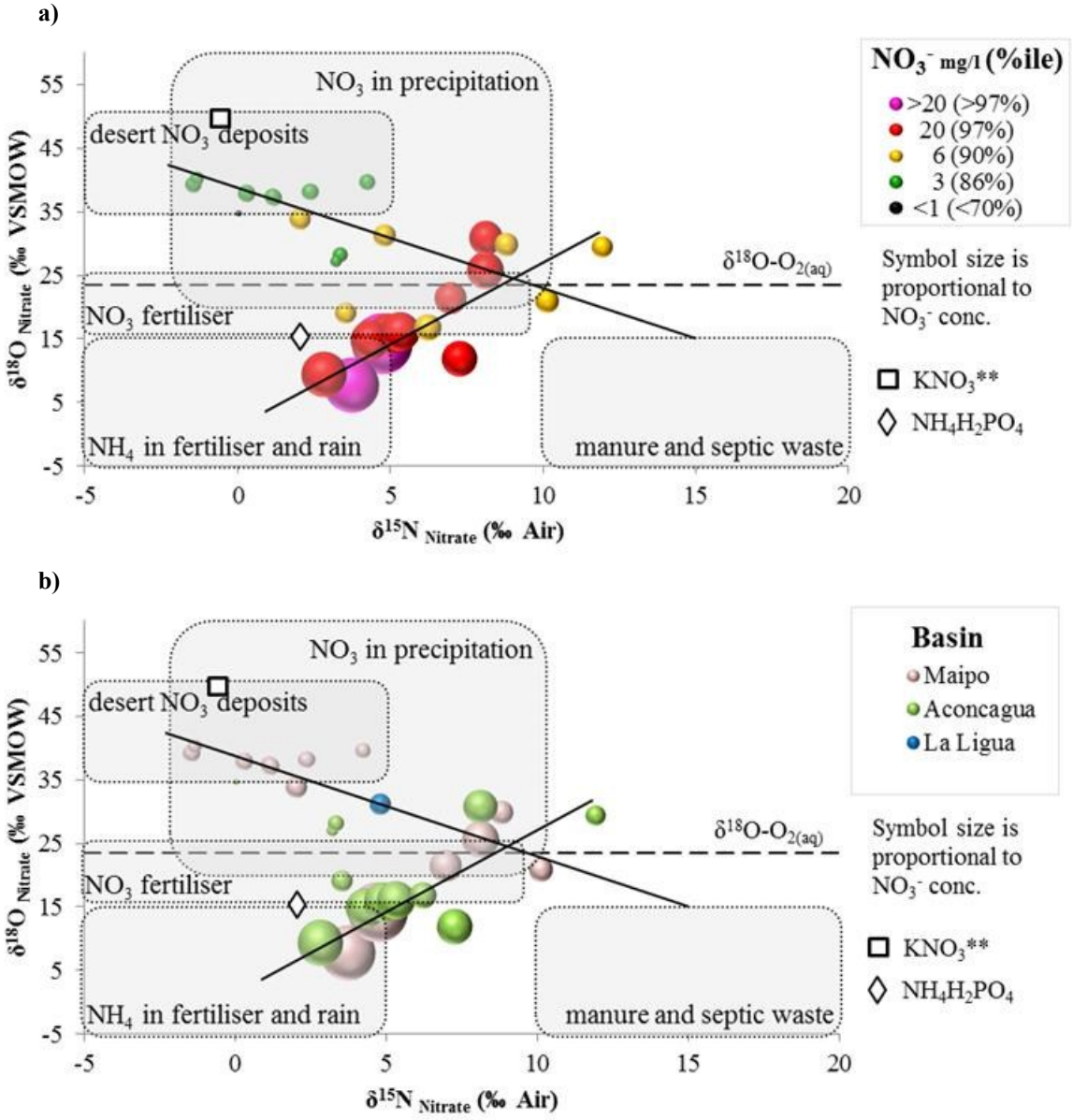


Figure 4.23: Modified from Jorquera et al. (2012). Typical $\delta^{15}N$ and $\delta^{18}O$ values of various nitrate reservoirs (after Kendall 1998) shown in boxes. The size of the symbol corresponds to the dissolved nitrate in mg/l. Value of atmospheric oxygen of 23.5‰ (Kroopnick & Craig 1972) is shown as a dashed line. Fertiliser isotopic data are shown for the KNO_3** Chilean fertiliser (Vitòria et al. 2004) and for $NH_4H_2PO_4$ (Jorquera et al. 2012) determined for this study. Two possible mixing lines are shown by continuous black lines. (a) The symbol colour represents the nitrate frequency population, and in (b) the symbol colour represents the three basins, the La Ligua, Aconcagua and Maipo.

4.5 Sources of anomalous geochemistry in Central Chile

The calculated area of the watersheds with anomalously high geochemistry was ~5000 sq.km. The main sources of anomalously high levels of chemicals found in stream water in that area were from the natural sources: geology (70%, 3600 sq.km.), hydrothermally

altered areas (7%, 380 sq.km.), and Cu-mineralised areas (4%, 190 sq.km.). There was also contamination from anthropogenic sources: agriculture and sewage (14%, 710 sq.km.), human settlements (4%, 210 sq.km.) and mining (1%, 60 sq.km.).

4.5.1 Geology

The major ion geochemistry of the stream waters in Central Chile is dominated by their interaction with evaporites, carbonates in marine sediments, andesites and granodiorites. The evaporites, which outcrop over a large area in the headwaters of the Maipo and Aconcagua valleys, comprise mainly Upper Jurassic gypsum inter-bedded and as diapirs with stratified volcano-sedimentary rocks, carbonates and marine formations (Figure 4.16). The carbonate rocks in marine sedimentary rocks also outcrop in the CC (Figure 4.4). Andesites and granodiorites are the dominant rock type in the AC (Table 4.2), whereas marine sedimentary rocks dominate in the CV.

Waters draining evaporites (Figures 4.24 a and b) extend over ~3600 sq. km. downstream in almost all of the Maipo Basin and in the headwaters of the Aconcagua River. They are Ca and SO_4^{-2} dominant trending to Na-K-Cl type waters (Figures 4.15 a and c) with high TDS and alkaline pH values (Table 4.13) and as defined by Factor 1 (Table 4.9). These waters also have anomalous concentrations of Ca, Cl, K, SO_4^{-2}, Na and TDS (Figure 4.17) that are significantly correlated (Table 4.7). The $\delta^{34}S$ values of these waters range from almost 9‰ to 14‰ with $\delta^{18}O_{SO4}$ values from approximately 5‰ to 15‰, consistent with an evaporitic sulphate source for the waters (Figure 4.21). The $\delta^{15}N$ value of 4.2‰ with a $\delta^{18}O_{NO3}$ value of 40‰ indicates that the nitrate in the waters is from atmospheric sources comparable with values in other waters elsewhere in the Andes (Figure 4.23) (Kendall 1998; Michalski et al. 2004; Jorquera et al. 2012). Waters draining carbonates, andesites

and granodiorites were found to be of Ca-HCO_3 type with low TDS and alkaline pH values (Table 4.13).

Table 4.13: Lithology reflected in ternary diagrams and anomalous water samples. Ranges of concentrations are shown in brackets.

Lithology	pH	TDS mg/l	Anomalously high concentrations
Evaporite rocks	7 - 8.5	<500 - 1500	SO_4^{-2} (300 to ~1300 mg/l), Ca (120 to ~300 mg/l), Na (70 to ~200 mg/l), Cl (80 to ~130 mg/l), K (3 to ~8 mg/l)
Carbonate rocks	7 - 9	<500	N/A
Marine intercalations in sedimentary rocks, andesite and granite	7 - 9	<500	N/A

N/A: Not applicable

4.5.2 Hydrothermally altered and mineralised areas

Fifteen water samples covering ~380 sq. km. in the AC have a distinctive geochemistry that reflects the influence of extensive areas of hydrothermal alteration and mineralisation in their catchments. They occur at five locations: viz. in the headwaters of the Colorado, Riecillos, Arrayán and San Francisco rivers, and the area between the Tupungato and Maipo volcanoes (Figure 4.3 and Table 4.14).

The Colorado River areas of hydrothermal alteration and mineralisation in the Aconcagua Basin are reflected in the chemistry of the stream waters over an area of ~200 sq. km. The waters have an almost neutral pH (mean 7.1) with low TDS (mean ~360 mg/l) and anomalous concentrations of Cd, Fe, Hg, Ni and Zn (Table 4.14). Cadmium, Ni and Zn are highly positively correlated (Table 4.7). The $\delta^{34}S$ values of -0.6‰ to 3.5‰ with $\delta^{18}O_{SO4}$ values of -3.4‰ to 8.3‰ are consistent with waters that have oxidised sulphide sources (Figure 4.21).

The Riecillos River areas of hydrothermal alteration and mineralisation in the Aconcagua Basin are reflected in the chemistry of the stream waters over an area of ~10 sq. km. The waters have an almost neutral pH (mean 7.5) with low TDS values (mean ~150 mg/l) and anomalously high values of As and Mo (Table 4.14). The $\delta^{34}S$ values are in the range 0.5‰ to 5.9‰ with $\delta^{18}O_{SO4}$ values of -3.4‰ to -1‰ and reflect the presence of waters that have reacted with sulphide sources (Figure 4.21). In the Agua Mala stream (Site 5, Figure 4.3), a tributary of the Riecillos River, local farmers have reported cattle dying after drinking the water (field observation) and this might be related to the concentration of As in the waters.

The Arrayán (Figure 4.24c) and San Francisco rivers areas of hydrothermal alteration and mineralisation in the Maipo Basin are reflected in the chemistry of the stream waters over an area of ~55 sq. km. The waters have relatively low pH (mean 5.2), TDS values with a mean of ~250 mg/l and anomalously high values of Al, Fe, Hg, Mo, Ni, P, SO_4^{-2} and Zn (Table 4.14). Aluminium, Ni, SO_4^{-2} and Zn are highly positively correlated (Table 4.7). The $\delta^{34}S$ values range -3.8‰ to 4.3‰ with $\delta^{18}O_{SO4}$ values of -7.7 to -4.5‰ which are consistent with the oxidation of sulphide (Figure 4.21). The $\delta^{15}N$ value of 2‰ with a $\delta^{18}O_{NO3}$ value of 34‰ are consistent with an atmospheric source (Jorquera et al. 2012) (Figure 4.23).



Figure 4.24: Field pictures. (a) Gypsum outcrop in the Volcán River. (b) Gypsum crushing and stockpiling plant in the Volcán River Valley. The dust in the valley is from the processing plant and dust deposited on the road. (c) Argillic alteration in the headwaters of Arrayán River. (d) An area of sulphide mineralisation in the headwaters of the Yerba Loca Stream. (e) The El Melón River draining agricultural and grazing land and (f) a canal draining into the El Melón River from agricultural land with small settlements

Table 4.14: Anomalously high elemental concentrations and specific isotopic compositions associated with hydrothermally altered and mineralised areas. Peak values are shown in brackets. See Figure 4.3 for the sampling site number location.

Sample Site N°	Area ID	pH	TDS mg/l	Anomalous chemistry and isotopic compositions
	Colorado River, 203 sq. km.			
1	Colorado River	7.7	334	Cd (0.8 µg/l), Ni (5.6 µg/l), $\delta^{34}S$ (3.5‰), $\delta^{18}O_{SO4}$ (-3.4‰)
2	Blanco River (*T)	5.9	407	Cd (3.3 µg/l), Fe (6 mg/l), Ni (14.5 µg/l), Zn (175 µg/l), $\delta^{34}S$ (-0.6‰), $\delta^{18}O_{SO4}$ (8.3‰)
3	Colorado River	7.4	355	Cd (1.4 µg/l), Hg (3.4 µg/l), Ni (11 µg/l)
4	Colorado River	7.5	336	Ni (7.3 µg/l), $\delta^{34}S$ (2.1‰), $\delta^{18}O_{SO4}$ (1.2‰)
	Riecillos River, 11 sq. km.			
5	Agua Mala (*T)	7.2	86	As (65.9 µg/l), Mo (8.1 µg/l), $\delta^{34}S$ (0.5‰), $\delta^{18}O_{SO4}$ (-1‰)
6	Riecillos River	7.7	198	As (11.3 µg/l), $\delta^{34}S$ (5.9‰), $\delta^{18}O_{SO4}$ (-3.4‰)
	Arrayán and San Francisco rivers, 55 sq. km.			
7	Ortiga (*T)	4.8	106	Al (0.3 mg/l), F^- (480 µg/l), $\delta^{34}S$ (2.8‰), $\delta^{18}O_{SO4}$ (3‰)
8	Del Rayo (*T)	3.2	206	Al (4 mg/l), F^- (838 µg/l), Fe (5 mg/l), Ni (21 µg/l), Zn (40 µg/l), $\delta^{34}S$ (-3.8‰), $\delta^{18}O_{SO4}$ (-7.7‰)
9	Ortiga (*T)	3.4	334	Al (6 mg/l), F^- (380 µg/l), Fe (5 mg/l), Hg (3.1 µg/l), Ni (33 µg/l), Zn (83 µg/l), $\delta^{34}S$ (-3.8‰), $\delta^{18}O_{SO4}$ (-4.5‰)
10	Valle Largo (*T)	4.7	437	Al (5 mg/l), F^- (504 µg/l), Fe (0.8 mg/l), Ni (28 µg/l), SO_4^{-2} (357 mg/l), Zn (31 µg/l), $\delta^{34}S$ (-0.7‰), $\delta^{18}O_{SO4}$ (4.5‰), $\delta^{15}N$ (2‰), $\delta^{18}O_{NO3}$ (34‰)
11	El Plomo (*T)	6.8	137	Ni (6.5 µg/l), Zn (102 µg/l), $\delta^{34}S$ (-2‰), $\delta^{18}O_{SO4}$ (-4.8‰)
12	Duarte (*T)	8	204	Mo (9.3 µg/l), P (68 µg/l), $\delta^{34}S$ (4.3‰), $\delta^{18}O_{SO4}$ (-2.9‰)
	Tupungato and Maipo Volcanoes, 110 sq. km.			
13	Rabicano (*T)	7.6	1008	SO_4^{-2} (354 mg/l), Zn (71 µg/l)
14	Las Amarillas (*T)	7.9	1076	Mg (29 mg/l), Ni (16 µg/l), SO_4^{-2} (953 mg/l), $\delta^{34}S$ (0.3‰), $\delta^{18}O_{SO4}$ (-4.1‰)
15	Barroso River	7.1	1352	As (17 µg/l), Fe (3043 µg/l), Mg (38 mg/l), Ni (40 µg/l), $\delta^{34}S$ (10.2‰), $\delta^{18}O_{SO4}$ (-2.1‰)

(*T) Tributary of a main river or stream in the area

The areas of hydrothermal alteration and mineralisation between the Tupungato and Maipo volcanoes in the Maipo Basin are reflected in the chemistry of the stream waters over an area of ~110 sq. km. The waters have a near neutral pH (mean 7.6) and high TDS (mean ~1000 mg/l) reflecting buffering by the evaporites in the area. The waters also

have anomalously high values of As, Fe, Mg, Ni, SO_4^{-2} and Zn (Table 4.14). Nickel, SO_4^{-2} and Zn are highly positively correlated (Table 4.7). The $\delta^{34}S$ values range 0.3‰ to 10.2‰ with $\delta^{18}O_{SO4}$ values of -4.1‰ to -2.1‰) which are consistent with waters that have interacted with oxidising sulphide sources (Figure 4.21) and possibly mixing with hydrothermal springs seen in the field associated with volcanoes in the area such as the Maipo Volcano. In the Barroso River Valley, local farmers have also reported cattle deaths after drinking the water (field observation).

4.5.3 Copper mineralisation

For the purpose of this study, copper mineralisation is defined by the presence of highly anomalous stream waters in areas with no known historic or current mining. Seven samples from the survey have a distinctive geochemistry reflecting the presence of copper sulphide mineralisation at four locations, viz.: Colorado, Barriga and San Francisco rivers and the Yerba Loca Stream (Table 4.15). These areas extend over a total of ~190 sq. km. in the AC.

The Cu-mineralisation in the Colorado River area in the Aconcagua Basin is reflected by the chemistry of the stream waters over an area of ~8 sq. km. The stream waters have low pH (2.8) with low TDS (506 mg/l) and anomalously high values of Al, Cd, Cu, Fe, Ni, Pb, SO_4^{-2} and Zn (Table 4.15). Aluminium, Cd, Cu, Ni, SO_4^{-2} and Zn are highly positively correlated (Table 4.7). The $\delta^{34}S$ value of 4.3‰ with a $\delta^{18}O_{SO4}$ value of -1.8‰ is consistent with waters that have reacted with oxidising sulphide sources (Figure 4.21).

The Barriga River area of Cu-mineralisation in the Aconcagua Basin is reflected in the geochemistry of stream waters over ~17 sq. km. The stream waters are moderately acid,

pH 5.4 and have relatively high TDS 905 mg/l with anomalously high values of Al, Ca, Cd, Cu, EC, F^-, Fe, Hg, Mg, Ni, SO_4^{-2} and Zn (Table 4.15). Aluminium, Cd, Cu, F, Ni, SO_4^{-2} and Zn are highly positively correlated (Table 4.7). The $\delta^{34}S$ value of -0.2‰ with a $\delta^{18}O_{SO4}$ value of -4.5‰ are consistent with oxidising sulphide sources (Figure 4.21). The $\delta^{15}N$ value of 0‰ with a $\delta^{18}O_{NO3}$ value of 34.8‰ are most consistent with an atmospheric source (Jorquera et al. 2012) (Figure 4.23).

Table 4.15: Anomalously high concentrations and specific isotopic compositions associated with the Cu-mineralised areas. Peak values are shown in brackets. See Figure 4.3 for the sampling site number location.

Sample Site N°	Area ID	pH	TDS mg/l	Anomalous chemistry and isotopes
	Colorado River, 8 sq. km.			
16	Torin (*T)	2.8	506	Al (12 mg/l), Cd (1.3 µg/l), Cu (457 µg/l), Fe (8 mg/l), Ni (19 µg/l), Pb (1.4 µg/l), SO_4^{-2} (368 mg/l), Zn (219 µg/l), pH (2.8), $\delta^{34}S$ (4.3‰), $\delta^{18}O_{SO4}$ (-1.8‰)
	Barriga River, 17 sq. km.			
17	Barriga River	5.4	905	Al (8 mg/l), Ca (215 mg/l), Cd (0.89 µg/l), Cu, (120 µg/l), F^- (650 µg/l), Fe (1 mg/l), Hg (1.3 µg/l), Mg (26 mg/l), Ni (59.1 µg/l), SO_4^{-2} (968 mg/l), Zn (265 µg/l), EC (1136 µS/cm), pH (5.4), TDS (905 mg/l), $\delta^{34}S$ (-0.2‰), $\delta^{18}O_{SO4}$ (-4.5‰), $\delta^{15}N$ (0.0‰), $\delta^{18}O_{NO3}$ (34.8‰)
	San Francisco River, 12 sq. km.			
18	Dolores (*T)	6.3	326	Cd (0.79 µg/l), Cu (258 µg/l), Fe (0.7 mg/l), Ni (6.5 µg/l), Zn (345 µg/l), pH (6.3), $\delta^{34}S$ (4.3‰), $\delta^{18}O_{SO4}$ (-2.5‰)
19	San Francisco	6.6	277	Cu (803 µg/l), Ni (12 µg/l), Zn (131 µg/l), $\delta^{34}S$ (2.9‰), $\delta^{15}N$ (0.3‰), $\delta^{18}O_{NO3}$ (38‰)
	Yerba Loca Stream, 155 sq. km.			
20	Yerba Loca headwaters	2.0	1070	Al (6 mg/l), As (14 µg/l), Cu (11693 µg/l), Fe (45 mg/l), Ni (26 µg/l), P (694 µg/l), SO_4^{-2} (446 mg/l), Zn (124 µg/l), $\delta^{34}S$ (4.2‰), $\delta^{18}O_{SO4}$ (-0.4‰)
21	Yerba Loca	5.7	262	Al (0.2 mg/l), Cu (3275 µg/l), Ni (18 µg/l), Zn (173 µg/l), $\delta^{34}S$ (3.2‰), $\delta^{18}O_{SO4}$ (-0.4‰), $\delta^{15}N$ (-1.5‰), $\delta^{18}O_{NO3}$ (39.4‰)
22	Yerba Loca	5.1	310	Al (1 mg/l), Cu (4185 µg/l), Ni (18 µg/l), Zn (175 µg/l), $\delta^{34}S$ (2.9‰)

(*T) Tributary of a main river or stream in the area.

The San Francisco River area in the Maipo Basin reflects the presence of Cu-mineralisation in the chemistry of the stream waters from ~12 sq. km. The waters have slightly acid pH 6.3 with low TDS 326 mg/l and anomalously high values of Cd, Cu, Fe,

Ni and Zn (Table 4.15). Cadmium, Cu, Ni and Zn are highly positively correlated (Table 4.7). The $\delta^{34}S$ value of 4.3‰ with a $\delta^{18}O_{SO4}$ value of -2.5‰ is consistent with oxidising sulphide sources (Figure 4.21).

The Yerba Loca area water chemistry reflects the presence of Cu-mineralisation in the headwaters of the Yerba Loca Stream in the Maipo Basin over ~155 sq. km. (Figure 4.24d). The waters have acid pH values (mean 4.3) with low TDS (mean 547 mg/l) and anomalously high values of Al, As, Cu, Fe, Ni, P, SO_4^{-2} and Zn (Table 4.15). Aluminium, Cu, Ni, SO_4^{-2} and Zn are highly positively correlated (Table 4.7). The $\delta^{34}S$ values of 2.9‰ to 4.2‰ with a $\delta^{18}O_{SO4}$ value of -0.4‰ are consistent with oxidising sulphide sources (Figure 4.21). The $\delta^{15}N$ values of -1.5‰ to 0.3‰ with $\delta^{18}O_{NO3}$ values of ~35‰ to ~40‰ are consistent with an atmospheric source (Jorquera et al. 2012) (Figure 4.23).

4.5.4 Agriculture and sewage

The chemistry of twenty five stream water samples reflects the presence of agriculture and/or sewage. These areas which are in the CV and CC cover an area totalling ~700 sq. km. The waters are grouped according to the principal source affecting the water chemistry, viz.: fertilisers, sewage and a mixture of nitrate sources (Table 4.16). These were defined by their anomalous geochemistry and the nitrogen and oxygen isotopic compositions of nitrate (Figure 4.23).

The area affected by fertilisers extends over ~270 sq. km. in the valleys of the CC, in the Aconcagua near Catemu and in the CV in the Mapocho River (Figures 4.3 and 4.24e). The waters have a slightly alkaline pH (mean 7.7), low TDS (mean ~480 mg/l) and anomalously high concentrations of HCO_3^-, K, Mg, NO_3^- and P (Table 4.16 and Figure

4.17). Alkalinity, Mg and NO_3^- are highly positively correlated (Table 4.7). The $\delta^{34}S$ values of 3‰ to 11‰) with $\delta^{18}O_{SO4}$ values of 2.5‰ to 27.2‰ are consistent with mixtures of sulphur sources including sulphides, evaporites, and atmospheric deposition sources and anthropogenic sources such as fertilisers and detergents (Figure 4.21). The $\delta^{15}N$ values of 2.8‰ to 6.2‰ with $\delta^{18}O_{NO3}$ values of 7.8‰ to 19.2‰ reflect mixing of nitrate and ammonium based fertilisers (Jorquera et al. 2012) (Figure 4.23).

The areas affected by sewage extend over ~160 sq km. in the Aconcagua River near the La Calera Township and in the Mapocho River downstream of Santiago (Figures 4.3 and 4.24f). The stream waters have a slightly alkaline pH (mean 8.0) with low TDS (mean ~760 mg/l) and anomalous F^-, HCO_3^-, K, Mo, NO_3^- and P (Table 4.16). Alkalinity, F^-, and NO_3^- are highly positively correlated (Table 4.7). The $\delta^{34}S$ values of 4.8‰ to 12.7‰ with $\delta^{18}O_{SO4}$ values of 2.3‰ to 8.3‰ are consistent with mixing of sulphides, evaporites, and atmospheric deposition with fertilisers (Figure 4.21). The $\delta^{15}N$ values of 10.1‰ to 11.9‰ with $\delta^{18}O_{NO3}$ values of 21‰ to 29.5‰ indicate a sewage source with some mixing with atmospheric oxygen (Jorquera et al. 2012) (Figure 4.23).

The waters which reflect mixed nitrate sources extend over an area of ~280 sq. km. in the CC and in the CV. The stream waters have a slightly alkaline pH (mean 7.8) and low TDS (mean ~450 mg/l) with anomalous values of HCO_3^-, K, Mg, NO_3^- and P (Table 4.16). Alkalinity, Mg and NO_3^- are highly positively correlated (Table 4.7). The $\delta^{34}S$ values of 0.4‰ to 11‰ with $\delta^{18}O_{SO4}$ values of 3‰ to 10.2‰ reflect mixing of sulphides, evaporites, and atmospheric deposition with fertilisers (Figure 4.21). The $\delta^{15}N$ values of 4.8‰ to 8.8‰ with $\delta^{18}O_{NO3}$ values of 12‰ to 31.3‰ indicate the mixing of fertilisers and NO_3^- from atmospheric precipitation (Jorquera et al. 2012) (Figure 4.23).

Table 4.16: Anomalously high concentrations of elements associated with agricultural areas by nitrate source. Peak values are shown in brackets. See Figure 4.3 for the sampling site number location.

Sample Site N°	Source ID/ Area ID	pH	TDS mg/l	Anomalous chemistry and isotopes
	Fertilisers, 270 sq. km.			
23	Carretón (*T)	7.5	353	HCO_3^- (152 mg/l), Mg (24 mg/l), NO_3^- (4 mg/l), P (89 µg/l), $\delta^{34}S$ (4.9‰), $\delta^{18}O_{SO4}$ (3.8‰), $\delta^{15}N$ (3.5‰), $\delta^{18}O_{NO3}$ (19.2‰)
24	El Melón Stream	7.1	440	HCO_3^- (161 mg/l), Mg (23 mg/l), NO_3^- (14 mg/l), P (105 µg/l), $\delta^{34}S$ (4.4‰), $\delta^{18}O_{SO4}$ (3.2‰), $\delta^{15}N$ (5.3‰), $\delta^{18}O_{NO3}$ (16.2‰)
25	Aconcagua River	8.4	361	NO_3^- (6 mg/l), $\delta^{34}S$ (5.7 ‰), $\delta^{18}O_{SO4}$ (19.8‰), $\delta^{15}N$ (6.2‰), $\delta^{18}O_{NO3}$ (16.9‰)
26	Catemu (*T)	6.9	422	HCO_3^- (174 mg/l), Mg (20 mg/l), NO_3^- (20 mg/l), P (105 µg/l), $\delta^{34}S$ (5.9‰), $\delta^{18}O_{SO4}$ (3.8‰), $\delta^{15}N$ (2.8‰), $\delta^{18}O_{NO3}$ (9.5‰)
27	Los Loros (*T)	7.1	497	HCO_3^- (195 mg/l), NO_3^- (15 mg/l), $\delta^{34}S$ (3.5‰), $\delta^{15}N$ (4.9‰), $\delta^{18}O_{NO3}$ (15.9‰)
28	Ocoa (*T)	8.5	519	HCO_3^- (199 mg/l), Mg (24 mg/l), NO_3^- (14 mg/l), P (155 µg/l), $\delta^{34}S$ (5.1‰), $\delta^{18}O_{SO4}$ (2.5‰), $\delta^{15}N$ (4.3‰), $\delta^{18}O_{NO3}$ (14.9‰)
29	Colina Stream	8.1	320	HCO_3^- (154 mg/l), NO_3^- (29 mg/l), $\delta^{34}S$ (3 ‰), $\delta^{18}O_{SO4}$ (12.5‰), $\delta^{15}N$ (3.7‰), $\delta^{18}O_{NO3}$ (7.8‰)
30	Mapocho River	7.9	932	HCO_3^- (191 mg/l), K (8 mg/l), Mg (24 mg/l), NO_3^- (34 mg/l), P (1613 µg/l), $\delta^{34}S$ (11‰), $\delta^{18}O_{SO4}$ (27.2‰), $\delta^{15}N$ (4.7‰), $\delta^{18}O_{NO3}$ (14.3‰)
	Sewage, 160 sq. km.			
31	Aconcagua River	8.5	349	NO_3^- (4 mg/l), $\delta^{34}S$ (4.8‰), $\delta^{18}O_{SO4}$ (2.3‰), $\delta^{15}N$ (11.9‰), $\delta^{18}O_{NO3}$ (29.5‰)
32	Mapocho River	7.4	1180	F^- (390 µg/l), HCO_3^- (220 mg/l), K (17 mg/l), Mo (8.6 µg/l), NO_3^- (5 mg/l), P (9021 µg/l), $\delta^{34}S$ (12.7‰), $\delta^{18}O_{SO4}$ (8.3‰), $\delta^{15}N$ (10.1‰), $\delta^{18}O_{NO3}$ (21‰)
	Mixed nitrate sources, 280 sq. km.			
33	La Ligua River	8.4	262	K (5.2 mg/l), NO_3^- (4 mg/l), P (664 µg/l), $\delta^{34}S$ (3.4‰), $\delta^{18}O_{SO4}$ (10.2‰), $\delta^{15}N$ (4.8‰), $\delta^{18}O_{NO3}$ (31.3‰)
34	El Melón Stream	6.6	563	HCO_3^- (158 mg/l), Mg (36 mg/l), NO_3^- (11 mg/l), P (495 µg/l), $\delta^{34}S$ (3.2‰), $\delta^{18}O_{SO4}$ (5.5‰), $\delta^{15}N$ (8.1‰), $\delta^{18}O_{NO3}$ (30.9‰)
35	Aconcagua River	8.1	404	HCO_3^- (154 mg/l), NO_3^- (12 mg/l), $\delta^{34}S$ (4.5‰), $\delta^{18}O_{SO4}$ (3‰), $\delta^{15}N$ (7.2‰), $\delta^{18}O_{NO3}$ (12‰)
36	El Arrayán Stream	7.7	287	NO_3^- (9 mg/l), $\delta^{34}S$ (0.4‰), $\delta^{18}O_{SO4}$ (6.2‰), $\delta^{15}N$ (6.9‰), $\delta^{18}O_{NO3}$ (21.5‰)
37	Picarquín (*T)	7.3	351	NO_3^- (12 mg/l), P (68 µg/l), $\delta^{34}S$ (5.8‰), $\delta^{18}O_{SO4}$ (7.1‰), $\delta^{15}N$ (8.1‰), $\delta^{18}O_{NO3}$ (25.8‰)
38	Maipo River	8.5	854	K (6 mg/l), NO_3^- (5 mg/l), P (98 µg/l), $\delta^{34}S$ (11‰), $\delta^{18}O_{SO4}$ (10.1‰), $\delta^{15}N$ (8.8‰), $\delta^{18}O_{NO3}$ (29.9‰)

(*T) Tributary of a main river or stream in the area

4.5.5 Human settlements

Eight samples have a distinctive geochemistry reflecting the presence of human settlements and other type of built environments. They extend over ~210 sq. km. in the CV, the CC and downstream of the ski resorts in the AC.

In the vicinity of Colina, Pirque and Mostazal townships in the CV and in the vicinity of Calera Township in the CC (Sites 39, 40, 37 and 28 respectively, Figure 4.3), the stream waters have anomalous values of lead (0.9 to 4 µg/l) which is suggested to be associated with fly-tipping of batteries, paint or lead pipes (There are no official landfill sites here).

In the Mapocho River downstream of Santiago (Site 30, Figure 4.3), the stream water has anomalously high Hg concentration of 1.6 µg/l, which may reflect the presence of Santiago waste disposal, illegal incineration and/or pesticides.

In the El Manzanito Stream, a tributary of San Francisco River downstream of the ski resorts near Santiago in the AC (Site 43, Figure 4.3), stream waters have an anomalous value of P (185 µg/l), which is thought to be associated with detergents in waste waters. Indeed foam was seen at the time the sample was taken (field observation).

4.5.6 Mine area waters

For the purpose of this study, mine area waters are defined as follows. They do not reflect the mining operation because all mine and process waters are diverted to tailing dams up to 50 km. away in the CV. Moreover, fresh water streams near the mine are diverted from around mining operations into major streams, hence waters downstream from major mines in the district have a near neutral pH and low metal contents. Waters near to mines

which have highly anomalous concentrations of chemicals in stream waters reflect the presence of high grade mineralisation and alteration or potentially contaminated with road dust.

Four samples have a distinctive geochemistry which reflects the presence of such waters. These include the Andina - Los Bronces Cu-Mo districts in the AC and the El Soldado Cu district and the abandoned La Poza and Restauradora Pb-Zn mines in the CC (Table 4.17). The stream waters which indicate the presence of high grade mineralisation and alteration diluted by fresh waters extend over ~60 sq. km.

One water sample draining the Andina mine area represents ~10 sq. km. of the Blanco River valley. It has a neutral to alkaline pH (7.7), low TDS (~264 mg/l) and an anomalous value of Mo (Table 4.17 and Mo map, Figure 4.17) which is in solution in more alkaline environments. The $\delta^{34}S$ value of 2.3‰ with a $\delta^{18}O_{SO4}$ value of -0.3‰ is consistent with oxidising sulphide sources.

One water sample draining the Los Bronces mine area represents ~24 sq. km. of the San Francisco River valley. It has a near neutral pH (7.9), low TDS (~468 mg/l) with anomalously high values of Cd, Cl, Na and Zn (Table 4.17). Cadmium and Zn are highly positively correlated (Figure 4.10 and Table 4.7) as defined by Factor 2 reflecting mineralisation (Table 4.9). Cl and Na are also highly positively correlated (Figure 4.10 and Table 4.7) and as defined by Factor 1 (Table 4.9) indicating dissolved salts. The $\delta^{34}S$ value of 2.2‰ with a $\delta^{18}O_{SO4}$ value of -2.4‰ is consistent with sulphide sources. The $\delta^{15}N$ value of 1.1‰ with a $\delta^{18}O_{NO3}$ value of 37.5‰ is most consistent with an atmospheric source (Jorquera et al. 2012).

One water sample draining from the El Soldado mine represents an area of only 0.2 sq. km. of the El Gallo Stream valley. It has an alkaline pH of 8.4 with low TDS (~700 mg/l) and anomalously high values of Fe, Mg, Mo, and SO_4^{-2} (Table 4.17). Magnesium and SO_4^{-2} are highly positively correlated (Table 4.7). The $\delta^{34}S$ value of 3.7‰ with a $\delta^{18}O_{SO4}$ value of 0.7‰ is consistent with oxidising sulphide sources.

One water sample draining the abandoned La Poza and Restauradora Pb-Zn mines near Catemu (Figure 4.3) represents ~20 sq. km. It has near neutral pH (7.1) and low TDS (~350 mg/l), with anomalously high values of HCO_3^-, Pb and Zn (Table 4.17). The $\delta^{34}S$ value of -1.1‰ with a $\delta^{18}O_{SO4}$ value of -0.4‰ is consistent with oxidising sulphide sources.

Table 4.17: Anomalously high concentrations of elements and specific isotopic compositions in mine area waters. Peak values are shown in brackets. See Figure 4.3 for the sampling site number location.

Sample Site N°	Area ID	Area sq. km.	pH	TDS mg/l	Anomalous chemistry and isotopes
44	Andina	10	7.7	264	Mo (17 µg/l), $\delta^{34}S$ (2.3‰), $\delta^{18}O_{SO4}$ (-3.0‰)
45	Los Bronces	24	7.9	468	Cd (0.89 µg/l), Cl (82 mg/l), Na (51 mg/l), Zn (91.3 µg/l), $\delta^{34}S$ (2.2‰), $\delta^{18}O_{SO4}$ (-2.4‰), $\delta^{15}N$ (1.1‰), $\delta^{18}O_{NO3}$ (37.5‰)
46	El Soldado	0.2	8.4	672	Fe (178 µg/l), Mg (34 mg/l), Mo (12 µg/l), SO_4^{-2} (324 mg/l), $\delta^{34}S$ (3.7‰), $\delta^{18}O_{SO4}$ (0.7‰)
47	La Poza and Restauradora	20	7.1	324	HCO_3^- (178 mg/l), Pb (1.1 µg/l), Zn (87 µg/l), $\delta^{34}S$ (-1.1‰), $\delta^{18}O_{SO4}$ (-0.4‰)

4.6 Comparison of the hydrogeochemical data of the Maipo Basin with water quality regulation data

The percentage differences of fifteen parameters including EC, DO, pH, sodium absorption ratio (RAS), Al, As, Cl, Cr, Cu, Fe, Mn, Mo, Pb, SO_4, and Zn were calculated (Table 4.18). The overall means of the percentage differences of all the parameters below or equal to zero for all sites are -65% with respect to the mean of the regional

hydrogeochemical data for the Maipo Basin and -65% to the 66th percentile of the regional hydrogeochemical data for the Maipo Basin (Table 4.18).

With respect to the regulation values, the overall means of the percentage differences above zero considering all the sites are 45% for the mean of the regional hydrogeochemical data for the Maipo Basin and 42% to the 66th percentile of the regional hydrogeochemical data for the Maipo Basin (Table 4.18). The parameters higher than the regulated levels (or with a positive difference) are EC, DO, pH, RAS, Cl, Cu, Mn, Mo, SO_4 and Zn (Table 4.18).

Table 4.18: Mean of the percentage difference between the regional hydrogeochemical data for the Maipo Basin (mean and 66th percentile) and regulated values. The codes of the sub-basins are those used in the draft regulation. Parameters higher than the regulation values are listed for each sub-basin. The percentage differences are shown in brackets. Very high differences are shown in bold.

Sub-basin	River or stream name /and segment	Mean of % Diff. > 0%		Parameters % Diff. > 0%	
		cf. mean	*cf.* 66th percentile	*cf.* mean	*cf.* 66th percentile
SF-TR-10	San Francisco	113	5	Mn (113%)	pH (7%), Cu (4%), Mn (149%)
YL-TR-10	Yerba Loca	**511**	**173**	**Zn (511%)**	EC (20%), DO (8%), Cu (17%), Zn **(646%)**
MO-TR-10	Molina	3	27	pH (3%)	DO (47%), pH (7%)
AR-TR-10	Arrayán	3	41	EC (3%)	EC (39%), DO (42%)
VO-TR-10	Volcán	41	60	EC (4%), RAS (73%), Cl (46%)	EC (29%), RAS (89%), Cl (63%)
YE-TR-10	Yeso upstream the dam	48	36	SO_4 (55%), Mn (41%)	EC (24%), pH (%), SO_4 (74%), Mn (47%)
YE-TR-20	Yeso upstream Maipo	45	104	EC (9%), SO_4 (82%)	EC (38%), SO_4 (170%)
CO-TR-10	Colorado	N/A	10		EC (10%), DO (18%), pH (1%)
OL-TR-10	Olivares	6	5	pH (6%)	DO (1%), pH (9%)
EEM-TR-10	El Manzano	31	93	SO_4 (31%)	SO_4 (93%)
QR-TR-10	Quebrada San Ramón	37	76	EC (25%), Mn (50%)	EC (38%), Mn (115%)
LA-TR-10	Lampa	9	25	EC (16%), DO (6%), pH (3%), Mo (12%)	EC (31%), DO (41%), pH (9%), SO_4 (10%), Mo (37%)
MP-TR-10	Mapocho upstream Arrayán	1	10	pH (1%)	EC (3%), DO (26%), pH (3%)
MP-TR-31	Mapocho upstream Peñaflor	25	37	EC (41%), DO (14%), RAS (19%)	EC (63%), DO (42%), RAS (38%), Cl (27%), SO_4 (16%)
MP-TR-32	Mapocho upstream Maipo	17	45	DO (22%), SO_4 (13%)	DO (114%), pH (4%), SO_4 (18%)
MA-TR-10	Maipo upstream Volcán	6	21	EC (1%), SO_4 (11%)	EC (17%), DO (20%), SO_4 (26%)
MA-TR-20	Maipo upstream Colorado	5	21	DO (9%), SO_4 (2%)	EC (10%), DO (35%), SO_4 (18%)
MA-TR-32	Maipo upstream Clarillo	N/A	5		EC (3%), DO (5%), SO_4 (6%)
MA-TR-33	Maipo upstream Angostura	6	10	DO (6%)	EC (1%), DO (37%), pH (1%), SO_4 (1%)
MA-TR-40	Maipo upstream Mapocho	19	42	DO (31%), pH (5%), SO_4 (22%)	DO (90%), pH (6%), SO_4 (29%)
AN-TR-10	Angostura	20	35	DO (39%), pH (2%)	DO (62%), pH (9%)
EC-TR-10	Colina	27	43	EC (77%), pH (2%), SO_4 (4%)	EC (129%), DO (24%), pH (4%), RAS (13%), SO_4 (45%)
OVERALL		**45**	**42**	**-**	**-**

CHAPTER 5: DISCUSSION

5.1 Introduction

The research area for this study extends over ~20000 sq. km. of Central Chile and extends from the mountainous terrains of the Andes to the Coastal Cordillera including the Central Valley and covers the 3 principal catchment basins of La Ligua, Aconcagua and Maipo. It also includes part of the classic copper district of Central Chile, the porphyry Cu-Mo deposits of Andina-Los Bronces. Nine hundred and fifty eight water samples were collected over agricultural valleys and the copper district of Central Chile with the sampling being carried out over the high flow and low flow seasons of October to May, 2006-2007 and 2007-2008. Electrical conductivity (EC), pH, dissolved oxygen (DO), temperature and alkalinity were measured in the field. The samples were analysed using a range of multi-elemental techniques including ICP-MS and ion chromatography at Acme Analytical Laboratories Ltd.©, Vancouver. In addition, stable isotopes (δD, $\delta^{18}O$ in water; $\delta^{34}S$ and $\delta^{18}O$ in sulphate; and $\delta^{15}N$ and $\delta^{18}O$ in nitrate) were prepared and determined at the Queen's Facility for Isotope Research (QFIR) at Queen's University, Kingston, Ontario.

5.2 Reliability of the analytical data

The results of the QA/QC data analysis showed that the majority of chemical levels were within the degree of variation defined as acceptable. Only aluminium concentrations for the certified reference materials (CRMs) were slightly above the limit, but they showed high reproducibility and the results did not affect the overall sample data and they were considered acceptable. Overall the dataset was found to have a high level of accuracy and precision and hence could be used for both this hydrogeochemical baseline study, and importantly also to compare with current drinking water guideline and regulatory values.

Most samples have acceptable charge imbalance (CI) results, however the samples with low pH (<5) and some samples with pH near 8 have a highly negative CI (<-50%). These samples reflect the presence of hydrothermal alteration and mineralisation, and it is suggested that maybe the highly anomalous trace metals in these areas affect the ionic balance. This is exemplified for the pH and Cu content of the regional dataset where samples with low pH and high Cu concentration have the most negative charge imbalances (Figure 5.1). It is suggested that, in calculating the CI for waters of low pH, speciation must be calculated (Nordstrom et al. 2009). In this study speciation was not calculated, but it is thought that the speciation of ions and compounds may be affecting the waters with high negative charge imbalance.

5.3 Geochemistry of the trace elements and compounds

One hundred and forty five samples collected over the low flow season, February to May of 2008, were used to prepare the hydrogeochemical baseline and to characterise the geochemistry of the stream waters in the region. This sampling campaign covered more rivers and streams of the study area and showed generally less dilution than over the high flow season (Figure 4.9).

The ternary diagrams of major ions reflect the main lithological units in the region. Waters with low TDS levels are dominantly of Ca-HCO_3 type and reflect the presence of carbonate rocks in the marine formations and marine intercalations in continental formations in the region. This type of water was found also in areas with outcrops of marine intercalations in sedimentary sequences and of andesites and granodiorites. Waters with high TDS values, which are dominantly of Ca-SO_4 trending to Na-K-Cl type, reflect interaction with evaporites as defined by Factor 1 (Table 4.9) composed mainly of

gypsum (Figure 4.24a). The ternary diagram for nitrate and other anions (Figure 4.15e) shows one sample with low TDS levels that is NO_3^- dominant. This is thought to reflect the presence of fertilisers and sewage in the drainage from a local agricultural community.

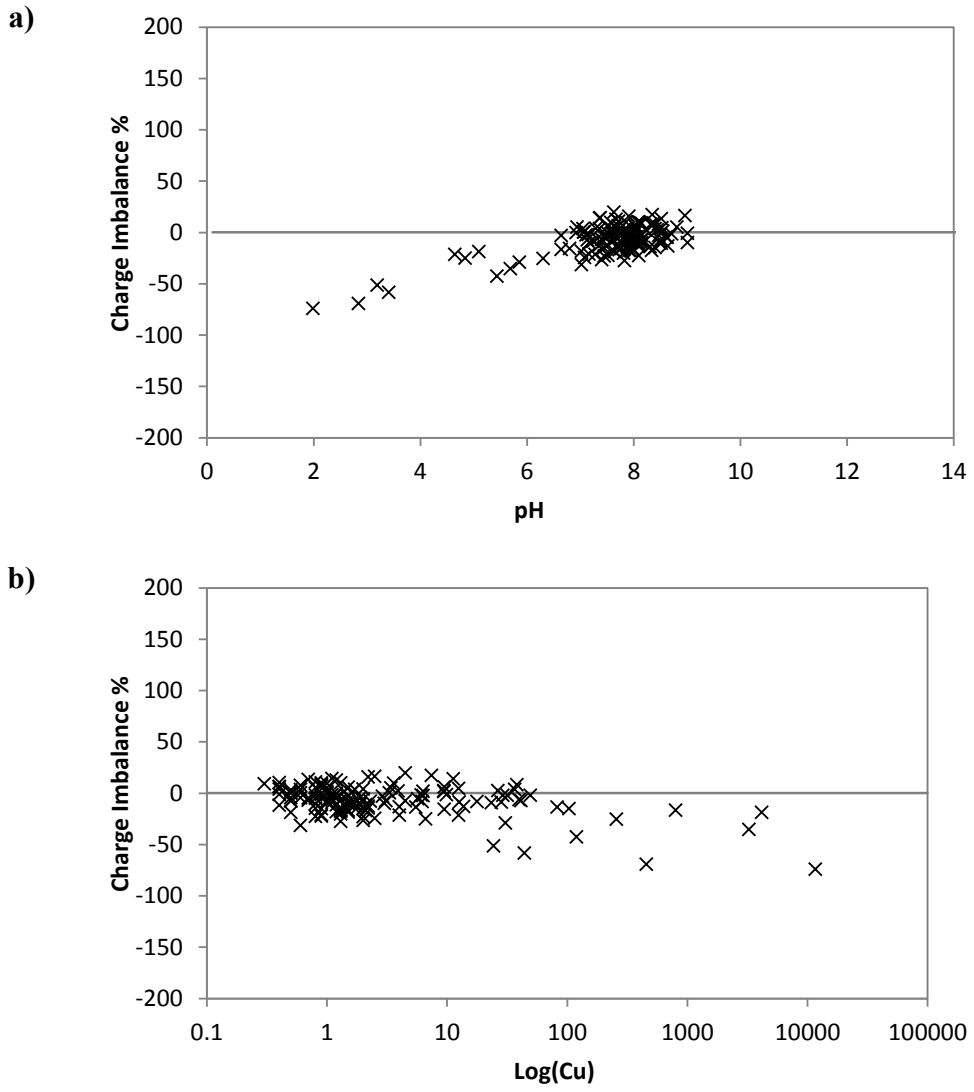


Figure 5.1: Charge imbalance for regional samples. (a) CI versus pH and (b) CI versus the logarithm of Cu in µg/l

Compared to the guideline values for drinking water (WGVs) of Chile, Europe, the US and the WHO (Table 2.1), most of the data concentrations are below the WGVs, except for SO_4^{-2} in 8.3% of the samples (12 samples), As in 6.9% (10 samples), Hg in 4.8% (7

samples) and Cu in 2% (3 samples) (Table 4.6) which are discussed further in section 6.6. Other parameters regulated for aesthetic purposes also had concentrations outside the guideline values, these being Al in 6.9% (10 samples), Cl in 0.7% (1 sample), Fe in 6.9% (10 samples), pH in 13.8% (20 samples) and TDS in 0.7% (1 sample). These can affect the taste and colour of drinking water but do not expose a risk to human health. The thresholds identified for the background levels of the chemicals are below the WGVs with the exception of pH with an upper guideline value of 8.5 which is lower than the pH threshold of 9 (Table 4.6).

Acid to neutral water samples with values below the lower WGVs for pH 6.5 are significantly correlated with Cd, Zn and Mn, and are all in the headwaters of the Colorado and Mapocho rivers in the AC, in areas of mineralisation and hydrothermal alteration. In these areas are also located the samples above the WGV for Al which in turn is highly correlated with Mn, Cu, F, Zn, Cd, Ni and SO_4^{-2}.

Water samples with SO_4^{-2} concentrations above the WGVs are significantly correlated with Ca, TDS, EC, K, F, Cl and Na and are in most of the Maipo Basin related to the occurrence of evaporites in the headwaters of the Maipo Basin. In the Central Valley, there are samples with high concentrations of HCO_3^-, NO_3^-, Mg and P which are significantly correlated; these concentrations are not above the WGVs however.

5.4 Stable isotope geochemistry

5.4.1 Hydrogen (δD) and oxygen ($\delta^{18}O$) isotopes in the waters

The relationship between δD and $\delta^{18}O$ in the waters of the three basins is linear (Figure 4.19) and intersects with the SMWL with a slightly smaller slope. This indicates that the

waters in all three basins are of meteoric origin and indicated evaporation downstream. Two end member sources define the relationship between the isotopic compositions of the water in the three basins; the first has high δD and $\delta^{18}O$ values closer to the isotopic values of seawater (0‰) and characterises the waters in the CC. The second source has low δD and $\delta^{18}O$ values and characterises the waters from the AC which reflect depletion of D and ^{18}O during fractionation of the meteoric water. Samples from the CV and along the west side of the AC have values between the two end member sources.

The slopes of the regression lines between δD and $\delta^{18}O$ values for the La Ligua (5.922), Aconcagua (7.349) and Maipo (7.251) basins data are lower than the SMWL slope (8.279) (Figure 4.19) which reflects evaporation and the associated isotopic fractionation of water downstream. The La Ligua basin has the lowest slope reflecting the greatest degree of evaporation. Isotopic fractionation of D and ^{18}O in the waters occurs from the coast towards the Andes because of what is known as the continental effect (Figure 5.2a) (Clark & Fritz 1997). This causes coastal precipitation to be isotopically enriched but to become more depleted as the vapour mass moves eastward over the continent. This fractionation can be also explained by the rainout effect (Clark & Fritz 1997), because as precipitation occurs the vapour mass becomes progressively more isotopically depleted in D and ^{18}O. Altitude also affects isotopic fractionation (Figure 5.2b) as reflected in the values for samples along the west side of the Andes (Figure 4.18). As vapour rises and cools at higher altitudes over the CV, precipitation occurs depleting D and ^{18}O in the vapour. The combination of these effects can be seen in Figure 5.2c where the altitude and the east coordinate show a nearly exponential relationship and D decreases with both.

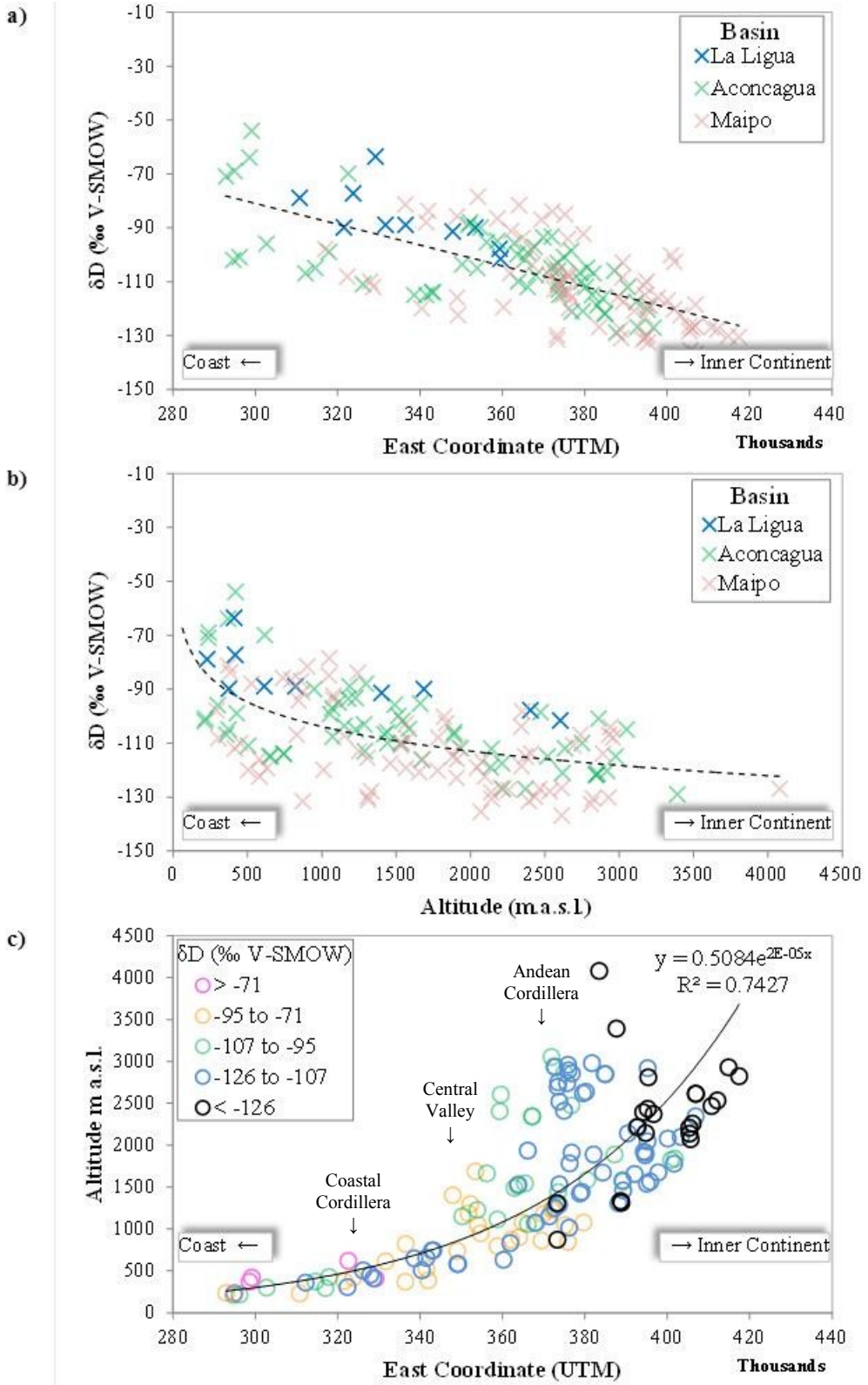


Figure 5.2: (a) δD versus east UTM coordinate (E) by basin shows the continental effect. Regression line for all data shown dashed (δD = -0.0004 x E + 34.944; R^2 = 0.46; n = 145). (b) δD versus altitude (A) by basin shows the altitude effect (Clark & Fritz 1997). Logarithmic trendline for all data shown dashed (δD = -13.13 ln(A) – 13.177; R^2 = 0.33; n = 145). (c) Altitude versus E coloured by different population for δD. Exponential trendline shown in chart. Central Valley, Coastal and Andean cordilleras indicated.

5.4.2 Sulphur and oxygen isotopes in sulphate

The relationship between $\delta^{34}S$ and $\delta^{18}O$ in SO_4^{-2} in the waters reflects the mixing of different sulphur sources including sulphides, sulphate, fertilisers and detergent and the oxygen in the dissolved sulphate indicates mixing with atmospheric oxygen in the waters (Figure 4.21). Three end member sources define the relationship between the isotopic compositions; the first source, sulphates, has high $\delta^{34}S$ (>9‰) and $\delta^{18}O_{SO4}$ (~14‰) values trending towards the signature of the Jurassic evaporites ($\delta^{34}S$ ~17‰ CDT and $\delta^{18}O_{SO4}$ ~13‰ V-SMOW, Claypool et al. 1980). This source characterises the waters draining the Upper Jurassic marine evaporites which outcrop in the headwaters of the Maipo and Aconcagua basins in the AC (Figure 4.4).

The second end member source, sulphides, has much lower $\delta^{34}S$ (<5‰) and $\delta^{18}O_{SO4}$ (~0‰) values reflecting the leaching and oxidation of sulphides in igneous rocks ($\delta^{34}S$ ~0‰ CDT). Oxidation of sulphides by bacteria involves oxygen from surface water and atmospheric $O_{2(aq)}$ and is accelerated by the exposure of fresh sulphides to weathering resulting in a higher content of $\delta^{18}O\text{-}H_2O$ compared to $O_{2(aq)}$ (Wright & Nordstrom 1999). This source reflects the presence of waters draining areas of hydrothermal alteration, mineralisation and mining in the AC and the CC.

The third end member source indicated by the variation of the oxygen (-8 to +27‰) in the sulphate indicates a mixture of atmospheric oxygen ($\delta^{18}O\text{-}O_{2(aq)}$ = 23.5‰ V-SMOW) and oxygen in the water molecule ($\delta^{18}O\text{-}H_2O$ = ~ -18 to -7‰ V-SMOW, in the regional stream water data, Table 4.11). Aqueous sulphate reflects the $\delta^{18}O_{SO4}$ values of the evaporite source (Upper Jurassic evaporites ~10 to ~15‰ V-SMOW) mixing with the oxidation of sulphides by bacteria, and with sulphate from fertilisers and detergents.

5.4.3 Nitrogen and oxygen isotopes in nitrate

The relationship between $\delta^{15}N$ and $\delta^{18}O$ in NO_3^- in the waters is complex and indicates at least two mixing lines between three main end member sources (Figure 4.23), including atmospheric nitrate, a sewage source and fertilisers from agriculture. The first end member source has low $\delta^{15}N$ (< -1.5‰) and high $\delta^{18}O_{NO3}$ (> 40‰) and is isotopically similar to nitrate deposits in the Atacama Desert ($\delta^{15}N$ -4.9 to 4.1‰ and $\delta^{18}O_{NO3}$ 36 to 50‰, after Böhlke et al. 1997) (Figure 4.23). The accumulation of nitrate in the Atacama Desert has been shown to have been produced by photochemical reactions in the atmosphere using the ^{17}O isotope analysis in nitrate (Michalski et al. 2004). This suggests that the deposition of nitrate in the Andean Cordillera of Central Chile could also be derived predominantly from atmospheric photochemical reactions however the very low nitrate concentration (mean ~2 mg/l), suggests that these values reflect considerable dilution (Jorquera et al. 2012). This source is characteristic of all the water samples collected at high altitudes (2,000 to 4,000 m) in the AC.

The second end member source, manure and septic waste, has much higher $\delta^{15}N$ values (> 12‰) with $\delta^{18}O_{NO3}$ (<15‰) (Figure 4.23). The $\delta^{18}O_{NO3}$ values of theses samples are systematically higher than values typical of manure and septic waste, however this is most likely due to mixing with $\delta^{18}O_{NO3}$ derived from oxygen in the atmosphere (Jorquera et al. 2012). Even though $\delta^{15}N$ and $\delta^{18}O_{NO3}$ increase systematically the content of nitrate does not decrease, hence there is no evidence of denitrification. This source reflects the presence of sewage in the area, principally in the CV. A previous study of nitrogen and oxygen isotopes in the north Santiago aquifer found values ranging 3.7 to 12.5‰ for $\delta^{15}N$ and 1.8 to 7.17‰ for $\delta^{18}O_{NO3}$ and that the main source of nitrate was from the sewage system (Iriarte et al. 2009). This is consistent with the isotope values found in the

Mapocho River downstream of Santiago, the $\delta^{18}O_{NO3}$ values are generally higher in this study however.

The third end member source is fertilisers, which have low $\delta^{15}N$ (< 2.5‰) with $\delta^{18}O_{NO3}$ (< 25‰) values trending towards those typical of ammonium and nitrate fertilisers (Figure 4.23). Isotopic analysis of fertilisers (monoammonium phosphate and muriate of potash) sampled in this study from the Catemu area in Central Chile have very low $\delta^{15}N$ values (1.0 and -3.4‰) with a $\delta^{18}O_{NO3}$ value of 15.6‰ which are consistent with published values (Kendall 1998). This is consistent with fertilisers being a major source of nitrogen (Jorquera et al. 2012) and the associated elements K and P in these waters. This source is agricultural areas in the CV.

5.5 Sources of anomalous chemistry

Of the ~20000 sq. km. research area, ~5000 sq. km. (25% of the area) has anomalously high stream water concentrations of one or more of the following parameters: the major cations Ca, Mg, Na, K, Al and Fe; the major anions Cl^-, NO_3^- and SO_4^{-2}; the trace elements As, Cd, Cu, F, Hg, Mo, Ni, P, Pb and Zn, and HCO_3^-, pH, and TDS. The sources of these chemicals are natural viz. geology, hydrothermally altered areas and mineralised areas, but in other cases reflect contamination from human activities viz. agriculture, human settlements and mining.

5.5.1 Natural sources of anomalous geochemistry

Of the ~5000 sq. km. area which has anomalously high concentrations of chemicals including Al, As, Cd, Cu, Fe, Ni, SO_4^{-2} and Zn in waters (Figure 4.17), ~4000 sq. km. (80%) reflect dominantly natural sources. These include bedrock geology, ~3600 sq. km.

(70%) (Table 4.13); hydrothermally altered and mineralised rocks, ~380 sq. km. (7%) (Table 4.14) and copper sulphide mineralisation, ~190 sq. km. (4%) (Table 4.15) (Figure 5.3).

In the headwaters of the Maipo and Aconcagua rivers the geochemistry of bedrock geology is dominated by outcropping evaporites. These are associated with high SO_4^{-2} levels in the waters which extend over a catchment area of ~3600 sq. km. The stream waters in this area have anomalously high Ca, Cl, K, SO_4^{-2} and Na concentrations (Figure 4.17) with a range pH of 7 to 8.5, and a mean of 8 and TDS range of ~100 to ~1500, with a mean of ~790 mg/l (Table 4.13). The high $\delta^{34}S$ values of 9‰ to 14‰ indicate that the sulphate in these waters is derived largely from the dissolution of evaporites (Figure 4.21). The $\delta^{18}O_{SO4}$ values of 5‰ to 15‰ also indicate that the SO_4 is derived largely from Upper Jurassic evaporites with $\delta^{18}O_{SO4}$ of ~13‰ (Claypool et al. 1980). The variation towards lower values of $\delta^{18}O_{SO4}$ indicates mixing with meteoric waters which are between -18‰ to -7‰ V-SMOW (Table 4.11) and towards higher values of $\delta^{18}O_{SO4}$ mixing with atmospheric oxygen ~24‰ V-SMOW (Kroopnick & Craig 1972). The $\delta^{15}N$ value of 4.2‰ with a $\delta^{18}O_{NO3}$ value of 40‰ indicates that the nitrogen in the waters is derived from the atmosphere (Jorquera et al. 2012) (Figure 4.23).

The presence of argillic hydrothermally altered rocks and Zn-Cd mineralisation is reflected by the anomalously high in Al, As, Cd, Fe, Hg, Ni and Zn values (Figure 4.17) and pH range of 3.2 to 8.0, with a mean of 6.5 (Table 4.14) extending over ~380 sq. km. Low $\delta^{34}S$ values of -3.8‰ to 5.9‰, mean 0.7‰ indicate that the source of the dissolved sulphate is from oxidising sulphides (Figure 4.21). The $\delta^{34}S$ value of 10‰ in the Barroso River (Table 4.14) is an exception and may indicate the dominance of sulphate

dissolution from evaporites over the hydrothermal alteration and mineralisation or mixing with volcanic sulphate sources with $\delta^{34}S$ values between ~3‰ to ~15‰ (Clark & Fritz 1997) from the volcanoes in the area. The low $\delta^{18}O_{SO4}$ values of -7.7‰ to 8.3‰, mean -1.3‰ indicate that most of the oxygen is mainly from oxidation of sulphides to sulphate by stream water (Wright & Nordstrom 1999). The $\delta^{15}N$ value of 2‰ with a high $\delta^{18}O_{NO3}$ value of 34‰ is consistent with an atmospheric source (Jorquera et al. 2012).

Areas of unmined copper sulphide mineralisation are reflected by the chemistry of the stream waters over an area of ~190 sq. km. in the AC. The waters have anomalously high Al, As, Cd, Cu, Fe, Ni, SO_4^{-2} and Zn values (Figure 4.17) with low pH values in the range 2 to 6.3 and a mean of 5.1 (Table 4.15) which are defined by Factor 2 (Table 4.9). Low $\delta^{34}S$ values of -0.2‰ to 4.3‰ indicate that the sulphate source is sulphide oxidation (Figure 4.21) and low $\delta^{18}O_{SO4}$ values of -4.5‰ to -0.4‰ indicate that most of the oxygen in the sulphate is from ambient stream water. The low $\delta^{15}N$ values of -1.5‰ to 0.3‰ with high $\delta^{18}O_{NO3}$ values of ~35‰ to ~40‰ indicate that the dissolved nitrate is most likely atmospheric (Jorquera et al. 2012). The waters are generally acid near to sulphide sources (3.2 to 5.9, mean 4.4), but as they mix with neutral to slightly alkaline pH stream waters (7.7 to 8.1, mean 7.9) the pH increases resulting in nearly neutral pH values (7.4 to 8, mean 7.7) and generally the concentrations of metals decrease as discussed and exemplified in section 5.5.3. Acid waters have anomalously high Al, Cu, Fe and SO_4^{-2} concentrations and low $\delta^{34}S$ and $\delta^{18}O_{SO4}$ values which reflect the oxidation of Cu and Fe sulphides by bacteria (Wright & Nordstrom 1999), particularly in the mineralised areas of Torin, Condell and Yerba Loca.

The extent of the effects of the evaporite source in the Maipo Basin indicates that species such as sulphate and calcium (Table 4.9) although diluted stay in the aqueous environment downstream for at least ~150 km (Figures 4.16 and 4.17 Ca and SO4 maps). Some of this water is also diverted to the Mapocho River to the north of the Maipo Basin through the San Carlos Canal (Figure 4.3) where the waters mix; the geochemical composition of the Maipo River waters dominating those of the Mapocho River (Table 4.10).

The change in the water chemistry of the Mapocho River due to the San Carlos Canal and Santiago is reflected in the compositions of the samples upstream (next to site 36, Figure 4.3) and downstream Santiago (site 32, Figure 4.3). The water upstream of Santiago has all the chemical concentrations within the background range and the low $\delta^{34}S$ value of 4.6‰ with $\delta^{18}O_{SO4}$ of 8.2‰ and the low $\delta^{15}N$ value of 2.3‰ with high $\delta^{18}O_{NO3}$ of 38.3‰ suggest the sulphate is from sulphide oxidation and the nitrate from the atmosphere as the other samples in the AC. In contrast, the sample downstream from Santiago has concentrations above the background range for HCO_3^-, K, NO_3^- and P with a $\delta^{15}N$ value of 10‰ and a $\delta^{18}O_{NO3}$ value of 21‰ which reflect the sewage source and also anomalously high concentrations of SO_4^{-2}, Ca, Cl and Na with a $\delta^{34}S$ value of 12.7‰ and a $\delta^{18}O_{SO4}$ value of 8.3‰ which reflect the sulphate coming from the evaporites. This is also consistent with a isotopic study that showed the mixing of the waters of the San Carlos Canal within the aquifer north of Santiago (Iriarte et al. 2009).

Other natural sources such as hydrothermally altered areas and mineralised areas are highly localised, indicating that the species released by sulphide oxidation are quickly

precipitated downstream as the pH increase. This is exemplified for the Yerba Loca Cu-mineralised area in section 5.5.3.

5.5.2 Anthropogenic sources of anomalous geochemistry

Nitrate isotopic data were used to distinguish between fertilisers, sewage and mixtures of these sources. Of the ~5000 sq. km. area with anomalous chemistry, ~1000 sq. km. (20%) reflect the dominant influence of anthropogenic sources, with high levels of Al, Cd, Cl, F, Fe, HCO_3^-, Hg, K, Mg, Mo, Na, NO_3^-, P, Pb, SO_4^{-2} or Zn. These include agriculture, ~710 sq. km. (14%), from fertilisers, sewage and mixtures of these sources with atmospheric nitrate; human settlements, ~210 sq. km. (4%), and mine area waters, ~60 sq. km. (1%) (Figure 5.3).

Stream water catchments where fertiliser is the principal source of nitrate extend over ~270 sq. km. in tributaries of the Aconcagua River in the CC and in tributaries of the Maipo River in the CV (Sites 23 – 30, Figure 4.3). The waters also have anomalously high HCO_3^-, K, Mg, NO_3^- and P (Table 4.16 and Figure 4.17) which also reflect the use of fertilisers (Fitzpatrick et al. 2007; Ohte et al. 2008). The variable but high $\delta^{34}S$ values of 3‰ to 11‰ with $\delta^{18}O_{SO4}$ values of ~2‰ to ~30‰ in these waters indicate mixing of a range of sulphate sources including sulphides and sulphates, and anthropogenic sources of fertilisers and household chemicals such as detergents (Figure 4.21). The low $\delta^{15}N$ values of ~3‰ to ~6‰ with low $\delta^{18}O_{NO3}$ values of ~8‰ to ~19‰ indicate that ammonium and nitrate fertilisers are the principal source of the dissolved nitrate (Jorquera et al. 2012). The $\delta^{15}N_{NO3}$ values determined for the fertilisers $NH_4H_2PO_4$ of 1‰ and KCl -3.4‰ found in this study are consistent with published values (Kendall 1998), but differ from the

Chilean KNO_3 fertiliser isotopic values in another study (Vitòria et al. 2004) (Figure 4.23).

Stream water catchments in which sewage is the principal source of nitrate extend over ~160 sq. km. in the CV in the Mapocho River near Santiago and in the Aconcagua River (Sites 31 – 32, Figure 4.3). The waters have anomalously high values of F^-, HCO_3^-, K, Mo, NO_3^- and P^- (Table 4.16 and Figure 4.17), which are related to the presence of agricultural communities and sewage (Neal et al. 2010; Muscutt & Withers 1996). The $\delta^{34}S$ values of ~4‰ to ~13‰ with $\delta^{18}O_{SO4}$ values of ~2‰ to ~8‰ in the waters also indicate mixing of sulphate, sulphide and anthropogenic sources such as fertilisers (Figure 4.21). The high $\delta^{15}N$ values of ~10‰ to ~12‰ indicate that manure and septic waste in sewage are the principal source of dissolved nitrate. The expected values for $\delta^{18}O_{NO3}$ are much higher 21‰ to ~30‰ however, this is thought to be due to mixing with oxygen isotopes derived from the atmosphere (Jorquera et al. 2012).

Stream water catchments with mixed sources of nitrate extend over ~280 sq. km. in the La Ligua and Aconcagua River in the CC and in tributaries of the Maipo River in the CV (Sites 33 – 38, Figure 4.3). The waters have anomalously high values of HCO_3^-, K, Mg, NO_3^- and P (Table 4.16 and Figure 4.17) which reflect the presence of agricultural communities. The $\delta^{34}S$ values of ~0‰ to 11‰ with $\delta^{18}O_{SO4}$ values of 3‰ to 10.2‰ indicate mixed evaporites, sulphide oxidation, fertilisers and household chemicals such as detergents (Figure 4.21). The $\delta^{15}N$ values of ~5‰ to ~9‰ with $\delta^{18}O_{NO3}$ values of 12‰ to ~31‰ indicate mixed nitrate sources including fertilisers, sewage and atmospheric nitrogen (Jorquera et al. 2012).

Stream waters with localised anomalously high concentrations of Pb, Hg, and P (Figure 4.17) near human settlements extend over ~150 sq. km. in the vicinity of townships in the CV and the CC (Sites 28, 30, 37, 39, 40, Figure 4.3) and downstream from the ski resorts in the AC (Site 43, Figure 4.3). The localised highly anomalous concentrations of Pb and Hg, in waters dominated by the composition of evaporites which are not a source of these elements, are suggested to be associated with fly-tipping of batteries, paint, lead pipes, and/or thermometers, the use of pesticides and/or illegal incineration, because there is no authorised landfill in the area and the occurrences are localised near to towns. The isolated anomalously high value of P downstream the ski resorts is suggested to be associated with detergents in waste waters based on field observation, but no anomalous values of Boron were found associated with this sample (B map, Appendix D) noting that Boron is commonly associated with detergents in stream waters (Neal et al. 2010).

The mine area waters, which extend over ~60 sq. km., have anomalously high concentrations of Cd, Cl, Mo, Na, and Zn with pH values in the range 7.7 to 7.9, with a mean of 7.8 at Andina and Los Bronces; Fe, Mg, Mo and SO_4^{-2} with pH 8.4 at El Soldado; and Pb and Zn values with pH 7.1 in the La Poza and Restauradora abandoned Pb-mines areas (Table 4.17). Anomalously high Na and Cl concentrations in these areas in the AC reflect salting of mine roads. The Cd, Mo and Zn values are thought to reflect a combination of mineralisation in the area as well as dust from mine roads adjacent to the rivers. Anomalously high Pb and Zn concentrations reflect the La Poza and Restauradora Pb-Zn mines and are thought to be related to the abandoned smelter in the area. The low $\delta^{34}S$ values of -1.1‰ to 3.7‰ indicate that the source of dissolved sulphate in these waters is from sulphide oxidation (Figure 4.21). The low $\delta^{18}O_{SO4}$ values of -3.0‰ to 0.7‰ indicate that the oxygen in the sulphate is mainly from ambient stream water. The

near atmospheric $\delta^{15}N$ value of 1.1‰ and high $\delta^{18}O_{NO3}$ value of 37‰ indicate that the dissolved nitrate is from an atmospheric source at Andina and Los Bronces districts.

Another possible source of NO_3^- in the AC would be from explosives used in mining. One sample in the mine area waters of Los Bronces had nitrate isotopes values of 1.1‰ $\delta^{15}N_{NO3}$ and 37‰ $\delta^{18}O_{NO3}$ with NO_3^- contents ~2 mg/l. These values are the same as the isotopic composition of the non-mine-related waters found elsewhere in the AC which range $\delta^{15}N_{NO3}$ from -1.5‰ to 4.2‰ with $\delta^{18}O_{NO3}$ from 34‰ to 39.7‰ and NO_3^- contents from 0.3 to ~4 mg/l, indicating no measurable contribution of NO_3^- from explosives (Jorquera et al. 2012).

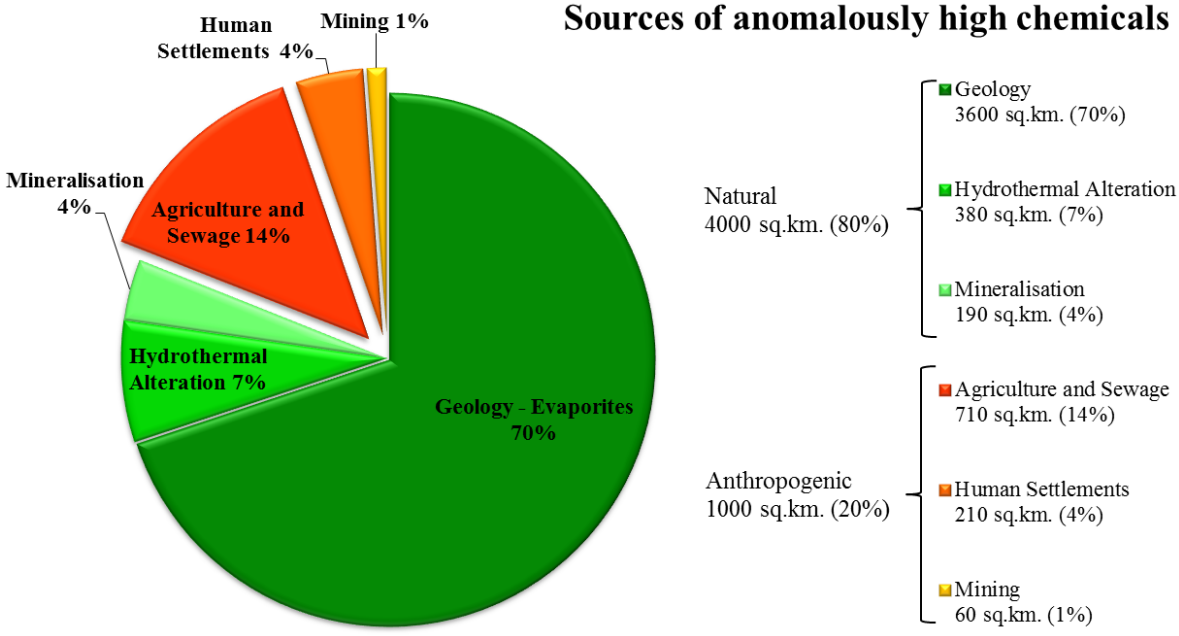


Figure 5.3: Sources of anomalously high concentration of chemicals by the estimated proportion of catchment areas they cover. Green colours are used for natural sources and warm colours for anthropogenic sources.

The greatest extent of pollution was found in the agricultural areas associated with fertilisers and sewage. The chemicals related to this source including NO_3^- and P can

cause eutrophication of waters (Muscutt & Withers 1996; Edmunds 2009) leading to the development of hazardous species such as blue algae.

5.5.3 Cu-Mineralisation and mine area waters in the headwaters of Mapocho River: The Yerba Loca Stream and the San Francisco River

Waters draining the Cu-mineralisation in the headwaters of the Yerba Loca Stream have higher levels of Cu (11693 µg/l), Ni (26 µg/l) and Al (6 mg/l) and a low pH of 2 than ~20 km. downstream where values are Cu (4185 µg/l), Ni (18 µg/l, Al (1 mg/l) (Table 4.15) with a pH of 5.1, which suggests precipitation has occurred downstream. The exception is for Zn which has a slightly lower value of 124 µg/l than Zn downstream (175 µg/l). The anomalously high values of As (14 µg/l), Fe (45 mg/l), P (694 µg/l) and SO_4^{-2} (446 mg/l) in the Yerba Loca headwaters all decrease to background levels over the same distance. This reflects the oxidation of sulphides close to the Cu-mineralisation and the rapid dilution and precipitation of trace elements such as As which decreases markedly to <0.5 µg/l by the end of the Yerba Loca Valley. The origin of the anomalous P is most likely apatite associated with the mineralisation (Oyarzún 2000) which is soluble in the acid environment precipitating under more neutral pH downstream.

In contrast, the mine area waters in the San Francisco River Valley ~20 km. downstream from the mine operations have values within the background range for Al (0.016 mg/l), Cu (41 µg/l) and Ni (4.3 µg/l) (Table 4.17), which are lower than the levels at the end of the Yerba Loca Valley, ~20 km. downstream of the mineralisation. Also, the mine area waters have lower Zn concentrations (91 µg/l) and a significantly higher pH of 7.9 compared with a pH of 5.1 at the end of the Yerba Loca Valley. This reflects more diluted

mineralisation signatures in the San Francisco River and the input of the fresh water streams diverted around the mine operations into the river.

In the mine area waters of the San Francisco River and the water draining mineralisation in the Yerba Loca Stream, the sulphate and nitrate isotopes values are almost identical. The sulphate isotopes reflect the presence of sulphides at both localities and the nitrate isotopes an atmospheric origin and also that there is no measurable contribution to nitrate levels from the use of explosives in mining (Jorquera et al. 2012).

5.6 Application of the geochemical baseline to water regulation

5.6.1 Regional hydrogeochemical data compared with regulation and guideline values

The regional hydrogeochemical data of Central Chile were compared with the regulation and guideline values for drinking water (WGVs) of Chile, Europe, the US and the WHO (Table 2.1). Most of the data concentrations are below the WGVs, except for SO_4^{-2} in 8.3% of the samples (12 samples), As in 6.9% (10 samples), Hg in 4.8% (7 samples) and Cu in 2% (3 samples) (Table 4.6). The sources of these high concentrations are all natural, with the SO_4^{-2} being derived from evaporites, As and Cu reflecting copper sulphide mineralisation and Hg from hydrothermal alteration and mineralisation. The only exceptions are 3 samples high in Hg that are thought to be reflecting the presence of batteries, thermometers from fly-tipping or pesticides. Other parameters had also concentrations outside the guideline values including Al, Cl, Fe, pH and TDS which are all regulated for aesthetic purposes only and will not be considered further for discussion.

Chilean drinking water regulation values have historically followed international guidelines (Table 2.1), which are not useful for regulating stream water levels because they do not take into account natural sources of chemicals that here reflect the lithology, hydrothermal alteration and mineralisation of the rocks they drain. This issue has been considered in the Chilean Government draft regulations on surface water quality, for example for the Maipo Basin (CONAMA 2004). The regulation defines the surface water quality for each sub-basin in the Maipo Basin. The regulated levels are defined by calculating the 66^{th} percentile of the data for each sub-basin. However, the sampling sites and dates of data collection are not specified.

The regional hydrogeochemical data prepared in this study were compared to the draft regulation values for stream waters. Most of the regional hydrogeochemical data for the Maipo Basin were found to be well below the stream water draft regulation levels for most chemicals and not greater than 10% above the regulation levels, except for Cu and Zn in the headwaters of the Mapocho River and SO_4^{-2} in the headwaters of El Yeso River upstream (Figure 5.4).

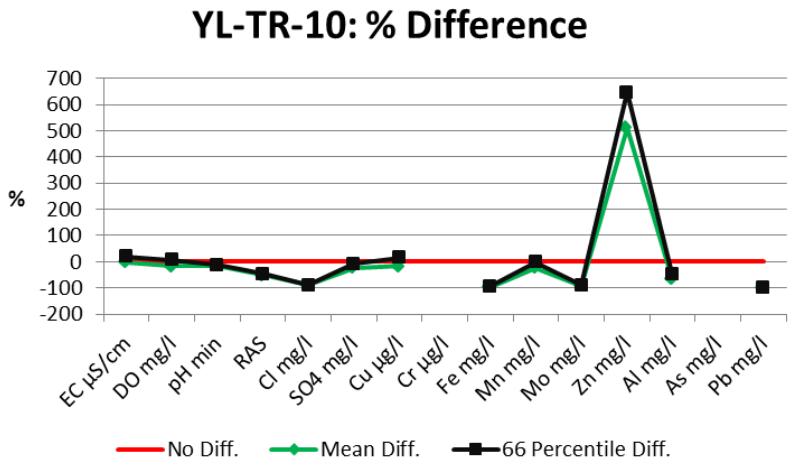
The highest differences were found in the Yerba Loca Stream for Zn with a relative difference of ~500% cf. mean and ~650% cf. 66^{th} percentile (Figure 5.4a); in the San Francisco River for Mn with a relative difference of ~100% cf. mean and ~150% cf. 66^{th} percentile (Figure 5.4b); and in the El Yeso River upstream the junction with the Maipo River for SO_4^{-2} with a relative difference of ~80% cf. mean and ~170% cf. 66^{th} percentile (Figure 5.4c).

For the Yerba Loca Stream in the headwaters of the Mapocho River, Zn has a mean and 66th percentile value of ~0.2 mg/l which is one order of magnitude higher than the regulated value of 0.025 mg/l (CONAMA 2004). The anomalously high concentrations of Zn here were found to reflect the presence of mineralisation in these waters; and overall the regional hydrogeochemical data are generally consistent with the draft regulation levels, thus this difference is believed to be an error in the draft regulation data. This is most likely a typing error as the regulated values are based on a report prepared by the Chilean supervisory entity DGA (Dirección General de Aguas) where the published value of 0.25 mg/l Zn for summer for the Yerba Loca Stream (DGA 2004b) is consistent with those found in this study ~0.2 mg/l.

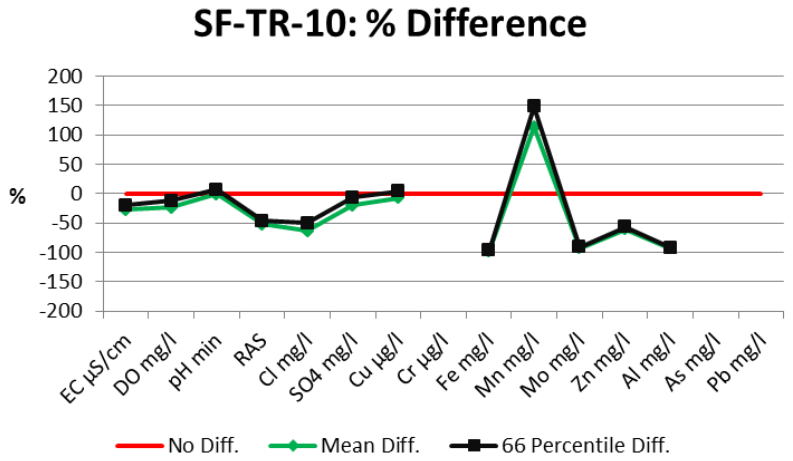
For the San Francisco River, Mn has a mean and 66th percentile value of ~0.4 mg/l which is only twice the regulated level for Mn of ~0.2 mg/l (CONAMA 2004). This difference is thought to be due to seasonal or annual variation (Figure 4.9) since the anomalously high concentrations of Mn here (Appendix D) were found to be associated with the presence of mineralisation and hydrothermal alteration.

For El Yeso River, SO_4^{-2} has a mean of 273 mg/l and a 66th percentile value of 405 mg/l which are higher than the regulated value of 150 mg/l (CONAMA 2004). This difference may also reflect seasonal or annual variation since these values are all near the threshold of 314 mg/l (Table 4.6) and they were found here to reflect the presence of extensive evaporites in the headwaters.

a)



b)



c)

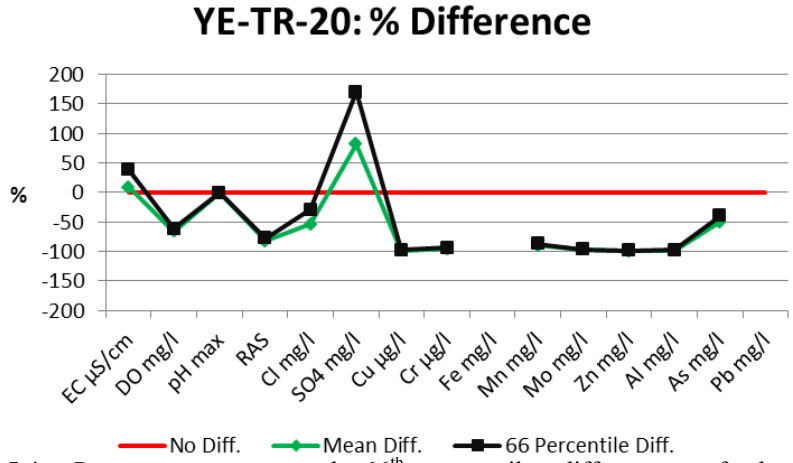


Figure 5.4: Percentage mean and 66th percentile differences of the regional hydrogeochemical data compared to the draft regulation values. The red line indicates zero difference and negative percentages reflect concentration of chemicals lower than the draft regulated values. (a) Yerba Loca Stream, most parameters are below zero or not higher than 10% except for Zn, and for the 66th percentile differences of EC and Cu which are ~20%; (b) San Francisco River, most parameters are below zero or not higher than 10% except for Mn; (c) El Yeso River, most parameters are below zero or not higher than 10% except for SO_4, and for the 66th percentile percentage difference of EC.

The differences for the dissolved oxygen (DO) are not significantly high and as they represent the minimum level to protect and preserve aquatic life, thus it is not a problem and it is most likely derived from seasonal variation. Other parameters that have higher values than the regulated levels (Table 4.18) in other sub-basins have not significantly high differences however. They are mostly related to the presence of the evaporites such as SO_4^{-2}, EC, RAS (sodium absorption ratio) and Cl and thus are thought to be related to seasonal or annual variations.

5.7 Summary

The international sampling and analytical procedures followed in this research were demonstrated to be effective in generating high quality data through the QA/QC evaluation. This evaluation is critical to validate all the findings, and current and future applications of the data not only for environmental but also for exploration purposes.

The physicochemical characteristics of the waters vary depending on the source and control the presence of species in solution and precipitation, and thus the distance from the source they are still identified in the waters according to the detection limits of the analytical methods used. For example, the sulphate diluted from evaporites extends significantly further downstream compared to the sulphate from oxidised sulphides in hydrothermally altered and mineralised areas which is highly local and the metals associated precipitate quickly downstream.

The area of water contaminated with fertilisers and sewage was found to be significantly greater than areas with water locally polluted with Hg and Pb, and from the mining area waters. The agricultural communities, covering most of the Central Valley and the valleys

in the Coastal Cordillera were found to contaminate the water mainly with NO_3^- and P which even though are below WGVs (P is not regulated in drinking water however) were found to locally generate eutrophication.

The integration of the stable isotope results with the regional hydrogeochemical baseline data resulted in the accurate identification of the sources of anomalously high geochemistry. This identification and geochemical characterisation of the sources of chemicals in the stream water environment have a variety of application such us agricultural, human health and mineral exploration.

In order for legislation to have a sound basis, systematic geochemical baseline data must be used in its formulation. Such baselines should be based on and provide information on background levels of chemical elements appropriate for the region (Salminen et al. 2005). For example, during contamination incidents (either naturally occurring such as volcanic eruptions or of anthropogenic origin) information about the previous naturally occurring concentrations of chemical elements is required, to reliably evaluate and predict potential environmental impacts.

Geochemical baselines are needed for environmental legislation and political decision making (Van Den Oever 2000), such as for remediation and land use planning. Being the Maipo Basin one of the main sources for drinking and irrigation water in Santiago, it is important to distinguish the background levels and sources of chemicals when regulating. The high quality of the hydrogeochemical data and baseline prepared in this study fit those purposes.

CHAPTER 6: CONCLUSIONS

The regional hydrogeochemical baseline prepared for this research extended over ~20000 sq. km. of Central Chile including the classic Andina – Los Bronces copper mining district. Approximately 5000 sq. km. (25% of the area) have highly anomalous concentrations of one or more of the following in stream water: the major cations Ca, Mg, Na, K, Al and Fe; the major anions Cl^-, NO_3^- and SO_4^{-2}; the trace elements As, Cd, Cu, F, Hg, Mo, Ni, P, Pb and Zn and/or HCO_3^-, pH and TDS. The sources of the anomalously high levels of elements were identified using trace and major element chemistry and isotope geochemistry. Within the ~5000 sq. km., anomalously high concentrations extending over ~4000 sq. km. reflect the influence of natural sources comprising bedrock geology (70% of the affected areas), hydrothermal alteration (7%) and mineralisation (4%). The remaining ~1000 sq. km. is contamination from anthropogenic sources including agriculture (14% of the affected areas), fertilisers, sewage, fly-tipping (4%) and mining (1%).

The greatest natural source found is the bedrock geology, principally the Upper Jurassic evaporites outcropping in the headwaters of the Maipo Basin in the AC where the high concentrations of SO_4^{-2}, Ca, Na, Cl and K extend in solution downstream in the CV for at least ~150 km. Anomalously high concentrations of chemicals in waters draining hydrothermally altered and mineralised areas are dominantly Al, As, Cd, Fe, Hg, Ni and Zn and are highly restricted to sources such as in the hydrothermal alteration of Zn-Hg sulphide-rich intrusions in andesites in the headwaters of the Colorado River and particularly the argillic alteration in the Arrayán Stream in the AC which is very high in Al reflecting the dissolution of clays. Similarly, anomalously high concentrations of Al, As, Cd, Fe, Ni, and Zn were found in the waters draining copper mineralised areas but

these are particularly high in Cu and SO_4^{-2} and are also restricted to sources such as in the headwaters of the Barriga River and Yerba Loca Stream in the AC and dilute rapidly downstream. Isotopic compositions of sulphate distinguished the sulphate from evaporites and sulphide oxidation.

The major anthropogenic source of anomalously high levels of NO_3^-, P, HCO_3^-, F^-, K, Mg, and Mo is from fertilisers in agriculture and sewage from communities in the CV and the CC. Isotopic compositions of nitrate distinguish nitrate and ammonium based fertilisers used in agriculture, as well as sewage and mixed sources. Fertilisers are reflected in the waters of tributaries of the Aconcagua River in the CV and in the Maipo River. Sewage is reflected in the Mapocho River downstream of Santiago and also in the Aconcagua River. Mixed nitrate sources, including fertilisers, sewage and atmospheric oxygen in nitrate, occur in the CC in the Aconcagua River, some of its tributaries and in the CV in the Maipo River and some of its tributaries. Stream waters contaminated locally with anomalously high concentrations of Pb or Hg from human settlements occur near seven townships across the region. Water downstream from the ski resorts has locally high values of P reflecting contamination from household chemicals. Anomalously high levels of Cd, Cl, Na, Mo and Zn in the mine area waters proximal to the Andina and Los Bronces mines are related to waters from mineralisation and alteration and from salting of mine roads in the AC, which are rapidly diluted downstream to background levels over a distance of ~20 km. The waters draining the abandoned La Poza and Restauradora Pb-Zn mines are highly anomalous in Pb and Zn downstream for ~10 km. from the mines.

The waters in the Yerba Loca Valley reflect the oxidation of sulphides close to the Cu-mineralisation and the rapid dilution and precipitation of most of the trace elements downstream. These waters have significantly higher Cu and Ni levels than the mine area waters in the San Francisco River and a much lower pH. The isotopic composition of these waters indicates the same natural sources of dissolved sulphate and nitrate with no measurable contribution from the use of explosives in the mining district. In this context, the isotopic analysis of explosives used in mining in Central Chile would corroborate this finding.

With respect to national and international drinking water guideline values, the majority of concentrations are lower than stipulated levels. Some parameters with potential health effects have concentrations outside the WGVs, these being As, Cu, Hg and SO_4^{-2}. The SO_4^{-2} and As were found to be derived from natural sources and Hg from both natural and anthropogenic sources.

Whether the cattle deaths in the Agua Mala stream and the Barroso river areas are due to the anomalous levels of As or the overall anomalous water chemistry would require research to determine for example the bioavailability of those chemicals to the cattle. This study would be local rather than regional however.

The majority of the concentrations for the regional hydrogeochemical baseline are below the Chilean draft water quality regulation values for the Maipo Basin. Higher values are related to natural sources including copper sulphide mineralisation (Cu, Zn) and evaporites (SO_4^{-2}) and are probably due to seasonal variations. The quantitative comparison highlights the high correspondence in the two databases but also that

regulation should be aided by and based on geochemical baselines which provide information on background levels of chemical elements appropriate for a region and the identification of their sources.

A range of potential applications of high quality geochemical datasets to environmental studies in mining districts are identified. Geochemical baselines can be of value to mining companies especially in helping to understand the geochemistry of mineralised areas and define baseline levels of chemicals prior to their mining operations and as a basis for monitoring.

Having high quality hydrogeochemistry of a region is invaluable to reliably evaluate and predict potential environmental impacts after contamination incidents. Areas with trace element deficiencies or toxicity can also be identified using geochemical baselines and risk evaluated.

It is recommended to conduct stream sediments studies in the region to identify the mechanically deposited and precipitated species in the streams and to understand the pathways of the chemicals in the drainage system. It would be valuable to incorporate groundwaters in areas with no surficial drainage to cover the whole region.

Seasonal and annual variations were identified in this study in the comparison with the draft regulated values for the Maipo Basin, however this can be studied further and quantified for the whole region.

REFERENCES

Abernathy, C., Thomas, D. & Calderon, R., 2003. Health effects and risk assessment of arsenic. *The Journal of Nutrition*, 133(5), pp.1536–1538.

Ackerman, J.J.H. et al., 1979. Effect of halide complexation of cadmium(II) on cadmium-113 chemical shifts. *Journal of American Chemical Society*, 101(2), pp.341–347.

Alvarez, P. et al., 1997. Estratigrafía del Jurásico de la Cordillera Principal de Argentina y Chile (33°45' - 34°00' LS). In *Actas VIII Congreso Geológico Chileno. Vol 1*. Antofagasta: Universidad Católica del Norte, pp. 425–429.

Alvarez, P. et al., 2000. Relationship between different depocenters of Triassic-Jurassic rift systems in the main Andes of Argentina and Chile. In *Proceedings XXIII Geological International Congress*. Rio de Janeiro.

ATSDR, 2007a. Case studies in environmental medicine. Nitrate/nitrite toxicity. , p.40. Available at: http://www.atsdr.cdc.gov/csem/csem.html.

ATSDR, 2006. *Toxicological profile for hydrogen sulfide*, Atlanta, GA.

ATSDR, 2007b. *Toxicological profile for lead*, Atlanta, GA.

ATSDR, 2005. *Toxicological profile for nickel*, Atlanta, GA.

ATSDR, 2012. *Toxicological profile for phosphate ester flame retardants*, Atlanta, GA.

ATSDR, 1998a. *Toxicological profile for sulfur dioxide*, Atlanta, GA.

ATSDR, 1998b. *Toxicological profile for sulfur trioxide and sulfuric acid*, Atlanta, GA.

Awadalla, F.T., Striez, C. & Lamb, K., 1994. Removal of ammonium and nitrate ions from mine effluents by membrane technology. *Separation Science and Technology*, 29(4), pp.483–495.

Ayers, J.C. & Watson, E.B., 1991. Solubility of apatite , monazite , zircon , and rutile in supercritical aqueous fluids with implications for subduction zone geochemistry. *Philosophical Transactions: Physical Sciences and Engineering*, 335(1638), pp.365–375.

Barceloux, D.G., 1999. Nickel. *Clinical Toxicology*, 37, pp.239–258.

Barrett, J.H. et al., 1998. Nitrate in drinking water and the incidence of gastric, esophageal, and brain cancer in Yorkshire, England. *Cancer Causes & Control*, 9(2), pp.153–159.

Benson, J.M. et al., 1994. Fate of inhaled nickel oxide and nickel subsulfide in F344/N rats. *Inhalation Toxicology*, 6, pp.167–183.

Berleur, M.P. & Cordier, S., 1995. The role of chemical, physical, or viral exposures and health factors in neurocarcinogenesis: implications for epidemiologic studies of brain tumors. *Cancer Causes & Control*, 6(3), pp.240–256.

Böhlke, J.K., Ericksen, G.E. & Revesz, K., 1997. Stable isotope evidence for an atmospheric origin of desert nitrate deposits in northern Chile and southern California, U.S.A. *Chemical Geology*, 136(1-2), pp.135–152.

Boric, R., 2002. The geology of the El Soldado manto type Cu-(Ag) deposit, Central Chile. In T. M. Porter, ed. *Hydrothermal iron oxide copper-gold and related deposits: a global perspective*. Adelaide: PGC Publishing, pp. 163–184.

Bouzari, F. et al., 2011. *Porphyry Indicator Minerals (PIMS): A new exploration tool for concealed deposits in south-central British Columbia*,

Boyle, R.W. et al., 1968. *Minor and trace element distribution in the heavy minerals of the rivers and streams of the Bathurst-Jacquet River District, New Brunswick*, Ottawa.

Boyle, R.W. & Garrett, R.G., 1970. Geochemical Prospecting - A Review of its status and future. *Earth Science Reviews*, 6, pp.51–75.

Caceres, D.D. et al., 2005. Exposure to inorganic arsenic in drinking water and total urinary arsenic concentration in a Chilean population. *Environmental Research*, 98(2), pp.151–159.

Callender, E., 2003. Heavy Metals in the Environment-Historical Trends. In B. S. Lollar, ed. *Treatise on Geochemistry, Vol. 9: Environmental Geochemistry*. Elsevier Ltd, pp. 67–105.

Cameron, E.M. et al., 2004. Finding deeply buried deposits using geochemistry. *Geochemistry: Exploration, Environment, Analysis*, 4(1), pp.7–32.

Campos, V.L. et al., 2011. Arsenic mobilization by epilithic bacterial communities associated with volcanic rocks from Camarones River, Atacama Desert, northern Chile. *Archives of environmental contamination and toxicology*, 61(2), pp.185–92.

De Caritat, P. et al., 2009. Using groundwater chemical and isotopic composition in the search for base metal deposits: hydrogeochemical investigations in the Hinta and Kayar Pb-Zn districts, India. *Geochemistry: Exploration, Environment, Analysis*, 9(3), pp.215–226.

CCME, 2001. Canadian sediment quality guidelines for the protection of aquatic life: Introduction. Updated. In *Canadian environmental quality guidelines, 1999*. Winnipeg: Canadian Council of Ministers of the Environment.

CCME, 1999. Canadian water quality guidelines for the protection of aquatic life: Introduction. In *Canadian environmental quality guidelines, 1999*. Winnipeg: Canadian Council of Ministers of the Environment.

Central Energía, 2012. SIC installed capacity. *Central de información y discusión de energía en Chile*. Available at: http://www.centralenergia.cl/en/power-plants-chile/sic-installed-capacity/ [Accessed October 23, 2013].

Charlson, R.J., Anderson, T.L. & McDuff, R.E., 2000. The sulfur cycle. In M. C. Jacobson et al., eds. *International Geophysics*. Academic Press, pp. 343–359.

Charrier, R., 2002. Evidence for Cenozoic extensional basin development and tectonic inversion south of the flat-slab segment, southern Central Andes, Chile 33° - 36°S.L.). *Journal of South American Earth Sciences*, 15(1), pp.117–139.

Charrier, R., Pinto, L. & Rodríguez, M., 2007. Tectonostratigraphic evolution of the Andean Orogen in Chile. In T. Moreno & W. Gibbsons, eds. *The Geology of Chile*. Bath: The Geological Society Publishing House, pp. 21–114.

Clark, I.D. & Fritz, P., 1997. *Environmental Isotopes in hydrogeology*, Boca Raton: Lewis Publishers.

Claypool, G.E. et al., 1980. The age curves of sulfur and oxygen isotopes in marine sulfate and their mutual interpretation. *Chemical Geology*, 28(2003), pp.199–260.

CONAMA, 2004. *Anteproyecto de Normas Secundarias de Calidad Ambiental Para la Protección de las Aguas Continentales Superficiales de la Cuenca del Río Maipo*, Chile.

Cotter-Howells, J., 1996. Lead phosphate formation in soils. *Environmental pollution (Barking, Essex : 1987)*, 93(1), pp.9–16.

Craig, H., 1961. Standard for Reporting Concentrations of Deuterium and Oxygen-18 in Natural Waters. *Science, New Series*, 133(3467), pp.1833–1834.

Darnley, A.G. et al., 1995. *A global geochemical database for environmental and resource management - Final Report of IGCP Project 259*, Paris.

Darnley, A.G., 1997. A global geochemical reference network: the foundation for geochemical baselines. *Journal of Geochemical Exploration*, 60, pp.1–5.

Davies, T.D., 2007. Sulphate toxicity to the aquatic moss, Fontinalis antipyretica. *Chemosphere*, 66(3), pp.444–451.

DGA, 2004a. *Diagnóstico y Clasificación de los Cursos y Cuerpos de Agua Segun Objetivos de Calidad: Cuenca del Río Aconcagua*,
DGA, 2004b. *Diagnóstico y Clasificación de los Cursos y Cuerpos de Agua Segun Objetivos de Calidad: Cuenca del Río Maipo*, Santiago.
EC & European Commission, 1998. *The drinking water directive. Council Directive 98/83/EC*, European Commission: Official journal of the European Communities.
Edmunds, W.M., 2009. Geochemistry's vital contribution to solving water resource problems. *Applied Geochemistry*, 24(6), pp.1058–1073.
Emsley, J., 2011. *Nature's Building Blocks: An A-Z Guide to the Elements*, Oxford University Press.
EPA, 2009. *National Primary Drinking Water Regulations. EPA 816-F-09-004*, Washington DC.
EPA, 2002. *Using biosolids for reclamation and remediation of disturbed soils*, Washington DC.
European Commission, 2003. *Directive 2003/17/EC amending Directive 98/70/EC relating to the quality of petrol and diesel fuels*, EU.
European Commission, 1998. *Directive 98/70/EC relating to the quality of petrol and diesel fuels*, EU.
Fanning, D.S. & Burch, S.N., 2001. Sulfate and Sulfide Minerals. In R. Lal, ed. *Encyclopedia of Soil Science*. New York: Marcel Dekker, pp. 1714–1716.
Fersman, A.E., 1935. *The scientific study of Soviet mineral resources* C. P. Dutt, ed., London: Martin Lawrence Limited.
Fitzgerald, W.F. & Lamborg, C.H., 2003. Geochemistry of Mercury in the Environment. In B. S. Lollar, ed. *Treatise on Geochemistry, Vol. 9: Environmental Geochemistry*. Elsevier Ltd, pp. 107–148.
Fitzpatrick, M.L., Long, D.T. & Pijanowski, B.C., 2007. Exploring the effects of urban and agricultural land use on surface water chemistry, across a regional watershed, using multivariate statistics. *Applied Geochemistry*, 22(8), pp.1825–1840.
Fletcher, W.K., 1997. Stream sediment geochemistry in today's exploration world. In A. G. Gubins, ed. *Exploration 97: Fourth Decennial Internation Conference on Mineral Exploration*. Toronto, pp. 249–260.
FOREGS, 2005. Geochemical Atlas of Europe. Part 2. *Forum of the European Geological Surveys Directors*. Available at: http://weppi.gtk.fi/publ/foregsatlas/ [Accessed May 18, 2013].
Gana, P. & Wall, R., 1997. Evidencias Geocronológicas 40Ar/39Ar y K-Ar de un hiatus Cretásico Superior-Eoceno en Chile Central (33° - 33°30' S). *Revista Geológica de Chile*, 24(2), pp.145–163.
Garrett, R.G. et al., 2008. From geochemical prospecting to international geochemical mapping : a historical overview. *Geochemistry: Exploration, Environment, Analysis*, 8(1939), pp.205–217.
Garrett, R.G., 1969. The determination of sampling and analytical errors in exploration geochemistry. *Economic Geology*, 64, pp.568–569.
Garrett, R.G., 1991. The managment, analysis and display of exploration geochemical data. In J. M. Franklin et al., eds. *Exploration Geochemistry Workshop - Open File 2390*. Geological Survey of Canada, pp. 9–1 to 9–41.
Giblin, A., 1994. Natural waters as sample media in drainage geochemistry. In M. Hale & J. A. Plant, eds. *Drainage Geochemistry*. Amsterdam: Elsevier, pp. 269–303.
Haber, L.T. et al., 2000. Hazard identification and dose response of ingested nickel-soluble salts. *Regulatory Toxicology and Pharmacology*, 31, pp.231–241.

HACH, 2006. Alkalinity, phenolphthalein and total method. *Digital Titrator Model 16900*, (June), pp.41–48. Available at: http://www.hach.com/asset-get.download-en.jsa?id=7639982643 [Accessed May 21, 2012].

Hale, M., 1994. Strategic choices in drainage geochemistry. In M. Hale & J. A. Plant, eds. *Drainage Geochemistry*. Amsterdam: Elsevier, pp. 111–144.

Hall, G.E.M. et al., 1996. The effect of using different 0.45 μm filter membranes on "dissolved" element concentrations in natural waters. *Applied Geochemistry*, 11(1-2), pp.243–249.

Hawkes, H.E., 1976. The early days of exploration geochemistry. *Journal of Geochemical Exploration*, 6(1-2), pp.1–11.

Hawkes, H.E. & Webb, J.S., 1962. *Geochemistry in mineral exploration* 1st ed., New York: Harper Collins.

Health Canada, 2012. *Guidelines for Canadian Drinking Water Quality - Summary Table*, Ottawa, Ontario: Water, Air and Climate Change Bureau, Healthy Environments and Consumer Saftey Branch, Health Canada.

Horowitz, A.J. et al., 1996. Problems Associated with Using Filtration To Define Dissolved Trace Element Concentrations in Natural Water Samples. *Environmental Science & Technology*, 30(3), pp.954–963.

Howarth, R.J. & Thornton, I., 1983. Regional Geochemical mapping and its Application to Environmental Studies. In Iain Thornton, ed. *Applied Environmental Geochemistry*. London: Academic Press, pp. 41–73.

Iavicoli, I., Fontana, L. & Bergamaschi, A., 2009. The effects of metals as endocrine disruptors. *Journal of toxicology and environmental health. Part B, Critical reviews*, 12(3), pp.206–23.

Inacio, M., Pereira, V. & Pinto, M., 2008. The Soil Geochemical Atlas of Portugal: Overview and applications. *Journal of Geochemical Exploration*, 98(1-2), pp.22–33.

INE, 2012a. *Síntesis Geográfica Nacional*,

INE, 2012b. *Síntesis Geográfica Regional*, Santiago.

INN, 2005. *Agua potable - Parte 1 - Requisitos*, Chile.

INN, 1978. *NCh 1333. Requisitos de calidad del agua para diferentes usos*, Chile: Instituto Nacional de Normalización.

Iriarte, S. et al., 2009. Aquifer recharge and contamination determination using environmental isotopes: Santiago basin, Chile. A study case. In *Estudios de Hidrología Isotópica en América Latina 2006*. Vienna: IAEA, pp. 97–112.

James, C.H. & Radford, N.W., 1980. Some recent advances in mathematical geology: apportionment of error in geochemical prospecting data. *Proceedings of the Geologists' Association*, 91(1-2), pp.69–70.

Johnson, C.C. et al., 2005. G-BASE: baseline geochemical mapping of Great Britain and Northern Ireland. *Geochemistry: Exploration, Environment, Analysis*, 5(4), pp.347–357.

Jorquera, C.O. et al., 2012. The application of N and O isotopes to the identification of sources of nitrate in stream waters in Central Chile. In *XIII Congreso Geológico Chileno*. Antofagasta, Chile, pp. 774–776.

Kabata-Pendias, A., 2011. *Trace elements in soils and plants* 4th ed., USA, CRC.

Kabata-Pendias, A. & Pendias, H., 2001. *Trace elements in soils and plants* 3rd ed., USA, CRC.

Kattner, G., 1999. Storage of dissolved inorganic nutrients in seawater: poisoning with mercuric chloride. *Marine Chemistry*, 67(1-2), pp.61–66.

Kendall, C., 1998. Tracing nitrogen sources and cycling in catchments. In C. Kendall & J. J. McDonnell, eds. *Isotope Tracers in Catchment Hydrology*. New York: Elsevier Science, pp. 519–576.

Klock, J.C., 1975. Nonocclusive coronary disease after chronic exposure to nitrates: Evidence for physiologic nitrate dependence. *American Heart Journal*, 89(4), pp.510–513.

Knobeloch, L. et al., 2000. Blue babies and nitrate-contaminated well water. *Environmental Health Perspectives*, 108(7), pp.675–678.

Kroopnick, P. & Craig, H., 1972. Atmospheric oxygen: isotopic composition and solubility fractionation. *Science*, 175(4017), pp.54–55.

Krouse, H. & Mayer, B., 2000. Sulphur and Oxygen Isotopes in Sulphate. In P. Cook & A. Herczeg, eds. *Environmental Tracers in Subsurface Hydrology*. Boston: Kluwer Academic Press, pp. 195–231.

Lenntech B.V., 2013. SAR hazard of irrigation. Available at: http://www.lenntech.com/applications/irrigation/sar/sar-hazard-of-irrigation-water.htm [Accessed October 3, 2013].

Leybourne, M.I. & Cameron, E.M., 2010. Groundwater in geochemical exploration. *Geochemistry: Exploration, Environment, Analysis*, 10(2), pp.99–118.

Macko, S.A. & Ostrom, N.E., 1994. Pollution studies using stable isotopes. In K. Lajtha & R. M. Michener, eds. *Stable Isotopes in Ecology and Environmental Science*. Oxford: Blackwell Scientific Publishers, pp. 45–62.

Mészáros, E., 1988. On the possible role of the biosphere in the control of atmospheric clouds and precipitation. *Atmospheric Environment*, 22(2), pp.423–424.

Michalski, G., Böhlke, J.K. & Thiemens, M., 2004. Long term atmospheric deposition as the source of nitrate and other salts in the Atacama Desert, Chile: New evidence from mass-independent oxygen isotopic compositions. *Geochimica et Cosmochimica Acta*, 68(20), pp.4023–4038.

Miesch, A., 1967. *Theory of Error in Geochemical Data* Vol. 574., U.S. Government Printing Office.

Moscoso, R., Padilla, H. & Rivano, S., 1982. Hoja Los Andes, Región de Valparaiso. Carta Geológica de Chile No. 52. Geological map scale 1:250,000. , p.67.

Mukhopadhyay, R., 2008. The rise of instruments during World War II. *Analytical chemistry*, 80(15), pp.5684–91.

Muñoz, M. et al., 2006. Abanico East Formation: petrology and geochemistry of volcanic rocks behind the Cenozoic arc front in the Andean Cordillera, Central Chile (33°50'S). *Revista Geológica de Chile*, 33(1), pp.109–140.

Muscutt, A.D. & Withers, P.J.A., 1996. The phosphorus content of rivers in England and Wales. *Water Research*, 30(5), pp.1258–1268.

Neal, C. et al., 2010. The strategic significance of wastewater sources to pollutant phosphorus levels in English rivers and to environmental management for rural, agricultural and urban catchments. *The Science of the total environment*, 408(7), pp.1485–500.

Nordstrom, D.K., McCleskey, R.B. & Ball, J.W., 2009. Sulfur geochemistry of hydrothermal waters in Yellowstone National Park: IV Acid–sulfate waters. *Applied Geochemistry*, 24(2), pp.191–207.

O'Reilly, J. et al., 2010. Arsenic contamination of natural waters in San Juan and La Pampa, Argentina. *Environmental geochemistry and health*, 32(6), pp.491–515.

Van Den Oever, F., 2000. Aruba – a geochemical baseline study. *Journal Of Geosciences*, 79(4), pp.467–477.

Ohte, N. et al., 2008. Nitrogen and oxygen isotope measurements of nitrate to survey the sources and transformation of nitrogen loads in rivers. In *International Workshop on Integrated Watershed Management for Sustainable Water Use in a Humid Tropical Region*. Tsukuba, pp. 31–39.

Ottesen, R.T. & Theobald, P.K., 1994. Stream sediments in mineral exploration. In M. Hale & J. A. Plant, eds. *Drainage Geochemistry*. Amsterdam: Elsevier, pp. 147–184.

Oyarzún, J., 2000. Andean Metallogenesis: a Synoptical Review and Interpretation. In U. G. Cordani et al., eds. *Tectonic Evolution of South America*. Rio de Janeiro: International Geological Congress No. 31, pp. 726–753.

Pan, J. et al., 2012. Toxic Trace Elements. In J. A. Plant, N. Voulvoulis, & K. V. Ragnarsdottir, eds. *Pollutants, Human Health and the Environment*. John Wiley & Sons, Ltd, pp. 87–114.

Parslow, R.C. et al., 1997. Incidence of childhood diabetes mellitus in Yorkshire, northern England, is associated with nitrate in drinking water: an ecological analysis. *Diabetologia*, 40(5), pp.550–6.

Phoon, X., Ander, E.L. & Plant, J.A., 2012. Essential and Beneficial Trace Elements. In J. A. Plant, N. Voulvoulis, & K. V. Ragnarsdottir, eds. *Pollutants, Human Health and the Environment*. John Wiley & Sons, Ltd, pp. 53–86.

Piracés, R. & Maksaev, V., 1977. Geología de la Hoja de Quillota, IV y V Región. Geological map 1:250,000. , p.140.

Plant, J.A. et al., 2005. Arsenic and selenium. In B. S. Lollar, ed. *Treatise on Geochemistry, Vol. 9: Environmental Geochemistry*. Elsevier Ltd, pp. 17–66.

Plant, J.A., 1997. The Forum of European Geological Surveys Geochemistry Task Group inventory 1994–1996. *Journal of Geochemical Exploration*, 59(2), pp.123–146.

Plant, J.A. et al., 1975. The systematic determination of accuracy and precision in geochemical exploration data. *Journal of Geochemical Exploration*, 4, pp.467–486.

Plant, J.A., Baldock, J.W. & Smith, B., 1996. The role of geochemistry in environmental and epidemiological studies in developing countries: a review. *Geological Society, London, Special Publications*, 113(1), pp.7–22.

Plant, J.A. & Hale, M., 1994. Introduction: the foundations of modern drainage geochemistry. In M. Hale & J. A. Plant, eds. *Drainage Geochemistry*. Amsterdam: Elseiver, pp. 3–9.

Plant, J.A. & Raiswell, R.W., 1994. Modifications to the geochemical signatures of ore deposits and their associated rocks in different surface environments. In M. Hale & J. A. Plant, eds. *Drainage Geochemistry*. Amsterdam: Elsevier, pp. 73–109.

Ravichandran, M., 2004. Interactions between mercury and dissolved organic matter--a review. *Chemosphere*, 55(3), pp.319–31.

Reimann, C. et al., 2009. Arsenic distribution in the environment: The effects of scale. *Applied Geochemistry*, 24(7), pp.1147–1167.

Reimann, C. & de Caritat, P., 1998. *Chemical Elements in the Environment: Factsheets for the Geochemist and Environmental Scientist*, Springer.

Reimann, C. & Garrett, R.G., 2005. Geochemical background--concept and reality. *The Science of the total environment*, 350(1-3), pp.12–27.

Richardson, D.B., Terschüren, C. & Hoffmann, W., 2008. Occupational risk factors for non-Hodgkin's lymphoma: a population-based case-control study in Northern Germany. *American journal of industrial medicine*, 51(4), pp.258–68.

Rivano, S. et al., 1993. *Hojas Quillota y Portillo No 73. Carta Geológica de Chile 1:250,000*, Santiago.

Rollinson, H.R., 1993. *Using Geochemical Data: Evaluation, Presentation, Interpretation*, Harlow: Pearson Education Limited.
Romero, L. et al., 2003. Arsenic enrichment in waters and sediments of the Rio Loa (Second Region, Chile). *Applied Geochemistry*, 18(9), pp.1399–1416.
Salminen, R. et al., 1998. *FOREGS geochemical mapping field manual*, Geologian tutkimuskeskus.
Salminen, R. & Tarvainen, T., 1997. The problem of defining geochemical baselines. A case study of selected elements and geological materials in Finland. *Journal of Geochemical Exploration*, 60, pp.91–98.
Sellés, G. & Gana, P., 2001. Mapa geológico del área de Talagante-San Francisco de Mostazal, regiones Metropolitana de Santiago y del Libertador General Bernardo O'Higgins. Serie geológica básica No. 74. Geological map scale 1:100,000. , p.33.
SERNAGEOMIN, 2003. Carta Geológica de Chile. Geological map scale 1:1,000,000.
Shacklette, H.T. & Boerngen, J.G., 1984. Element concentrations in soils and other surficial materials of the conterminous United States. *Professional Paper, US Geological Survey*, p.105.
Silva, S.R., Chang, C.C.Y. & Avanzino, R.J., 2000. A new method for collection of nitrate from fresh water and the analysis of nitrogen and oxygen isotope ratios Kendall, C. Wilkison, D.H. Ziegler, A.C. *Journal of Hydrology*, 228(1-2), pp.22–36.
Simpson, P. et al., 1993. Geochemical mapping of stream water for environmental studies and mineral exploration in the UK. *Journal of Geochemical Exploration*, 49(1-2), pp.63–88.
Smith, D.B. et al., 2006. Natural and Man-Made Chemicals in North American Soils — Continental-Scale Pilot Study Completed. *US Geological Survey Fact Sheet*, (October), pp.2006–3115.
Smith, D.B. & Reimann, C., 2008. Low-density geochemical mapping and the robustness of geochemical patterns. *Geochemistry: Exploration, Environment, Analysis*, 8(3-4), pp.219–227.
Smith, E.A., Mayfield, C.I. & Wong, P.T.S., 1977. Physical and chemical characterization of selected natural and apatites in synthetic and natural aqueous solutions. *Water, Air, and Soil Pollution*, 8, pp.401–415.
Soucek, D.J. & Kennedy, A.J., 2005. Effects of hardness, chloride, and acclimation on the acute toxicity of sulfate to freshwater invertebrates. *Environmental toxicology and chemistry / SETAC*, 24(5), pp.1204–1210.
Stanley, C., 1988. PROBPLOT - An Intercative Computer Program to Fit Mixtures of Normal (or Log-Normal) Distributions using Maximum Likelihood Optimization Procedures. In *Special Volume #14, Association of Exploration Geochemist*. Ontario, p. 40.
Sunderman, F.W., 1973. The current status of nickel carcinogenesis. *Annals of Clinical and Laboratory Science*, 3, pp.156–180.
Taufen, P.M., 1997. Ground waters and surface waters in exploration geochemical surveys. In A. G. Gubins, ed. *Proceedings of Exploration 97: Fourth Decenial International Conference on Mineral Exploration*. pp. 271–284.
Thiele, R., 1980. Hoja Santiago, Región Metropolitana. Carta Geológica de Chile No. 39. Geological map scale 1:250,000. , p.21.
Thomas, H., 1958. Geología de la Cordillera de la Costa entre valle La Ligua y la cuesta Barriga.
Thompson, M., 1997. Comparability and Traceability in Analytical Measurements and Reference Materials†. *The Analyst*, 122(11), pp.1201–1206.

Thompson, M. & Howarth, R.J., 1973. The rapid estimation and control of precision by duplicate determinations. *The Analyst*, 98(1164), pp.153–160.
Thornton, I. et al., 1994. Lead contamination of UK dusts and soils and implications for childhood exposure: An overview of the work of the Environmental Geochemistry Research Group, Imperial College, London, England 1981–1992. *Environmental Geochemistry and Health*, 16-16(3-4), pp.113–122.
Thornton, I., 2010. Research in Applied Environmental Geochemistry, with particular reference to Geochemistry and Health. *Geochemistry: Exploration, Environment, Analysis*, 10(3), pp.317–329.
Uganda. Geological Survey and Mines Department & Reedman, A.J., 1973. *Geochemical Atlas of Uganda (compiled by A.J. Reedman)*, Geological Survey and Mines Department.
Vaughan, D.J., 2006. Arsenic. *Elements*, 2(2), pp.71–75.
Vitòria, L. et al., 2004. Fertilizer characterization: isotopic data (N, S, O, C, and Sr). *Environmental Science & Technology*, 38(12), pp.3254–3262.
Vyskocil, A. et al., 1994. Biochemical renal changes in workers exposed to soluble nickel compounds. *Human and Experimental Toxicology*, 13, pp.257–261.
Wall, R., Sellés, G. & Gana, P., 1999. Area Tiltil-Santiago, Región Metropolitana. Geological map No. 11 scale 1:100,000.
Ward, M.H. et al., 1996. Drinking water nitrate and the risk of non-Hodgkin's lymphoma. *Epidemiology*, 7(5), pp.465–471.
Warnaars, F.W., 1985. Porphyry copper and tourmaline breccias at Los Bronces-Rio Blanco, Chile. *Economic Geology*, 80, pp.1544–1565.
Wasserman, M.D. et al., 1992. *Methods for separation and total stable isotope analysis of alunite*, Open-File Report 92-9.
Webster, J.D. et al., 1980. Acute nickel intoxication by dialysis. *Annals of Internal Medicine*, 92, pp.631–634.
WHO, 2011a. *Cadmium in Drinking-water*, WHO.
WHO, 2011b. *Guidelines for drinking-water quality* 4th ed., WHO.
WHO, 1991a. *Nickel, nickel carbonyl, and some nickel compounds: health and safety guide 62*, Geneva: WHO.
WHO, 1991b. *Nickel: Environmental health criteria 108*, Geneva: WHO.
WHO, 2011c. *Nitrate and nitrite in drinking-water*, Geneva: WHO.
Williams, S.A. & Cesbron, F.P., 1977. Rutile and apatite: useful prospecting guides for porphyry copper deposits. *Mineralogical Magazine*, 41, pp.288–292.
Wright, W.G. & Nordstrom, D.K., 1999. Oxygen Isotopes of Dissolved Sulfate as a Tool to Distinguish Natural and Mining-Related Dissolved Constituents. In *US Geological Survey Toxic Substances Hydrology Program Procedings of the Technical Meeting*. California: U.S. Geological Survey, pp. 67–73.
Xie, X., 1997. Geochemical mapping in China. *Journal of Geochemical Exploration*, 60(1), pp.99–113.
Xie, X. et al., 2008. Multi-scale geochemical mapping in China. *Geochemistry: Exploration, Environment, Analysis*, 8(3-4), pp.333–341.

APPENDIX A: Sampling protocol to collect stream waters

Geochemical Sampling and Analytical Protocol

Stream Water Sampling Protocol

Author: Carmina Jorquera

Reviewer: Christian Ihlenfeld

In order to collect a high quality water sample, it is important to ensure cleanness and avoid contamination at all stages in the process, from preparing full sampling to the shipment of the samples to a laboratory.

Selecting sampling sites

Prior to collecting a sample it is important to carry out a study of potential sampling sites. This should include a review of the geology, the hydrogeology, the land use and any possible source of anthropogenic contamination.

All samples should be collected where there is a continuous uniform stream flow away from junctions, sources of contamination and manmade structures.

Equipment and supplies

The basic equipment for the sampling process at the field is:

- Peristaltic pump
- Multi-parameter meter (pH, conductivity, dissolved oxygen, temperature)
- 5 x 60 ml and 4 x 125 ml HDPE wide mouth Nalgene^{TM} bottles
- <0.45 μm filters
- Cooler (electric or with ice packs)

- Powder-free latex or nitrile gloves
- GPS

Chemical reagents and CRM

- Ultrapure nitric acid (e.g. 65% Suprapur® Merck or 70% AR HACH)
- Mercury chloride (directions: dissolve 15.75 g of HgCl2 in 450 ml of deionised water)
- Ultra pure deionised water (e.g. chromatography water)
- Buffer solutions for pH (4.01, 7.01 and 10.01) and conductivity (e.g. 1413 µS/cm)
- Water standards (e.g. TROIS-94 and TM-23.3)

Supplies for labelling

- Permanent markers (black, blue and red)
- Adhesive tape
- Ziploc plastic bags

Others supplies

- 1000 µl Pipette and appropriated tips
- Table to hold samples
- Camera
- Paper towels

Sampling procedure

The clean hands/ dirty hands practice will be used based on two samplers to avoid cross-contamination during the sampling process.

Clean hands (CH): this person can handle and touch the sample bottles, chemical reagents and filters. The details of the responsibilities of CH sampler are given below.

Dirty hands (DH): this person is responsible for manipulating non critical sampling equipment and carrying out any tasks that could be a possible source of contamination. The details of the responsibilities of DH sampler are given below.

Both CH and DH samplers should remove all rings and jewellery prior to sampling and then thoroughly wash their hands in the water to be sampled. Both CH and DH must wear only their own latex (or nitrile) gloves during sampling, and not touch their skin especially if they are using sunscreen.

Daily bottle preparation (CH)

The size of bottles used in the sampling process depends on laboratory requirements. Sizes shown here are for the Acme and the Queen's University laboratories.

1. Wear latex (or nitrile) gloves.
2. With a permanent marker label the prefix (depending on the analytical method will be used, see below) and the number of the sample. Use red colour on bottles for HNO_3 acidification for cation analysis, use blue colour on bottles for $HgCl_2$ for nitrogen isotope analysis and use black in any other:
    a. 1x60 ml bottle for cation analysis in filtered sample. Prefix CFAA
    b. 1x60 ml bottle for cation analysis in unfiltered sample. Prefix CUAA collected for future research project
    c. 1x60 ml bottle for anion analysis in filtered sample. Prefix AFUA
    d. 1x60 ml bottle for anion analysis in unfiltered sample. Prefix AUUA

e. 1x60 ml bottle for DOC analysis in filtered sample. Prefix KFUA

f. 1x125 ml bottle for physiochemical analysis in filtered sample. Prefix PFUA

g. 1x125 ml bottle for O, H and S isotope analyses in filtered sample. Prefix IFUQ

h. 2x125 ml bottle for N isotope analysis in filtered sample. Prefix NFUQ

3. Cover the label with adhesive tape.
4. If AAplc standard labels are being used, place the paper label below the adhesive tape and under the label marked.
5. Place all bottles with same number label into a Ziploc bag.
6. Add 1 ml of HNO_3 into bottles for cation analyses, those in red.
7. Add 20 drops of $HgCl_2$ into bottles for nitrogen isotope analysis, those in blue.

Note: DH can help wearing gloves.

Daily instrument calibration (DH)

1. At the beginning of the day the pH and conductivity meters are checked with appropriate buffer, and recalibrate as necessary.
2. Use pH 4.01, 7.01 and 10.01 buffer solutions to check/calibrate the meter following the manufacturer's instructions.
3. Pour out conductivity solution in a beaker to check/calibrate the meter following the manufacturer's instructions.
4. Used solutions are discharged and never reuse
5. The equipment is cleaned and packed for the field

6. Hands washed

On arrival at sampling sites

1. Set up the multiparameter instrument down flow of the site collection (DH).
2. Log the coordinates of the site, sample number, type of sample (original, duplicate or process blank), date and time (CH) in the field sheet.
3. Log any potential source of contamination, geology and vegetation (CH).
4. Log special features such the water colour; the width, the depth and the relative speed of the stream flow and any relevant comment (CH).
5. Take pictures if necessary and log the number of the picture (CH).

Preparing to sample (both CH and DH sampler must wear latex or nitrile gloves)

1. Prepare the site for collecting the sample (DH): set up the peristaltic pump and the sampler table near the border of the stream, fix the free tip of the hose under the water but not touching the base of the stream.
2. Prepare sampling bottles on to the sampler table (CH).
3. Place 2 water filters in easy reach, although only one is normally used (CH).

Sampling of stream water

1. Pump the water from the stream (DH), once water reaches the sampling tip of the hose pump 100 times more. This was done to equilibrate the sampling system with the water being collected and for consistency across all sampling sites.
2. Remove caps of bottles for unfiltered samples (CH), take the unfiltered sample filling the bottle until the top and close tighten the bottles avoiding bubbles inside.

3. Remove the filter from its package (CH) and put it into the sampling tip of the hose.
4. Pump water, once the water reaches the tip of the filter and pump 100 times more (DH).
5. Remove caps of bottles for filtered samples (CH), take the filtered samples filling the bottle until the top and close the bottles tighten avoiding bubbles inside.
6. Place all bottles into the Ziploc bag (CH), seal it and store in an electrical cooler or add ice pack. Take care all bottles are standing straight.
7. Remove the gloves.

On completion of sampling

1. Log pH, EC, DO and temperature once the meter stabilized (CH).
2. Measure the alkalinity following the manufacturer's instructions (CH) if more time is required to do this fill a bottle (at least 500 ml), rinsing three times before collecting the water and measure at cabinet/office at the end of the day.
3. Discard unused water from the hose and filter (DH).
4. Label the filter and retain for future research.
5. Ensure the field sheet is completed.
6. Place all waste residues into a rubbish bag. Ensure no material is left at the site.

At cabinet/office

1. Transfer the field sheet into a digital copy.
2. Measure the alkalinity if it wasn't done in the field.
3. Store the samples in a refrigerator.

After survey

1. Sort out the sample packaging bottles for different analyses.
2. Use film paper to package the sample bottles and protect the packs with bubble paper in the boxes. Ensure bottles always standing straight.
3. Dispatch waters to the required laboratory.

Quality assurance

1. Field duplicates (in the field)
    - Collect a duplicate every 10th original samples collected.
    - Repeating the entire sampling procedure at the same site as the original sample.
2. Process blank (in the field)
    - A process blank must be taken every 20th original samples collected.
    - Rinse with ultra pure deionised water a 1Lt Nalgene^{TM} bottle at least three times and fill it with ultra pure deionised water.
    - Repeat the sampling process using the ultra pure deionised water into the bottle.
3. Simple blank (in the cabinet/office)
    - A simple blank must be inserted every 20th original samples.
    - Add ultra pure water directly into the bottles.
4. Standards (in the cabinet/office)
    - A standard must be inserted every 20th original samples.

- Add water standard into bottles directly.
- Use TM-23.3 or TM-27.2 for cation analyses.
- Use TROIS-94 for anion, physiochemical and DOC analyses.

Note: Do not add HNO_3 to the standard for cation analysis as it already contains this.

APPENDIX B: QA/QC evaluation

Table B-1: Accuracy assessment for the TM-27.2 CRM

Element	Al_ppb	As_ppb	Ba_ppb	Be_ppb	Cd_ppb	Co_ppb	Cr_ppb	Cu_ppb	Fe_ppb	Li_ppb	Mn_ppb	Mo_ppb	Ni_ppb
Within 2 SD					x	x						x	x
Within 3 SD		x	x	x				x		x			
Within ±25%													
≤3 outside ±25%													
Outside limits	x						x		x		x		
Evaluation	†						∏		§		∏		
Mean TM-27.2 data	18	2.5	4.99	1.46	1.21	2.28	1.8	4.7	10	4.0	2.75	2.5	2.4
Mean TM-27.2	15	2.4	5.1	1.4	1.2	2.30	1.8	4.6	11	3.9	2.60	2.4	2.6
Bias[1]	3	0.1	-0.11	0.06	0.01	-0.02	0.03	0.1	-1	0.1	0.15	0.1	-0.2
% Bias[2]	23.0	4.4	-2.1	4.2	0.5	-0.8	1.6	3.1	-12.3	1.5	5.8	3.4	-7.3
Mean of data	1209	6.0	17.49	0.22	1	14.15	0.9	3997.7	1531	8.8	980.05	117.2	7.9
Median of data	13	2.5	14.22	0.025	0.03	0.08	0.3	2.4	12	2.6	11.05	1.8	0.1
Detection limit	1	0.5	0.05	0.05	0.05	0.02	0.5	0.1	10	0.1	0.05	0.1	0.2
10x det. limit	10	5	0.5	0.5	0.5	0.2	5	1	100	1	0.5	1	2

Element	Pb_ppb	Sb_ppb	Se_ppb	Sr_ppb	Tl_ppb	U_ppb	V_ppb
Within 2 SD		x	x			x	
Within 3 SD	x						x
Within ±25%				x	x		
≤3 outside ±25%							
Outside limits							
Evaluation							
Mean TM-27.2 data	3.1	2.13	1.6	52.17	1.94	2.073	2.4
Mean TM-27.2	3.2	1.9	1.6	54.4	1.80	2.000	2.4
Bias[1]	-0.1	0.23	0.02	-2.23	0.14	0.072	0.0
% Bias[2]	-2.8	11.9	1	-4.1	8	3.6	-0.3
Mean of data	0.3	0.35	1.2	465.85	0.04	1.717	3.4
Median of data	0.05	0.13	0.5	238.09	0.005	0.240	1.1
Detection limit	0.1	0.05	0.5	0.01	0.01	0.02	0.2
10x det. limit	1	0.5	5	0.1	0.1	0.2	2

† Where the initial 2s and 3s parameter are > +/-25%

∏ Standards are too close to DL

§ More than 50% of standards are below the DL

[1] bias = (x̄ data - x̄ standard)

[2]% bias = bias/certified mean *100

% bias colour code

	>10%
	5 to 10%
	2 to 5%
	-2 to 2%
	-2 to -5%
	-5 to -10%
	<-10%

Table B-2: Accuracy assessment for the TM-23.3 CRM

Element	Al_ppb	As_ppb	Ba_ppb	Be_ppb	Cd_ppb	Co_ppb	Cr_ppb	Cu_ppb	Fe_ppb	Li_ppb	Mn_ppb	Mo_ppb	Ni_ppb
Within 2 SD													x
Within 3 SD		x		x						x			
Within ±25%			x			x		x			x		
≤3 outside ±25%							x					x	
Outside limits	x				x				x				
Evaluation	Ω				†				§				
Mean TM-23.3 data	130	8.8	15.44	1.64	2.81	7.69	8.0	10.3	19	2.8	10.04	5.3	5.3
Mean TM-23.3	96	7.6	14.3	1.5	2.5	6.7	6.6	9.1	15	2.5	8.7	4.4	5.4
Bias[1]	34	1.2	1.14	0.14	0.31	0.99	1.4	1.2	4	0.3	1.34	0.9	-0.2
% Bias[2]	35.7	16.1	8	9.3	12.3	14.8	20.6	12.7	23.3	11.6	15.4	20	-2.8
Mean of data	1209	6.0	17.49	0.22	1	14.15	0.9	3997.7	1531	8.8	980.05	117.2	7.9
Median of data	13	2.5	14.22	0.025	0.03	0.08	0.3	2.4	12	2.6	11.05	1.8	0.1
Detection limit	1	0.5	0.05	0.05	0.05	0.02	0.5	0.1	10	0.1	0.05	0.1	0.2
10x det. limit	10	5	0.5	0.5	0.5	0.2	5	1	100	1	0.5	1	2

Element	Pb_ppb	Sb_ppb	Se_ppb	Sn_ppb	Sr_ppb	Ti_ppb	Tl_ppb	U_ppb	V_ppb
Within 2 SD									
Within 3 SD		x	x	x					x
Within ±25%					x				
≤3 outside ±25%							x	x	
Outside limits	x					x			
Evaluation	†					§			
Mean TM-23.3 data	3.6	3.27	7.0	3.44	76.83	<10	4.34	6.05	2.4
Mean TM-23.3	3.2	2.5	4.2	2.7	70.6	3.2	3.8	5.10	2.1
Bias[1]	0.4	0.77	2.8	0.7	6.23	N/A	0.54	0.95	0.3
% Bias[2]	13.8	30.8	65.5	27.4	8.8	N/A	14.2	18.5	12.4
Mean of data	0.3	0.35	1.2	0.1	465.85	<10	0.04	1.717	3.4
Median of data	0.05	0.13	0.5	<0.05	238.09	<10	0.005	0.240	1.1
Detection limit	0.1	0.05	0.5	0.05	0.01	10	0.01	0.02	0.2
10x det. limit	1	0.5	5	1	0.1	100	0.1	0.2	2

Ω Good reproducibility, but biased

§ More than 50% of stds are < DL

† Initial 2s and 3s are > ±25%

[1] bias = (x̄ data - x̄ standard)

[2]% bias = bias/certified mean *100

% bias colour code

	>10%
	5 to 10%
	2 to 5%
	-2 to 2%
	-2 to -5%
	-5 to -10%
	<-10%

Table B-3: Accuracy assessment for the TROIS-94 CRM

Analyte	Alkalinity	DOC	pH	EC	NO3-N
Within 2 SD					
Within 3 SD		x			
Within ±25%			x		
≤3 outside ±25%					
Outside limits	x			x	x
Evaluation	§			§	§
Mean TROIS-94 data	7	5	7.0	24	0.054
Mean TROIS-94	5	6	6.7	32	0.071
Bias[1]	2	-1	0.3	-8.2	-0.017
% Bias[2]	33.6	-12.8	4.4	-25.8	-24.0
Mean of data	88	1	7.3	885	1.19
Median of data	72	1	7.5	541	0.12
Detection limit	1	1	0.1	3	0.01
10x det. limit	10	10	1.0	30.0	0.1

§ More than 50% of std are below the DL

[1] bias = ($\bar{x}$ data - $\bar{x}$ standard)

[2]% bias = bias/certified mean *100

% bias colour code

	>10%
	5 to 10%
	2 to 5%
	-2 to 2%
	-2 to -5%
	-5 to -10%
	<-10%

Table B-4: Precision assessment for field duplicates

Analyte	Ag_ppb	Al_ppb	As_ppb	Au_ppb	B_ppb	Ba_ppb	Be_ppb	Bi_ppb	Br_ppb	Ca_ppb	Cd_ppb	Ce_ppb	Cl_ppm
10x det. limit	0.5	10	5	0.5	50	0.5	0.5	0.5	50	500	0.5	1.5	10
Samples outside ±20%		5			5	6				0			
% within ±20%		92			93	94				100			
≥95% data within ±20%										x			
Samples <10x det. limit	x		x	x			x	x	x		x	x	x
<95% within ±20%		x			x	x							
Ave % Rel. Dif.	N/A	10.09	N/A	N/A	7.99	8.01	N/A	N/A	N/A	2.97	N/A	N/A	N/A
Analyte	Co_ppb	Cr_ppb	Cs_ppb	Cu_ppb	Dy_ppb	Er_ppb	Eu_ppb	Fe_ppb	Ga_ppb	Gd_ppb	Ge_ppb	Hf_ppb	Hg_ppb
10x det. limit	0.2	5	0.1	1	0.1	1.1	0.1	100	0.5	0.1	0.5	0.2	1
Samples outside ±20%				11									
% within ±20%				86									
≥95% data within ±20%													
Samples <10x det. limit	x	x	x		x	x	x	x	x	x	x	x	x
<95% within ±20%				x									
Ave % Rel. Dif.	N/A	N/A	N/A	15.43	N/A	N/A	N/A	N/A	N/A	N/A	N/A	N/A	N/A
Analyte	Ho_ppb	In_ppb	Ir_ppb	K_ppb	La_ppb	Li_ppb	Lu_ppb	Mg_ppb	Mn_ppb	Mo_ppb	Na_ppb	Nb_ppb	Nd_ppb
10x det. limit	0.1	0.1	0.5	500	0.1	1	0.1	500	0.5	1	500	0.1	1.1
Samples outside ±20%				1		4		1	10	3	0		
% within ±20%				99		95		99	89	96	100		
≥95% data within ±20%				x		x		x		x	x		
Samples <10x det. limit	x	x	x		x		x					x	x
<95% within ±20%									x				
Ave % Rel. Dif.	N/A	N/A	N/A	4.58	N/A	9.36	N/A	3.56	10.80	6.89	3.50	N/A	N/A
Analyte	Ni_ppb	Os_ppb	P_ppb	Pb_ppb	Pd_ppb	Pr_ppb	Pt_ppb	Rb_ppb	Re_ppb	Rh_ppb	Ru_ppb	S_ppm	Sb_ppb
10x det. limit	2	0.5	200	1	2	0.1	0.1	0.1	0.1	1.1	0.5	10	0.5
Samples outside ±20%								5				10	
% within ±20%								95				89	
≥95% data within ±20%								x					
Samples <10x det. limit	x	x	x	x	x	x	x		x	x	x		x
<95% within ±20%												x	
Ave % Rel. Dif.	N/A	N/A	N/A	N/A	N/A	N/A	N/A	6.32	N/A	N/A	N/A	7.98	N/A
Analyte	Sc_ppb	Se_ppb	Si_ppb	Sm_ppb	Sn_ppb	Sr_ppb	Ta_ppb	Tb_ppb	Te_ppb	Th_ppb	Ti_ppb	Tl_ppb	Tm_ppb
10x det. limit	10	5	400	0.2	0.5	0.1	0.2	0.1	0.5	1.5	100	0.1	0.1
Samples outside ±20%			2			2							
% within ±20%			98			98							
≥95% data within ±20%			x			x							
Samples <10x det. limit	x	x		x	x		x	x	x	x	x	x	x
<95% within ±20%													
Ave % Rel. Dif.	N/A	N/A	5.32	N/A	N/A	5.97	N/A	N/A	N/A	N/A	N/A	N/A	N/A
Analyte	U_ppb	V_ppb	W_ppb	Y_ppb	Yb_ppb	Zn_ppb	Zr_ppb	NO3_ppm	ALK_mg/L	DOC_ppm	F_ppb	pH_units	EC_µS/cm
10x det. limit	0.2	2	0.2	0.1	0.1	5	0.2	0.5	10	10	200	1	30
Samples outside ±20%	0					19			1			2	0
% within ±20%	100					63			98			97	100
≥95% data within ±20%	x								x			x	x
Samples <10x det. limit		x	x	x	x		x	x		x	x		
<95% within ±20%						x							
Ave % Rel. Dif.	4.76	N/A	N/A	N/A	N/A	31.77	N/A	N/A	4.39	N/A	N/A	5.00	2.88

Analyte	TDS_ppm
10x det. limit	20
Samples outside ±20%	0
% within ±20%	100
≥95% data within ±20%	x
Samples <10x det. limit	
<95% within ±20%	
Ave % Rel. Dif.	2.85

Table B-5: Cross-contamination assessment for simple blank (B1) of distilled water

Element	Ag_ppb	Al_ppb	As_ppb	Au_ppb	B_ppb	Ba_ppb	Be_ppb	Bi_ppb	Br_ppb	Ca_ppb	Cd_ppb	Ce_ppb	Cl_ppm
3xDL	0.15	3	1.5	0.15	15	0.15	0.15	0.15	15	150	0.15	0.03	3
Samples >3xDL	0	7	0	0	11	19	0	0	0	2	1	0	0
% outside	0	37	0	0	58	100	0	0	0	11	5	0	0
Samples >10xDL	0	0	0	0	2	4	0	0	0	0	0	0	0
Data below 3xDL	x		x	x			x	x	x			x	x
Data below 10xDL	x	x	x	x			x	x	x	x	x	x	x
Data above 3xDL		x			x	x				x	x		
Data above 10xDL					x	x							
Max. of blanks	<0.05	8	<0.5	<0.05	129	1.27	0.07	<0.05	15	164	0.26	0.03	3
Median of blanks	<0.05	3	0.25	<0.05	18	0.23	<0.05	<0.05	<5	<50	<0.05	<0.01	1
Minimum of data	<0.05	1	<0.5	<0.05	<5	0.1	<0.05	<0.05	<5	1163	<0.05	<0.01	<1
Mean of data	0.05	1869	4.4	<0.05	105	15.39	0.35	<0.05	50	89599	1.67	3.03	31
Median of data	<0.05	20	2.3	<0.05	66	12.72	<0.05	<0.05	15	47598	<0.05	0.01	8
Element	Co_ppb	Cr_ppb	Cs_ppb	Cu_ppb	Dy_ppb	Er_ppb	Eu_ppb	Fe_ppb	Ga_ppb	Gd_ppb	Ge_ppb	Hf_ppb	Hg_ppb
3xDL	0.06	1.5	0.03	0.3	0.03	0.03	0.03	30	0.15	0.03	0.15	0.06	0.3
Samples >3xDL	0	0	0	15	0	0	0	0	0	0	0	0	0
% outside	0	0	0	79	0	0	0	0	0	0	0	0	0
Samples >10xDL	0	0	0	2	0	0	0	0	0	0	0	0	0
Data below 3xDL	x	x	x		x	x	x	x	x	x	x	x	x
Data below 10xDL	x	x	x		x	x	x	x	x	x	x	x	x
Data above 3xDL				x									
Data above 10xDL				x									
Max. of blanks	0.06	1	<0.01	1.9	<0.01	<0.01	<0.01	25	<0.05	<0.01	<0.05	<0.02	0.2
Median of blanks	0.03	<0.5	<0.01	0.5	<0.01	<0.01	<0.01	<10	<0.05	<0.01	<0.05	<0.02	<0.1
Minimum of data	<0.02	<0.5	<0.01	<0.1	<0.01	<0.01	<0.01	<10	<0.05	<0.01	<0.05	<0.02	<0.1
Mean of data	22.77	0.9	1.18	6981	0.83	0.36	0.24	2654	0.06	0.95	0.05	<0.02	0.1
Median of data	0.08	<0.5	0.6	2.4	<0.01	<0.01	<0.01	<10	<0.05	<0.01	<0.05	<0.02	<0.1
Element	Ho_ppb	In_ppb	Ir_ppb	K_ppb	La_ppb	Li_ppb	Lu_ppb	Mg_ppb	Mn_ppb	Mo_ppb	Na_ppb	Nb_ppb	Nd_ppb
3xDL	0.03	0.03	0.15	150	0.03	0.3	0.03	150	0.15	0.3	150	0.03	0.03
Samples >3xDL	0	0	0	0	0	9	0	0	8	1	0	0	0
% outside	0	0	0	0	0	47	0	0	42	5	0	0	0
Samples >10xDL	0	0	0	0	0	9	0	0	1	0	0	0	0
Data below 3xDL	x	x	x	x	x		x	x			x	x	x
Data below 10xDL	x	x	x	x	x		x	x		x	x	x	x
Data above 3xDL						x			x	x			
Data above 10xDL						x			x				
Max. of blanks	<0.01	<0.01	<0.05	52	<0.01	1.8	<0.01	<50	1	0.5	146	0.03	0.02
Median of blanks	<0.01	<0.01	<0.05	<50	<0.01	0.2	<0.01	<50	0.14	<0.1	81	<0.01	<0.01
Minimum of data	<0.01	<0.01	<0.05	<50	<0.01	<0.1	<0.01	100	<0.05	<0.1	492	<0.01	<0.01
Mean of data	0.15	0.01	<0.05	3679	1.1	8.8	0.04	13102	1310	81.6	30293	0.01	2.68
Median of data	<0.01	<0.01	<0.05	851	<0.01	2.7	<0.01	7967	9	1.7	11158	<0.01	0.01
Element	Ni_ppb	Os_ppb	P_ppb	Pb_ppb	Pd_ppb	Pr_ppb	Pt_ppb	Rb_ppb	Re_ppb	Rh_ppb	Ru_ppb	S_ppm	Sb_ppb
3xDL	0.6	0.15	60	0.3	0.6	0.03	0.03	0.03	0.03	0.03	0.15	3	0.15
Samples >3xDL	0	0	1	2	0	0	0	0	0	0	0	0	0
% outside	0	0	5	11	0	0	0	0	0	0	0	0	0
Samples >10xDL	0	0	0	1	0	0	0	0	0	0	0	0	0
Data below 3xDL	x	x			x	x	x	x	x	x	x	x	x
Data below 10xDL	x	x	x		x	x	x	x	x	x	x	x	x
Data above 3xDL			x	x									
Data above 10xDL				x									
Max. of blanks	0.4	<0.05	62	1.8	<0.2	0.01	<0.01	0.02	<0.01	<0.01	<0.05	3	<0.05
Median of blanks	<0.2	<0.05	29	0.1	<0.2	<0.01	<0.01	<0.01	<0.01	<0.01	<0.05	1	<0.05
Minimum of data	<0.2	<0.05	<20	<0.1	<0.2	<0.01	<0.01	0.04	<0.01	<0.01	<0.05	<1	<0.05
Mean of data	12.5	<0.05	64	0.2	<0.2	0.51	<0.01	4.28	0.33	0.01	<0.05	91	0.28
Median of data	<0.2	<0.05	35	<0.1	<0.2	<0.01	<0.01	1.17	0.02	<0.01	<0.05	34	0.12
Element	Sc_ppb	Se_ppb	Si_ppb	Sm_ppb	Sn_ppb	Sr_ppb	Ta_ppb	Tb_ppb	Te_ppb	Th_ppb	Ti_ppb	Tl_ppb	Tm_ppb
3xDL	3	1.5	120	0.06	0.15	0.03	0.06	0.03	0.15	0.15	30	0.03	0.03
Samples >3xDL	0	0	6	0	0	17	0	0	0	0	0	0	0
% outside	0	0	32	0	0	89	0	0	0	0	0	0	0
Samples >10xDL	0	0	2	0	0	4	0	0	0	0	0	0	0
Data below 3xDL	x	x		x	x		x	x	x	x	x	x	x
Data below 10xDL	x	x		x	x		x	x	x	x	x	x	x
Data above 3xDL			x			x							
Data above 10xDL			x			x							
Max. of blanks	<1	<0.5	500	<0.02	0.11	0.26	<0.02	<0.01	<0.05	<0.05	<10	<0.01	<0.01
Median of blanks	<1	<0.5	100	<0.02	<0.05	0.08	<0.02	<0.01	<0.05	<0.05	<10	<0.01	<0.01
Minimum of data	<1	<0.5	708	<0.02	<0.05	3.75	<0.02	<0.01	<0.05	<0.05	<10	<0.01	<0.01
Mean of data	3	0.9	7774	0.74	0.05	440	<0.02	0.15	<0.05	0.46	<10	0.01	0.05
Median of data	1	<0.5	6277	<0.02	<0.05	221	<0.02	<0.01	<0.05	<0.05	<10	<0.01	<0.01
Element	U_ppb	V_ppb	W_ppb	Y_ppb	Yb_ppb	Zn_ppb	Zr_ppb	NO3_ppm	ALK_mg/L	DOC_ppm	F_ppb	EC_µs/cm	TDS_ppm
3xDL	0.06	0.6	0.06	0.03	0.03	1.5	0.06	0.15	3	3	60	9	6
Samples >3xDL	0	1	0	0	0	16	0	0	0	0	0	0	0
% outside	0	5	0	0	0	84	0	0	0	0	0	0	0
Samples >10xDL	0	0	0	0	0	16	0	0	0	0	0	0	0
Data below 3xDL	x		x	x	x		x	x	x	x	x	x	x
Data below 10xDL	x	x	x	x	x		x	x	x	x	x	x	x
Data above 3xDL		x				x							
Data above 10xDL						x							
Max. of blanks	<0.02	0.7	0.03	0.01	0.01	32.6	<0.02	<0.05	2	1	20	3	2
Median of blanks	<0.02	<0.2	<0.02	<0.01	<0.01	13.0	<0.02	<0.05	2	<1	20	2	2
Minimum of data	<0.02	<0.2	<0.02	<0.01	<0.01	<0.5	<0.02	<0.05	<1	<1	50	500	337
Mean of data	2.42	3	0.36	4.42	0.27	400.3	0.03	4	77	1	295	1264	898
Median of data	0.2	1.1	0.02	0.02	<0.01	3.7	<0.02	0.37	63	<1	100	1097	774

Table B-6: Cross-contamination assessment for process blank (B2) of distilled water

Element	Ag_ppb	Al_ppb	As_ppb	Au_ppb	B_ppb	Ba_ppb	Be_ppb	Bi_ppb	Br_ppb	Ca_ppb	Cd_ppb	Ce_ppb	Cl_ppm
3xDL	0.15	3	1.5	0.15	15	0.15	0.15	0.15	15	150	0.15	0.03	3
Samples >3xDL	0	9	0	0	11	11	0	0	0	5	0	0	0
% outside	0	47	0	0	58	58	0	0	0	26	0	0	0
Samples >10xDL	0	3	0	0	2	4	0	0	0	0	0	0	0
Data below 3xDL	x		x	x			x	x	x		x	x	x
Data below 10xDL	x		x	x			x	x	x	x	x	x	x
Data above 3xDL		x			x	x				x			
Data above 10xDL		x			x	x							
Max. of blanks	0.07	19	<0.5	0.08	132	1.26	0.08	<0.05	10	316	0.15	0.01	3
Median of blanks	<0.05	3	<0.5	<0.05	17	0.19	<0.05	<0.05	<5	81	<0.05	<0.01	1
Minimum of data	<0.05	1	<0.5	<0.05	<5	0.1	<0.05	<0.05	<5	1163	<0.05	<0.01	<1
Mean of data	0.05	1869	4.4	<0.05	105	15.39	0.35	<0.05	50	89599	1.67	3.03	31
Median of data	<0.05	20	2.3	<0.05	66	12.72	<0.05	<0.05	15	47598	<0.05	0.01	8
Element	Co_ppb	Cr_ppb	Cs_ppb	Cu_ppb	Dy_ppb	Er_ppb	Eu_ppb	Fe_ppb	Ga_ppb	Gd_ppb	Ge_ppb	Hf_ppb	Hg_ppb
3xDL	0.06	1.5	0.03	0.3	0.03	0.03	0.03	30	0.15	0.03	0.15	0.06	0.3
Samples >3xDL	0	0	0	11	0	0	0	1	0	0	0	0	0
% outside	0	0	0	58	0	0	0	5	0	0	0	0	0
Samples >10xDL	0	0	0	5	0	0	0	0	0	0	0	0	0
Data below 3xDL	x	x	x		x	x	x		x	x	x	x	x
Data below 10xDL	x	x	x		x	x	x	x	x	x	x	x	x
Data above 3xDL				x				x					
Data above 10xDL				x									
Max. of blanks	0.03	0.9	0.02	2.1	<0.01	<0.01	<0.01	51	<0.05	<0.01	<0.05	<0.02	0.3
Median of blanks	<0.02	<0.5	<0.01	1	<0.01	<0.01	<0.01	<10	<0.05	<0.01	<0.05	<0.02	<0.1
Minimum of data	<0.02	<0.5	<0.01	<0.1	<0.01	<0.01	<0.01	<10	<0.05	<0.01	<0.05	<0.02	<0.1
Mean of data	22.77	0.9	1.18	6981	0.83	0.36	0.24	2654	0.06	0.95	0.05	<0.02	0.1
Median of data	0.08	<0.5	0.6	2.4	<0.01	<0.01	<0.01	<10	<0.05	<0.01	<0.05	<0.02	<0.1
Element	Ho_ppb	In_ppb	Ir_ppb	K_ppb	La_ppb	Li_ppb	Lu_ppb	Mg_ppb	Mn_ppb	Mo_ppb	Na_ppb	Nb_ppb	Nd_ppb
3xDL	0.03	0.03	0.15	150	0.03	0.3	0.03	150	0.15	0.3	150	0.03	0.03
Samples >3xDL	0	0	0	0	0	11	0	0	10	1	1	0	0
% outside	0	0	0	0	0	58	0	0	53	5	5	0	0
Samples >10xDL	0	0	0	0	0	9	0	0	1	0	0	0	0
Data below 3xDL	x	x	x	x	x		x	x				x	x
Data below 10xDL	x	x	x	x	x		x	x		x	x	x	x
Data above 3xDL						x			x	x	x		
Data above 10xDL						x			x				
Max. of blanks	<0.01	<0.01	<0.05	53	0.01	4.9	<0.01	<50	0.75	0.7	416	0.02	0.01
Median of blanks	<0.01	<0.01	<0.05	<50	<0.01	0.4	<0.01	<50	0.19	<0.1	83	<0.01	<0.01
Minimum of data	<0.01	<0.01	<0.05	<50	<0.01	<0.1	<0.01	100	<0.05	<0.1	492	<0.01	<0.01
Mean of data	0.15	0.01	<0.05	3679	1.1	8.8	0.04	13102	1310	81.6	30293	0.01	2.68
Median of data	<0.01	<0.01	<0.05	851	<0.01	2.7	<0.01	7967	9	1.7	11158	<0.01	0.01
Element	Ni_ppb	Os_ppb	P_ppb	Pb_ppb	Pd_ppb	Pr_ppb	Pt_ppb	Rb_ppb	Re_ppb	Rh_ppb	Ru_ppb	S_ppm	Sb_ppb
3xDL	0.6	0.15	60	0.3	0.6	0.03	0.03	0.03	0.03	0.03	0.15	3	0.15
Samples >3xDL	0	0	1	1	0	0	0	0	0	0	0	0	1
% outside	0	0	5	5	0	0	0	0	0	0	0	0	5
Samples >10xDL	0	0	0	0	0	0	0	0	0	0	0	0	1
Data below 3xDL	x	x			x	x	x	x	x	x	x	x	
Data below 10xDL	x	x	x	x	x	x	x	x	x	x	x	x	
Data above 3xDL			x	x									x
Data above 10xDL													x
Max. of blanks	0.2	<0.05	66	0.6	<0.2	<0.01	<0.01	0.03	<0.01	<0.01	<0.05	2	0.61
Median of blanks	0.2	<0.05	30	<0.1	<0.2	<0.01	<0.01	0.01	<0.01	<0.01	<0.05	1	<0.05
Minimum of data	<0.2	<0.05	<20	<0.1	<0.2	<0.01	<0.01	0.04	<0.01	<0.01	<0.05	<1	<0.05
Mean of data	12.5	<0.05	64	0.2	<0.2	0.51	<0.01	4.28	0.33	0.01	<0.05	91	0.28
Median of data	<0.2	<0.05	35	<0.1	<0.2	<0.01	<0.01	1.17	0.02	<0.01	<0.05	34	0.12
Element	Sc_ppb	Se_ppb	Si_ppb	Sm_ppb	Sn_ppb	Sr_ppb	Ta_ppb	Tb_ppb	Te_ppb	Th_ppb	Ti_ppb	Tl_ppb	Tm_ppb
3xDL	3	1.5	120	0.06	0.15	0.03	0.06	0.03	0.15	0.15	30	0.03	0.03
Samples >3xDL	0	0	7	0	0	19	0	0	0	0	0	0	0
% outside	0	0	37	0	0	100	0	0	0	0	0	0	0
Samples >10xDL	0	0	2	0	0	13	0	0	0	0	0	0	0
Data below 3xDL	x	x		x	x		x	x	x	x	x	x	x
Data below 10xDL	x	x		x	x		x	x	x	x	x	x	x
Data above 3xDL			x			x							
Data above 10xDL			x			x							
Max. of blanks	<1	<0.5	512	<0.02	0.06	0.99	<0.02	<0.01	0.06	0.08	<10	<0.01	<0.01
Median of blanks	<1	<0.5	115	<0.02	<0.05	0.2	<0.02	<0.01	<0.05	<0.05	<10	<0.01	<0.01
Minimum of data	<1	<0.5	708	<0.02	<0.05	3.75	<0.02	<0.01	<0.05	<0.05	<10	<0.01	<0.01
Mean of data	3	0.9	7774	0.74	0.05	440	<0.02	0.15	<0.05	0.46	<10	0.01	0.05
Median of data	1	<0.5	6277	<0.02	<0.05	221	<0.02	<0.01	<0.05	<0.05	<10	<0.01	<0.01
Element	U_ppb	V_ppb	W_ppb	Y_ppb	Yb_ppb	Zn_ppb	Zr_ppb	NO3_ppm	ALK_mg/L	DOC_ppm	F_ppb	EC_µs/cm	TDS_ppm
3xDL	0.06	0.6	0.06	0.03	0.03	1.5	0.06	0.15	3	3	60	9	6
Samples >3xDL	0	1	0	0	0	16	0	0	0	0	0	0	0
% outside	0	5	0	0	0	84	0	0	0	0	0	0	0
Samples >10xDL	0	0	0	0	0	12	0	0	0	0	0	0	0
Data below 3xDL	x		x	x	x		x	x	x	x	x	x	x
Data below 10xDL	x	x	x	x	x		x	x	x	x	x	x	x
Data above 3xDL		x				x							
Data above 10xDL						x							
Max. of blanks	<0.02	0.7	0.03	0.01	<0.01	23.6	<0.02	0.08	3	2.4	20	3	2
Median of blanks	<0.02	<0.2	<0.02	<0.01	<0.01	5.7	<0.02	<0.05	2	<1	20	2	<1
Minimum of data	<0.02	<0.2	<0.02	<0.01	<0.01	<0.5	<0.02	<0.05	<1	<1	50	500	337
Mean of data	2.42	3	0.36	4.42	0.27	400.3	0.03	4	77	1	295	1264	898
Median of data	0.2	1.1	0.02	0.02	<0.01	3.7	<0.02	0.37	63	<1	100	1097	774

Table B-7: Cross-contamination assessment for simple blank (B1) of deionised water

Element	Ag_ppb	Al_ppb	As_ppb	Au_ppb	B_ppb	Ba_ppb	Be_ppb	Bi_ppb	Br_ppb	Ca_ppb	Cd_ppb	Ce_ppb	Cl_ppm
3xDL	0.15	3	1.5	0.15	15	0.15	0.15	0.15	15	150	0.15	0.03	3
Samples >3xDL	0	27	0	0	0	27	0	0	0	27	0	21	0
% outside	0	87	0	0	0	87	0	0	0	87	0	68	0
Samples >10xDL	0	27	0	0	0	27	0	0	0	20	0	20	0
Data below 3xDL	x		x	x	x		x	x	x		x		x
Data below 10xDL	x		x	x	x		x	x	x		x		x
Data above 3xDL		x				x				x		x	
Data above 10xDL		x				x				x		x	
Max. of blanks	<0.05	71	<0.5	0.06	6	2.94	<0.05	<0.05	15	907	<0.05	0.19	2
Median of blanks	<0.05	49	<0.5	<0.05	<5	2	<0.05	<0.05	<5	572	<0.05	0.12	1
Minimum of data	<0.05	<1	<0.5	<0.05	<5	<0.05	<0.05	<0.05	<5	<50	<0.05	<0.01	<1
Mean of data	0.05	715	7	<0.05	134	19	0.115	<0.05	95	109856	0.5	1.26	39
Median of data	<0.05	10	2.5	<0.05	82	15	<0.05	<0.05	25	57302	<0.05	0.01	12
Element	Co_ppb	Cr_ppb	Cs_ppb	Cu_ppb	Dy_ppb	Er_ppb	Eu_ppb	Fe_ppb	Ga_ppb	Gd_ppb	Ge_ppb	Hf_ppb	Hg_ppb
3xDL	0.06	1.5	0.03	0.3	0.03	0.03	0.03	30	0.15	0.03	0.15	0.06	0.3
Samples >3xDL	0	0	0	20	0	0	0	0	0	0	0	0	2
% outside	0	0	0	65	0	0	0	0	0	0	0	0	6
Samples >10xDL	0	0	0	1	0	0	0	0	0	0	0	0	1
Data below 3xDL	x	x	x		x	x	x	x	x	x	x	x	
Data below 10xDL	x	x	x		x	x	x	x	x	x	x	x	
Data above 3xDL				x									x
Data above 10xDL				x									x
Max. of blanks	<0.02	0.8	0.01	1.3	<0.01	<0.01	<0.01	<10	<0.05	0.01	<0.05	<0.02	1.4
Median of blanks	<0.02	<0.5	<0.01	0.5	<0.01	<0.01	<0.01	<10	<0.05	<0.01	<0.05	<0.02	0.1
Minimum of data	<0.02	<0.5	<0.01	<0.1	<0.01	<0.01	<0.01	<10	<0.05	<0.01	<0.05	<0.02	<0.1
Mean of data	7.7	0.7	0.5	1767	0.29	0.14	0.1	691	0.1	0.37	0.05	<0.02	0.6
Median of data	0.08	<0.5	0.05	2.4	<0.01	<0.01	<0.01	15	<0.05	<0.01	<0.05	<0.02	0.3
Element	Ho_ppb	In_ppb	Ir_ppb	K_ppb	La_ppb	Li_ppb	Lu_ppb	Mg_ppb	Mn_ppb	Mo_ppb	Na_ppb	Nb_ppb	Nd_ppb
3xDL	0.03	0.03	0.15	150	0.03	0.3	0.03	150	0.15	0.3	150	0.03	0.03
Samples >3xDL	0	0	0	0	2	0	0	1	22	0	27	0	0
% outside	0	0	0	0	6	0	0	3	71	0	87	0	0
Samples >10xDL	0	0	0	0	0	0	0	0	0	0	26	0	0
Data below 3xDL	x	x	x	x		x	x			x		x	x
Data below 10xDL	x	x	x	x	x	x	x	x	x	x		x	x
Data above 3xDL					x			x	x		x		
Data above 10xDL											x		
Max. of blanks	<0.01	<0.01	<0.05	83	0.04	0.3	<0.01	158	0.42	0.3	1178	0.03	0.03
Median of blanks	<0.01	<0.01	<0.05	<50	0.03	0.2	<0.01	109	0.23	<0.1	880	0.01	0.02
Minimum of data	<0.01	<0.01	<0.05	<50	<0.01	<0.1	<0.01	<50	0.08	<0.1	<50	<0.01	<0.01
Mean of data	0.06	0.01	<0.05	7523	0.43	8.8	0.02	18626	733	144	45642	0.01	0.99
Median of data	<0.01	<0.01	<0.05	1025	0.01	2.6	<0.01	9603	14	1.8	16171	0.01	0.01
Element	Ni_ppb	Os_ppb	P_ppb	Pb_ppb	Pd_ppb	Pr_ppb	Pt_ppb	Rb_ppb	Re_ppb	Rh_ppb	Ru_ppb	S_ppm	Sb_ppb
3xDL	0.6	0.15	60	0.3	0.6	0.03	0.03	0.03	0.03	0.03	0.15	3	0.15
Samples >3xDL	0	0	0	3	0	0	0	27	0	0	0	0	0
% outside	0	0	0	10	0	0	0	87	0	0	0	0	0
Samples >10xDL	0	0	0	0	0	0	0	27	0	0	0	0	0
Data below 3xDL	x	x	x		x	x	x		x	x	x	x	x
Data below 10xDL	x	x	x	x	x	x	x		x	x	x	x	x
Data above 3xDL				x				x					
Data above 10xDL								x					
Max. of blanks	0.2	<0.05	43	1	<0.2	0.01	<0.01	0.26	<0.01	<0.01	<0.05	1	0.09
Median of blanks	<0.2	<0.05	25	0.1	<0.2	0.01	<0.01	0.19	<0.01	<0.01	<0.05	<1	<0.05
Minimum of data	<0.2	<0.05	<20	<0.1	<0.2	<0.01	<0.01	<0.01	<0.01	<0.01	<0.05	<1	<0.05
Mean of data	4.4	<0.05	95	0.4	0.2	0.19	0.01	5.7	0.5	0.02	<0.05	120	0.4
Median of data	<0.2	<0.05	39	<0.1	<0.2	<0.01	<0.01	1.26	0.03	<0.01	<0.05	41	0.13
Element	Sc_ppb	Se_ppb	Si_ppb	Sm_ppb	Sn_ppb	Sr_ppb	Ta_ppb	Tb_ppb	Te_ppb	Th_ppb	Ti_ppb	Tl_ppb	Tm_ppb
3xDL	3	1.5	120	0.06	0.15	0.03	0.06	0.03	0.15	0.15	30	0.03	0.03
Samples >3xDL	0	0	27	0	18	31	0	0	0	0	0	0	0
% outside	0	0	87	0	58	100	0	0	0	0	0	0	0
Samples >10xDL	0	0	27	0	8	28	0	0	0	0	0	0	0
Data below 3xDL	x	x		x			x	x	x	x	x	x	x
Data below 10xDL	x	x		x			x	x	x	x	x	x	x
Data above 3xDL			x		x	x							
Data above 10xDL			x		x	x							
Max. of blanks	1	<0.5	3713	<0.02	1.74	0.96	<0.02	<0.01	<0.05	<0.05	<10	<0.01	<0.01
Median of blanks	1	<0.5	2765	<0.02	0.17	0.71	<0.02	<0.01	<0.05	<0.05	<10	<0.01	<0.01
Minimum of data	<1	<0.5	<40	<0.02	<0.05	0.24	<0.02	<0.01	<0.05	<0.05	<10	<0.01	<0.01
Mean of data	3	1.5	9450	0.28	0.05	485	<0.02	0.06	<0.05	0.16	<10	0.05	0.03
Median of data	2	0.5	7922	<0.02	<0.05	257	<0.02	<0.01	<0.05	<0.05	<10	<0.01	<0.01
Element	U_ppb	V_ppb	W_ppb	Y_ppb	Yb_ppb	Zn_ppb	Zr_ppb	NO3_ppm	ALK_mg/L	DOC_ppm	F_ppb	EC_µs/cm	TDS_ppm
3xDL	0.06	0.6	0.06	0.03	0.03	1.5	0.06	0.15	3	3	60	9	6
Samples >3xDL	0	0	0	0	0	4	22	3	24	0	1	1	1
% outside	0	0	0	0	0	13	71	10	77	0	3	3	3
Samples >10xDL	0	0	0	0	0	4	17	0	0	0	0	0	0
Data below 3xDL	x	x	x	x	x					x			
Data below 10xDL	x	x	x	x	x			x	x	x	x	x	x
Data above 3xDL						x	x	x	x		x	x	x
Data above 10xDL						x	x						
Max. of blanks	<0.02	0.4	0.05	0.02	<0.01	25	0.46	0.33	9	1	67	11	7
Median of blanks	<0.02	<0.2	<0.02	0.01	<0.01	<0.5	0.23	<0.05	6	<1	28	6	4
Minimum of data	<0.02	<0.2	<0.02	<0.01	<0.01	<0.5	<0.02	<0.05	<1	<1	<20	7	5
Mean of data	1.19	3.7	0.6	1.54	0.1	222	0.02	6.04	89	1	162	854	588
Median of data	0.27	1.2	0.02	0.02	<0.01	6.2	<0.02	0.62	75	1	104	508	342

Table B-8: Cross-contamination assessment for process blank (B2) of deionised water

Element	Ag_ppb	Al_ppb	As_ppb	Au_ppb	B_ppb	Ba_ppb	Be_ppb	Bi_ppb	Br_ppb	Ca_ppb	Cd_ppb	Ce_ppb	Cl_ppm
3xDL	0.15	3	1.5	0.15	15	0.15	0.15	0.15	15	150	0.15	0.03	3
Samples >3xDL	0	25	0	0	0	26	0	0	1	26	0	24	1
% outside	0	83	0	0	0	87	0	0	3	87	0	80	3
Samples >10xDL	0	25	0	0	0	25	0	0	0	25	0	8	0
Data below 3xDL	x		x	x	x		x	x			x		
Data below 10xDL	x		x	x	x		x	x	x		x		x
Data above 3xDL		x				x			x	x		x	x
Data above 10xDL		x				x				x		x	
Max. of blanks	<0.05	76	<0.5	0.08	5	2.57	<0.05	<0.05	17	917	<0.05	0.15	4
Median of blanks	<0.05	54	<0.5	<0.05	<5	1.91	<0.05	<0.05	<5	683	<0.05	0.1	1
Minimum of data	<0.05	<1	<0.5	<0.05	<5	<0.05	<0.05	<0.05	<5	<50	<0.05	<0.01	<1
Mean of data	0.05	715	7	<0.05	134	19	0.115	<0.05	95	109856	0.5	1.26	39
Median of data	<0.05	10	2.5	<0.05	82	15	<0.05	<0.05	25	57302	<0.05	0.01	12
Element	Co_ppb	Cr_ppb	Cs_ppb	Cu_ppb	Dy_ppb	Er_ppb	Eu_ppb	Fe_ppb	Ga_ppb	Gd_ppb	Ge_ppb	Hf_ppb	Hg_ppb
3xDL	0.06	1.5	0.03	0.3	0.03	0.03	0.03	30	0.15	0.03	0.15	0.06	0.3
Samples >3xDL	0	1	1	26	0	0	0	1	0	0	0	0	3
% outside	0	3	3	87	0	0	0	3	0	0	0	0	10
Samples >10xDL	0	0	0	10	0	0	0	0	0	0	0	0	1
Data below 3xDL	x				x	x	x		x	x	x	x	
Data below 10xDL	x	x	x		x	x	x	x	x	x	x	x	
Data above 3xDL		x	x	x				x					x
Data above 10xDL				x									x
Max. of blanks	0.03	3	0.04	3.5	0.01	<0.01	<0.01	51	<0.05	0.01	<0.05	<0.02	1.1
Median of blanks	0.01	<0.5	0.01	0.7	<0.01	<0.01	<0.01	<10	<0.05	<0.01	<0.05	<0.02	0.1
Minimum of data	<0.02	<0.5	<0.01	<0.1	<0.01	<0.01	<0.01	<10	<0.05	<0.01	<0.05	<0.02	<0.1
Mean of data	7.7	0.7	0.5	1767	0.29	0.14	0.1	691	0.1	0.37	0.05	<0.02	0.6
Median of data	0.08	<0.5	0.05	2.4	<0.01	<0.01	<0.01	15	<0.05	<0.01	<0.05	<0.02	0.3
Element	Ho_ppb	In_ppb	Ir_ppb	K_ppb	La_ppb	Li_ppb	Lu_ppb	Mg_ppb	Mn_ppb	Mo_ppb	Na_ppb	Nb_ppb	Nd_ppb
3xDL	0.03	0.03	0.15	150	0.03	0.3	0.03	150	0.15	0.3	150	0.03	0.03
Samples >3xDL	0	0	0	0	0	1	0	2	22	0	25	0	0
% outside	0	0	0	0	0	3	0	7	73	0	83	0	0
Samples >10xDL	0	0	0	0	0	0	0	0	1	0	25	0	0
Data below 3xDL	x	x	x	x	x		x			x		x	x
Data below 10xDL	x	x	x	x	x	x	x	x		x		x	x
Data above 3xDL						x		x	x		x		
Data above 10xDL									x		x		
Max. of blanks	<0.01	<0.01	<0.05	80	0.03	0.5	<0.01	156	3.06	0.3	1259	0.03	0.03
Median of blanks	<0.01	<0.01	<0.05	52.5	0.02	0.2	<0.01	118	0.2	<0.1	971	0.01	0.02
Minimum of data	<0.01	<0.01	<0.05	<50	<0.01	<0.1	<0.01	<50	0.08	<0.1	<50	<0.01	<0.01
Mean of data	0.06	0.01	<0.05	7523	0.43	8.8	0.02	18626	733	144	45642	0.01	0.99
Median of data	<0.01	<0.01	<0.05	1025	0.01	2.6	<0.01	9603	14	1.8	16171	0.01	0.01
Element	Ni_ppb	Os_ppb	P_ppb	Pb_ppb	Pd_ppb	Pr_ppb	Pt_ppb	Rb_ppb	Re_ppb	Rh_ppb	Ru_ppb	S_ppm	Sb_ppb
3xDL	0.6	0.15	60	0.3	0.6	0.03	0.03	0.03	0.03	0.03	0.15	3	0.15
Samples >3xDL	0	0	0	2	0	0	0	26	0	0	0	0	0
% outside	0	0	0	7	0	0	0	87	0	0	0	0	0
Samples >10xDL	0	0	0	0	0	0	0	25	0	0	0	0	0
Data below 3xDL	x	x	x		x	x	x		x	x	x	x	x
Data below 10xDL	x	x	x	x	x	x	x		x	x	x	x	x
Data above 3xDL				x				x					
Data above 10xDL								x					
Max. of blanks	0.4	<0.05	37	0.5	<0.2	0.01	<0.01	0.28	<0.01	<0.01	<0.05	1	0.14
Median of blanks	<0.2	<0.05	25	0.1	<0.2	<0.01	<0.01	0.20	<0.01	<0.01	<0.05	<1	<0.05
Minimum of data	<0.2	<0.05	<20	<0.1	<0.2	<0.01	<0.01	<0.01	<0.01	<0.01	<0.05	<1	<0.05
Mean of data	4.4	<0.05	95	0.4	0.2	0.19	0.01	5.7	0.5	0.02	<0.05	120	0.4
Median of data	<0.2	<0.05	39	<0.1	<0.2	<0.01	<0.01	1.26	0.03	<0.01	<0.05	41	0.13
Element	Sc_ppb	Se_ppb	Si_ppb	Sm_ppb	Sn_ppb	Sr_ppb	Ta_ppb	Tb_ppb	Te_ppb	Th_ppb	Ti_ppb	Tl_ppb	Tm_ppb
3xDL	3	1.5	120	0.06	0.15	0.03	0.06	0.03	0.15	0.15	30	0.03	0.03
Samples >3xDL	0	0	26	0	18	30	0	0	0	0	0	0	0
% outside	0	0	87	0	60	100	0	0	0	0	0	0	0
Samples >10xDL	0	0	25	0	8	28	0	0	0	0	0	0	0
Data below 3xDL	x	x		x			x	x	x	x	x	x	x
Data below 10xDL	x	x		x			x	x	x	x	x	x	x
Data above 3xDL			x		x	x							
Data above 10xDL			x		x	x							
Max. of blanks	1	<0.5	3769	<0.02	1.2	1.8	<0.02	<0.01	<0.05	0.06	<10	<0.01	<0.01
Median of blanks	1	<0.5	2892	<0.02	0.26	0.87	<0.02	<0.01	<0.05	<0.05	<10	<0.01	<0.01
Minimum of data	<1	<0.5	<40	<0.02	<0.05	0.24	<0.02	<0.01	<0.05	<0.05	<10	<0.01	<0.01
Mean of data	3	1.5	9450	0.28	0.05	485	<0.02	0.06	<0.05	0.16	<10	0.05	0.03
Median of data	2	0.5	7922	<0.02	<0.05	257	<0.02	<0.01	<0.05	<0.05	<10	<0.01	<0.01
Element	U_ppb	V_ppb	W_ppb	Y_ppb	Yb_ppb	Zn_ppb	Zr_ppb	NO3_ppm	ALK_mg/L	DOC_ppm	F_ppb	EC_µs/cm	TDS_ppm
3xDL	0.06	0.6	0.06	0.03	0.03	1.5	0.06	0.15	3	3	60	9	6
Samples >3xDL	0	1	0	0	0	6	24	3	24	0	1	0	0
% outside	0	3	0	0	0	20	80	10	80	0	3	0	0
Samples >10xDL	0	0	0	0	0	5	11	0	0	0	0	0	0
Data below 3xDL	x		x	x	x					x		x	x
Data below 10xDL	x	x	x	x	x			x	x	x	x	x	x
Data above 3xDL		x				x	x	x	x		x		
Data above 10xDL						x	x						
Max. of blanks	<0.02	0.7	0.05	0.01	0.01	21.2	0.36	0.33	9	2	119	9	6
Median of blanks	<0.02	<0.2	<0.02	0.01	<0.01	0.6	0.18	<0.05	6	1	28	6	4
Minimum of data	<0.02	<0.2	<0.02	<0.01	<0.01	<0.5	<0.02	<0.05	<1	<1	<20	7	5
Mean of data	1.19	3.7	0.6	1.54	0.1	222	0.02	6.04	89	1	162	854	588
Median of data	0.27	1.2	0.02	0.02	<0.01	6.2	<0.02	0.62	75	1	104	508	342

APPENDIX C: Anomalously high geochemistry

Chemical	Background Range /Mean	Thld	WGV	Anomalous Location	No. of Anomalous Samples	Sample Value	Anomalously High Chemicals Associated by Source							Comment
							Natural			Anthropogenic			Unknown	
							Hydrothermal Alteration	Mineralisation	Geology	Agriculture /Sewage	Settlements	Mining		
Al (mg/l)	0.001-0.2 /0.03	0.2	0.2	Yerba Loca	3	**6**		As (13.5), Cu (11693), Fe (45), Ni (26.4), P (694), SO4 (446), Zn (123.6), pH (1.99), TDS (1070)						Be (0.87), Cr (2.6), Mn (641.94)
						2.4		Cu (3275), Ni (17.5), Zn (173.1), pH (5.69)						Mn (654)
						1.4		Cu (4185), Ni (17.9), Zn (175), pH (5.1)						Mn (781)
				Ortiga	3	**0.3**	F (480), pH (4.84)							
						4.4	F (838), Fe (4.6), Ni (21.1), Zn (40.2), pH (3.19)							Tl (0.15)
						6.1	F (380), Fe (5.1), Hg (3.1), Ni (32.5), Zn (83.3), pH (3.41)							Be (0.46), Mn (415.46), Tl (0.16)
				Arrayán	1	**4.6**	F (504), Fe (0.8), Ni (27.5), SO4 (357), Zn (31.1), pH (4.65)							Mn (406.33), Tl (0.48)
				El Manzanito	1	**0.7**					Fe (0.7), P (185)			detergent (foams at sampling site)
				Barriga	1	**8.2**		Ca (215), Cd (0.89), Cu, (119.8), F (650), Fe (1), Hg (1.3), Mg (25.8), Ni (59.1), SO4 (968), Zn (264.7), EC (1136), pH (5.44), TDS (905)						Be (0.74), Mn (1920.08), Se (5.1)

				Torin	5	**12.3**		Cd (1.31), Cu (457.3), Fe (8.5), Ni (19.1), Pb (1.4), SO4 (368), Zn (218.8), pH (2.84)					Be (0.56), Mn (688.26)
As (µg/l)	<0.5-10 /3.2	10	10	Riecillos	2	**65.9**	Mo (8.1)						Se (1.7)
						11.3	None						
				Rocín	1	**24.5**			None				
				Aconcagua	1	**23.8**						None	
				Colina	1	**14.8**					Pb (4)		B (350)
				Yerba Loca	1	**13.5**		Al (6), Cu (11693), Fe (45), Ni (26.4), P (694), SO4 (446), Zn (123.6), pH (1.99), TDS (1070)					Be (0.87), Cr (2.6), Mn (641.94)
				Maipo, Maipo Vn.	1	**16.6**	Fe (3), Mg (38), Ni (40.3)		Ca (377), Cl (116), F (1010), K (7.6), Na (62), SO4 (1360), EC (1307), TDS (1352)				B (823), Se (2.1), Mn (1658.84), Tl (0.14)
				Arrayán	1	**46.5**			NO3 (4.18)				
				Colorado	1	**16.6**			Cl (270), Na (161), EC (1099), pH (8.52), TDS (932)			None	Tl (0.07)
				Lampa	1	**13.6**				Ca (143), Cl (177), Fe (0.2), K (25), Mg (24), Mo (8.6), Na (145), NO3 (27.27), P (993), SO4 (491), HCO3- (200), EC (1505), TDS (1088)	None		B (339), Mn (265.66)
Ca (mg/l)	8-98 /43	98	N/A	Juncal	2	128			SO4 (327)				

		130			SO4 (398)			
Barriga	1	215		Al (8), Cd (0.89), Cu, (119.8), F (650), Fe (1), Hg (1.3), Mg (26), Ni (59.1), SO4 (968), Zn (264.7), EC (1136), pH (5.44), TDS (905)				Be (0.74), Mn (1920.08), Se (5.1),
El Soldado	1	127				HCO3- (172), K (5.7), Na (50), NO3 (24.07), P (732), EC (1085)	Fe (0.2), Mg (34), Mo (11.6), SO4 (324)	
Parraguirre	1	157			SO4 (419)			
Rabicano	1	163	Zn (71.1)		P (87), SO4 (354), Sn (0.12)			Se (4.5)
Colorado	3	216			Mg (29), SO4 (638), TDS (912)			Se (1.4), Tl (0.06)
		129			Na (57), SO4 (315)			
		123			SO4 (333)			
Yeso	4	156			Pb (1), SO4 (470)			
		171			SO4 (539)			
		243			SO4 (683), TDS (846)			
		307			Mg (23), SO4 (869), TDS (1058)			
El Volcán	5	140			Cl (86), Na (59), SO4 (333)			
		131			Cl (89), Na (600)			
		146			Na (54), SO4 (386)			

		213		SO4 (590)		
		294	Mg (29), Ni (16.1), SO4 (953)	F (480), EC (1374), TDS (1076)		Mn (796)
Maipo, Maipo Vn.	6	229		Cl (165), F (438), K (11), Na (95), SO4 (617), EC (1165), TDS (1132)		B (508), Se (1.6), Mn (387.26), Tl (0.23)
		305		SO4 (836), EC (1000), TDS (980)		
		366		Cl (84), K (5.4), Na (56), SO4 (929), EC (1340), TDS (1268)		Se (1.4), Tl (0.07)
		196		Cl (426), F (360), K (6), Na (240), SO4 (611), EC (1551), TDS (1524)		B (548), Se (2), Mn (276.28)
		377	As (16.6), Fe (3), Mg (38), Ni (40.3)	Cl (116), F (1010), K (7.6), Na (62), SO4 (1360), EC (1307), TDS (1352)		B (823), Mn (1658.84), Se (2.1), Tl (0.14)
		163		Cl (311), K (4.8), Na (186), SO4 (485), EC (1313), TDS (1168)		B (391), Se (1.7)
Clarillo	1	146		Cl (107), Na (719), SO4 (404)	K (5.3), P (95), NO3 (9.57), HCO3- (147.6)	

				Maipo	5	120		Cl (83), Na (59), SO4 (339)			
						122		Cl (99), Na (66), SO4 (377)		Pb (3.5)	
						124		Cl (103), Na (63), SO4 (383)			
						152		Cl (128), Na (79), SO4 (401), EC (1111), TDS (854)	K (5.5), NO3 (5.16), P (98)		
						173		Cl (194), K (4.4), Na (127), SO4 (467), EC (1173), TDS (1002)		Hg (2.1)	
				Lampa	1	143		Cl (177), Na (145), EC (1505), TDS (1088)	Fe (0.2), K (25), Mg (24), Mo (8.6), NO3 (27.27), P (993), SO4 (491), HCO3- (200)	As (13.6)	B (339), Mn (265.66)
				Mapocho	2	164		Cl (144), Na (85), EC (1209), TDS (932)	K (8.3), Mg (24), P (1613), SO4 (374), NO3 (34.31), HCO3- (191)	Hg (1.6)	Se (1.4)
						141		Cl (209), Na (146), EC (1577), TDS (1180)	K (17), F (390), Mo (8.6), NO3 (5.24), P (9021), SO4 (383), Zn (37.9), HCO3- (220)	Sn (0.4)	Cr (2), Se (1.6)
Cd (µg/l)	<0.05-0.63 /0.07	0.6	10	Los Bronces	2	0.89					Cl (82), Na (51), Zn (91.3)

				Dolores		0.79		Cu (257.7), Fe (0.7), Ni (6.5), Zn (344.8), pH (6.3)			Mn (992)
				Barriga	1	0.89		Al (8), Ca (215), Cu, (119.8), F (650), Fe (1), Hg (1.3), Mg (26), Ni (59.1), SO4 (968), Zn (264.7), EC (1136), pH (5.44), TDS (905)			Be (0.74), Mn (1920.08), Se (5.1)
				Colorado (Aconcagua)	5	1.31		Al (12), Cu (457.3), Fe (8.5), Ni (19.1), Pb (1.4), SO4 (368), Zn (218.8), pH (2.84)			Be (0.56), Mn (688.26)
						1.37	Hg (3.4), Ni (11)				Mn (510.83), Tl (0.12)
						0.83	Ni (5.6)				Mn (886)
						3.31	Fe (5.6), Ni (14.5), Zn (174.9), pH (5.86)				Tl (0.26)
						0.89	Ni (7.3)				Mn (456.1), Tl (0.09)
Cl (mg/l)	<1-81 /11.81	81	400	Los Bronces	1	82				Cd (0.89), Na (51), Zn (91.3)	
				Colorado	1	270				As (16.6), Na (161), EC (1099), pH (8.52), TDS (932)	Tl (0.07)
				Olivares	2	385		K (7.6), Na (214), HCO3- (161), EC (1166), TDS (1096)			B (1473)
						147		K (3.9), Na (84), pH (8.71)			B (572)

Maipo, Maipo Vn.	5	165		Ca (229), F (438), K (11), Na (95), SO4 (617), EC (1165), TDS (1132)		B (508), Se (1.6), Mn (387.26), Tl (0.23)
		84		Ca (366), K (5.4), Na (56), SO4 (929), EC (1340), TDS (1268)		Se (1.4), Tl (0.07)
		116	As (16.6), Fe (3), Mg (38), Ni (40.3)	Ca (377), F (1010), K (7.6), Na (62), SO4 (1360), EC (1307), TDS (1352)		B (823), Mn (1658.84), Se (2.1), Tl (0.14)
		311		Ca (163), K (4.8), Na (186), SO4 (485), EC (1313), TDS (1168)		B (391), Se (1.7)
		426		Ca (196), F (360), K (6.1), Na (240), SO4 (611), EC (1551), TDS (1524)		B (548), Se (2), Mn (276.28)
El Volcán	2	86		Ca (140), Na (59), SO4 (333)		
		89		Ca (131), Na (60)		
Clarillo	1	107		Ca (146), Na (72), SO4 (404)	K (5.3), P (95), NO3 (9.57), HCO3-	

				Maipo	5	83		Ca (120), Na (59), SO4 (339)				
						99		Ca (122), Na (66), SO4 (377)		Pb (3.5)		
						103		Ca (124), Na (63), SO4 (383)				
						128		Ca (152), Na (79), SO4 (401), EC (1111), TDS (854)	K (5.5), NO3 (5.16), P (98)			
						194		Ca (173), K (4.4), Na (127), SO4 (467), EC (1173), TDS (1002)		Hg (2.1)		
				Lampa	1	177		Ca (143), Na (145), EC (1505), TDS (1088)	Fe (0.2), K (25), Mg (24), Mo (8.6), NO3 (27.27), P (993), SO4 (491), HCO3- (200)	As (13.6)		B (339), Mn (265.66)
				Mapocho	2	144		Ca (164), Na (85), EC (1209), TDS (932)	K (8.3), Mg (24), P (1613), SO4 (374), NO3 (34.31), HCO3- (191)	Hg (1.6)		Se (1.4)
						209		Ca (141), Na (146), EC (1577), TDS (1180)	K (17), F (390), Mo (8.6), NO3 (5.24), P (9021), SO4 (383), Zn (37.9), HCO3- (220)	Sn (0.4)		Cr (2), Se (1.6)
Cu (µg/l)	0.3-83 /6.2	83	2000	Aconcagua	1	103.9					Zn (42.3)	
				Dolores	1	257.7	Cd (0.79), Fe (0.7), Ni (6.5), Zn (344.8), pH (6.3)					Mn (992.29)

				Barriga	1	119.8		Al (8), Ca (215), Cd (0.89), F (650), Fe (1), Hg (1.3), Mg (26), Ni (59.1), SO4 (968), Zn (264.7), EC (1136), pH (5.44), TDS (905)	Be (0.74), Mn (1920.08), Se (5.1)
				Torin	1	457.3		Al (12), Cd (1.31), Fe (8.5), Ni (19.1), Pb (1.4), SO4 (368), Zn (218.8), pH (2.84)	Be (0.56), Mn (688.26)
				Yerba Loca	3	**11693**		Al (6), As (13.5), Fe (45), Ni (26.4), P (694), SO4 (446), Zn (123.6), pH (1.99), TDS (1070)	Be (0.87), Cr (2.6), Mn (641.94)
						3275.1		Al (0.2), Ni (17.5), Zn (173.1), pH (5.69)	Mn (654)
						4185		Al (1.4), Ni (17.9), Zn (175), pH (5.1)	Mn (781)
				San Francisco	1	802.6		Ni (12.2), Zn (130.7)	Mn (493)
F (µg/l)	22-335 /136	335	1500	Barriga	1	650		Al (8), Ca (215), Cd (0.89), Cu (119.8), Fe (1), Hg (1.3), Mg (26), Ni (59.1), SO4 (968), Zn (264.7), EC (1136), pH (5.44), TDS (905)	Be (0.74), Mn (1920.08), Se (5.1)
				Ortiga	3	380	Al (6), Fe (5.1), Hg (3.1), Ni (32.5), Zn (83.3), pH (3.41)		Be (0.46), Mn (415.46),
						480	Al (0.3), pH (4.84)		
						838	Al (4.4), Fe (4.6), Ni (21.1), Zn (40.2), pH (3.19)		Tl (0.15)

				Maipo, Maipo Vn.	3	360		Ca (196), Cl (426), K (6.1), Na (240), SO4 (611), EC (1551), TDS (1524)				B (548), Mn (276.28), Se (2)
						438		Ca (229), Cl (165), K (11), Na (95), SO4 (617), EC (1165), TDS (1132)				B (508), Mn (387.26), Se (1.6), Tl (0.23)
						1010	As (16.6), Fe (3), Mg (38), Ni (40.3)	Ca (377), Cl (116), K (7.6), Na (62), SO4 (1360), EC (1307), TDS (1352)				B (823), Mn (1658.84), Se (2.1), Tl (0.14)
				Mapocho	1	390		Ca (141), Cl (209), Na (146), EC (1577), TDS (1180)	K (17), Mo (8.6), NO3 (5.24), P (9021), SO4 (383), Zn (37.9), HCO3- (220)	Sn (0.4)		Cr (2), Se (1.6)
				El Volcán	1	480	Mg (29), Ni (16.1), SO4 (953)	Ca (294), EC (1374), TDS (1076)				Mn (796)
				Arrayán	1	504	Al (4.6), Fe (0.8), Ni (27.5), SO4 (357), Zn (31.1), pH (4.65)					Mn (406.33), Tl (0.48)
Fe (mg/l)	<0.01-0.1 /19	0.1	0.3	El Soldado	1	0.2			Ca (127), HCO3- (172), K (5.7), Na (50), NO3 (24.07), P (732), EC (1085)		Mg (34), Mo (11.6),SO4 (324)	sewage

Lampa	1	0.2				As (13.6), Ca (143), Cl (177), K (25), Mg (24), Mo (8.6), Na (145), NO3 (27.27), P (993), SO4 (491), HCO3- (200), EC (1505), TDS (1088)		B (339), Mn (264.66)
El Manzanito	1	**0.7**					Al (0.7), P (185)	detergent (foams at sampling site)
Dolores	1	**0.7**		Cd (0.79), Cu (257.7), Ni (6.5), Zn (344.8), pH (6.3)				Mn (992.29)
Arrayán	1	**0.8**	Al (4.6), F (504), Ni (27.5), SO4 (357), Zn (31.1), pH (4.65)					Mn (406.33), Tl (0.48)
Ortiga	2	**4.6**	Al (4.4), F (838), Ni (21.1), Zn (40.2), pH (3.19)					Tl (0.15)
		5.1	Al (6), F (380), Hg (3.1), Ni (32.5), Zn (83.3), pH (3.41)					Be (0.46), Mn (415.46),
Barriga	1	**1**		Al (8), Ca (215), Cd (0.89), Cu (119.8), F (650), Hg (1.3), Mg (26), Ni (59.1), SO4 (968), Zn (264.7), pH (5.44), EC (1136), TDS (905)				Be (0.74), Mn (1920.08), Se (5.1)
Maipo, Maipo Vn.	1	**3**	As (16.6), Mg (38), Ni (40.3)		Ca (377), Cl (116), F (1010), K (7.6), Na (62), SO4 (1360), EC (1307), TDS (1352)			B (823), Mn (1658.84), Se (2.1), Tl (0.14)

				Colorado (Aconcagua)	2	**5.6**	Cd (3.31), Ni (14.5), Zn (174.9), pH (5.86)					Tl (0.26)
						8.5		Al (12), Cd (1.31), Cu (457.3), Ni (19.1), Pb (1.4), SO4 (368), Zn (218.8), pH (2.84)				Be (0.56), Mn (688.26)
				Yerba Loca	1	**45**		Al (6), As (13.5), Cu (11693), Ni (26.4), P (694), SO4 (446), Zn (123.6), pH (1.99), TDS (1070)				Be (0.87), Cr (2.6), Mn (641.94)
HCO3- (mg/l)	0-145 /67	145	N/A	Olivares	1	161			Cl (385), K (7.6), Na (214), EC (1166), TDS (1096)			B (1473)
				Clarillo	1	148			Ca (146), Cl (107), Na (72), SO4 (404)	K (5.3), P (95), NO3 (9.57)		
				Angostura	1	148				None		
				Colina	1	154				NO3 (28.62)		
				Lampa	1	200			Ca (143), Cl (177), Na (145), EC (1505), TDS (1088)	As (13.6), Fe (0.2), K (25.2), Mg (24), Mo (8.6), NO3 (27.27), P (993), SO4 (491)		B (339), Mn (265.66)
				Mapocho	2	220			Ca (141), Cl (209), Na (146), EC (1577), TDS (1180)	K (17), F (390), Mo (8.6), NO3 (5.24), P (9021), SO4 (383), Zn	Sn (0.4)	Cr (2), Se (1.6)
						191			Ca (164), Cl (144), Na (85), EC (1209), SO4 (374), TDS (932)	K (8), Mg (24), NO3 (34.31), P (1613)	Hg (1.6)	Se (1.4)

				El Soldado	1	172			Ca (127), K (5.7), Na (50), NO3 (24.07), P (732), EC (1085)		Fe (0.2), Mg (345), Mo (11.6), SO4 (324)		
				Calera	3	152			Mg (24), NO3 (4.05), P (89)				
						158			Mg (36), NO3 (10.7), P (495)				
						161			Mg (23), NO3 (13.76), P (105)				
				Aconcagua	2	154			NO3 (11.63)				
						195			NO3 (14.58)				
				La Poza	1	178					Pb (1.1), Zn (87)		Tl (0.14)
				Catemu	1	174			Mg (20), NO3 (19.5), P (105)				
				Ocoa	1	199			Mg (24), NO3 (14.28), P (155)	Pb (0.9)			
				Los Angeles	1	196						None	
				La Ligua	1	154			NO3 (9.89), pH (8.96)				Se (13.4)
Hg (µg/l)	<0.1-0.7 /0.3	0.7	1	Barriga	1	**1.3**		Al (8), Ca (215), Cd (0.89), Cu (119.8), F (650), Fe (1), Mg (26), Ni (59.1), SO4 (968), Zn (264.7), EC (1136), pH (5.44), TDS (905)					Be (0.74), Mn (1920.08), Se (5.1)
				Molina	1	**1.4**						None	
				Ortiga	1	**3.1**	Al (6), F (380), Fe (5.1), Ni (32.5), Zn (83.3), pH (3.41)						Be (0.46), Mn (415.5), Tl (0.16)

				Mapocho	1	**1.6**			Ca (164), Cl (144), K (8.3), Mg (24), Na (85), P (1613), SO4 (374), NO3 (34.31), HCO3- (191), EC (1209), TDS (932)	None	Se (1.4)
				Maipo	1	**2.1**		Ca (173), Cl (194), K (4.4), Na (127), SO4 (467), EC (1173), TDS (1002)		None	
				Colorado (Aconcagua)	1	**3.4**	Cd (1.37), Ni (11)				Mn (510.83), Tl (0.12)
				Riecillos	1	**8.6**				P (80)	
K (mg/l)	0.1-3.7 /1.2	3.7	N/A	El Soldado	1	5.7			Ca (127), HCO3- (172), Na (50), NO3 (24.07), P (732), EC (1085)	Fe (0.2), Mg (34), Mo (11.6), SO4 (324)	sewage
				Olivares	2	7.6		Cl (385), Na (214), HCO3- (161), EC (1166), TDS (1096)			B (1473)
						3.9		Cl (147), Na (84), pH (8.71)			B (572)
				Maipo, Maipo Vn.	5	11.3		Ca (229), Cl (165), F (438), Na (95), SO4 (617), EC (1165), TDS (1132)			B (508), Se (1.6), Mn (387.26), Tl (0.23)

		5.4		Ca (366), Cl (84), Na (56), SO4 (929), EC (1340), TDS (1268)			Se (1.4), Tl (0.07)
		7.6	As (16.6), Fe (3), Mg (38), Ni (40.3)	Ca (377), Cl (116), F (1010), Na (62), SO4 (1360), EC (1307), TDS (1352)			B (823), Mn (1658.84), Se (2.1), Tl (0.14)
		4.8		Ca (163), Cl (311), Na (186), SO4 (485), EC (1313), TDS (1168)			B (391), Se (1.7)
		6.1		Ca (196), Cl (426), F (360), Na (240), SO4 (611), EC (1551), TDS (1524)			B (548), Se (2), Mn (276.28)
Clarillo	1	5.3		Ca (146), Cl (107), Na (72), SO4 (404)	NO3 (9.57), P (95), HCO3- (147.6)		
Maipo	2	4.4		Ca (173), Cl (194), Na (127), SO4 (467), EC (1173), TDS (1002)		Hg (2.1)	
		5.5		Ca (152), Cl (128), Na (79), SO4 (401), EC (1111), TDS (854)	NO3 (5.16), P (98)		

				Lampa	1	25.2			Ca (143), Cl (177), Na (145), EC (1505), TDS (1088)	As (13.6), Fe (0.2), Mg (24), Mo (8.6), NO3 (27.27), P (993), SO4 (491), HCO3- (200)		B (339), Mn (265.6)
				Mapocho	2	16.8			Ca (141), Cl (209), Na (146), EC (1577), TDS (1180)	F (390), Mo (8.6), NO3 (5.24), P (9021), SO4 (383), Zn (37.9), HCO3- (220)	Sn (0.4)	Cr (2), Se (1.6)
						8.3			Ca (164), Cl (144), Na (85), EC (1209), TDS (932)	Mg (24), NO3 (34.31), P (1613), SO4 (374), HCO3- (191)	Hg (1.6)	Se (1.4)
				La Ligua	1	5.2				NO3 (4.24), P (664)		
Mg (mg/l)	0.8-20 /8	20	125	Barriga	1	26	Al (8), Ca (215), Cd (0.89), Cu (962), F (650), Fe (1), Hg (1.3), Ni (59.1), SO4 (968), Zn (264.7), EC (1136), pH (5.44), TDS (905)					Be (0.74), Mn (1920.08), Se (5.1)
				Catemu	1	20				NO3 (19.5), P (105), HCO3- (174)		
				Ocoa	1	24				NO3 (14.28), P (155), HCO3- (199)	Pb (0.9)	
				El Soldado	1	34				Ca (127), HCO3- (172), K (5.7), Na (50), NO3 (24.07), P (732), EC (1085)		Fe (0.2), Mo (11.6), SO4 (324)
				Calera	3	24				NO3 (4.05), P (89), HCO3- (152)		

		23			NO3 (13.76), P (105), HCO3- (161)		
		36			NO3 (10.7), P (495), HCO3- (158)		
Maipo, Maipo Vn.	1	38	As (16.6), Fe (3), Ni (40.3)	Ca (377), Cl (116), F (1010), K (7.6), Na (62), SO4 (1360), EC (1307), TDS (1352)			B (823), Mn (1658.84), Se (2.1), Tl (0.14)
El Volcán		29	Ni (16.1)	Ca (294), F (480), SO4 (953), EC (1374), TDS (1076)			Mn (796)
Yeso	1	23		Ca (307), SO4 (869), TDS (1058)			
Colorado	1	29		Ca (216), SO4 (638), TDS (912)			Se (1.4), Tl (0.06)
Lampa	1	24			As (13.6), Ca (143), Cl (177), Fe (0.2), K (25), Mo (8.6), Na (145), P (993), SO4 (491), NO3 (27.27), HCO3- (200), EC (1505), TDS (1088)		B (339), Mn (265.66)
Mapocho	1	24			Ca (164), Cl (144), K (8.3), Na (85), P (1613), SO4 (374), NO3 (34.31), HCO3- (191), EC (1209), TDS (932)	Hg (1.6)	Se (1.4)

Mo (µg/l)	<0.1-7.3 /2.4	7.3	70	Riecillos	1	8.1	As (65.9)				Se (1.7)
				Duarte	1	9.3	P (68)				
				El Soldado	1	11.6		Ca (127), HCO3- (172), K (5.7), P (732), NO3 (24.07), EC (1085)		Fe (0.2), Mg (34), Na (50), SO4 (324)	sewage
				Andina	1	16.6				None	
				Colorado	1	10.8	None				
				Lampa	1	8.6		As (13.6), Ca (143), Cl (177), Fe (0.2), K (25), Mg (24), Na (145), P (993), SO4 (491), NO3 (27.27), HCO3- (200), EC (1505), TDS (1088)			B (339), Mn (265.66)
				Mapocho	1	8.6		Ca (141), Cl (209), K (17), F (390), Na (146), P (9021), SO4 (383), Zn (37.9), NO3 (5.24), HCO3- (220), EC (1577), TDS (1180)	Sn (0.4)		Cr (2), Se (1.6)
Na (mg/l)	0.2-42 /12	42	N/A	El Soldado	1	50		Ca (127), HCO3- (172), K (5.7), P (732), NO3 (24.07), EC (1085)		Fe (0.2), Mg (34), Mo (11.6), SO4 (324),	sewage
				Los Bronces	1	51				Cd (0.89), Cl (82), Zn (91.3)	
				Colorado	2	161				As (16.6), Cl (270), EC (1099), pH (8.52), TDS (932)	Tl (0.07)

		57		Ca (129), SO4 (315)	
Olivares	2	214		Cl (385), K (7.6), HCO3- (161), EC (1166), TDS (1096)	B (1473)
		840		Cl (147), K (3.9),pH (8.71)	B (572)
Maipo, Maipo Vn.	5	95		Ca (229), Cl (165), F (438), K (11), SO4 (617), EC (1165), TDS (1132)	B (508), Se (1.6), Mn (387.26), Tl (0.23)
		56		Ca (366), Cl (84), K (5.4), SO4 (929), EC (1340), TDS (1268)	Se (1.4), Tl (0.07)
		62	As (16.6), Fe (3), Mg (38), Ni (40.3)	Ca (377), Cl (116), F (1010), K (7.6), SO4 (1360), EC (1307), TDS (1352)	B (823), Mn (1658.84), Se (2.1), Tl (0.14)
		186		Ca (163), Cl (311), K (4.8), SO4 (485), EC (1313), TDS (1168)	B (391), Se (1.7)
		240		Ca (196), Cl (426), F (360), K (6.1), SO4 (611), EC (1551), TDS (1524)	B (548), Se (2), Mn (276.28)

El Volcán	3	59		Ca (140), Cl (86), SO4 (333)			
		54		Ca (146), SO4 (386)			
		60		Ca (131), Cl (89)			
Clarillo	1	72		Ca (146), Cl (107), SO4 (404)	K (5.3), P (95), NO3 (9.57), HCO3- (147.6)		
Maipo	5	59		Ca (120), Cl (83), SO4 (339)			
		66		Ca (122), Cl (99), SO4 (377)		Pb (3.5)	
		63		Ca (124), Cl (103), SO4 (383)			
		79		Ca (152), Cl (128), SO4 (401), EC (1111), TDS (854)	K (5.5), NO3 (5.16), P (98)		
		127		Ca (173), Cl (194), K (4.4), SO4 (467), EC (1173), TDS (1002)		Hg (2.1)	
Lampa	1	145		Ca (143), Cl (177), EC (1505), TDS (1088)	Fe (0.2), K (25), Mg (24), Mo (8.6), NO3 (27.27), P (993), SO4 (491), HCO3- (200)		As (13.6) B (339), Mn (265.66)

				Mapocho	2	85			Ca (164), Cl (144), EC (1209), TDS (932)	K (8.3), Mg (24), P (1613), SO4 (374), NO3 (34.31), HCO3- (191)	Hg (1.6)	Se (1.4)
						146			Ca (141), Cl (209), EC (1577), TDS (1180)	K (17), F (390), Mo (8.6), NO3 (5.24), P (9021), SO4 (383), Zn (37.9), HCO3- (220)	Sn (0.4)	Cr (2), Se (1.6)
Ni (µg/l)	<0.2-4.9 /<0.1	4.9	70	Colorado (Aconcagua)	5	5.6	Cd (0.83)					Mn (886)
						7.3	Cd (0.89)					Mn (456.1), Tl (0.09)
						11	Cd (1.37), Hg (3.4)					Mn (510.83), Tl (0.12)
						14.5	Cd (3.31), Fe (5.6), Zn (174.9), pH (5.86)					Tl (0.26)
						19.1		Al (12), Cd (1.31), Cu (457.3), Fe (8.5), Pb (1.4), SO4 (368), Zn (218.8), pH (2.84)				Be (0.56), Mn (688.26)
				Barriga	1	59.1		Al (8), Ca (215), Cd (0.89), Cu (962), Hg (1.3), F (650), Fe (1), Hg (1.3), Mg (26), SO4 (968), Zn (264.7), EC (1136), pH (5.44), TDS (905)				Be (0.74), Mn (1920.08), Se (5.1)
				Ortiga	2	21.1	Al (4.4), F (838), Fe (4.6), Zn (40.2), pH (3.19)					Tl (0.15)
						32.5	Al (6), F (380), Fe (5.1), Hg (3.1), Zn (83.3), pH (3.41)					Be (0.46), Mn (415.46), Tl (0.16)

				Arrayán		27.5	Al (4.6), F (504), Fe (0.8), SO4 (357), Zn (31.1), pH (4.65)					Mn (406.33), Tl (0.48)
				Dolores		6.5		Cd (0.79), Cu (257.7), Fe (0.7), Zn (344.8), pH (6.3)				Mn (992.29)
				Los Bronces	2	6.5	Zn (101.7)					
						7.4					Cd (1.91), Cl (114), Cu (114.3), Na (68), Zn (214.6)	B (413), Mn (795)
				Yerba Loca	3	26.4		Al (6), As (13.5), Cu (11693), Fe (45), P (694), SO4 (446), Zn (123.6), pH (1.99), TDS (1070)				Be (0.87), Cr (2.6), Mn (641.94)
						17.5		Al (0.2), Cu (3275.1), Zn (173.1), pH (5.69)				Mn (653.59)
						17.9		Al (1.4), Cu (4185), Ni (17.9), Zn (175), pH (5.1)				Mn (781)
				San Francisco	1	12.2		Cu (802.6), Zn (130.7)				Mn (493.47)
				El Volcán	1	16.1	Mg (29), SO4 (953)		Ca (294), F (480), EC (1374), TDS (1076)			Mn (796)
				Maipo, Maipo Vn.	1	40.3	As (16.6), Fe (3), Mg (38)		Ca (377), Cl (116), F (1010), K (7.6), Na (62), SO4 (1360), EC (1307), TDS (1352)			B (823), Mn (1658.84), Se (2.1), Tl (0.14)
NO3 (mg/l)	<0.05-2.68 /0.5	2.7	50	Arrayán	2	4.18				As (46.5), B (426)		

		9.32		None			
La Ligua	2	4.24 9.89		K (5.2), P (664) HCO3- (154), pH (8.96)			Se (13.4)
Maipo	1	5.16	Ca (152), Cl (128), Na (79), SO4 (401), EC (1111), TDS (854)	K (5.5), P (98)			
Clarillo	1	9.57	Ca (146), Cl (107), Na (72), SO4 (404)	K (5.3), P (95), HCO3- (147.6)			
Picarquín	1	12.46		P (68)	Pb (2.8)		Se (2), B (360)
Colina	1	28.62		HCO3- (154)			
Lampa	1	27.27	Ca (143), Cl (177), Na (145), EC (1505), TDS (1088)	As (13.6), Fe (0.2), K (25), Mg (24), Mo (8.6), P (993), SO4 (491), HCO3- (200)			B (339), Mn (265.66)
Mapocho	2	5.24	Ca (141), Cl (209), Na (146), EC (1577), TDS (1180)	K (17), F (390), Mo (8.6), P (9021), SO4 (383), Zn (37.9), HCO3- (220)	Sn (0.4)		Cr (2), Se (1.6)
		34.31	Ca (164), Cl (144), Na (85), EC (1209), TDS (932)	K (8.3), Mg (24), P (1613), SO4 (374), HCO3- (191)	Hg (1.6)		Se (1.4)
El Soldado	1	24.07		Ca (127), HCO3- (172), K (5.7), Na (50), P (732), EC (1085)		Fe (0.2), Mg (34), Mo (11.6), SO4 (324)	
Calera	4	3.9		pH (8.53)			

						4.05				Mg (24), P (89), HCO3- (152)		
						10.7				Mg (36), P (495), HCO3- (158)		
						13.76				Mg (23), P (105), HCO3- (161)		
				Aconcagua	3	6.41				None		
						11.63				HCO3- (154)		
						14.58				HCO3- (195)		
				Catemu	1	19.5				Mg (20), P (105), HCO3- (174)		
				Ocoa	1	14.28				Mg (24), P (155), HCO3- (199)	Pb (0.9)	
P (µg/l)	<20-67 /34	67	N/A	Duarte	1	68		Mo (9.3)				
				Yerba Loca	1	694		Al (6), As (13.5), Cu (11693), Fe (45), Ni (26.4), SO4 (446), Zn (123.6), pH (1.99), TDS (1070)				Be (0.87), Cr (2.6), Mn (641.94)
				Rabicano	1	87	Zn (71.1)		Ca (163), SO4 (354)			Se (4.5), Sn (0.12)
				El Manzanito	1	185					Al (0.7), Fe (0.7)	detergent
				Clarillo	1	95			Ca (146), Cl (107), Na (72), SO4 (404)	K (5.3), NO3 (9.57), HCO3- (147.6)		
				Maipo	1	98			Ca (152), Cl (128), Na (79), SO4 (401), EC (1111), TDS (854)	K (5.5), NO3 (5.16)		

Lampa	1	993		Ca (143), Cl (177), Na (145), EC (1505), TDS (1088)	As (13.6), Fe (0.2), K (25), Mg (24), Mo (8.6), NO3 (27.27), SO4 (491), HCO3- (200)			B (339), Mn (265.6)
Mapocho	2	9021		Ca (141), Cl (209), Na (146), EC (1577), TDS (1180)	K (17), F (390), Mo (8.6), NO3 (5.24), SO4 (383), Zn (37.9), HCO3- (220)	Sn (0.4)		Cr (2), Se (1.6)
		1613		Ca (164), Cl (144), Na (85), EC (1209), TDS (932)	K (8.3), Mg (24), NO3 (34.31), SO4 (374), HCO3- (191)	Hg (1.6)		Se (1.4)
Picarquín	1	68			NO3 (12.46)	Pb (2.8)		B (360), Se (2)
Riecillos	1	80					Hg (8.6)	
Los Andes	1	92			None			
Catemu	1	105			Mg (20), NO3 (19.5), HCO3- (174)			
Ocoa	1	155			Mg (24), NO3 (14.28), HCO3- (199)	Pb (0.9)		
El Soldado	1	732			Ca (127), HCO3- (172), K (5.7), Na (50), NO3 (24.07), EC (1085)		Fe (0.2), Mg (34), Mo (11.6), SO4 (324)	
Calera	1	89			Mg (24), NO3 (4.05), HCO3- (152)			
		105			Mg (23), NO3 (13.76), HCO3- (161)			

						495			Mg (36), NO3 (10.7), HCO3- (158)				
				La Ligua		664			K (5.2), NO3 (4.24)				
Pb (µg/l)	<0.1-0.8 /0.1	0.8	50	Ocoa	1	0.9			Mg (24), NO3 (14.28), P (155), HCO3- (199)	None			
				Yeso	1	1		Ca (156), SO4 (470)				None	
				La Poza	1	1.1					Zn (87), HCO3- (178)		Tl (0.14)
				Colorado (Aconcagua)	1	1.4	Al (12), Cd (1.31), Cu (457.3), Fe (8.5), Ni (19.1), SO4 (368), Zn (218.8), pH (2.84)						Be (0.56), Mn (688.26)
				Picarquin	1	2.8			NO3 (12.46), P (68)	None			B (360), Se (2)
				Maipo	1	3.5		Ca (122), Cl (99), Na (66), SO4 (377)		None			
				Colina	1	4				As (14.8)			B (350)
pH	6.6-8.5 /7.8	<6.6->8.	<6.5->8.5	La Ligua	1	**9**			NO3 (9.89), HCO3- (154)				Se (13.4)
				Chalaco	2	**8.6**		None					
						9		None					
				Pocuro	1	**8.6**		None					
				Covarrubias	1	**9**		None					
				Olivares	2	**8.7**		Cl (147), K (3.9), Na (84)					B (572)
				Yeso	1	**8.6**		None					

Coyanco	1	**8.8**		None		
El Manzano	1	**8.6**		None		
Dolores		**6.3**		Cd (0.79), Cu (257.7), Fe (0.7), Ni (6.5), Zn (345)		Mn (992)
Colorado (Aconcagua)	2	**5.9**	Cd (3.31), Fe (5.6), Ni (14.5), Zn (175)			Tl (0.26)
		2.8		Al (12), Cd (1.31), Cu (457.3), Fe (8.5), Ni (19.1), Pb (1.4), SO4 (368), Zn (218.8)		Be (0.56), Mn (688.26)
Yerba Loca	3	**2**		Al (6), As (13.5), Cu (11693), Fe (45), Ni (26.4), P (694), SO4 (446), Zn (123.6), TDS (1070)		Be (0.87), Cr (2.6), Mn (641.94)
		5.7		Al (0.2), Cu (3275), Ni (17.5), Zn (173.1)		Mn (654)
		5.1		Al (1.4), Cu (4185), Ni (17.9), Zn (175)		Mn (781)
Ortiga	3	**4.8**	Al (0.3), F (480)			
		3.2	Al (4.4), F (838), Fe (4.6), Ni (21.1), Zn (40.2)			Tl (0.15)
		3.4	Al (6), F (380), Fe (5.1), Hg (3.1), Ni (32.5), Zn (83.3)			Be (0.46), Mn (415.46), Tl (0.16)
Arrayán	1	**4.7**	Al (4.6), F (504), Fe (0.8), Ni (27.5), SO4 (357), Zn (31.1)			Tl (0.48), Mn (406.33)

				Barriga	1	**5.4**		Al (8), Ca (215), Cd (0.89), Cu, (119.8), F (650), Fe (1), Hg (1.3), Mg (26), Ni (59.1), SO4 (968), Zn (264.7), EC (1136), TDS (905)					Be (0.74), Mn (1920.08), Se (5.1)
SO4 (mg/l)	12-303 /99	303	500	Juncal	2	327			Ca (128)				
						398			Ca (130)				
				El Soldado	1	324				Ca (127), HCO3- (172), K (5.7), Na (50), NO3 (24.07), P (732), EC (1085)	Fe (0.2), Mg (34), Mo (11.6)		
				Barriga	1	**968**		Al (8), Ca (215), Cd (0.89), Cu, (119.8), F (650), Fe (1), Hg (1.3), Mg (26), Ni (59.1), Zn (264.7), EC (1136), pH (5.44), TDS (905)					Be (0.74), Mn (1920.08), Se (5.1)
				Colorado (Aconcagua)	1	368		Al (12), Cd (1.31), Cu (457.3), Fe (8.5), Ni (19.1), Pb (1.4), Zn (218.8), pH (2.84)					Be (0.56), Mn (688.26)
				Parraguirre	1	419			Ca (157)				
				Rabicano	1	354	Zn (71.1)		Ca (163), P (87)			Sn (0.12)	Se (4.5)
				Colorado	3	**638**			Ca (216), Mg (29), TDS (912)				Se (1.4), Tl (0.06)
						315			Ca (129), Na (57)				
						333			Ca (123)				

Yerba Loca	1	446		Al (6), As (13.5), Cu (11693), Fe (45), Ni (26.4), P (694), Zn (123.6), pH (1.99), TDS (1070)			Be (0.87), Cr (2.6), Mn (641.94)
Arrayán	1	357	Al (4.6), F (504), Fe (0.8), Ni (27.5), Zn (31.1), pH (4.65)				Tl (0.48), Mn (406.33)
Yeso	4	470		Ca (156), Pb (1)			
		539		Ca (171)			
		683		Ca (243), TDS (846)			
		869		Ca (307), Mg (23), TDS (1058)			
El Volcán	4	333		Ca (140), Cl (86), Na (59)			
		386		Ca (146), Na (54)			
		590		Ca (213)			
		953	Mg (29), Ni (16.1)	Ca (294), F (480), EC (1374), TDS (1076)			Mn (796)
Clarillo	1	404		Ca (146), Cl (107), Na (72), SO4 (404)	K (5.3), P (95), NO3 (9.57), HCO3- (147.6)		
Maipo, Maipo Vn.	6	485		Ca (163), Cl (311), K (4.8), Na (186), EC (1313), TDS (1168)			B (391), Se (1.7)

		611		Ca (196), Cl (426), F (360), K (6.1), Na (240), EC (1551), TDS (1524)		B (548), Se (2), Mn (276.28)
		617		Ca (229), Cl (165), F (438), K (11), Na (95), EC (1165), TDS (1132)		B (508), Se (1.6), Mn (387.26), Tl (0.23)
		836		Ca (305), EC (1000), TDS (980)		
		929		Ca (366), Cl (84), K (5.4), Na (56), EC (1340), TDS (1268)		Se (1.4), Tl (0.07)
		1360	As (16.6), Fe (3), Mg (38), Ni (40.3)	Ca (377), Cl (116), F (1010), K (7.6), Na (62), EC (1307), TDS (1352)		B (823), Se (2.1), Mn (1658.84), Tl (0.14)
Maipo	5	339		Ca (120), Cl (83), Na (59)		
		377		Ca (122), Cl (99), Na (66)	Pb (3.5)	
		383		Ca (124), Cl (103), Na (63)		
		467		Ca (173), Cl (194), K (4.4), Na (127), EC (1173), TDS (1002)	Hg (2.1)	

						401		Ca (152), Cl (128), Na (79), EC (1111), TDS (854)	K (5.5), NO3 (5.16), P (98)			
				Lampa	1	491		Ca (143), Cl (177), Na (145), EC (1505), TDS (1088)	Fe (0.2), K (25), Mg (24), Mo (8.6), NO3 (27.27), P (993), HCO3- (200)	As (13.6)		B (339), Mn (265.66)
				Mapocho	2	374		Ca (164), Cl (144), Na (85), EC (1209), TDS (932)	K (8.3), Mg (24), P (1613), NO3 (34.31), HCO3- (191)	Hg (1.6)		Se (1.4)
						383		Ca (141), Cl (209), Na (146), EC (1577), TDS (1180)	K (17), F (390), Mo (8.6), NO3 (5.24), P (9021), Zn (37.9), HCO3- (220)	Sn (0.4)		Cr (2), Se (1.6)
TDS (mg/l)	34-783 /290	783	1500	Yerba Loca	1	1070	Al (6), As (13.5), Cu (11693), Fe (45), Ni (26.4), P (694), SO4 (446), Zn (123.6), pH (1.99)					Be (0.87), Cr (2.6), Mn (641.94)
				Barriga	1	905	Al (8), Ca (215), Cd (0.89), Cu, (119.8), F (650), Fe (1), Hg (1.3), Mg (26), Ni (59.1), SO4 (968), Zn (264.7), EC (1136), pH (5.44)					Be (0.74), Mn (1920.08), Se (5.1)
				Colorado	2	912		Ca (216), Mg (29), SO4 (638)				Se (1.4), Tl (0.06)
						932					As (16.6), Cl (270), Mo (6.9), Na (161), EC (1099), pH (8.52)	Tl (0.07)

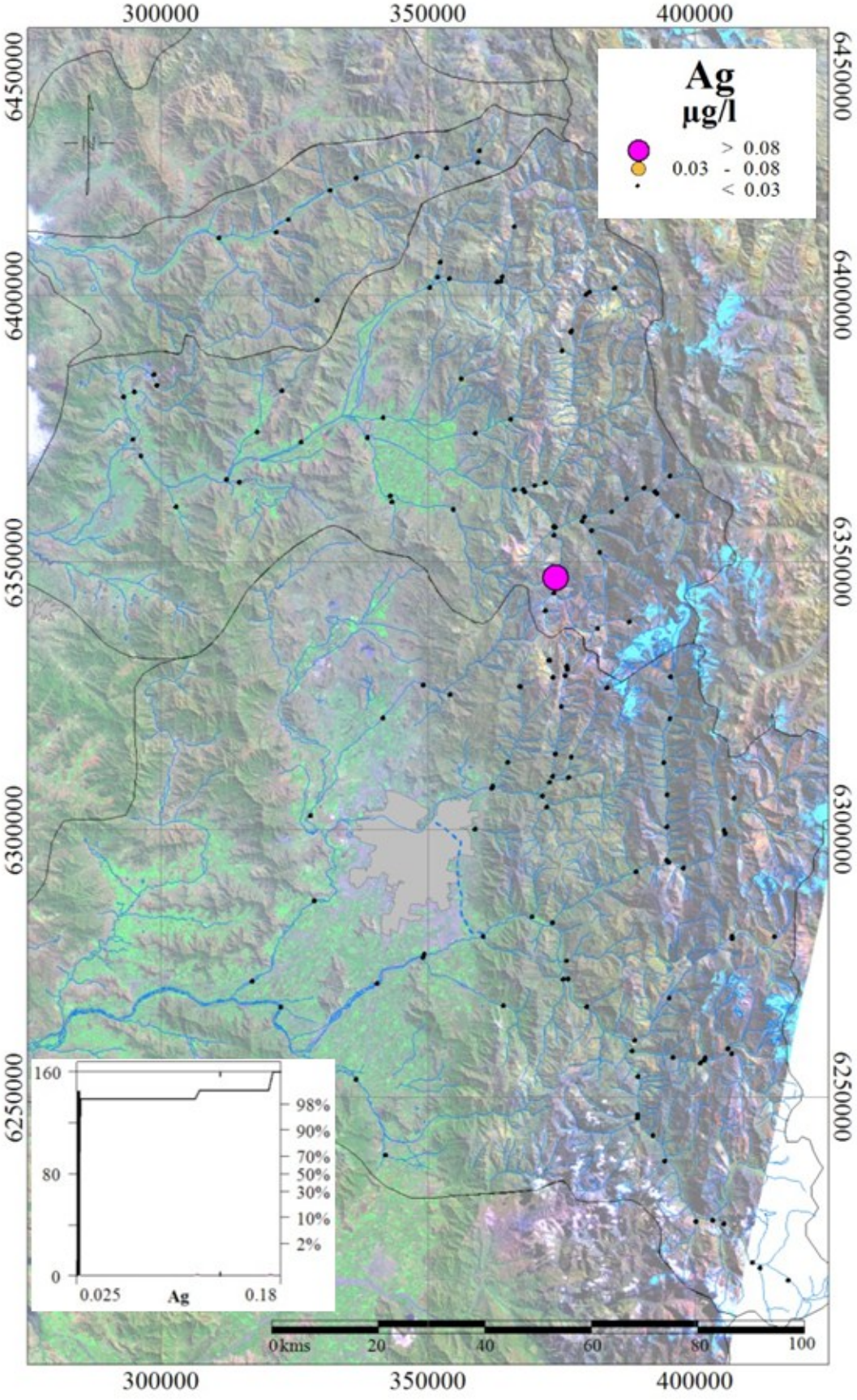
Olivares	1	1096		Cl (385), K (7.6), Na (214), HCO3- (161), EC (1166)	B (1473)
Yeso	2	1058		Ca (307), Mg (23), SO4 (869)	
		846		Ca (243), SO4 (683)	
El Volcán	1	1076	Mg (29), Ni (16.1), SO4 (953)	Ca (294), F (480), EC (1374)	Mn (796)
Maipo, Maipo Vn.		1352	As (16.6), Fe (3), Mg (38), Ni (40.3)	Ca (377), Cl (116), F (1010), K (7.6), Na (62), SO4 (1360), EC (1307)	B (823), Se (2.1), Mn (1659), Tl (0.14)
		1524		Ca (196), Cl (426), F (360), K (6.1), Na (240), SO4 (611), EC (1551)	B (548), Mn (276.28), Se (2)
		1268		Ca (366), Cl (84), K (5.4), Na (56), SO4 (929), EC (1340)	Se (1.4), Tl (0.07)
		1168		Ca (163), Cl (311), K (4.8), Na (186), SO4 (485), EC (1313)	B (391), Se (1.7)

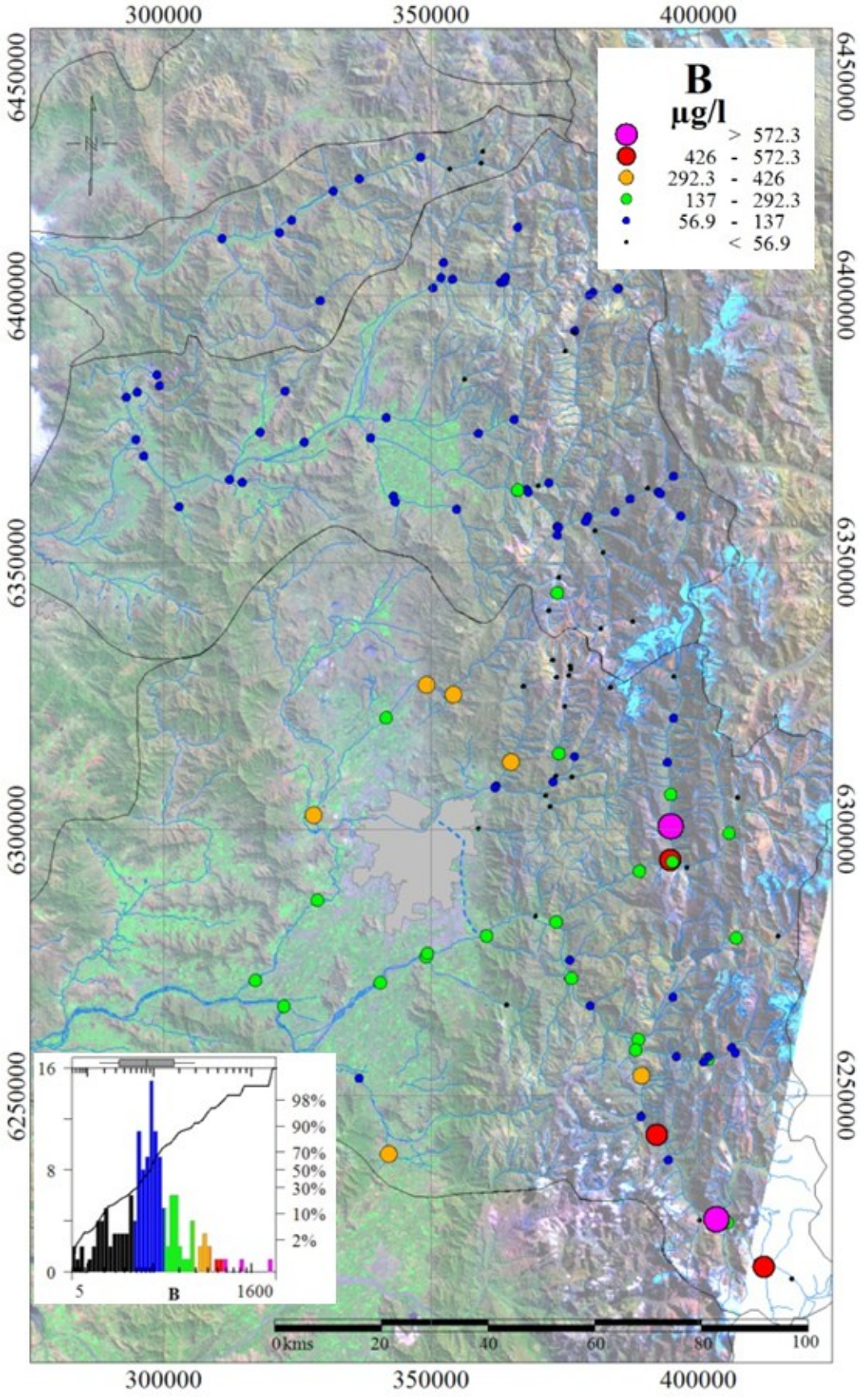
						1132			Ca (229), Cl (165), F (438), K (11), Na (95), SO4 (617), EC (1165)				B (508), Se (1.6), Mn (387.26), Tl (0.23)
						980			Ca (305), SO4 (836), EC (1000)				
				Maipo	2	1002			Ca (173), Cl (194), K (4.4), Na (127), SO4 (467), EC (1173)		Hg (2.1)		
z						854			Ca (152), Cl (128), Na (79), SO4 (401), EC (1111)	K (5.5), NO3 (5.16), P (98)			
				Mapocho	1	932			Ca (164), Cl (144), Na (85), EC (1209)	K (8.3), Mg (24), P (1613), NO3 (34.31), SO4 (374), HCO3- (191)	Hg (1.6)		Se (1.4)
				Lampa	1	1088			Ca (143), Cl (177), Na (145), EC (1505)	As (13.6), Fe (0.2), K (25), Mg (24), Mo (8.6), P (993), SO4 (491), NO3 (27.27), HCO3- (200)			B (339), Mn (265.66)
Zn (µg/l)	<0.5-27.6 /3.9	28	3000	Los Bronces	2	91.3						Cd (0.89), Cl (82), Na (51)	
						101.7	Ni (6.5)						
				Dolores	1	344.8		Cd (0.79), Cu (257.7), Fe (0.7), Ni (6.5), pH (6.3)					Mn (992)

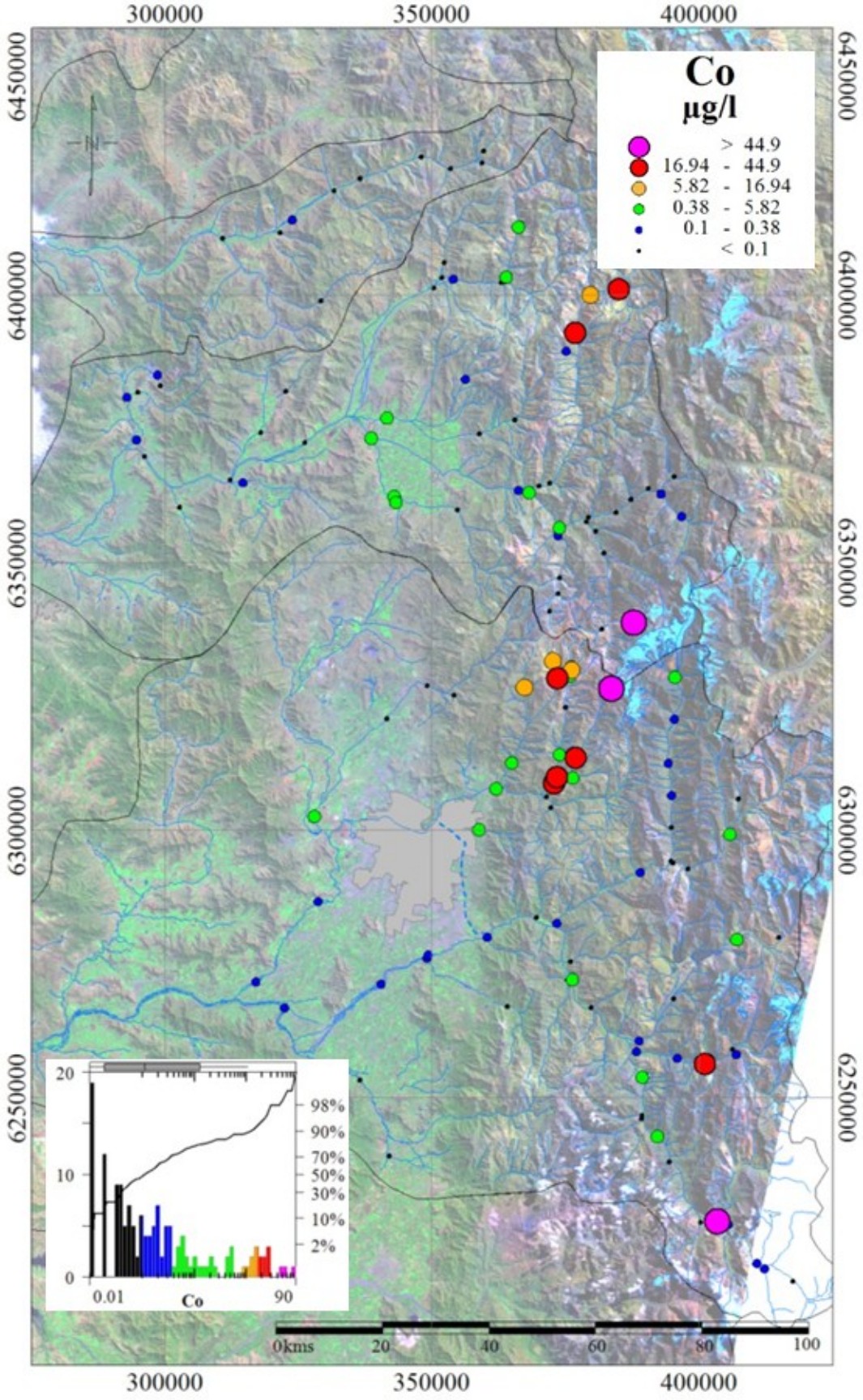
Yerba Loca	3	123.6		Al (6), As (13.5), Cu (11693), Fe (45), Ni (26.4), P (694), SO4 (446), pH (1.99), TDS (1070)					Be (0.87), Cr (2.6), Mn (641.94)
		173.1		Al (0.2), Cu (3275), Ni (17.5), pH (5.69)					Mn (654)
		175		Al (1.4), Cu (4185), Ni (17.9), pH (5.1)					Mn (781)
San Francisco	1	130.7		Cu (802.6), Ni (12.2)					Mn (493)
Ortiga	2	40.2	Al (4.4), F (838), Fe (4.6), Ni (21.1), pH (3.19)						Tl (0.15)
		83.3	Al (6), F (380), Fe (5.1), Hg (3.1), Ni (32.5), Zn (83.3), pH (3.41)						Be (0.46), Mn (415.46), Tl (0.16)
Arrayán	1	31.1	Al (4.6), F (504), Fe (0.8), Ni (27.5), SO4 (357), pH (4.65)						Mn (406.33), Tl (0.48)
Rabicano	1	71.1			Ca (163), P (87), SO4 (354)				Se (4.5), Sn (0.12)
Mapocho	1	37.9			Ca (141), Cl (209), Na (146), EC (1577), TDS (1180)	K (17), F (390), Mo (8.6), NO3 (5.24), P (9021), SO4 (383), HCO3- (220)	Sn (0.4)		Cr (2), Se (1.6)
Barriga	1	264.7		Al (8), Ca (215), Cd (0.89), Cu, (119.8), F (650), Fe (1), Hg (1.3), Mg (26), Ni (59.1), SO4 (968), EC (1136), pH (5.44), TDS (905)					Be (0.74), Mn (1920.08), Se (5.1)
Aconcagua	1	42.3						Cu (104)	

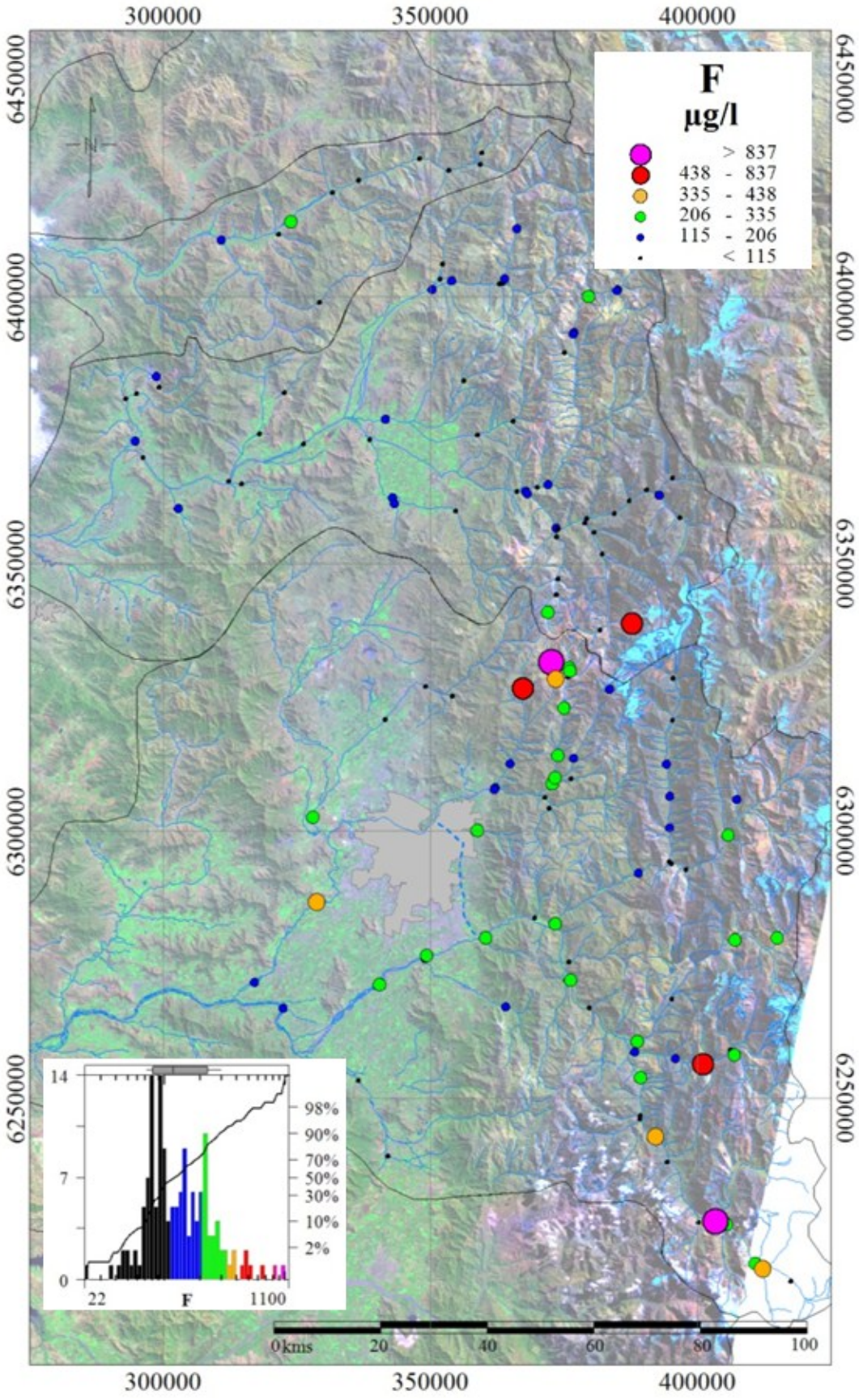
Colorado (Aconcagua)	2	174.9	Cd (3.31), Fe (5.6), Ni (14.5), pH (5.86)			Tl (0.26)
		218.8		Al (12), Cd (1.31), Cu (457.3), Fe (8.5), Ni (19.1), Pb (1.4), SO4 (368), pH (2.84)		Be (0.56), Mn (688.26)
La Poza	1	87			HCO3- (178), Pb (1.1)	Tl (0.14)

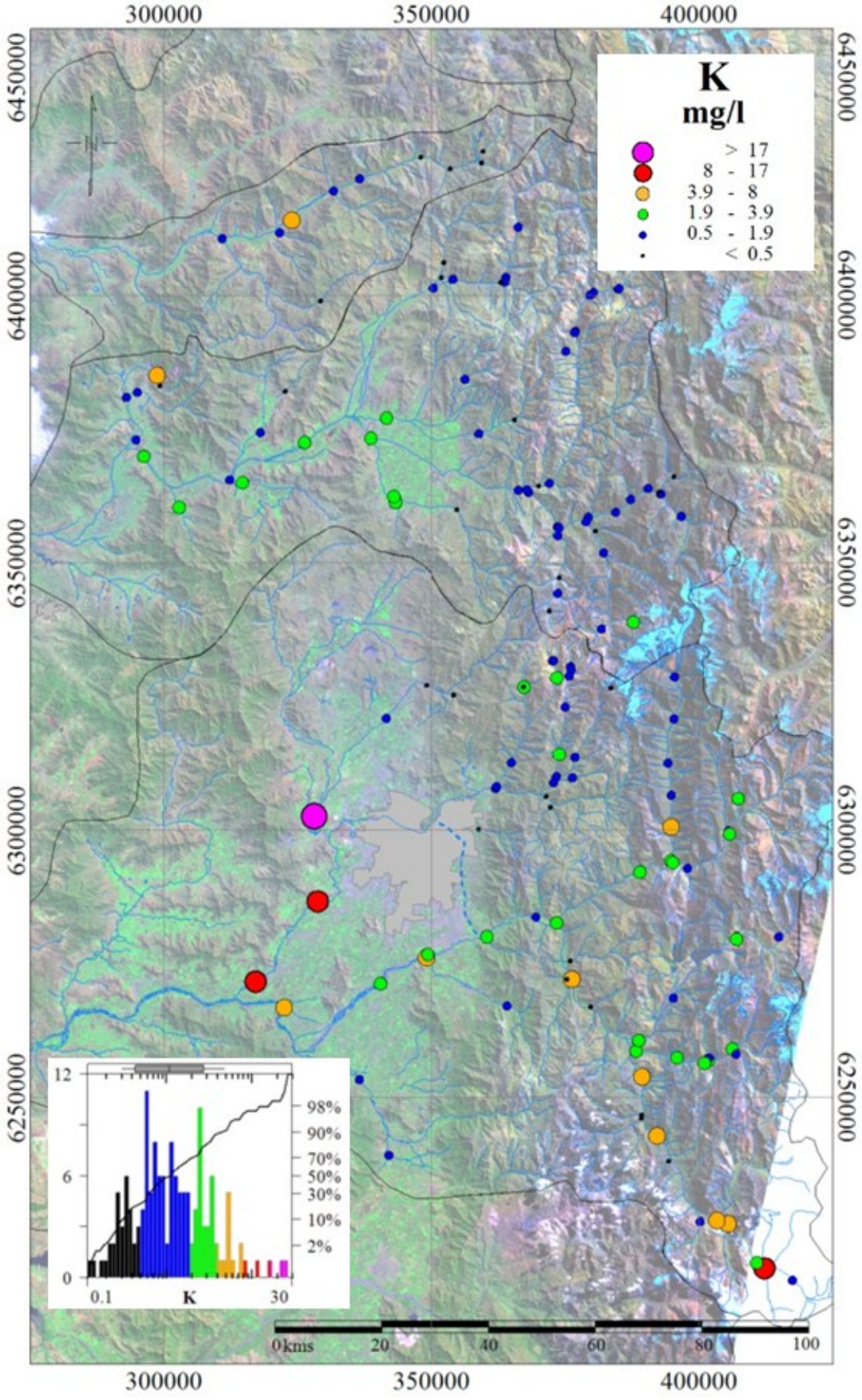
APPENDIX D: Hydrogeochemical baseline maps for Ag, B, Co, F, K, Mn, Sb, Se, Sn and Zn

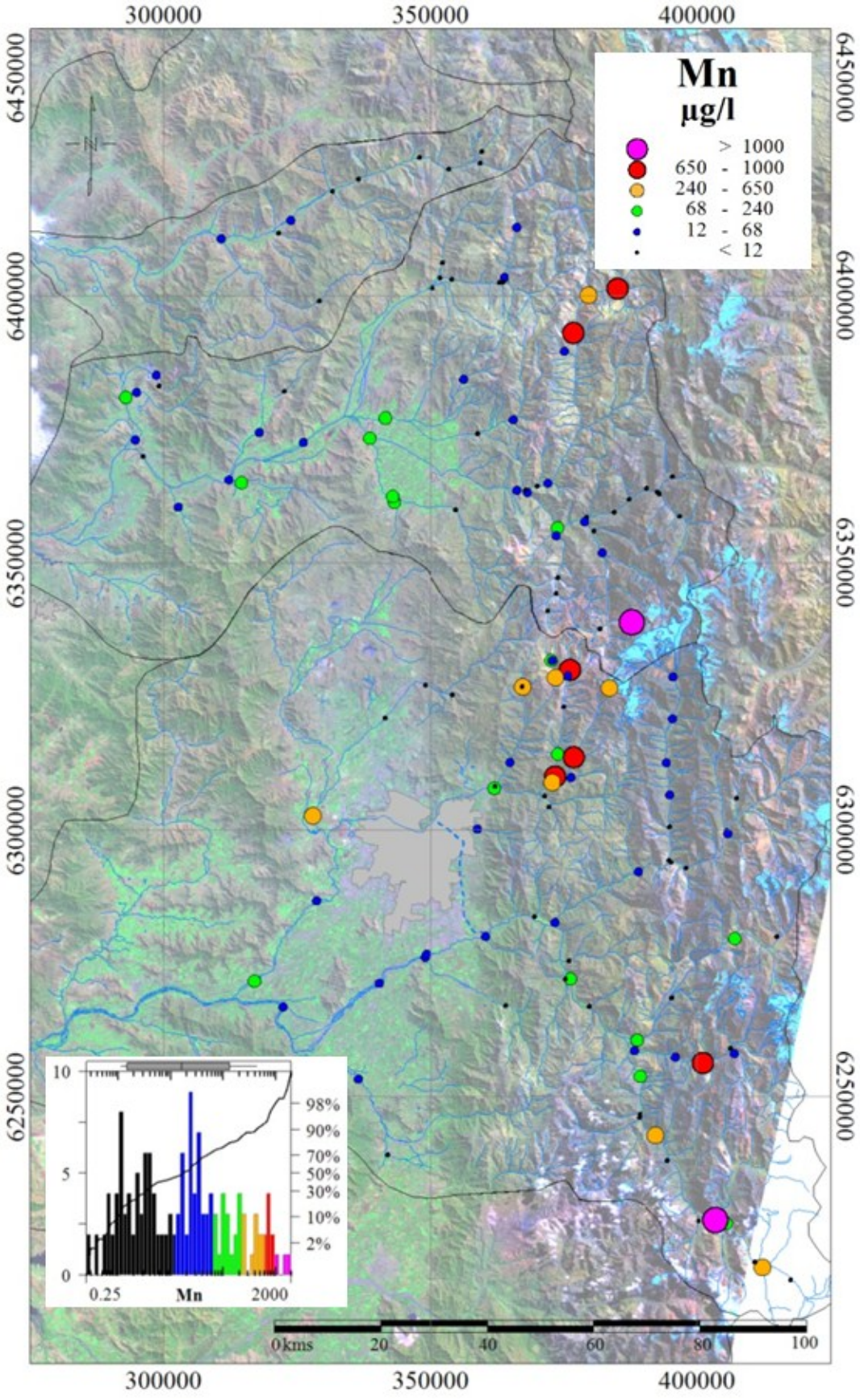

Ag
µg/l
> 0.08
0.03 - 0.08
< 0.03
300000
350000
400000
6450000
6400000
6350000
6300000
6250000
160
80
0
0.025
Ag
0.18
98%
90%
70%
50%
30%
10%
2%
0kms
20
40
60
80
100

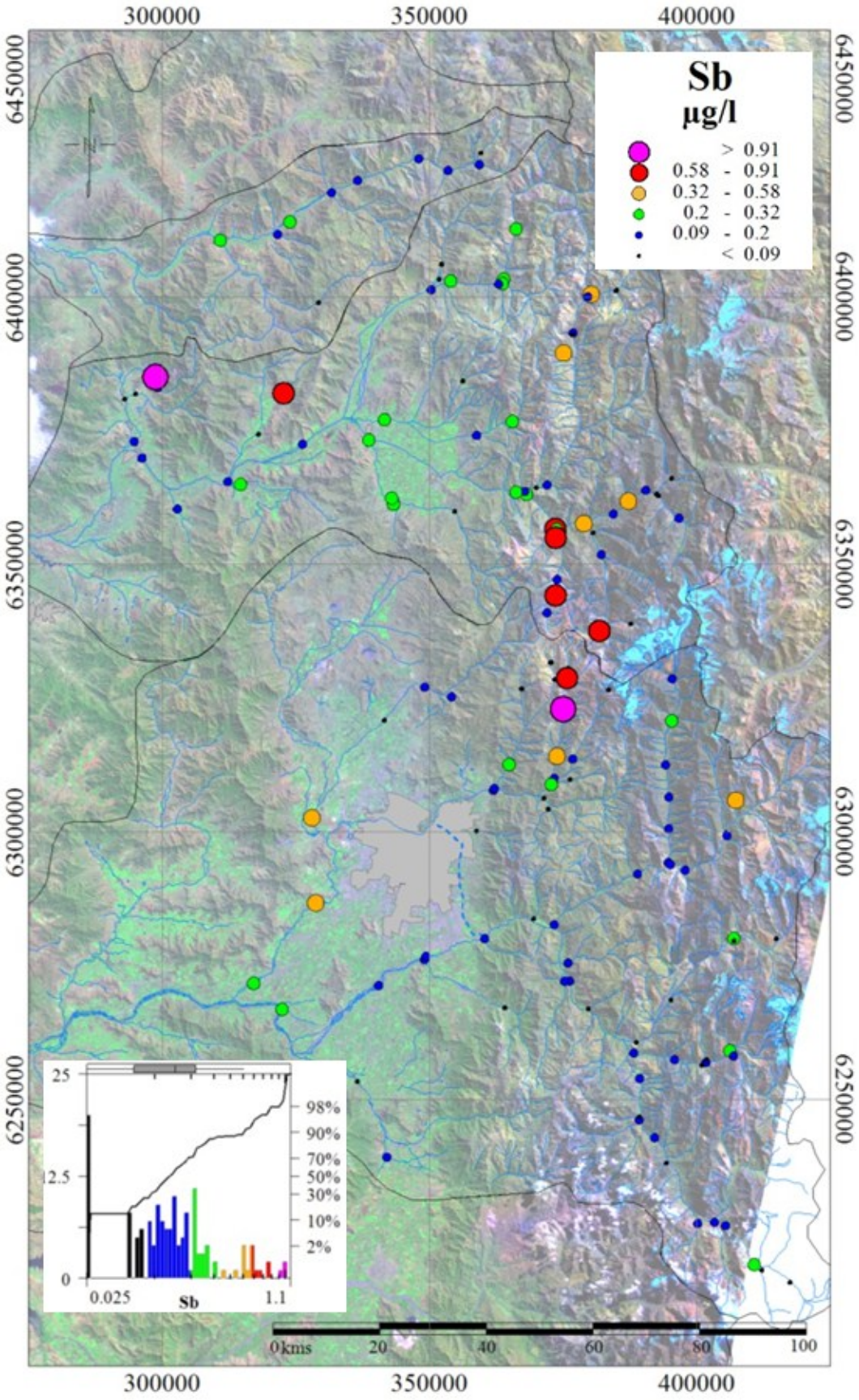

300000
350000
400000
6450000
6400000
6350000
6300000
6250000
B
µg/l
> 572.3
426 - 572.3
292.3 - 426
137 - 292.3
56.9 - 137
< 56.9
N
16
8
0
5
B
1600
98%
90%
70%
50%
30%
10%
2%
0kms
20
40
60
80
100

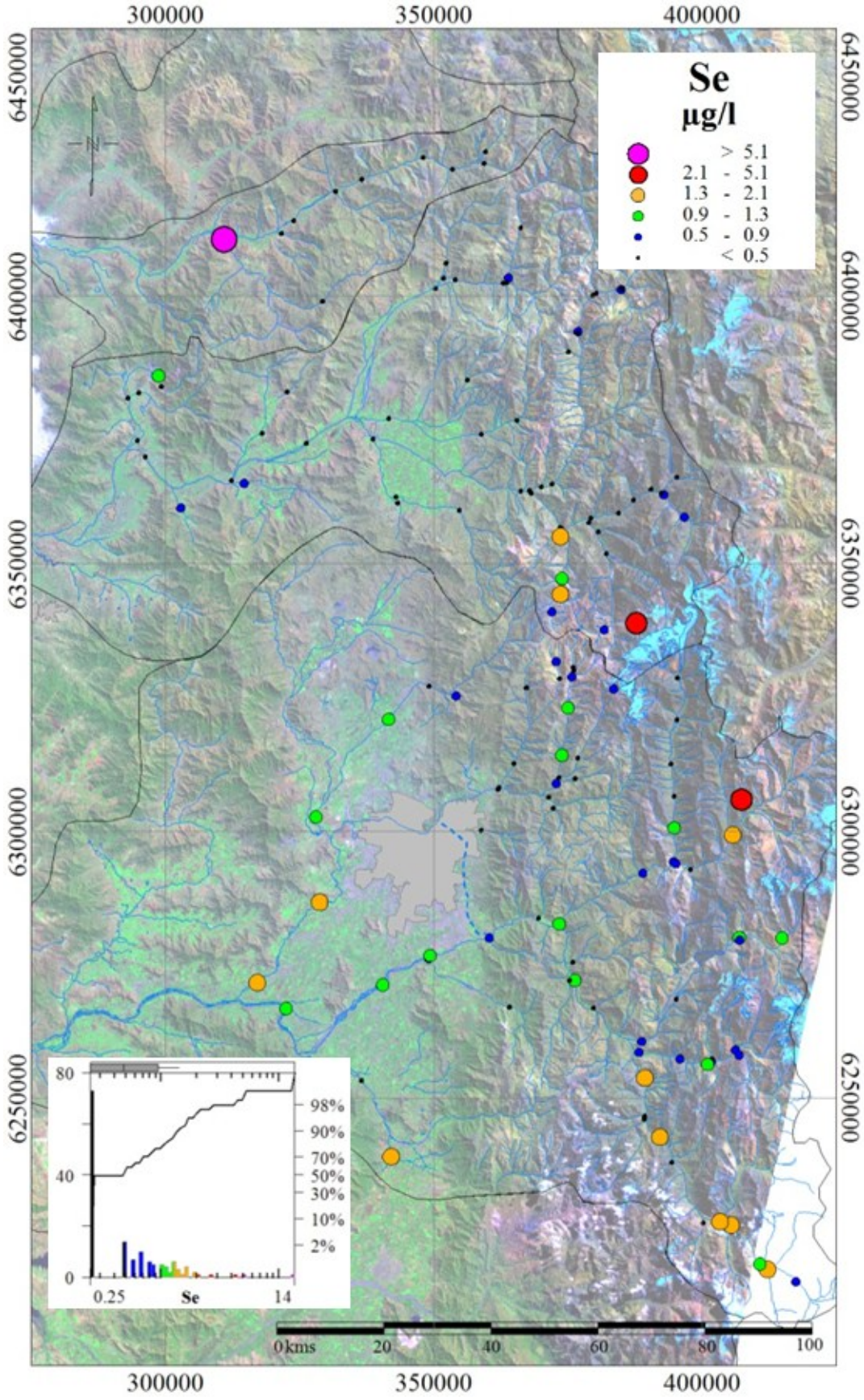

Co
µg/l
> 44.9
16.94 - 44.9
5.82 - 16.94
0.38 - 5.82
0.1 - 0.38
< 0.1
N
300000
350000
400000
6450000
6400000
6350000
6300000
6250000
20
10
0
98%
90%
70%
50%
30%
10%
2%
0.01
Co
90
0kms
20
40
60
80
100

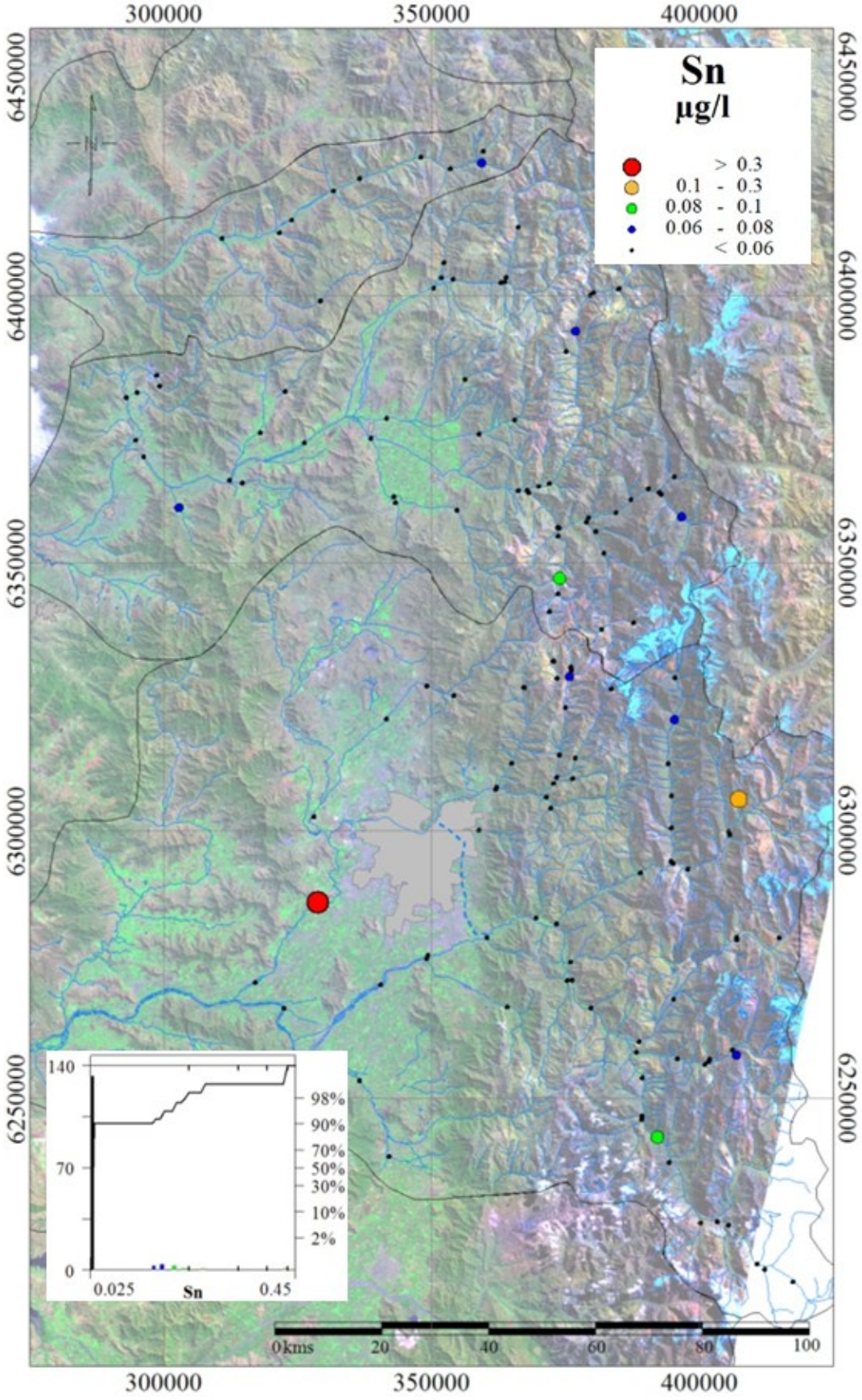

300000
350000
400000
6450000
6400000
6350000
6300000
6250000
F
µg/l
> 837
438 - 837
335 - 438
206 - 335
115 - 206
< 115
14
7
0
22
F
1100
98%
90%
70%
50%
30%
10%
2%
0kms
20
40
60
80
100

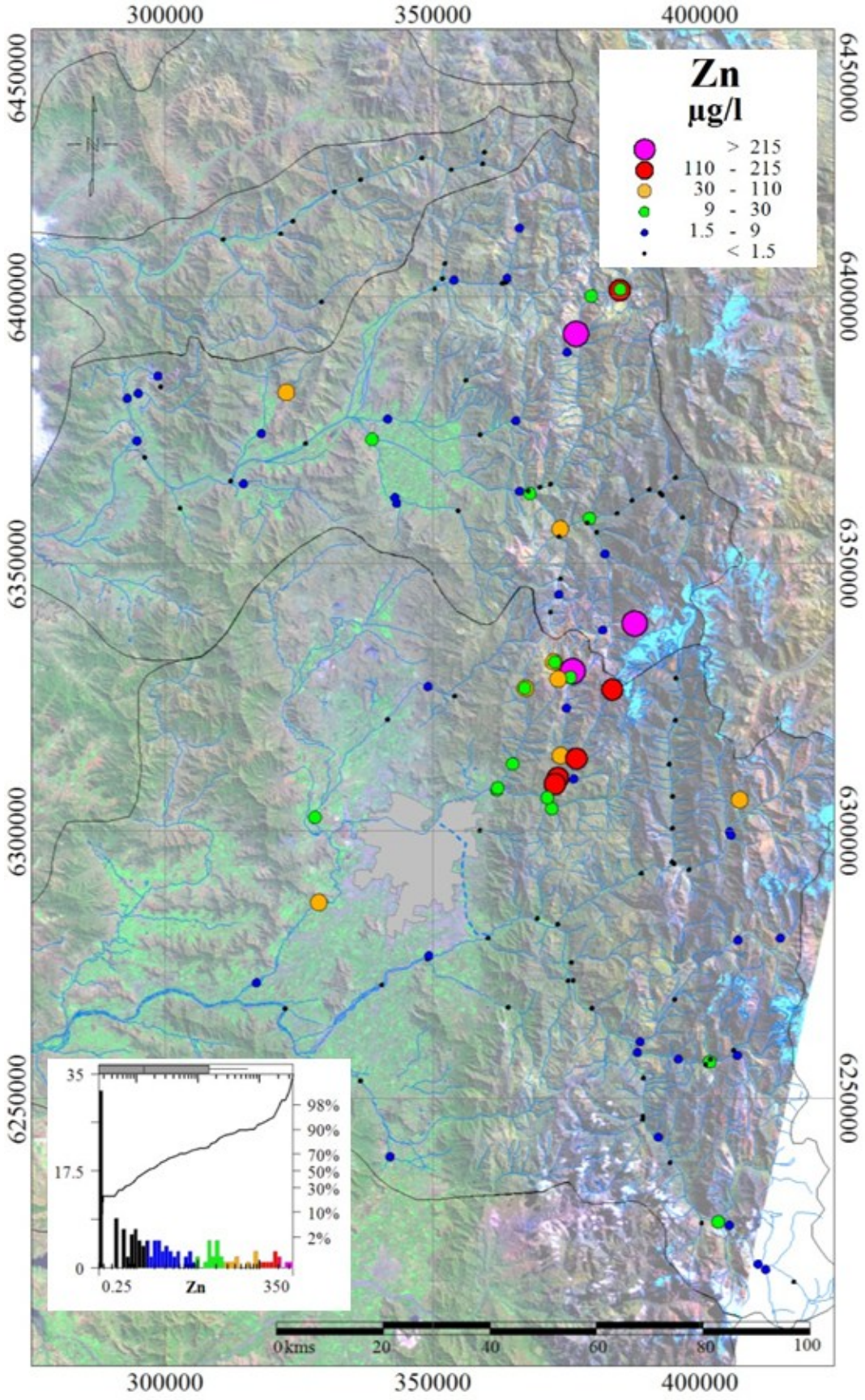

300000
350000
400000
6450000
6400000
6350000
6300000
6250000
K
mg/l
> 17
8 - 17
3.9 - 8
1.9 - 3.9
0.5 - 1.9
< 0.5
12
6
0
0.1
K
30
98%
90%
70%
50%
30%
10%
2%
0kms
20
40
60
80
100


Mn
µg/l
> 1000
650 - 1000
240 - 650
68 - 240
12 - 68
< 12
N
300000
350000
400000
6450000
6400000
6350000
6300000
6250000
10
5
0
0.25
Mn
2000
98%
90%
70%
50%
30%
10%
2%
0kms
20
40
60
80
100


300000
350000
400000
6450000
6400000
6350000
6300000
6250000
Sb
µg/l
> 0.91
0.58 - 0.91
0.32 - 0.58
0.2 - 0.32
0.09 - 0.2
< 0.09
25
12.5
0
98%
90%
70%
50%
30%
10%
2%
0.025
Sb
1.1
0kms
20
40
60
80
100


300000
350000
400000
6450000
6400000
6350000
6300000
6250000
Se
µg/l
> 5.1
2.1 - 5.1
1.3 - 2.1
0.9 - 1.3
0.5 - 0.9
< 0.5
N
80
40
0
98%
90%
70%
50%
30%
10%
2%
0.25
Se
14
0 kms
20
40
60
80
100


Sn
µg/l
> 0.3
0.1 - 0.3
0.08 - 0.1
0.06 - 0.08
< 0.06
300000
350000
400000
6450000
6400000
6350000
6300000
6250000
140
70
0
0.025
Sn
0.45
98%
90%
70%
50%
30%
10%
2%
0kms
20
40
60
80
100


Zn
µg/l
> 215
110 - 215
30 - 110
9 - 30
1.5 - 9
< 1.5
300000
350000
400000
6450000
6400000
6350000
6300000
6250000
35
17.5
0
0.25
Zn
350
98%
90%
70%
50%
30%
10%
2%
0kms
20
40
60
80
100

APPENDIX E: Statistical summary for the regional data

Table E-1: Statistical summary for the regional data. Values below detection limit (DL) were used as half of the DL value for calculation purposes. This distinguishes between values at DL and lower than DL.

Chemical	Unit	DL	Minimum	Median	Maximum	Mean	St.Dev.	%ile - 75	%ile - 98
Ag	µg/l	0.05	0.025	0.025	0.16	0.0263	0.012	0.025	0.025
Al	µg/l	1	1	15	12287	325.2585	1481.7	47.5	6050.24
As	µg/l	0.5	0.25	3.1	65.9	4.6881	7.3641	5.15	23.856
Au	µg/l	0.05	0.025	0.025	0.09	0.0257	0.0061	0.025	0.025
B	µg/l	5	5	91	1473	127.551	164.7202	133	549.92
Ba	µg/l	0.05	0.58	14.7	178.4	18.4478	19.7729	26.585	58.5836
Be	µg/l	0.05	0.025	0.025	0.87	0.0482	0.1098	0.025	0.468
Bi	µg/l	0.05	0.025	0.025	0.09	0.0257	0.0065	0.025	0.025
Br	µg/l	5	2.5	19	410	35.1497	47.5253	44.5	150.28
Ca	µg/l	50	8093	51149	377163	75527.76	70999.83	92231	305100.28
Cd	µg/l	0.05	0.025	0.025	3.31	0.1515	0.3928	0.025	1.3148
Ce	µg/l	0.01	0.005	0.01	14.84	0.3343	1.5283	0.02	4.9428
Cl	mg/l	1	0.5	8	426	34.0612	67.5044	23.5	273.28
Co	µg/l	0.02	0.01	0.1	88.07	3.4438	10.6562	0.56	30.6132
Cr	µg/l	0.5	0.25	0.25	2.6	0.3306	0.2925	0.25	1.224
Cs	µg/l	0.01	0.005	0.08	23.32	0.7288	2.6442	0.285	6.966
Cu	µg/l	0.1	0.3	1.6	11693	150.0313	1055.571	6.45	1000.4
DO	mg/l	0.01	1.78	14.41	27.87	13.3702	4.2626	15.815	19.8424
Dy	µg/l	0.01	0.005	0.005	4.55	0.0953	0.4652	0.01	1.3832
EC	µS/cm	0.1	66	324	1577	440.3333	355.8934	586.5	1384.48
Er	µg/l	0.01	0.005	0.005	1.71	0.0418	0.1831	0.005	0.5664
Eu	µg/l	0.01	0.005	0.005	1.58	0.0352	0.1638	0.005	0.444
F	µg/l	20	22	120	1010	163.9388	135.8377	203.5	515.68
Fe	µg/l	10	5	13	44860	528.3061	3822.007	30.5	5126.56
Ga	µg/l	0.05	0.025	0.025	0.29	0.0297	0.0291	0.025	0.0948
Gd	µg/l	0.01	0.005	0.005	6.67	0.1298	0.6566	0.01	1.8252
Ge	µg/l	0.05	0.025	0.025	0.13	0.0286	0.0153	0.025	0.0808
HCO3-	mg/l	0	0	78	220	80.0857	51.5807	111.2	196.24
Hf	µg/l	0.02	0.01	0.01	0.01	0.01	0	0.01	0.01
Hg	µg/l	0.1	0.05	0.2	8.6	0.3946	0.8114	0.4	2.18
Ho	µg/l	0.01	0.005	0.005	0.8	0.0208	0.082	0.005	0.254
In	µg/l	0.01	0.005	0.005	0.09	0.0056	0.007	0.005	0.005
Ir	µg/l	0.05	0.025	0.025	0.06	0.0252	0.0029	0.025	0.025
K	µg/l	50	121	1113	25165	2089.197	3339.646	2426.5	11777.2
La	µg/l	0.01	0.005	0.01	4.73	0.1217	0.4879	0.01	1.6192
Li	µg/l	0.1	0.1	4.3	216.7	14.9599	31.766	12.65	142.176
Lu	µg/l	0.01	0.005	0.005	0.13	0.0077	0.0134	0.005	0.05
Mg	µg/l	50	805	8426	37859	10148.67	7384.278	14645	29659.92
Mn	µg/l	0.05	0.25	17.7	1920.08	123.5873	285.4071	67.58	949.6572
Mo	µg/l	0.1	0.05	2.1	38.5	3.0296	3.8434	3.9	10.864
Na	µg/l	50	209	11970	239547	25894.5	39316.08	22735.5	163422.6
Nb	µg/l	0.01	0.005	0.005	0.03	0.0076	0.004	0.01	0.02
Nd	µg/l	0.01	0.005	0.01	13.99	0.3031	1.4414	0.02	4.4584
Ni	µg/l	0.2	0.1	0.1	59.1	2.8218	7.8692	0.6	27.9

Chemical	Unit	DL	Minimum	Median	Maximum	Mean	St.Dev.	%ile - 75	%ile - 98
NO3	mg/l	0.05	0.025	0.31	34.31	2.2815	5.5342	1.4	24.326
Os	µg/l	0.05	0.025	0.025	0.025	0.025	0	0.025	0.025
P	µg/l	20	10	34	9021	134.3129	759.9524	44.5	752.88
Pb	µg/l	0.1	0.05	0.05	4	0.2374	0.5284	0.2	1.512
Pd	µg/l	0.2	0.1	0.1	0.1	0.1	0	0.1	0.1
pH	pH	N/A	1.99	7.81	9.01	7.5737	1.0673	8.08	8.822
Pr	µg/l	0.01	0.005	0.005	2.42	0.0568	0.2502	0.005	0.818
Pt	µg/l	0.01	0.005	0.005	0.005	0.005	0	0.005	0.005
Rb	µg/l	0.01	0.16	1.5	54.35	3.97	8.3656	3.41	29.57
Re	µg/l	0.01	0.005	0.02	0.23	0.034	0.0406	0.04	0.1708
Rh	µg/l	0.01	0.005	0.005	0.05	0.0067	0.0067	0.005	0.04
Ru	µg/l	0.05	0.025	0.025	0.025	0.025	0	0.025	0.025
S	mg/l	1	4	38	454	68.2721	76.3007	97.5	310.64
Sb	µg/l	0.05	0.025	0.14	1.01	0.1893	0.1896	0.21	0.7536
Sc	µg/l	1	0.5	2	7	2.3129	1.2957	3	5.08
Se	µg/l	0.5	0.25	0.5	13.4	0.7439	1.2521	0.85	2.752
Si	µg/l	40	1475	7034	25229	7603.64	4369.017	9672.5	17360.32
Sm	µg/l	0.02	0.01	0.01	4.51	0.0964	0.4576	0.01	1.3284
Sn	µg/l	0.05	0.025	0.025	0.4	0.0322	0.0344	0.025	0.0908
SO4	mg/l	0.1	11.9836	113.8442	1360.139	204.5364	228.5894	292.1003	930.6464
Sr	µg/l	0.01	13.93	256.96	3173	509.5819	571.3549	708.295	2327.2268
Ta	µg/l	0.02	0.01	0.01	0.02	0.0101	0.0012	0.01	0.01
Tb	µg/l	0.01	0.005	0.005	0.88	0.0211	0.0875	0.005	0.2512
TDS	mg/l	2	34	287	1524	391.0748	319.5376	533	1187.04
Te	µg/l	0.05	0.025	0.025	0.13	0.0262	0.0102	0.025	0.025
Th	µg/l	0.05	0.025	0.025	1.46	0.0381	0.1191	0.025	0.1
Ti	µg/l	10	5	5	27	5.2313	2.0609	5	5
Tl	µg/l	0.01	0.005	0.005	0.48	0.0225	0.0541	0.01	0.1656
Tm	µg/l	0.01	0.005	0.005	0.2	0.0094	0.022	0.005	0.0716
TOC	mg/l	1	0.5	1	10	1.23	1.3825	1	7.04
U	µg/l	0.02	0.01	0.22	3.83	0.3913	0.5454	0.495	1.7772
V	µg/l	0.2	0.1	1.1	12.4	1.8694	1.9317	2.7	6.28
W	µg/l	0.02	0.01	0.02	5.2	0.0945	0.4424	0.05	0.5144
Y	µg/l	0.01	0.005	0.02	22.55	0.5043	2.3476	0.05	7.1112
Yb	µg/l	0.01	0.005	0.005	0.95	0.0269	0.1046	0.005	0.3408
Zn	µg/l	0.5	0.25	1.5	344.8	20.8782	53.6438	8.95	214.936
Zr	µg/l	0.02	0.01	0.01	0.23	0.0141	0.0206	0.01	0.0408

APPENDIX F: Regional geochemical data

- The file 'Appendix F_ Regional Geochemical Data.xlsx' contains the regional data used to develop the geochemical baselines of this study. The data included in the table are only those approved by the sponsoring company to be published